DOCTOR OF PHILOSOPHY

The role of salt-inducible kinase in the control of hepatic gluconeogenesis

Patel, Kashyap

Award date:
2014

DOCTOR OF PHILOSOPHY

The role of salt-inducible kinase in the control of hepatic gluconeogenesis

Kashyap Patel

2014

University of Dundee

The Role of Salt-inducible Kinase in the control of Hepatic Gluconeogenesis

By

Kashyap Amratlal Patel

A thesis submitted for the degree of Doctor of Philosophy

University of Dundee

September 2013

TABLE OF CONTENTS

List of Figures

List of Tables

Appendix

Abbreviations

°C	degree Celsius
aa	amino acid
ACC	acetyl-CoA carboxylase
AICAR	5-amino-1-β-D-ribofuranosyl-imidazole-4-carboxamide
AMP	adenosine monophosphate
AMPK	AMP-dependent protein kinase
ATP	adenosine 5'-triphosphate
BCA	bicinchoninic acid
BPG	bisphosphoglycerate
BRSK	brain-specific kinase
BSA	bovine serum albumin
Bt_2AMP	dibutyryl cyclic adenosine monophosphate
BTK	bruton agammaglobulinemia tyrosine kinase
C/EBP	CCAAT enhancer-binding protein
CaMK	Ca^{2+}/calmodulin-dependent protein kinase
CaMKK	Ca^{2+}/calmodulin-dependent protein kinase kinase
cAMP	cyclic adenosine monophosphate
CBP	CREB binding protein
CDK	cyclin dependent kinase
cDNA	complementary deoxyribonucleic acid
ChREBP	carbohydrate-responsive element-binding protein
CLK	cell division cycle like kinase
cpm	counts per minute
CREB	cAMP response element-binding protein
CRTC	cAMP response element-binding protein regulated transcription coactivator
DAX-1	Dosage-sensitive sex reversal adrenal hypoplasia congenital critical region on the X chromosome gene 1
DHAP	dihydroxyacetone phosphate
DMEM	dulbecco's modified eagles medium
DMSO	dimethyl sulphoxide
DNA	deoxyribonucleic acid
DSTT	division of signal transduction therapy
DTT	dithiothreitol
ECL	enhanced chemiluminescence
EDTA	ethylenediamine tetraacetic acid
EGTA	ethyleneglycol bis (2-aminoethylether)-N'N'tetraacetic acid
ES	embryonic stem
F1,6BP	fructose-1,6-bisphophatase
F1,6P2	fructose-1,6-bisphosphate
F6P	fructose-6-phosphate
FAS	fatty acid synthase
FBP1	fructose-1,6-bisphosphatase
FBS	foetal bovine serum

FGF	fibroblast Growth Factor
FoxO	forkhead O box
FXR	farnesoid X receptor
G1P	glucose-1-phosphate
G3P	glyceraldehyde-3-phosphate
G6P	glucose-6-phosphate
G6Pase	glucose-6-phosphatase
G6PDH	glucose-6-phosphate dehydrogenase
GDP	guanosine 5'-diphosphate
GFP	green fluorescent protein
GK	glucokinase
GLUT	glucose transporter
GNG	gluconeogenesis
GP	glycogen phosphorylase
GR	Glucocorticoid receptor
GS	glycogen synthase
GS	glycogen synthase
GSK3	glycogen synthase kinase 3
GST	glutathione-S-transferase
GTT	glucose tolerance test
HAT	histone deacetylase
HCl	hydrochloric acid
HDAC	class IIa Histone deacetylases
HEK293	human embryonic kidney 293
HEPES	4-(2-hydroxyethyl)-1-piperazineethanesulfonic acid
HGP	hepatic glucose production
HNF	hepatocyte nuclear factor
HPRT1	hypoxanthine phosphoribosyltransferase 1
HRP	horseradish peroxidase
HUNK	hormonally up-regulated neu-associated kinase
IC_{50}	half maximal inhibitory concentration
IGF-1	Insulin-like growth factor-1
IP3R	inositol-1,4,5-trisphosphate receptor
IPTG	isopropyl β-D-1-thiogalactopyranoside
IR	insulin receptor
IRS 1	insulin receptor substrate 1
kDa	kilodalton
LB	luria-berani
LC-MS	liquid chromatography–mass spectrometry
LCK	lymphocyte-specific protein tyrosine kinase
LKB1	liver kinase B1
LXR	liver X receptor
MARK	microtubule-affinity-regulating kinase
MDH	malate dehydrogenase
MEF2	myogenic enhancer factor 2
MELK	maternal embryonic leucine-zipper kinase
Mo25	mouse protein 25
MOI	multiplicities of infection

MOPS	3-(N-morpholino) propane sulphonic acid
MRC	Medical Research Council
mRNA	messenger ribonucleic acid
mTOR	mammalian target of rapamycin
NAD	nicotinamide adenine dinucleotide
NADPH	nicotinamide adenine dinucleotide phosphate
NEFA	non-esterified fatty acids
NUAK	sucrose-non-fermenting kinase-1 (SNF1)-like kinase
OD	optical density
PAGE	polyacrylamide gel electrophoresis
PAS	periodic acid schiff
PBS	phosphate-buffered saline
PC	pyruvate carboxykinase
PCR	polymerase chain reaction
PDK1	3-phosphoinositide-dependent protein kinase-1
PEI	polyethylenimine
PEP	phosphoenolpyruvate
PEPCK	phosphoenolpyruvate-carboxykinase
PFK	phosphofructokinase
PFKFB1	6-phosphofructokinase 2/fructose-2,6-bisphosphotase
PFU	plaque forming unit
PG	phosphoglycerate
PGC1α	proliferator-activated receptor Y coactivator-1 α
PI3K	phosphoinositide 3-kinase
PKA	cyclic-AMP dependent protein kinase A
PME-1	protein phosphatase methylesterase-1
PP2A	protein phosphatase 2A
PPU	protein phosphorylation and ubiquitination unit
qPCR	quantitative polymerase chain reaction
RNA	ribonucleic acid
rpm	revolutions per minute
RT-PCR	reverse transcriptase polymerase chain reaction
SD	standard deviation
SDS	sodium dodecyl sulphate
SE	standard error
SEM	standard error of the mean
SERBP	sterol regulatory element binding protein
SHP	small heterodimer partner
ShRNAi	short hairpin RNA interference
SIK	salt inducible kinase
SIRT1	sirtuin-1
SNRK	sucrose non-fermenting related kinase
SOC	super optimal broth with catabolite repression
SRC1	steroid receptor coactivator
SSTK	testis-specific serine kinase 6
StAR	steroidogenic acute regulatory protein
STAT3	signal transducer and activator of transcription 3
STRAD	ste20-related adaptor protein

TAK1	transforming growth factor β-activated kinase 1
TBS	tris-buffered saline
TBS-T	tris -buffered saline + tween-20
TCA	tricarboxylic acid
TEMED	tetramethylethylenediamine
Tris	tris(hydroxymethyl)aminomethane
TSC2	tuberous sclerosis 2
TSSK	testis-specific serine kinase
U	unit
UBA	ubiquitin association
v/v	volume by volume
VASP	Vasodilator-stimulated phosphoprotein
w/v	weight by volume
WT	wild-type
X5P	xylulose-5-phosphate
YES	v-yes-1 yamaguchi sarcoma viral oncogene homolog

Acknowledgements

I would like to thank Kei Sakamoto and Calum Sutherland for their excellent guidance and support during these past three years, without whom this research would not have materialised. I would like to thank Kei for directing design and plan of the experiments, interpretation of results, providing opportunity for collaboration to other groups and finally for thorough review of my thesis. I would also like to sincerely thank Calum for providing excellent guidance, thorough review of my thesis and allowing me to work in his lab for the last 8 months of my PhD in absence of Kei in Dundee.

I would also like to thank thesis monitoring committee Hari Hundal and Rory McCrimmon for their feedback on my work. In addition, I am grateful to my collaborators Morris Birnbaum and Marc Foretz, particularly Marc for teaching me the vital skill of mouse hepatocyte isolation. I would also like to thank Nathanael Gray for SIK inhibitors and Olga Göransson, Hiroshi Takemori and Robert Screaton for antibodies. I would also like to thank Proteomics team at MRC, particularly David Campbell for his help in SIK2 phosphopeptide mapping.

I am very grateful to the past and present members of Kei and Calum's group, Roger Hunter, Eriko Ohta and particularly Alex von Wilamowitz-Moellendorff for his excellent support throughout my research and teaching me the basic laboratory skills. I would also like to thank postdocs in MRC Unit in particular Ning Zhang and Martin Voss for many exciting brain-storming sessions, excellent laboratory tips and help with my thesis. In addition, I would like to thank Paul Davis for gel filtration experiments, George Allen for help with microscopy and lastly, all the MRC PhD students and postdocs for creating such helpful and supportive environment for work.

I would like to extend sincere gratitude to Dario Alessi and the support staff of MRC who have worked in the background to create excellent research environment, Kirsten McArdle and Janis Stark for their work in tissue culture, Mark Peggie, Thomas Macartney and Rachel Toth from

the DSTT Cloning team and Fiona Brown for purifying and supplying in-house antibodies. I would like to thank Allison Bridges, lab manager of MRC for her excellent help with my move to Calum's lab and making the transition as smooth as possible.

Finally, I would like to thank my family and friends but in particular my wife Hiral, whose excellent moral support, constant encouragement, great understating and charming personality has helped me greatly during the difficult times of my research and kept me sane.

Declarations

I hereby declare that the following thesis is based on the results of investigations conducted by myself and that this thesis is of my own composition. Work other than my own is clearly indicated in the text by reference to the relevant researchers or of their publications. This dissertation has not in whole, or in part, been previously submitted for a higher degree.

Kashyap A Patel

I certify that Kashyap A Patel has spent the equivalent of at least nine terms in research work at the School of Life Sciences, University of Dundee, and that he has fulfilled the conditions of the Ordinance General No. 14 of the University of Dundee and is qualified to submit the accompanying thesis in application for the degree of Doctor of Philosophy.

Kei Sakamoto Calum Sutherland

Summary

Regulation of hepatic gluconeogenesis by hormones insulin and glucagon is central to glucose homeostasis. Recent work has proposed that amongst the salt inducible kinase isoforms (SIK1, 2 and 3), members of the AMPK-related kinase family, the SIK2 isoform may play a role as signalling mediator in the control of insulin- and glucagon-regulated hepatic gluconeogenesis. However, the mechanisms of the hormonal-regulation of SIK2 in liver remain controversial, with much of the data based on the studies in non-hepatic tissues/cells. Therefore, the exact molecular regulation of SIK2 by these hormones in the liver required robust and intensive molecular/biochemical research coupled to physiological readout (e.g. gluconeogenesis).

My studies with phosphopeptide mapping by mass spectrometry followed by verification with well-characterised phospho-specific antibodies revealed that SIK2 was phosphorylated on Ser343, Ser358, Thr484 and Ser587 in response to glucagon and fasting but not following insulin treatment or refeeding in primary hepatocytes and liver *in vivo,* respectively. Unexpectedly, fasting- or glucagon-stimulated phosphorylation of SIK2 (individually or in combination) did not directly modulate kinase activity of SIK2 and its subcellular localisation. These findings collectively questioned the role of SIK2 in hepatic gluconeogenesis.

Thus to establish the role of SIK2 *in vivo*, liver-specific SIK2 knock-out mice were generated and analysed (in collaboration with Dr Marc Foretz, Institut Cochin, Paris). Surprisingly, the liver-specific SIK2 knock-out mice displayed normal blood glucose levels and gluconeogenic gene expression in both fasted and refed states compared to the control mice. The primary hepatocytes from these liver-specific SIK2 knock-out mice had unaltered basal and Bt_2-cAMP-stimulated glucose production and gluconeogenic gene expression compared to the control hepatocytes. These suggest that SIK2 is either not involved in hepatic gluconeogenesis or its loss is compensated by other SIK isoforms in the liver. This may indicate a possible redundancy amongst SIK isoforms for their role in hepatic gluconeogenesis.

To test this hypothesis, highly selective pan SIK inhibitors (HG-9-91-01 and KIN112) were characterised and used to study the importance of SIKs activity in hepatic glucose production employing mouse primary hepatocytes. Incubation of hepatocytes with SIK inhibitors significantly reduced CRTC2, CRTC3 and HDAC4 phosphorylation and robustly increased gluconeogenic gene expression and glucose production. The effects of HG-9-91-01 on hepatic gluconeogenesis were validated as SIK-specific, using HG-9-91-01-resistant SIK mutants, LKB1-null hepatocytes (cells where SIK activity was already depleted) and also AMPKα1/α2-null hepatocytes.

These experiments have proposed a novel insulin-independent pathway of gluconeogenesis suppression, in which SIK isoforms collectively work together as a 'molecular gatekeeper' to continually suppress hepatic gluconeogenesis. This inhibition is released following glucagon/fasting by inhibiting SIKs through a mechanism yet to be elucidated but likely to be dependent on phosphorylation of SIKs on multiple residues.

Importantly and contrary to the previous studies, my data demonstrates that SIK2 is clearly not the only or the dominant SIK isoform that regulates hepatic gluconeogenesis and glucagon regulates phosphorylation of four specific residues on SIK2, while insulin does not induce phosphorylation of SIK2 in liver. These data inform on how glucagon signals to these important kinases, but more work is required to decipher how phosphorylation actually changes SIKs function at the molecular and biochemical level and how such phosphorylation effects downstream targets and biological processes.

1 Introduction

1.1 Glucose homeostasis

Glucose is an essential source of energy for the body and accurate and precise regulation of blood glucose levels-glucose homeostasis, is the key to survival. Hyperglycaemia can lead to complications of diabetes while low blood glucose levels can cause coma or death, therefore blood glucose levels are tightly regulated in a narrow range (between 4-7 mmol/L) primarily by glucose disposal to peripheral tissues (e.g. muscle and adipose tissue) and glucose production in liver (Roden and Bernroider, 2003). Insulin and glucagon are the key hormones in maintaining glucose homeostasis and are responsible for acute and chronic regulation of glucose homeostasis by acting on multiple organs such as liver, skeletal muscle, adipose tissue, brain and pancreas (Aronoff et al., 2004; Stumvoll et al., 2005; Wasserman, 2009).

After a meal blood glucose increases, which stimulates insulin secretion from pancreatic β-cells (Figure 1.1). Insulin secretion is augmented by glucagon-like peptide 1 (GLP-1) and glucose-dependent insulinotropic polypeptide (GIP) secreted from intestinal L and K cells respectively (MacDonald et al., 2002). Insulin acts directly on the liver and increases glycogen synthesis, suppresses glycogenolysis and gluconeogenesis leading to a reduction in hepatic glucose production (Figure 1.1) (Cherrington, 1999; Rask-Madsen and Kahn, 2012). In peripheral tissues such as skeletal muscle and adipose tissue, insulin promotes glucose uptake by inducing translocation of GLUT4 (glucose transporter 4) to the cell membrane (Charron et al., 1989; Huang and Czech, 2007; James et al., 1989). Insulin also increases glycogen and protein synthesis and reduces protein degradation in skeletal muscle as well as suppresses lipolysis and increases lipogenesis in adipose tissue (Figure 1.1) (Rask-Madsen and Kahn, 2012). These actions collectively lead to a further reduction in gluconeogenesis by decreasing the availability of gluconeogenic substrates (i.e. glycerol and amino acids) (Saltiel and Kahn, 2001).

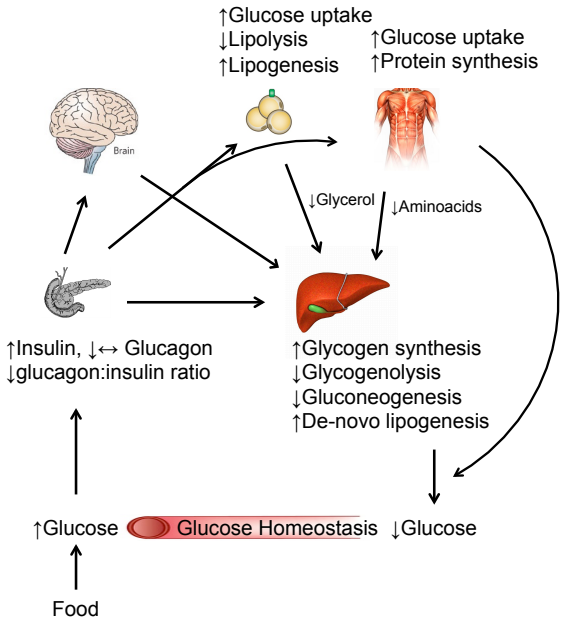

Figure 1.1 Control of glucose homeostasis: under feeding condition.

Rise in blood glucose after a meal stimulates insulin release and causes reduction in glucagon:insulin ratio. This leads to increase in glucose uptake in peripheral tissues such as adipose tissue and skeletal muscles and suppression of hepatic glucose production. Hepatic glucose production is reduced by direct action of hormones on the liver or indirectly via central nervous system and reduction in the availability of gluconeogenic substrates. These actions collectively maintain glucose homeostasis.

Insulin is thought to reduce hepatic glucose production indirectly through its action on brain. These effects have been studied in rodents by direct injection of insulin using intracerebroventricular cannula, which resulted in decreased hepatic glucose production mainly by suppression of gluconeogenesis (Obici et al., 2002; Pocai et al., 2005). This central action of insulin was noted to be antagonised by either co-infusion of K_{ATP} channel-blockers (glibenclamide) or by surgical resection of hepatic branch of vagal nerve (Pocai et al., 2005), while direct injection of the K_{ATP} channel-activator (diazoxide) in hypothalamus reduced hepatic glucose production (Obici et al., 2002; Pocai et al., 2005). Conversely, central antagonism of insulin signalling using insulin antibodies or wortmannin (PI3K inhibitor) (Obici et al., 2002)or glibenclamide (Pocai et al., 2005) impaired the ability of circulating insulin to inhibit hepatic glucose production. These findings suggest that insulin activates the K_{ATP} channel in the hypothalamus and reduces hepatic glucose production via vagal efferent nerves to the liver. However, studies in conscious dogs using hepatic-portal clamps and intra-arterial

(carotid/vertebral) insulin infusions noted minimal or no suppression of hepatic glucose production (reviewed in (Ramnanan et al., 2012)).

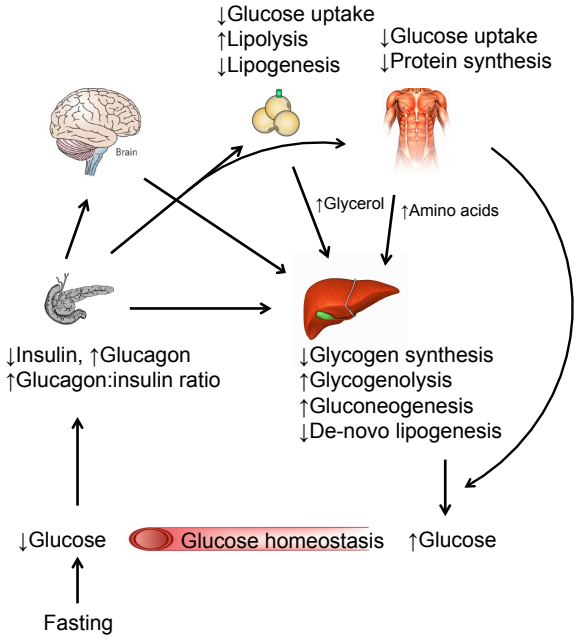

Figure 1.2 Control of glucose homeostasis: under fasting condition.

Fasting stimulates glucagon release and suppresses insulin secretion from pancreas. This leads to reduction in glucose uptake in peripheral tissues such as adipose tissue and skeletal muscles and robust increase in hepatic glucose production by direct action of hormones or indirectly via central nervous system and increase in gluconeogenic substrates. These actions collectively achieve glucose homeostasis.

During short-term fasting, reduction in blood glucose levels suppresses insulin secretion and increases glucagon secretion from pancreatic α-cells leading to a rise in glucagon:insulin ratio (Figure 1.2). Glucagon promotes glycogenolysis in the liver and increases hepatic glucose output while there is a reciprocal reduction in glucose uptake in peripheral organs due to reduced availability of insulin (Cherrington, 1999; Roden et al., 2001; Wasserman, 2009). During prolonged fasting, hepatic glucose production is maintained by glucagon through a direct up-regulation of hepatic gluconeogenesis, and indirectly by increasing gluconeogenic substrates (Figure 1.2) (Roden and Bernroider, 2003).

Apart from insulin and glucagon, several other hormones also contribute to glucose homeostasis such as incretins (GLP-1, GIP), epinephrine, cortisol and growth hormone, and adipokines (e.g. leptin, adiponectin, resistin) (Yeo and Sawdon, 2013).

1.2 Role of liver in glucose metabolism

The liver has a unique ability to modulate glucose production to match whole-body glucose utilisation, making it a key component of glucose homeostasis. Liver mediates this action by controlling metabolic flux through glycolysis, glycogen metabolism (synthesis/degradation) and gluconeogenesis (Figure 1.3) (Cherrington, 1999; Nordlie et al., 1999; Radziuk and Pye, 2001; Roden et al., 2001; Wu et al., 2005).

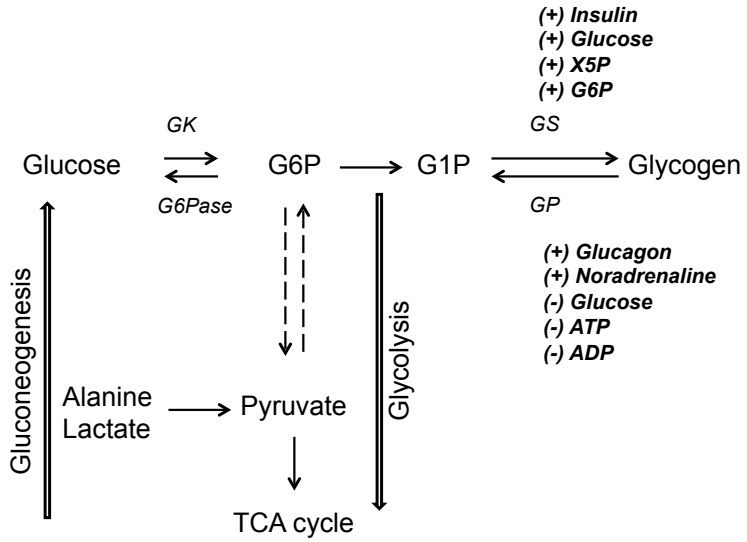

Figure 1.3 Fate of glucose in the liver.

Glucose from circulation can be stored as glycogen or metabolised via glycolytic pathway whereas liver produces glucose (which enters into circulation) by glycogenolysis and gluconeogenesis. Glycogen synthesis occurs by direct pathway from circulation-derived glucose and can also occur from gluconeogenic-derived glucose (indirect pathway). Glycogen metabolism is mainly regulated at the level of glycogen synthase (GS) and glycogen phosphorylase (GP) by multiple allosteric factors (and covalent modifications (not shown in this Figure)) and hormones as indicated in the Figure. GK (glucokinase), G6Pase (glucose-6-phosphatase), G6P (glucose-6-phoshphate), G1P (glucose-1-phosphate), X5P (xylulose-5-phosphate).

1.2.1 Hepatic glycogen metabolism

Glucose is stored primarily in liver and skeletal muscles as glycogen. However, only hepatic glycogen can be reconverted to glucose for entry into the circulation and delivery to peripheral tissues during fasting due to expression of the critical enzyme glucose-6-phosphatase (G6Pase) in liver. G6Pase is required for conversion of glucose-6-phosphate (G6P) to glucose, the final step of gluconeogenesis/glycogenolysis (Figure 1.3) (Nordlie et al., 1999).

Glycogen is directly generated from glucose after a meal or indirectly generated from gluconeogenic-derived glucose (Figure 1.3) (Roden and Bernroider, 2003). After an overnight fast, hepatic glycogenolysis contributes up to 50-65% of the total hepatic glucose production in humans but as fasting continues this contribution decreases and after 48 h glycogen stores are exhausted (Petersen et al., 1996; Rothman et al., 1991). Glycogen metabolism is principally regulated by the coordinated action of glycogen phosphorylase (GP) and glycogen synthase (GS) (Figure 1.3) (reviewed in (Agius, 2007)). These enzymes are tightly controlled by hormones such as glucagon, insulin and noradrenaline, as well as by allosteric regulators and substrate availability.

Glucagon activates GP. This is achieved by protein kinase A (PKA)-mediated phosphorylation and activation of GP kinase which in turn phosphorylates and activates GP (Agius, 2007). In contrast, insulin reduces GP activity by inducing dephosphorylation through glycogen phosphorylase phosphatase (type 1 phosphatase in complex with glycogen targeting subunit). Glycogen phosphorylase is also allosterically regulated by various metabolites and nucleotides such as glucose, G6P, and ATP (Agius, 2007). Glycogen synthase is activated by a key allosteric factor G6P (Bouskila et al., 2010) and the Akt (also known as protein kinase B)-glycogen synthase kinase 3 (GSK3) pathway by insulin (Cohen and Frame, 2001) and inhibited by PKA (e.g. by adrenaline and glucagon) and AMP-activated protein kinase (AMPK) (e.g. by energy stress) (Carling et al., 2012; Hardie et al., 2012).

Therefore during fasting, a rise in glucagon:insulin ratio activates GP and inactivates glycogen synthase. Furthermore, the relative reduction in glucose during fasting removes the allosteric inhibition on GP while the relative reduction in G6P reduces the allosteric activation of GS. These actions result in a rapid induction of glycogen breakdown and glucose release from the liver during fasting. The opposite regulation of these enzymes during feeding promotes glycogen synthesis and storage.

1.2.2 Hepatic gluconeogenesis

Gluconeogenesis is a process in which glucose is generated *de novo* from 3-carbon sources such as lactate, pyruvate, glycerol and amino acids (i.e. alanine, glutamine) (Exton and Park, 1967; Pilkis et al., 1988).Gluconeogenesis is an essential process for constant supply of glucose to the brain and erythrocytes, which are heavily dependent on glucose for energy, particularly during fasting. Liver, kidney and small intestine are the only organs that express the machinery for gluconeogenesis (i.e. the gluconeogenic enzymes) (Roden and Bernroider, 2003). Hepatic gluconeogenesis contributes to 35-50% of total hepatic glucose production after an overnight fast, and this steadily increases to almost 100% by 48-h fasting (Radziuk and Pye, 2001; Rothman et al., 1991). Renal gluconeogenesis is estimated to be negligible in the fed state but can increase to up to 23% during prolonged fast (Gerich et al., 2001), while the contribution of intestinal gluconeogenesis to overall glucose production is unknown (Previs et al., 2009).

1.2.2.1 Key enzymes of hepatic gluconeogenesis

Most of the enzymes required for gluconeogenesis are bidirectional and are shared with glycolysis. These enzymes are mainly controlled by the relative concentration of substrates and products (Exton and Park, 1967; Pilkis et al., 1988). However, there are four unidirectional gluconeogenic enzymes; pyruvate carboxylase, phosphoenolpyruvate carboxykinase (PEPCK), fructose-1,6-bisphosphatase (F1,6BP) G6Pase (Figure 1.4). In concert with their opposing glycolytic enzymes; pyruvate kinase, 6-phosphofructokinase 1 (6-PFK1) and glucokinase (GK), three very important substrate cycles are generated and represent rate-controlling steps in the pathway. Regulation of specifically these enzymes, by substrates and products, allosteric factors and hormones such as insulin and glucagon, provides a mechanism for balancing the need for glucose supply to the production of hepatic glucose (Figure 1.4) (Pilkis and Claus, 1991).

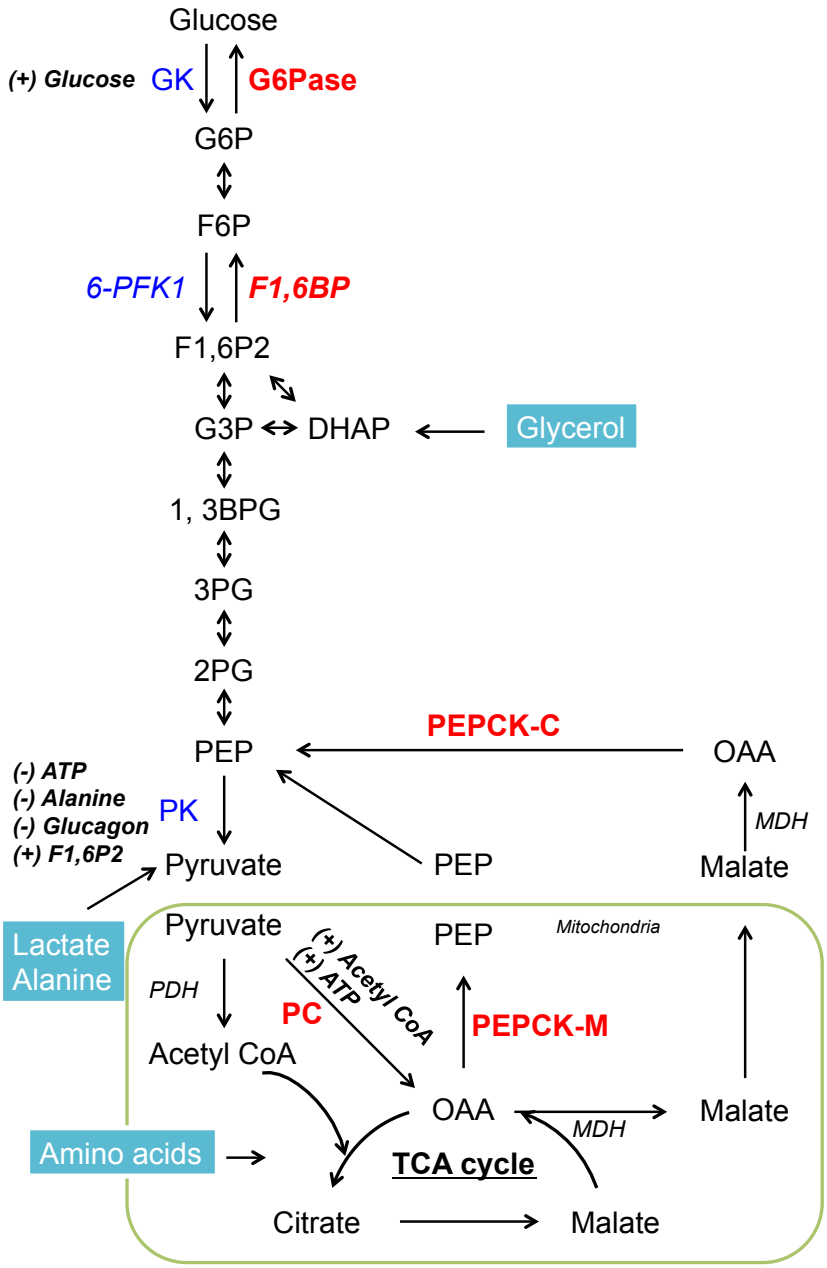

Figure 1.4 Gluconeogenesis pathway.

The key unidirectional gluconeogenic enzymes are highlighted in red and their counterpart glycolytic enzymes are highlighted in blue. Gluconeogenic substrates are highlighted and their entry point to pathway is indicated. GK (glucokinase), G6Pase (glucose-6-phosphatase), G6P (glucose-6-phoshphate), F6P (fructose-6-phosphate), F1,6P2 (fructose-1,6-bisphosphate), 6-PFK1 (6-phosphofructokinase 1), F1,6BP (fructose-1,6-bisphophatase), G3P (glyceraldehyde-3-phosphate), DHAP (dihydroxyacetone phosphate), 1,3BPG (1,3-bisphosphoglycerate), 3PG (3-phosphoglycerate), 2PG (2-phosphoglycerate), PEP (phosphoenolpyruvate), PK (pyruvate kinase), PC (pyruvate carboxylase), PEPCK (phosphoenolpyruvate carboxykinase)-C (cytoplasm), -M (mitochondria), OAA (oxaloacetate), PDH (pyruvate dehydrogenase), MDH (malate dehydrogenase).

For example, co-ordinated induction of pyruvate carboxylase, PEPCK, F1,6BP and G6Pase (along with inhibition of GP) generates glucose production, whereas induction of GK, 6-PFK1, pyruvate kinase and GS together will enhance glucose utilisation/storage in the liver.

Short-term regulation of gluconeogenesis is mainly mediated by allosteric and phosphorylation-dependent regulation of the unidirectional gluconeogenic enzymes and co-ordinated inhibition of their glycolytic counterpart enzymes (Hanson, 2003; Nordlie et al., 1999). Whereas, long-term regulation is mediated by transcriptional regulation of key unidirectional gluconeogenic enzymes PEPCK and G6Pase by hormones insulin and glucagon (Hanson, 2003; Nordlie et al., 1999; Roden and Bernroider, 2003).

1.2.2.2 Substrates for gluconeogenesis in liver

Lactate, glycerol and amino acids are the major substrates for gluconeogenesis. Lactate enters the gluconeogenesis pathway after converting to pyruvate in the liver. Glycerol is generated in adipose tissue by triglyceride metabolism and enters the pathway at triose-phosphate level (Figure 1.4) (Pilkis and Claus, 1991). Alanine enters gluconeogenesis pathway by converting to pyruvate (Figure 1.4), while other amino acids enter the pathway at various levels of the tricarboxylic acid (TCA) cycle (Figure 1.4) (Nuttall et al., 2008).

1.2.2.3 Short-term regulation of gluconeogenesis by allosteric factors and hormones

1.2.2.3.1 Pyruvate carboxylase and phosphoenolpyruvate carboxykinase

Pyruvate carboxylase catalyses the first step of gluconeogenesis, the carboxylation of pyruvate to oxaloacetate in mitochondria (Figure 1.4). Oxaloacetate is further decarboxylated to phosphoenolpyruvate by PEPCK using guanosine triphosphate (GTP) (Pilkis and Granner, 1992). In humans, this reaction is carried out either by mitochondrial-PEPCK or cytosolic-PEPCK (the products of different genes) (Hanson and Patel, 1994). Mice have minimal mitochondrial-PEPCK so oxaloacetate is reduced to malate and transported to cytoplasm where it is oxidised back to oxaloacetate (Figure 1.4). Thereafter, phosphoenolpyruvate continues on the gluconeogenesis pathway or can be converted back to pyruvate by pyruvate kinase creating the first substrate cycle (Figure 1.4). Pyruvate carboxylase is allosterically activated by acetyl-CoA and ATP and, inhibited by ADP (Attwood, 1993; Pilkis and Granner, 1992). Interestingly no such allosteric regulators of PEPCK have been identified or reported.

During prolonged fasting, liver primarily metabolises fatty acids to generate ATP and acetyl-CoA, while amino acids such as alanine are produced by protein catabolism in skeletal muscles (Attwood, 1993). Acetyl-CoA and ATP in mitochondria allosterically activate pyruvate carboxylase, thus promoting oxaloacetate generation. Oxaloacetate levels are further supplemented by the TCA cycle via amino acid anaplerosis. This leads to a rise in pyruvate levels (Figure 1.4). Along with this, co-ordinated inhibition of pyruvate kinase (a glycolytic enzyme) either by allosteric factors (alanine and ATP) or by glucagon during fasting diverts pyruvate for gluconeogenesis. Glucagon inhibits pyruvate kinase by PKA-dependent phosphorylation on Ser12 (Figure 1.4) (Pilkis and Granner, 1992).

1.2.2.3.2 Fructose-1,6-bisphosphatase

F1,6BP hydrolyses fructose-1,6-bisphosphate (F1,6P2) to provide fructose-6-phosphate (F6P) for gluconeogenesis. The reverse reaction in glycolysis is catalysed by 6-PFK1, creating a second substrate cycle (Figure 1.5). The major regulators of this cycle are fructose-2,6-bisphosphate (F2,6P2) and AMP, which allosterically inhibit F1,6BP and activate 6-PFK1 (Kurland and Pilkis, 1995; Pilkis et al., 1990) thereby driving the cycle towards production of F1,6P2 and glycolysis. F2,6P2 concentration in the liver is maintained by the bifunctional enzyme 6-phosphofructokinase 2/fructose-2,6-bisphosphatase (6-PFKFBP) (Figure 1.5).

During fasting, glucagon promotes phosphorylation of 6-PFKFBP on Ser33, activating its phosphatase activity and thus reducing F2,6P2 levels (Figure 1.5) (Kurland and Pilkis, 1995; Pilkis et al., 1990). This phosphatase activity is further enhanced by the reduction in glucose and insulin during fasting due to suppression of their inhibition on the phosphatase (Figure 1.5). Reduction of F2,6P2 reduces the activity of 6-PFK1 and enhances the activity of F1,6BP, thus driving the cycle towards gluconeogenesis (Kurland and Pilkis, 1995; Pilkis et al., 1990).

1.2.2.3.3 Glucose-6-phosphatase

G6Pase catalyses the final step in gluconeogenesis, the hydrolysis of G6P to glucose. The reverse reaction in glycolysis is catalysed by glucokinase, creating the last substrate cycle

(Figure 1.4). Although G6Pase is inhibited by multiple allosteric factors such as saturated fatty acids, fructose-1-phosphate and α-ketoglutarate *in vitro*, their contribution *in vivo* remains questionable (van de Werve et al., 2000).

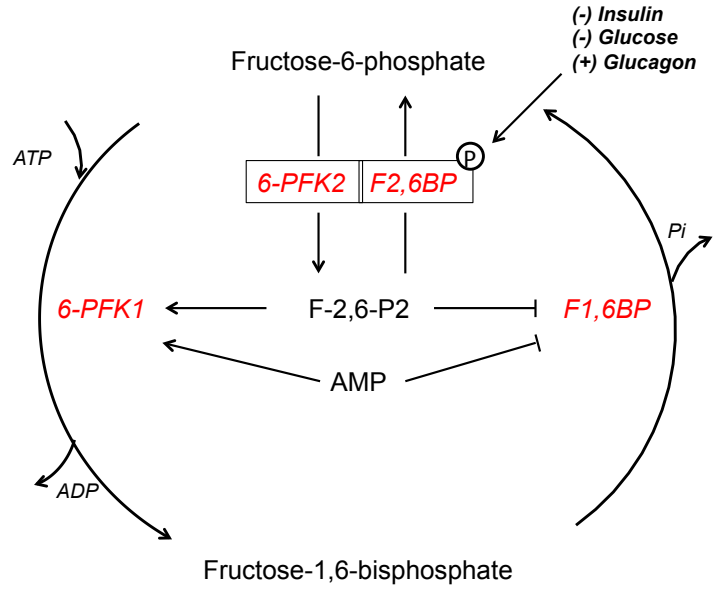

Figure 1.5 Regulation of Fructose-1,6-bisphosphatase (F1,6BP) and 6-phosphofructokinase 1 (6-PFK1). Both of these enzymes are heavily influenced by AMP and fructose-2,6-bisphosphate (F2,6P2) level in the liver. F2,6P2 level itself is further regulated by hormones and allosteric factors through their influence on kinase or phosphatase activity of bifunctional 6-PFK2/F2,6BP (6-phosphofructokinase 2/fructose-2,6-bisphosphotase) enzyme.

1.2.2.4 Long-term regulation of gluconeogenesis by transcriptional modulation in response to hormones

Metabolic hormones such as insulin and glucagon chronically influence gluconeogenesis by transcriptional regulation of the unidirectional gluconeogenic enzymes. In particular the transcription of two gluconeogenic enzymes PEPCK and G6Pase is potently and robustly regulated by glucagon, insulin and glucocorticoids. The transcriptional regulation of the other two gluconeogenic enzymes, pyruvate carboxylase and F1,6BP, by hormones is not well studied, but most studies suggest that transcriptional regulation may not be a major mechanism of regulation (Haase et al., 2011; Jitrapakdee et al., 2005; Kumashiro et al., 2013; Thonpho et al., 2010) but rather these enzymes are tightly controlled by allosteric factors that are in turn significantly influenced by hormones (see section 1.2.2.3.1, 1.2.2.3.2)

Fasting and glucagon exposure robustly increases PEPCK and G6Pase gene transcription in liver and hepatocytes, respectively (Chrapkiewicz et al., 1982; Iynedjian and Hanson, 1977; Lamers et al., 1982). In contrast, feeding and insulin exposure completely suppresses these genes in liver (and isolated hepatocytes) (Granner et al., 1983; Kioussis et al., 1978; Tilghman et al., 1974). The signal transduction pathways that connect these hormonal and nutritional cues to these hepatic gene promoters have been the focus of research for decades. Multiple transcription factors bind to numerous cis-elements in the gene promoters of PEPCK and G6Pase (reviewed in (Jitrapakdee, 2012)). Table 1-1 shows transcription factors and coactivators that are implicated in the regulation of PEPCK and G6Pase gene expression in the liver.

Table 1-1 Transcription factors and regulators of gluconeogenic genes in liver.

	Direct evidence of insulin and glucagon regulation	**Direct evidence of nutritional (Fasting and Feeding) regulation**	**Reference**
Transcription factors			
cAMP-response element-binding protein (CREB)	Yes	Yes	(Altarejos and Montminy, 2011; Herzig et al., 2001)
Forkhead O box (FoxO) 1, 3	Yes	Yes	(Benayoun et al., 2011; Haeusler et al., 2010; Matsumoto et al., 2007)
Hepatocyte nuclear factors (HNF1, 3 and 4)	No	No	(Kaestner et al., 1998; Rhee et al., 2003)
Glucocorticoid receptor (GR)	No	No	(Cassuto, 2005; Vander Kooi, 2005)
CCAAT enhancer-binding protein (C/EBP)	No	No	(Inoue, 2004; Wang et al., 1995)
Signal transducer and activator of transcription 3 (STAT3)	No	Yes	(Inoue et al., 2006; Inoue, 2004; Nie et al., 2009)
Farnesoid X receptor (FXR)	No	Yes	(Kemper, 2011; Ma, 2006a; Prawitt et al., 2011)
Transcriptional regulators			
CREB binding protein (CBP)	Yes	Yes	(Altarejos and Montminy, 2011; He et al., 2009; Ravnskjaer et al., 2007)
CREB-regulated transcription coactivator 2 (CRTC2)	Yes	Yes	(Altarejos and Montminy, 2011; Dentin et al., 2007; Koo et al., 2005)
Peroxisome proliferator-activated receptor-γ	Yes	Yes	(Koo et al., 2004; Liang and Ward, 2006; Liu and Lin, 2011)

coactivator-1α (PGC-1α)			
Class IIa Histone deacetylases (HDACs)	Yes	Yes	(Mihaylova et al., 2011)
Ca^{2+}/calmodulin-dependent protein kinase II (CaMKII)	Yes	Yes	(Ozcan et al., 2012; Wang et al., 2012)
Sirtuin-1 (SIRT1)	No	Yes	(Liu et al., 2008; Motta et al., 2004; Rodgers and Puigserver, 2007)
Small heterodimer partner (SHP)	No	Yes	(Kim et al., 2007; Ma, 2006b)
Steroid receptor coactivator 1 (SRC1)	No	Yes	(Chopra et al., 2011; Louet et al., 2010)
Dosage-sensitive sex reversal adrenal hypoplasia congenital critical region on the X chromosome gene 1 (DAX-1)	No	Yes	(Nedumaran et al., 2009)
Fibroblast Growth Factor (FGF) 15/19	No	Yes	(Belov and Mohammadi, 2013; Shin and Osborne, 2008)

Amongst these, CREB, CBP, CRTCs, FoxOs, PGC-1α, SIRT1 and class IIa HDACs are strongly linked to the hormonal- and nutritional-regulation of hepatic gluconeogenesis. Therefore their function and the signal transduction pathways regulating these proteins in response to nutritional cues (fasting and feeding) and hormones (glucagon and insulin) are discussed in more detail below (section 1.3). Salt-inducible kinase (SIK) isoforms influence the function of CRTC2, CBP and class IIa HDACs and thus could be integrators of hormone-regulation of PEPCK and G6Pase. Regulation and roles of SIK isoforms are also discussed in more detail below (section 1.5)

1.2.3 Role of liver in hyperglycaemia of diabetes

The liver plays a critical role in glucose homeostasis and loss of this hepatic function is a major contributor to the hyperglycaemia that defines diabetes. Diabetes is a chronic debilitating disease currently affecting nearly 347 million people worldwide (MD et al., 2011)**.** Diabetes is broadly divided into two types based on pathophysiological characteristics (reviewed in (Fowler, 2007)). Type 1 diabetes is caused by insulin deficiency due to β-cell loss, while type 2 diabetes (T2DM) is a progressive disease characterised by impaired insulin secretion from

pancreatic β-cells and insulin resistance - inadequate response of cells/tissues to insulin. About 80-90% of diabetes patients have type 2 diabetes. The etiology of type 2 diabetes is complex and largely mediated by a combination of genetic predisposition, obesity and environmental influences such as poor diet (high fat and sugar) and lack of exercise (reviewed in (Defronzo, 2004)).

Hepatic glucose production in type 2 diabetes patients is 10-50% higher becoming relatively more important when fasting glucose rises above 8-9 mmol/L (Basu et al., 2005; Staehr et al., 2004) and contributes to one third of hyperglyacemia in type 2 diabetes, while the remainder is due to reduced glucose uptake in the peripheral tissues, mainly skeletal muscles (Roden and Bernroider, 2003). Raised hepatic glucose production is mainly due to failure in appropriate suppression of hepatic gluconeogenesis and impaired glycogen synthesis secondary to hepatic insulin resistance, hyperglucagonemia and raised non-esterified fatty acids (Basu et al., 2005; Defronzo, 2004; Gastaldelli et al., 2001; Magnusson et al., 1992; Wu et al., 2005). Interestingly metformin, the most commonly used drug for type 2 diabetes, significantly reduces hyperglycaemia and this is thought to be primarily through suppression of hepatic glucose production via a decrease in hepatic gluconeogenesis (Defronzo, 2004; Rena et al., 2013).

In summary, proper control of hepatic gluconeogenesis is vital to prevent development of metabolic disease, and further understanding of signal transduction pathways that regulate hepatic gluconeogenesis may provide novel targets for clinical intervention.

1.3 Transcriptional regulation of gluconeogenesis

1.3.1 FoxO

The forkhead box O (FoxO) family is a subclass of the forkhead family of transcription factors (reviewed in (Benayoun et al., 2011; Eijkelenboom and Burgering, 2013)). It comprises four family members, FoxO1 (also known as FKHR), FoxO3 (also known as FKHRL1), FoxO4 (also known as AFX1) and FoxO6. They all bind to the same consensus DNA sequence (5'-TTGTTTAC-3') and thus there is a possibility of some redundancy in their function. However, isoform-

specific functions have been identified and are thought to be due to tissue-specific expression of the isoforms. Global FoxO3- and 4-null mice are viable but FoxO1-null mice are embryonically lethal (Hosaka et al., 2004). FoxO family members participate in regulation of various biological functions including aging, cellular oxidative stress, apoptosis, β-cell development, glucose and lipid metabolism (Carter and Brunet, 2007; Eijkelenboom and Burgering, 2013). FoxOs are mainly regulated by two canonical signalling pathways, an inhibitory phosphoinositide-3-kinase (PI3K)-Akt pathway (Figure 1.6) and an activating c-Jun N-terminal kinase (JNK) pathway. These pathways are stimulated by growth factors such as insulin and oxidative-stress respectively. Insulin-activated Akt phosphorylates FoxOs on three conserved residues (T24, S256 and S319 sites on human FoxO1) promoting binding to 14-3-3 proteins, which leads to cytoplasmic sequestration of FoxOs and inactivation of their transcriptional activity (Biggs et al., 1999; Brunet et al., 1999; Nakae, 1999; Nakae et al., 2001). In addition to these two well characterised signalling pathways, FoxOs are regulated by various upstream kinases such as AMPK (AMP-activated protein kinase), CDK1 (cyclin-dependent kinase 1), CKI (casein kinase I) and post-translational modifications including acetylation, methylation and ubiquiylation (Benayoun et al., 2011; Carter and Brunet, 2007).

1.3.1.1 Role of FoxO in hepatic gluconeogenesis

Contribution of FoxOs, particularly FoxO1 and 3, in the regulation of gluconeogenic genes was first highlighted by studies expressing dominant-negative (lacking transactivation domain) and constitutively-active (Akt phosphorylation-deficient, T24A/S253D/S316A) mutants of FoxO1 in mouse primary hepatocytes (Nakae et al., 2001) and in liver tissue (Altomonte et al., 2003). Forced expression of a dominant-negative mutant reduced fasted and fed blood glucose and reduced gluconeogenic gene expression in the liver of normal and diabetic *db/db* mice (Altomonte et al., 2003).

Role of FoxO1 in hepatic gluconeogenesis was further explored *in vivo* using liver-specific FoxO1-null mice (Matsumoto et al., 2007). These animals had mild reduction in blood glucose levels even after prolonged fasting (48 h) with minimal effect on hepatic PEPCK and G6Pase

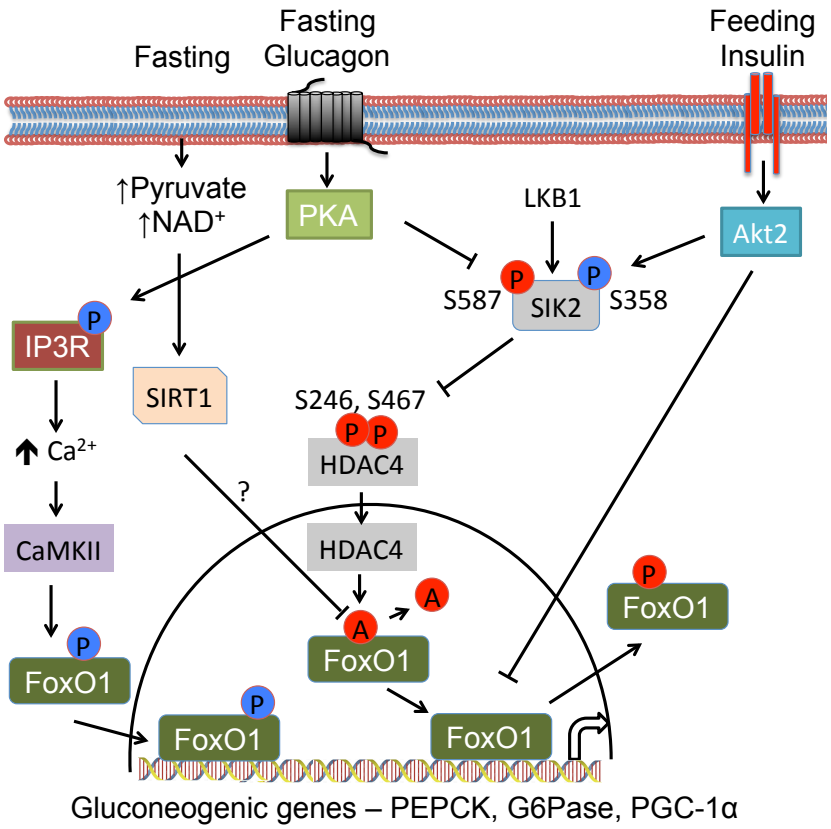

Figure 1.6 FoxO1 in hepatic gluconeogenesis.

Feeding and insulin activate Akt which phosphorylates FoxO1, induces its cytoplasmic translocation and thus inhibits gluconeogenic gene expression. Fasting activates CaMKII, secondary to increase in intracellular Ca^{2+}. CaMKII phosphorylates FoxO1 on multiple residues (non Akt-regulated sites) and promotes its nuclear translocation and thus activates gluconeogenic gene expression. Fasting can also increase FoxO1-dependent gene transcription by deacetylation of FoxO1 either by class IIa HDACs such as HDAC4 via SIK2 or by a class III NAD^{+}-dependent deacetylase SIRT1. However, SIRT1-mediated deacetylation has been disputed. P denotes phosphorylation and A denotes acetylation. Red coloured P or A are inhibitory modifications while blue coloured are activatory modifications. FoxO1 (forkhead box O 1), PKA (protein kinase A), SIK2 (salt-inducible kinase 2), IP3R (Inositol 1,4,5-trisphosphate receptor), CaMKII (Ca^{2+}/calmodulin-dependent protein kinases II), HDAC (histone deacetylase), SIRT1 (sirtuin 1)

mRNA expression. They also had a modest reduction in hepatic glucose production and gluconeogenesis during hyperinsulinaemic-euglycaemic clamp compared to wild-type mice. FoxO1-null mice had a blunted response to a pyruvate tolerance test. Contrary to *in vivo* results, hepatocytes from these mice had a significantly blunted response of gluconeogenic gene expression to cAMP stimulation (Matsumoto et al., 2007). Furthermore, hyperglycaemia associated with insulin receptor- or insulin receptor substrate 1- and 2-null mice was partially rescued by hepatic knock-out of FoxO1 (Dong et al., 2008; Matsumoto et al., 2007).

These studies have highlighted the importance of FoxOs not only in insulin-mediated inhibition of gluconeogenesis (Figure 1.6) but also in fasting-stimulated hepatic gluconeogenic gene expression. The latter effect may be mediated by activation of FoxOs by SIRT1 and more recently by class IIa HDACs and CaMKII during fasting (Figure 1.6) (Daitoku et al., 2004; Frescas, 2005; Mihaylova et al., 2011; Motta et al., 2004; Ozcan et al., 2012) and is discussed in detail below.

1.3.2 Class IIa HDACs

The family of mammalian class II histone deacetylases (HDACs) comprises of two subfamilies based on sequence homology; namely class IIa (HDAC 4, 5, 7 and 9) and class IIb (HDAC 6 and 10) (reviewed in (Mihaylova and Shaw, 2013; Verdin et al., 2003)). This family has very weak intrinsic deacetylase activity and their interaction with HDAC3 is thought to be required for their robust deacetylase activity (Fischle et al., 2002). Class IIa HDACs are regulated by nucleocytoplasmic translocation, where phosphorylation of key residues in the N-terminal domain (Ser246 and Ser467 for HDAC4) leads to their cytoplasmic translocation, 14-3-3 binding and ultimately leads to their inactivation (Yang and Seto, 2007). Class IIa HDACs are phosphorylated on these regulatory residues by multiple upstream kinases such as CaMK, protein kinase D (PKD) and Liver kinase B1 (LKB1)-activated kinases such as SIKs and AMPK). Class IIa HDACs have been implicated in myogenesis, adipocyte differentiation and recently in hormonal-regulation of hepatic gluconeogenesis (Mihaylova and Shaw, 2013).

1.3.2.1 Role of class IIa HDACs in hepatic gluconeogenesis

Class IIa HDACs have been implicated in fasting- and glucagon-mediated gluconeogenesis by deacetylation and activation of FoxOs (Mihaylova et al., 2011). Mihaylova and colleagues noted that glucagon and fasting promoted dephosphorylation (activation) and translocation of class IIa HDACs to the nucleus, where they interacted with HDAC3 on the FoxO1-regulated gluconeogenic gene promoters, which led to deacetylation of FoxO1 (Figure 1.6). Acute knock-down of class IIa HDACs in hepatocytes reduced glucagon-mediated induction of PEPCK and

G6Pase gene expression. This was associated with increased FoxO1 and 3 acetylation and reduced their promoter occupancy on gluconeogenic genes (Figure 1.6) (Mihaylova et al., 2011). Furthermore, shRNAi-mediated acute knock-down of HDACs in the liver reduced hyperglycaemia associated with multiple mouse models of diabetes including high fat diet-induced obese, *ob/ob* and *db/db*. LKB1-actiavted AMPK and SIKs can phosphorylate and inactivate class IIa HDACs in various cell lines (Berdeaux et al., 2007; Takemori et al., 2009; Walkinshaw et al., 2013). In liver-specific LKB1-null mice HDACs phosphorylation and fasting hyperglycaemia were reduced. Interestingly, acute shRNAi-mediated knock-down of HDACs in these mice significantly reduced their fasting glycaemia even further (Mihaylova et al., 2011). Fasting-mediated dephosphorylation and activation of HDAC was thought to be due to inactivation of SIKs during fasting (Mihaylova et al., 2011). However, it is important to note that the authors did not study inhibition of SIKs in the liver and the role of FoxO acetylation in gluconeogenic gene expression has been questioned (see section 1.3.4). Nonetheless, these results propose a role for class IIa HDACs-FoxO in fasting-induced gluconeogenesis.

1.3.3 CaMKII

Ca^{2+}/calmodulin-dependent protein kinase II (CaMKII) is a multifunctional serine/threonine kinase that is encoded by alpha, beta, gamma, and delta genes (reviewed in (Tombes et al., 2003)). It is activated by the Ca^{2+}-calmodulin complex and regulates many cellular processes including learning and memory (Tombes et al., 2003). Fasting and glucagon treatment was noted to activate CaMKII in liver by increasing intracellular Ca^{2+} levels through PKA-mediated phosphorylation and induction of lipid messenger inositol 1,4,5-trisphosphate receptor (IP3R) (Figure 1.11) (Ozcan et al., 2012; Wang et al., 2012). Mice that lack CaMKIIγ had lower fasting blood glucose and gluconeogenesis than wild-type counterparts. Similarly, ectopic expression of catalytically-inactive CaMKII in liver reduced fasting-stimulated gluconeogenic gene expression and blood glucose (Ozcan et al., 2012). These effects were associated with cytoplasmic translocation of FoxO1 and were rescued with expression of constitutively-nuclear

(T24A/S253D/S316A) FoxO1 mutant in liver (Figure 1.11) (Ozcan et al., 2012). Opposite results (on gluconeogenic gene induction and FoxO cellular location) were observed with ectopic expression of a constitutively-active CaMKII mutant in wild-type primary hepatocytes but not in FoxO1-null hepatocytes. Further experiments using CaMKIIγ-null hepatocytes, p38 inhibitor and p38α-null hepatocytes suggested that CaMKII exerted its effect on FoxO1 by phosphorylating it on 11 residues (S284, S295, S326, S467, S475, T24, S246, S253, S413, S415, and T553) directly or indirectly via p38α. These phosphorylation sites were identified by phosphopeptide mapping of recombinant FoxO1 in CaMKIIγ-null hepatocytes. Acute expression of catalytically-dead CaMKII in the liver of leptin-deficient *ob/ob* mice significantly reduced fasting blood glucose and gluconeogenic gene expression, further highlighting its role (Ozcan et al., 2012). Together these data implicate CaMKII, in concert with FoxO proteins, in the regulation of hepatic glucose production.

1.3.4 SIRT1

The mammalian homolog of yeast sir2, SIRT1, is a nicotinamide adenine dinucleotide (NAD^+)-dependent protein deacetylase that is activated following fasting due to a rise in NAD^+ levels (Rodgers et al., 2005). SIRT1 deacetylates multiple transcription factors and coactivators implicated in the regulation of hepatic gluconeogenesis, such as PGC-1α, FoxO1, STAT3, FXR and CRTC2 (reviewed in (Lin and Accili, 2011)). Acute loss and gain of function studies of SIRT1 in liver showed that fasting activated SIRT1 that increased gluconeogenesis. This effect was thought to be mediated by deacetylation and activation of PGC-1α (Figure 1.7) (Rodgers et al., 2005; 2008), deacetylation and inactivation of STAT3 (Nie et al., 2009) and deacetylation and activation of FXR (Kemper et al., 2009). Contrary to these studies, Liu and colleagues noted that SIRT1-mediated CRTC2 deacetylation during prolonged fasting decreased gluconeogenesis in liver (Figure 1.11) (see section1.3.8.1.1) (Liu et al., 2008). The role of SIRT1 was further question by *in vivo* studies with global or liver-specific SIRT1-null mice. Global SIRT1-null mice showed induction of gluconeogenic genes *in vivo* (Motta et al., 2004), while two liver-specific

SIRT1-null mouse strains reported normal regulation of blood glucose and gluconeogenic gene expression (Chen et al., 2008; Purushotham et al., 2009). Controversially a third liver-specific SIRT1-null mouse strain exhibited an increase in gluconeogenic gene expression following fasting and glucagon treatment (Liu et al., 2008). Thus, the importance of SIRT1 in hepatic gluconeogenesis remains unclear. The physiological role of SIRT1-mediated deacetylation of FoxOs is also not clear and contradictory results were observed in multiple studies (Figure 1.6) (reviewed in (Daitoku et al., 2011)). Motta and colleagues showed that deacetylation of FoxOs by SIRT1 represses its transcriptional activity (Motta et al., 2004), while others have shown opposite results using acetylation-deficient or -mimicking FoxO1 mutants (Banks et al., 2008; Daitoku et al., 2004) and SIRT1-activator resveratrol (Frescas, 2005). In addition, acetylation-deficient FoxO1 transgenic mice (K219R, K242R, K245R, K259R, K262R, K271R, and K291R) had unaltered suppression of G6Pase and PEPCK in liver following feeding and unaltered hepatic glucose production when measured using hyperinsulinaemic-euglycaemic clamp (Banks et al., 2011). These results collectively question the role of FoxO1 acetylation in hepatic gluconeogenesis.

1.3.5 PGC-1α

PGC-1 family is a group of multifunctional transcriptional coactivators containing closely related isoforms PGC-1α, PGC-1β and PRC (PGC-1-related coactivator) (Liang and Ward, 2006). PGC-1 interacts with various transcription factors/co-factors such as vitamin D, thyroid hormone, liver X receptor (LXR), estrogen receptors, PPARs, retinoid X receptors, mineralocorticoid and glucocorticoid receptors, as well as multiple histone acetyltransferase (HAT) complexes including CBP/p300 and steroid receptor coactivator-1 (Liang and Ward, 2006; Liu and Lin, 2011). Hence, PGC-1 is known to play an important role in multiple metabolic pathways including mitochondrial biogenesis, oxidative metabolism, thermogenesis, circadian rhythm, heart development, lipogenesis and gluconeogenesis. PGC-1 activity is

modulated by post-translational modifications such as phosphorylation and acetylation (Liang and Ward, 2006; Liu and Lin, 2011).

1.3.5.1 Role of PGC1-α in hepatic gluconeogenesis

Multiple studies have shown that fasting or glucagon treatment induces PGC-1α expression, mediated by the CREB-CRTC2 complex (Herzig et al., 2001; Koo et al., 2005; Yoon et al., 2001). PGC-1α is implicated as an upstream-regulator of gluconeogenic gene transcription (Figure 1.7). ShRNAi-mediated knock-down of PGC-1α in the liver blunted the response of PEPCK and G6Pase gene promoters to hormonal- or nutritional-stimulation and thereby reduced hepatic glucose production (Koo et al., 2004), while overexpression of PGC-1α in liver induced PEPCK and G6Pase expression and hence promoted hepatic gluconeogenesis (Yoon et al., 2001). This action of PGC-1α was thought to be mediated by activation of FoxO1 (Matsumoto et al., 2007), HNF4α (Rhee et al., 2003; Schilling et al., 2006; Yoon et al., 2001) and glucocorticoid receptors (Herzig et al., 2001; Yoon et al., 2001)(Figure 1.7).

Along with its regulation at the transcriptional level by fasting and glucagon, PGC-1α activity is also regulated by acetylation (Figure 1.7). Rodgers and colleagues noted that SIRT1 interacted with PGC-1α and deacetylated it on 13 residues, which in turn led to activation of PGC-1α and increased PEPCK and G6Pase gene expression in rat hepatoma cells (Rodgers et al., 2005). This was confirmed using overexpression of a PGC-1α acetylation-deficient mutant which enhanced expression of gluconeogenic genes in liver compared to wild-type PGC-1α (Rodgers et al., 2005).

PGC-1α has also been implicated in insulin-mediated inhibition of hepatic gluconeogenesis (Li et al., 2007; Rodgers et al., 2010). Insulin-activated Akt directly phosphorylated PGC-1α on Ser570 and this phosphorylation reduced recruitment of PGC-1α to the PEPCK and G6Pase gene promoters, and thus reduced the expression of these genes in the liver (Figure 1.7) (Li et al., 2007). Overexpression of a phosphorylation-defective mutant (S570A) of PGC-1α in liver blocked Akt-mediated gluconeogenic gene suppression. Interestingly, Akt can also indirectly

suppress PGC-1α activity by stabilising Clk (Cdc2-like kinase)-2 which in turn phosphorylates PGC-1α on multiple residues and inhibits its transcriptional activity (Figure 1.7) (Rodgers et al., 2010), but the exact amino acids involved are not known.

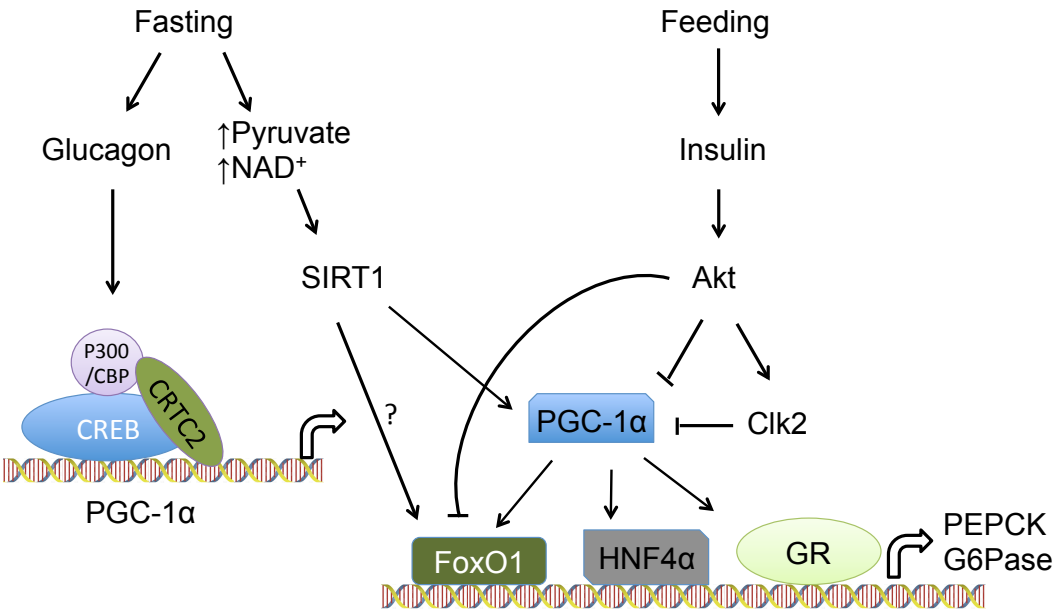

Figure 1.7 Role of PGC-1α in hepatic gluconeogenesis.

PGC-1α gene expression is regulated by CREB-CBP-CRTC2 complex similar to PEPCK and G6Pase such that its expression is induced with fasting and suppressed with feeding. In addition, PGC-1α further enhances PEPCK and G6Pase expression by activating FoxO1, HNF4α and GR. PGC-1α is inhibited directly by Akt- and Clk2-mediated phosphorylation during feeding and activated by deacetylation via SIRT1 during fasting. SIRT1 can also deacetylate FoxO1 and activate its transcriptional activity. However, this notion has been disputed. CREB (cAMP response element-binding protein), CBP (CREB-binding protein), CRTC2 (CREB regulated transcription coactivator 2), PGC-1α (peroxisome proliferator-activated receptor gamma coactivator 1-alpha), HNF4α (hepatocyte nuclear factor 4α), GR (glucocorticoid receptor).

Despite various studies highlighting the significant role of PGC-1α in hepatic gluconeogenesis, two independent strains of PGC-1α-null mice had unexpected phenotypes (Leone et al., 2005; Lin et al., 2004). generated PGC-1α-null mice with normal blood glucose levels during feeding and only a mild reduction in blood glucose after 24-h fasting (Lin et al., 2004). Fasting had no effect on gluconeogenic gene expression and paradoxically refed mice had raised gluconeogenic gene expression in liver relative to controls. The lack of an *in vivo* metabolic phenotype was attributed to compensation by C/EBPβ. These mice were resistant to high fat diet-induced obesity and had lower fasting blood glucose and improved insulin sensitivity following high fat diet compared to controls (Lin et al., 2004). Another group, Leone *et* al.,

generated PGC-1α knock-out mice with no defects in fasting/fed blood glucose, gluconeogenic gene expression or glucose tolerance (Leone et al., 2005). The use of different mouse strains may partly explain this discrepancy and the modest effect of PGC1-α knock-out may be partly due to compensation from PGC-1β (Sonoda et al., 2007). PGC-1α and β combined knock-out is embryonically lethal in mice (Liu and Lin, 2011). Thus liver-specific double-knock-out mice may be needed to clarify the *in vivo* role of PGC-1 in gluconeogenesis.

1.3.6 CREB

CREB (cAMP-response element binding protein) is a well-characterised transcription factor that belongs to basic-leucine-zipper family. CREB is ubiquitously expressed and proposed to regulate more than 100 genes in human cells (reviewed in (Johannessen et al., 2004)). It is involved in multiple cellular processes such as neuronal survival, β-cell growth, circadian rhythm, synaptic plasticity and glucose and lipid metabolism. CREB paralogues ATF-1 (activating transcription factor 1) (Hai et al., 1989) and CREM (cAMP-response element modulator) (Foulkes et al., 1991) are closely related to CREB and regulate gene transcription by forming heterodimers with CREB (reviewed in (De Cesare et al., 1999)). CREB binds to conserved cAMP-response elements (CRE) encompassing the sequence 'TGACGTCA' and regulates basal and cAMP-inducible gene expression (Johannessen et al., 2004). The CRE was first discovered by Goodman and colleagues during an investigation into cAMP induction of the somatostatin gene (Montminy et al., 1986). Subsequently, CREB was discovered as a protein bound to CRE in a pheochromocytoma cell line (Montminy and Bilezikjian, 1987). Thereafter, human (Hoeffler et al., 1988) and rat CREB (Gonzalez et al., 1989) were cloned, and Montminy and colleagues established that cAMP-dependent protein kinase A (PKA) phosphorylated CREB on Ser133 and increased CREB-mediated gene transcription (Gonzalez and Montminy, 1989; Mayr and Montminy, 2001). Ser133 lies within a central kinase inducible domain (KID) that is important for stimulus-dependent transcription (Figure 1.8 A). Either side of the KID, there are glutamine-rich domains Q1 and Q2, also called

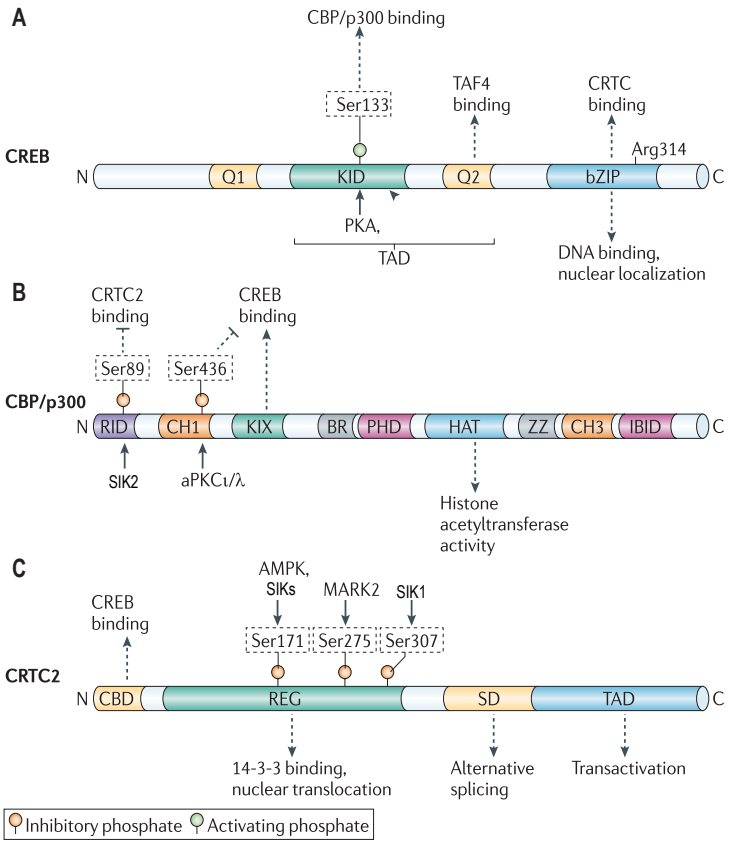

Figure 1.8 Domain structure and important regulatory phosphorylation sites for CREB, CBP/p300 and CRTC2.

Figure is adopted and modified from Altarejos *et* al. (Altarejos and Montminy, 2011) **A)** cAMP-responsive element-binding protein (CREB) contains two Glu-rich domains (Q1 and Q2), a central kinase-inducible domain (KID) and a c-terminal basic Leucine zipper (bZIP) domain. The KID domain and the Q2 domain make up the N-terminal transactivation domain (TAD). The Q2 domain binds to TBP-associated factor 4 (TAF4); phosphorylation of the KID domain at Ser133 promotes an interaction with CREB-binding protein (CBP) and its paralogue p300. Ser133 is phosphorylated by a number of basic directed kinases including protein kinase A (PKA). The bZIP domain promotes CREB DNA binding and dimerization; it also mediates CREB binding to cAMP-regulated transcriptional co-activators (CRTCs). Arg314 in the bZIP domain is critical for the CREB–CRTC interaction. **B)** Domain structure of CBP/p300, showing the nuclear receptor-interaction domain (RID), Cys- and His-rich region 1 (CH1), CREB-binding KIX domain, bromodomain (BR), plant homeodomain (PHD), histone acetyltransferase (HAT) domain, zinc-binding domain (ZZ), CH3 and interferon response factor-binding domain (IBID). Phosphorylation p300 at Ser89 by salt-inducible kinase (SIK) 2 inhibits CRTC2 binding and inhibits its HAT activity. Phosphorylation of CBP, but not p300, by atypical PKCι/λ (aPKCι/λ) at Ser436 within the CH1 region inhibits binding to CREB. **C)** Domain structure of the CRTC family of CREB co-activators, as exemplified by CRTC2. CRTCs contain an N-terminal CREB binding domain (CBD), a central regulatory region (REG), a splicing domain (SD) and a C-terminal TAD. CRTC2 phosphorylation at Ser171 (by AMPK and SIKs), Ser275 (by microtubule affinity-regulating kinase 2 (MARK2)) and Ser307 (by SIK1) promotes 14-3-3 protein binding and the cytoplasmic sequestration of CRTC2.

constitutive activation domains (CAD), which bind to the basal transcriptional machinery (RNA polymerase II, transcription factors TFIID, B, E and TAFII-130, TBP-associated factor 4) (Figure 1.8 A). CREB has a basic-leucine-zipper domain at its C-terminus that mediates DNA binding

and facilitates dimerisation (Figure 1.8 A) (Johannessen et al., 2004; Mayr and Montminy, 2001).

The phosphorylation of Ser133 recruits the coactivator CREB-binding protein (CBP) and its paralogue p300, thereby driving gene expression (Chrivia et al., 1993; Parker et al., 1996) (see section 1.3.7 for detail). There are numerous stimuli and kinases that can phosphorylate CREB on Ser133 such as cAMP-elevating signals (glucagon, forskolin) via PKA, Ca^{2+}-elevating signals via CaMK and stress or growth factor signals via mitogen- and stress-activated protein kinase (MSK) 1/2, and Ribosomal S6 kinase (RSK) 1/2 (Johannessen et al., 2004). CREB is also regulated by phosphorylation on sites other than Ser133 and by various post-translational modifications such as acetylation and glycosylation (Johannessen et al., 2004). Investigations into cell/signal specific CREB-regulated gene expression led to identification of more than 30 transcriptional coactivators or interacting proteins, which themselves have additional regulatory mechanisms. This provides a complex and multi-level regulation of CREB-dependent gene expression in both cell-and context-specific manners (Siu and Jin, 2007).

1.3.6.1 Role of CREB in hepatic gluconeogenesis

Long before the discovery of the CRE and CREB, it was noted that the PEPCK and G6Pase genes were transcriptionally induced in rat liver following cAMP treatment or fasting (Chrapkiewicz et al., 1982; Iynedjian and Hanson, 1977; Lamers et al., 1982) while they were suppressed following feeding or insulin treatment (Granner et al., 1983; Kioussis et al., 1978; Tilghman et al., 1974). Hanson and colleagues suggested a possible cAMP-regulatory region in the PEPCK promoter (Short et al., 1986; Wynshaw-Boris et al., 1984) and the CRE consensus sequence (Montminy et al., 1986) was subsequently identified in both the PEPCK promoter (Bokar et al., 1988; Quinn et al., 1988) and the G6Pase promoter (Lin et al., 1997). Further studies confirmed that CREB binds to the CRE of the PEPCK gene promoter and increases its transcription (Park et al., 1990; Quinn and Granner, 1990). However, it was Granner and Quinn who first proposed a PKA-mediated phosphorylation of CREB as the mechanism for glucagon-regulation of PEPCK gene transcription (Quinn and Granner, 1990).

During fasting, glucagon binds to its specific G protein-coupled receptor (GPCRs) promoting activation of the Gs protein (Figure 1.9) (reviewed in (Authier and Desbuquois, 2008; Ritter and Hall, 2009)). GTP-bound Gsα in turn activates adenylate cyclase resulting in generation of intracellular cAMP from ATP (Figure 1.9).

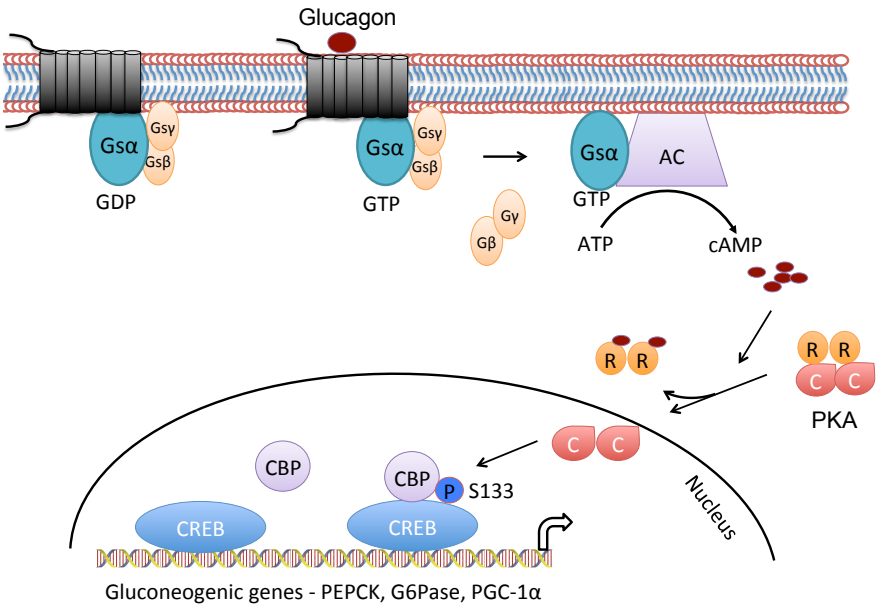

Figure 1.9 Role of CREB in Hepatic gluconeogenesis.

Glucagon binds to its G-coupled receptor and activates Gsα subunit of Gs protein by replacing GDP to GTP causing dissociation of Gsα from Gsβ and Gsγ subunits. GTP-bound Gsα activates adenylate cyclase (AC) leading to a rise in cAMP. cAMP binds to regulatory (R) subunits of PKA and dissociates them from the catalytic (C) subunits. Catalytic subunits diffuse into the nucleus and phosphorylate CREB on Ser133. This promotes recruitment of CBP on gluconeogenic genes promoter and increases their expression. P denotes phosphorylation and blue coloured P is an activatory modification.

This cAMP binds to the regulatory (inhibitory) subunits of PKA in cytosol which causes dissociation of the catalytic subunits of PKA which diffuse into the nucleus and phosphorylate CREB on Ser133 (Figure 1.9) (Krebs, 1989; Taylor et al., 1988). CREB phosphorylation leads to recruitment of CBP/p300 resulting in enhanced gene transcription (Figure 1.9).

In vivo studies have analysed hepatic gluconeogenesis in various transgenic models of disrupted CREB function including $CREB^{-/+}$ heterozygous mice (CREB knock-out is embryonically lethal) and mice expressing a dominant-negative CREB mutant (A-CREB). $CREB^{-/+}$ mice had lower fasting blood glucose, which was rescued by overexpression of PGC-1α but this study lacked a full characterisation of hepatic gluconeogenesis (Herzig et al., 2001). Mice expressing A-CREB in the liver had significant fasting hypoglycaemia and reduced expression of PEPCK and

G6Pase and PGC-1α. Again these defects were rescued with adenovirus-mediated overexpression of PGC-1α in the liver (Herzig et al., 2001). Acute knock-down of CREB in rat with antisense oligonucleotide showed no effect on glucose metabolism in normal chow-diet fed animals (Erion et al., 2009). However, CREB knock-down in a rat model of diabetes reduced fasting blood glucose, PEPCK expression and hepatic steatosis, but these animals had normal hepatic glucose production. The lack of a significant alteration in gluconeogenesis in these rats may be due to incomplete knock-down or the ability of the CREB paralogues ATF1 and CREM to compensate for its loss (Hummler et al., 1994; Rudolph et al., 1998).

Surprisingly, CREB is equally phosphorylated at Ser133 in the liver following fasting/glucagon or insulin/refeeding (He et al., 2009; Koo et al., 2005). In addition, CREB occupancy on the gluconeogenic gene promoters in the liver is not altered following fasting and refeeding (He et al., 2009; Zhou et al., 2004).

Collectively, these studies suggest that CREB is an important transcription factor for basal gluconeogenesis, but question the relative contribution of CREB Ser133 phosphorylation in the hormonal-control of gluconeogenesis. Liver-specific CREB Ser133Ala knock-in mice may be needed to clarify the role of CREB Ser133 phosphorylation in fasting-mediated hepatic gluconeogenesis. These studies also suggest that inducible CREB-dependent gene expression is likely to be mediated by mechanisms in addition to Ser133 phosphorylation. With this in mind, CBP and CRTC2 have been identified as important transcriptional coactivators that regulate CREB-dependent gluconeogenic gene expression by interacting with CREB in a Ser133 phosphorylation-independent manner and this is discussed in the sections below.

1.3.7 CBP

CREB binding protein (CBP) and its paralogue p300 were originally identified as binding proteins of CREB (Chrivia et al., 1993) and adenoviral E1A (Arany et al., 1994) respectively. CBP contains a nuclear receptor-interaction domain (RID), Cys- and His-rich region 1 (CH1), CREB-binding KIX domain, bromodomain (BR), plant homeodomain (PHD), histone acetyltransferase

(HAT) domain, zinc-binding domain (ZZ), CH3 and interferon response factor-binding domain (IBID) (Figure 1.8 B) (Iyer et al., 2004). CBP/p300 act as coactivators provide a bridge between numerous transcription factors (such as CREB) and the basal transcription machinery that includes RNA polymerase II (Kwok et al., 1994; Mueller, 1996; Nakajima et al., 1997). In addition, its endogenous HAT activity opens up the chromatin structure (Bannister and Kouzarides, 1996; Korzus, 1998) and allows it to act as a scaffold interacting with more than 30 proteins involved in transcription of the target gene (reviewed in (Chan and La Thangue, 2001)). CBP/p300 function is not only associated with the regulation of glucose metabolism but also cell cycle regulation, cell growth and cancer (reviewed in (Iyer et al., 2004)). Thus, this protein may provide some link between growth and metabolism and it is perhaps not surprising that CBP/p300 knock-out in mice is embryonically lethal (Yao et al., 1998).

1.3.7.1 Role of CBP/p300 in hepatic gluconeogenesis

Early studies proposed that Ser133 phosphorylation of CREB promoted binding to CBP/p300 through the KIX domain on CBP/p300 and this was the principle mechanism for cAMP-mediated induction of gene transcription (Figure 1.10) (Gonzalez et al., 1989; Gonzalez and Montminy, 1989).

However, transgenic mice expressing a CBP/p300 with a mutated KIX domain (CREB non-binding) exhibited normal blood glucose levels and hepatic gluconeogenic gene expression in response to fasting and feeding (Kasper et al., 2002; Koo et al., 2005). In support of this finding, a global microarray analysis of cAMP-induced gene transcription found only a modest reduction (20-30%) in cAMP responsiveness of CBP/p300 KIX mutant mouse embryonic fibroblasts (MEF) and in the same cells CBP recruitment to cAMP-responsive gene promoters was only partially reduced (Xu et al., 2007). Therefore, CBP recruitment to DNA in response to cAMP is clearly not solely dependent on CREB Ser133 phosphorylation. Indeed, CBP interacts with CREB phosphorylated on sites other than Ser133, and the CREB-CBP interaction is also regulated by post-translational modifications of CBP itself, including phosphorylation and acetylation (Goodman and Smolik, 2000; Lonze and Ginty, 2002).

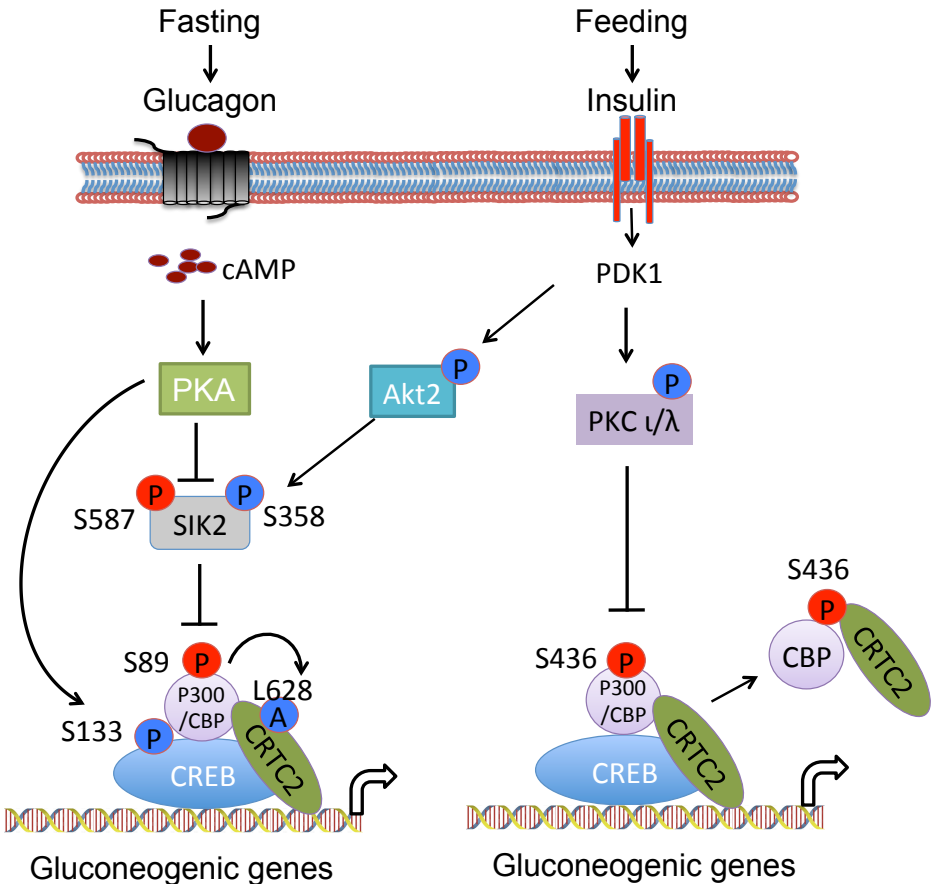

Figure 1.10 Role of CBP in hepatic gluconeogenesis.

Feeding and insulin activate Akt2 and PKCι/λ via PDK1 (phosphoinositide dependent protein kinase-1). PKCι/λ further phosphorylates S436 on CBP causing dissociation of CBP-CRTC2 complex from CREB and repression of gluconeogenesis. Akt2 phosphorylates on Ser358 and activates SIK2 thereby increasing Ser89 phosphorylation on p300. This causes a reduction in its acetylase activity towards CRTC2 making it available for proteasomal degradation and thus causes suppression of gluconeogenic gene expression. In contrast, fasting inhibits SIK2 by PKA-mediated phosphorylation on Ser587. This causes a reduction in p 300 phosphorylation and activation of its acetylatase activity towards CRTC2. Acetylated CRTC2 is resistant to proteasomal degradation, is retained in nucleus and subsequently increases gluconeogenic gene expression. P denotes phosphorylation and A denotes acetylation. Red coloured P or A are inhibitory modifications while blue coloured are activatory modifications.

For example, short term fasting (6-h) reduced Ser89 phosphorylation of p300, which in turn increased its HAT activity and interaction towards the transcriptional coactivator CRTC2 (Figure 1.10) (Liu et al., 2008). It was proposed that inhibition of SIK activity following glucagon stimulation of cells was responsible for the reduction in Ser89 phosphorylation of p300. Acetylated CRTC2 (on Lys628) was resistant to proteasomal degradation and increased hepatic gluconeogenic gene expression. Acute knock-down of CBP in mouse liver using adenovirus-mediated delivery of shRNAi reduced fasting blood glucose as well as PEPCK, G6Pase and PGC-

1α gene expression, highlighting a requirement for CBP in proper control of hepatic gluconeogenesis (Liu et al., 2008).

CBP is also implicated in the response of gluconeogenesis to feeding and insulin. Feeding/insulin promoted phosphorylation and activation of PKCι/λ downstream of PI3K and PDK1 (Figure 1.10) (He et al., 2009). PKCι/λ phosphorylated CBP on Ser436 which correlated with dissociation of CBP from the PEPCK/G6Pase gene promoters as well as disruption of the CREB-CBP complex and suppression of hepatic gluconeogenesis (Figure 1.10). In addition, transgenic mice that express a S436A mutant (PKCι/λ resistant CBP) were insulin resistant, had higher fasting glucose, higher hepatic glucose production and increased hepatic PEPCK and PGC-1α expression (He et al., 2009). In contrast, liver specific PKCι/λ knock-out mice had normal fasting glucose and the response of PEPCK and G6Pase mRNA to hormones was normal (Matsumoto et al., 2003). It was argued that the normal hepatic glucose metabolism in these mice was due to a compensatory improvement in insulin sensitivity secondary to a reduction in hepatic triglycerides (He et al., 2009; Matsumoto et al., 2003).

CBP/p300 can acetylate the transcription factors forkhead box O (FoxO) and farnesoid X receptor (FXR), both of which have been implicated in glucose homeostasis control. Acetylation of FoxOs (mainly FoxO1, FoxO4) by CBP/p300 reduces their transcriptional activity. Although the exact mechanism is not yet known, it is proposed that acetylation reduces DNA binding or enhances inhibitory phosphorylation of FoxOs (Kemper et al., 2009; Perrot and Rechler, 2005; Qiang et al., 2010; 2008). However, the contribution and direct role of CBP/p300-mediated acetylation of FoxOs and FXR in hepatic gluconeogenesis has not been studied.

These studies collectively suggest that CBP/p300 contributes to hormonal-regulation of hepatic gluconeogenesis but potentially involves multiple protein complexes including CREB-CBP, SIK2-CBP-CRTC2 and Akt-PKC-CBP (Figure 1.10). However, the relative importance and fine details of each of these signalling pathways remains to be clarified.

1.3.8 CRTC2

Earlier studies showed that cAMP-mediated transcription was mainly regulated via CREB Ser133 phosphorylation. However, this mechanism did not explain the diversity and cell-specific/stimulus-specific control of CREB-dependent gene transcription and led to a search for additional coactivators that could modulate CREB activity independent of Ser133 phosphorylation. Genome-wide studies with CRE-reporter assays by two independent groups identified CRTCs as mediators of cAMP- and calcium-signalling-regulated CREB activity, independent of CREB Ser133 phosphorylation (Bittinger et al., 2004; Conkright et al., 2003; Iourgenko et al., 2003; Screaton et al., 2004).

There are three closely related isoforms of CRTC, namely 1, 2, and 3. CRTCs are basally phosphorylated, bound to 14-3-3 proteins and sequestered in the cytoplasm. Upon stimulation of cells with cAMP and calcium, CRTCs dephosphorylate, translocate to the nucleus and bind to the bZIP domain of CREB (Bittinger et al., 2004; Conkright et al., 2003; Screaton et al., 2004). This leads to an increase in recruitment of TAFII130 and CBP to the CRE of the target gene promoter and an increase in CREB-dependent transcription, independent of Ser133 phosphorylation (Conkright et al., 2003; Ravnskjaer et al., 2007). CRTCs have been implicated in neuronal survival (Sasaki et al., 2011), steroidogenesis (Takemori et al., 2007), β-cell function (Eberhard et al., 2013) and recently in innate immunity (Clark et al., 2012).

CRTC2 is the most extensively studied isoform that is implicated in hepatic gluconeogenesis and contains an N-terminal CREB-binding domain (CBD), a central regulatory (REG) domain, a splicing domain (SD) and a C-terminal transactivation domain (TAD) (Figure 1.8 C) (Altarejos and Montminy, 2011).

1.3.8.1 Role of CRTC2 in hepatic gluconeogenesis

1.3.8.1.1 Fasting- and glucagon-mediated regulation

Short-term fasting or treatment of hepatocytes with glucagon promoted CRTC2 dephosphorylation (particularly at Ser171) (Figure 1.11), translocation to the nucleus and

induction of the transcription of PEPCK, G6Pase and PGC-1α (Figure 1.11) (Herzig et al., 2001; Koo et al., 2005). Adenovirus-mediated ectopic expression of wild-type CRTC2 in the liver increased hepatic gluconeogenic gene expression and blood glucose, while shRNAi-mediated knock-down of CRTC2 in the liver had opposite (Koo et al., 2005). CRTC2 dephosphorylation on Ser171 was critical to this effect and this residue is phosphorylated by SIKs which are in turn inhibited by PKA (Koo et al., 2005; Screaton et al., 2004). This provided a proposed pathway from glucagon, through cAMP-PKA to SIK inhibition, CRTC2 dephosphorylation and induction of PEPCK and G6Pase gene transcription. In support of this, adenovirus-mediated SIK1 and SIK2 overexpression in liver reduced blood glucose and gluconeogenic gene expression, while shRNAi-mediated knock-down of SIK1 and SIK2 in liver had the opposite effects (Ahmed et al., 2010; Koo et al., 2005; Wang et al., 2012). Furthermore, a S171A CRTC2 mutant was constitutively nuclear, rescued the repressive effects of SIK1 or 2 overexpression on the gluconeogenic genes and enhanced basal- and forskolin- mediated stimulation of gluconeogenic gene expression in primary hepatocytes and liver (Dentin et al., 2007; Koo et al., 2005). This suggested that phosphorylation of Ser171 played a central role in the control of CRTC2 activity.

Recently, a SIK-independent mechanism of dephosphorylation of CRTC2 in liver during fasting has been suggested. Glucagon-activated protein phosphatase 2B/calcineurin caused dephosphorylation of CRTC2 in the liver following an increase in intracellular Ca^{2+} in an inositol 1,4,5-trisphosphate receptor (IP3R)-dependent manner (Wang et al., 2012). Wang and colleagues employed a calcineurin inhibitor (cyclosporine A), transient overexpression and shRNAi-mediated knock-down of calcineurin in liver and primary hepatocytes and showed that calcineurin bound and dephosphorylated CRTC2 on Ser171 and Ser275 sites following glucagon/fasting with a subsequent increase in gluconeogenic gene expression. In support of these findings, a CRTC2 S171A/S275A double-mutant had enhanced CRE-reporter activity, which was resistant to inhibition by cyclosporine A, whereas a CRTC2-calcineurin non-binding

mutant (CRTC2 T619G, Δ259-258) had reduced CRE-reporter activity following glucagon treatment in primary hepatocytes (Figure 1.11) (Wang et al., 2012).

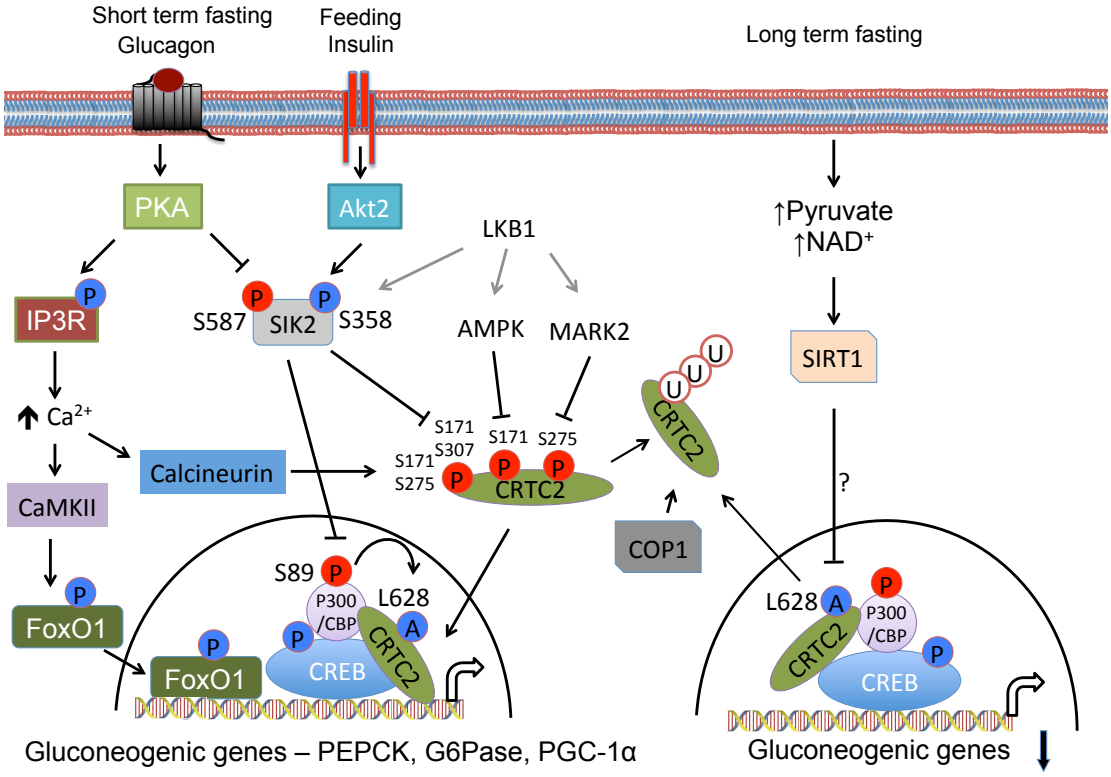

Figure 1.11 Role of CRTC2 in hepatic gluconeogenesis.

Short-tem fasting and glucagon activate PKA that in turn phosphorylates and activates IP3R and inhibits SIK2 by Ser587 phosphorylation. Inhibition of SIK2 leads to increased acetylation, dephosphorylation and nuclear translocation of CRTC2, which subsequently increases gluconeogenesis by forming complex with CREB and CBP. Glucagon also increases intracellular calcium in IP3R-dependent manner and activates calcineurin. Activated calcineurin dephosphorylates CRTC2 and promotes its nuclear translocation. Elevated calcium also activates CaMKII that in turn phosphorylates and activates FoxO1, further increasing gluconeogenic gene expression. In contrast, feeding- and insulin-activated Akt2 activates SIK2 by Ser358 phosphorylation. This leads to an increase in CRTC2 phosphorylation, nuclear export and subsequent proteasomal degradation with COP1 E3 ubiquitin ligase. Similarly, long term fasting-activated SIRT1 deacetylates CRTC2 and promotes its degradation and reduction in gluconeogenic gene expression. Long term fasting-mediated degradation of CRTC2 has been disputed. LKB1-activated kinases, AMPK and MARK2 phosphorylate CRTC2 on indicated residues. U, P and A denote ubiquitylation, phosphorylation and acetylation respectively. Red coloured P or A are inhibitory modifications while blue coloured are activatory modifications.

As mentioned earlier in section 1.3.7.1, acetylation of CRTC2 on Lys628 by CBP/p300 prevented its proteasomal degradation and prolonged CRTC2 activity while overexpression of a K628R CRTC2 (an acetylation-deficient mutant) decreased blood glucose levels (Liu et al., 2008). During prolonged fasting (24-h) CRTC2 was deacetylated by SIRT1 (Figure 1.11). The subsequent degradation of CRTC2 in the liver led to a paradoxical suppression of

gluconeogenesis (Liu et al., 2008). However, LeLay and colleagues did not observe CRTC2 degradation in the liver after 24-h fast in mice (Le Lay et al., 2009) and hence the role of SIRT1 in hepatic gluconeogenesis remains controversial (see section 1.3.4), and prolonged fasting-mediated regulation of CRTC2 needs further confirmation.

Strikingly, CRTC2 acetylation was also regulated by SIK2-mediated phosphorylation of CBP/p300 (Ser89 on p300). A reduction in Ser89 phosphorylation following fasting/glucagon was proposed to be caused by SIK2 inhibition following phosphorylation by PKA on Ser587 and was associated with increased CRTC2 acetylation (Figure 1.11) (Liu et al., 2008).

Thus, SIKs act on two of the key transcriptional co-activators, CRTC2 and CBP/p300, to co-ordinate cAMP-regulation of gluconeogenic gene transcription.

1.3.8.1.2 Feeding- and insulin-mediated regulation

Dentin and colleagues proposed that insulin-activated Akt2 promoted phosphorylation of SIK2 at Ser358 (see below section 1.5.5.4), which in turn increased CRTC2 phosphorylation on Ser171 and caused its nuclear exclusion (Figure 1.11) (Dentin et al., 2007). Phosphorylated cytoplasmic CRTC2 was shown to be ubiquitylated on Lys628 by the E3 ubiquitin ligase COP1 (constitutive photomorphogenesis protein 1), promoting its degradation and leading to suppression of gluconeogenic gene expression (Figure 1.11) (Dentin et al., 2007).

In support of this model, ectopic expression of a S171A CRTC2 mutant in the liver led to stabilisation of CRTC2, rise in both fasting and fed blood glucose along with unsuppressed gluconeogenic gene expression and lack of degradation of CRTC2. Similarly, shRNAi-mediated knock-down of SIK2 or COP1 in liver, prevented CRTC2 degradation during refeeding and increased gluconeogenic gene expression (Dentin et al., 2007).

In addition, SIK2 activation following phosphorylation by Akt2 also increased the phosphorylation of p300 by SIK2 at Ser89 leading to reduced acetylation of Lys628 of CRTC2 (Liu et al., 2008). Deacetylated CRTC2 was subsequently ubiquitylated and targeted for COP1-mediated degradation.

These findings provide two mechanisms possibly linking Akt2-mediated activation of SIK2 to the inhibition of CRTC2-CBP/p300 and the suppression of hepatic gluconeogenesis. However, it is important to note that Akt2-mediated phosphorylation of SIK2 was only studied using recombinant protein in HEK293 cells and also lacked confirmation with a phospho-specific antibody (see section 1.5.5.4 for detail)

1.3.8.1.3 CRTC2 knock-out mice

CRTC2 has been investigated *in vivo* by two independent studies using different strains of CRTC2 knock-out mice (Le Lay et al., 2009; Wang et al., 2011). LeLay and colleagues observed that mice lacking CRTC2 (exon 4-11 deletion) had normal fasting blood glucose, a normal glucose response to pyruvate challenge and only a slightly blunted gluconeogenic gene transcription response to 24-h fast (Le Lay et al., 2009). Similarly, hepatic glucose production was normal before and during a hyperinsulinaemic-hypoglycaemic clamp and the lack of CRTC2 had no effect on whole body insulin sensitivity (Le Lay et al., 2009). In contrast, primary hepatocytes isolated from these mice had a minor reduction in glucose production and gluconeogenic gene expression in response to glucagon treatment.

Contradictory to the above findings, a different strain of CRTC2 knock-out mice (exon 1 deletion) showed reduced fasting blood glucose and gluconeogenic gene expression along with a blunted response to a pyruvate tolerance test (Wang et al., 2010). Furthermore, these mice were insulin sensitive on normal chow diet and were protected against high-fat diet-induced hyperglycaemia and insulin resistance. Wang and colleagues proposed that the targeting vector used to disrupt the CRTC2 gene by Le lay *et* al. could have generated an in-frame polypeptide with comparable activity to wild-type CRTC2 and may explain the lack of phenotype. The difference in the results could be due to the difference in genetic strategy used to delete CRTC2 and/or the different mouse strains employed, but the striking contrast in the data does question the role of CRTC2 in the regulation of hepatic gluconeogenesis.

Along with these, a recent report on intraperitoneal administration of anti-sense oligonucleotide- (twice a week for 4 weeks) mediated acute knock-down of CRTC2 in rats showed reduced hepatic glucose production, fasting glucose and G6Pase mRNA expression, only in the streptozotocin induced type 1 diabetes model but not in a type 2 diabetes rat model (Erion et al., 2013). The lack of difference was not due to the efficiency of knock-down as both models had 90% reduction in CRTC2 mRNA expression in the liver. However, the authors claimed that the higher level of glucagon in the CRTC2 knock-down type 2 diabetes rat led to compensation and lack of effect on hepatic glucose production.

The confounding effects of *in vivo* compensation on CRTC2 deletion/knock-down must also be considered, especially the potential for redundancy between the CRTC isoforms due to the following observations that, 1) overexpression of CRTC1 in primary hepatocytes augmented forskolin-promoted glucose production similar to CRTC2 (Koo et al., 2005), 2) All the isoforms shared similar modes of regulation by cAMP and calcium signalling (Bittinger et al., 2004; Conkright et al., 2003; Iourgenko et al., 2003; Takemori et al., 2007) and were able to increase steroidogenesis with equal efficiency in cultured cells (Takemori et al., 2007), 3) SIKs can also phosphorylate CRTC1 and 3 with equal efficiency as CRTC2 (Katoh et al., 2006) and 4) the only reason that CRTC2 has been extensively studied in the liver is because it is claimed to be the most abundant isoform in the liver (Koo et al., 2005).

1.3.8.1.4 CRTC2 phosphorylation

While studying the role of CRTC2 in cAMP and calcium signalling, Screaton and colleagues noticed that CRTC2 was localised to the cytoplasm under basal condition and translocated to the nucleus following forskolin treatment of ATYB1 fibroblast cells (Screaton et al., 2004). Interestingly, the authors noticed that under basal condition, cytoplasmic CRTC2 was phosphorylated (slower migrating band on western blotting) and nuclear CRTC2 was dephosphorylated (faster migrating CRTC2 band), whereas forskolin and KCl treatment led to dephosphorylation (increase in faster migrating CRTC2 band) and nuclear translocalisation of CRTC2. These findings led authors to investigate the role of CRTC2 phosphorylation in its

cellular localisation (Screaton et al., 2004). Mass spectrometry analysis of immunoprecipitated recombinant CRTC2 from unstimulated HEK293 cells identified 12 putative phosphorylated serine residues on CRTC2 (Screaton et al., 2004). Further analysis of ^{32}P-labeled CRTC2 in mouse insulinoma cells using 2-dimensional tryptic mapping identified five hot-spots, where the fifth spot corresponded to Ser171. This fifth spot accounted for more than half of ^{32}P-incorporation in basal cells, which was significantly reduced following forskolin treatment (Screaton et al., 2004). These led the authors to propose that Ser171 was the major phosphorylation site of CRTC2 in HEK293 and mouse insulinoma cells (Figure 1.11). A S171A CRTC2 mutant was constitutively nuclear in location in ATYB1 fibroblast cells and had reduced but not abolished 14-3-3 binding. It also promoted higher CRE-reporter activity than wild-type CRTC2 in HEK293 cells and mouse insulinoma cells following forskolin and KCl treatment, respectively. Therefore, Ser171 was proposed as the principle regulatory site for CRTC2. Further investigation in HEK293 cells revealed that Ser171 was phosphorylated by SIK2 and dephosphorylated in response to forskolin treatment (Screaton et al., 2004). However, the lack of analysis on CRTC2 phosphorylation following cAMP stimulation and the significant residual 14-3-3 binding of the S171A mutant raised the possibility of regulatory roles for additional phosphorylation sites.

Site-directed mutagenesis analysis to identify additional 14-3-3 binding sites revealed Ser275 as a potential regulatory phosphorylation site on CRTC2 in mouse insulinoma cells. (Figure 1.11) (Jansson et al., 2008). A S275A mutant of CRTC2 had reduced 14-3-3 binding and enhanced CRE-activity when overexpressed in these cells. Interestingly, the double mutant (S171A, S275A) showed significantly higher CRE-activity than the single point mutants and 14-3-3 binding was completely abolished in mouse insulinoma cells. *In vitro* kinase assay screening using 180 human protein kinases (purified from reverse transfected HEK239T cells) identified MARK2 (Microtubule affinity-regulating kinase 2), an AMPK-related kinase, as the kinase that phosphorylated Ser275 (Figure 1.11) (Jansson et al., 2008). Authors further conducted *in vitro* kinase assays with CRTC2 WT (267-283) and S275A mutant peptide with recombinant MARK2

from HEK293 cells to support their conclusion. However, this study lacked validation of MARK2 in intact cells using gain and loss of function experiments. Experiments using a phospho-specific antibody against endogenous Ser275 CRTC2 showed that high glucose (20 mM) treatment of β-cells (Jansson et al., 2008) and glucagon stimulation of primary hepatocytes caused dephosphorylation of Ser275 CRTC2 (Wang et al., 2012), thus validating phosphorylation of this site in intact cells. Dephosphorylation of Ser171 and Ser275 following glucagon stimulation of primary hepatocytes appeared to require the phosphatase calcineurin (discussed above in section 1.3.8.1.1) (Figure 1.11) (Wang et al., 2012).

Interestingly, Uebi *et* al. noticed that the S171A/S275A CRTC2 double mutant, similar to wild-type CRTC2, continued to translocate to cytoplasm following SIK1 overexpression in COS7 cells, suggesting additional SIK1-regulated phosphorylation sites on CRTC2 (Uebi et al., 2010). This led the authors to perform site-directed mutagenesis analysis near the nuclear-export signal of CRTC2 (276-286) and identify Ser307 as a SIK1-regulated phosphorylation site (Figure 1.11). The phosphorylation of this site was confirmed with a phospho-specific antibody and SIK1 loss and gain of function studies in COS7 cells and liver (Uebi et al., 2010). A S307G mutant of CRTC2 demonstrated similar properties of enhanced forskolin-stimulated CRE-reporter activity in COS7 cells and nuclear localisation in liver to those of the S171A and S275A following forskolin treatment. The phosphorylation of Ser307 was shown to reduce following fasting and forskolin treatment in the liver and COS7 cells respectively (Uebi et al., 2010).

In addition, mass spectrometry analysis of CRTC2 following *in vitro* incubation with SIK1 or SIK3 demonstrated that CRTC2 became phosphorylated on Ser171, Ser70 and Ser348 (Al-Hakim et al., 2005).

CRTC2 is also phosphorylated by AMPK (AMP-activated protein kinase) *in vitro* and also in intact cells on Ser171, the same residue that is regulated by SIKs (Figure 1.11) (Foretz et al., 2010; Koo et al., 2005). In addition, treatment of primary hepatocytes with the AMPK activator, AICAR (5-amino-1-β-D-ribofuranosyl-imidazole-4-carboxamide) inhibited glucagon-induction of gluconeogenic gene transcription (Koo et al., 2005). However, AICAR-mediated

inhibition of gluconeogenic gene transcription and hepatic glucose production were not altered in the primary hepatocytes lacking AMPKα1/α2 (Foretz et al., 2010), suggesting that the effect of AICAR on gluconeogenesis did not require AMPK. To support this, a structurally and mechanistically distinct activator of AMPK (A-769662) had no effect on Bt_2-cAMP stimulated gluconeogenic gene expression and hepatic glucose production and the mice lacking any AMPK in the liver had normal fasting and fed blood glucose (Foretz et al., 2010). The primary hepatocytes from these mice showed unaltered cAMP-mediated gluconeogenic gene expression and hepatic glucose production compared to the wild-type hepatocytes. These data query the contribution of endogenous AMPK to the regulation of gluconeogenesis.

Collectively, these studies question the claim that Ser171 is the only regulatory site on CRTC2 that influences the control of hepatic gluconeogenesis and highlight the need for a more unbiased proteomics approach to identify basal- and glucagon/fasting-regulated phosphorylation sites on hepatic CRTC2.

As discussed above, AMPK and MARK2 along with SIKs phosphorylate CRTC2 while both AMPK and SIKs phosphorylate Class IIa HDACs (see section 1.3.2). These kinases belongs to a subfamily called 'AMPK-related kinases' and share some biochemical properties such as activation by conserved T-loop phosphorylation by the LKB1-STRD-MO25 complex (Figure 1.12) (Lizcano et al., 2004). There was dephosphorylation and nuclear localisation of CRTC2 and HDACs in the liver of LKB1-null mice as well as fasting hyperglycaemia with increased PEPCK, G6Pase and PGC-1α gene expression (Mihaylova et al., 2011; Shaw, 2005). ShRNAi-mediated knock-down of CRTC2 (Shaw, 2005) or HDACs (Mihaylova et al., 2011) in the liver partially rescued this hyperglycemia and reduced gluconeogenic gene expression. However, the relative contribution AMPK, MARK2 and SIKs to this phenotype is not known. Nonetheless, these highlight the importance of AMPK-related kinases in hepatic gluconeogenesis and are discussed below (Figure 1.12).

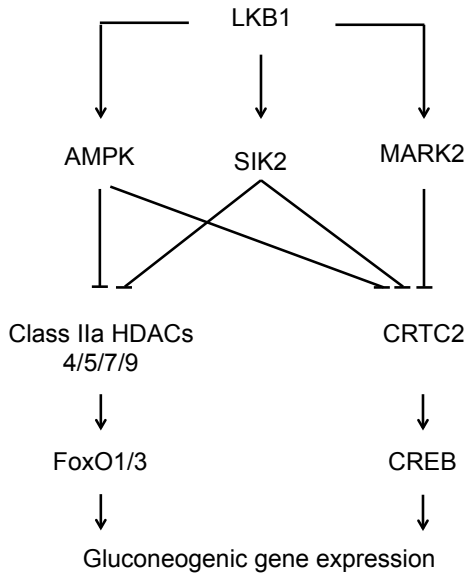

Figure 1.12 Proposed role of LKB1-activated kinases in hepatic gluconeogenesis.

LKB1-STRAD-MO25 complex activates AMPK, SIK2 and MARK2 by T-loop phosphorylation on conserved Thr residue (Thr 172 for AMPK). AMPK and MARK2 along with SIKs phosphorylate CRTC2 while both AMPK and SIKs phosphorylate Class IIa HDACs and thus can influence hepatic gluconeogenesis by inhibition of HDAC-FoxO- or CRTC2-CREB-mediated gluconeogenic gene expression of PEPCK, G6Pase and PGC-1α.

In summary, the hormonal-regulation of hepatic gluconeogenesis involves multiple signal transduction pathways and is dominated by pathways involving CREB-CBP-CRTC and FoxO as described above. Interestingly, both insulin and glucagon are proposed to mediate their effect on these pathways by modulating activity of SIK2, suggesting that SIK2 may be central to the co-ordination of hormonal-regulation of hepatic gluconeogenesis (Figure 1.15). SIK2 is proposed as the predominant isoform of SIKs and thought to regulate this gluconeogenic gene expression through phosphorylation of CRTC2, CBP and class IIa HDACs (Figure 1.15). SIK2 belongs to a family called 'AMPK-related kinases' and these are discussed below.

1.4 AMPK-related kinases

1.4.1 Classification of the AMPK-related kinases

AMP-activated protein kinase (AMPK) is a highly conserved protein kinase that plays a key role in energy homeostasis in all eukaryotes. It is a heterotrimeric protein complex comprising of a catalytic-α subunit and two regulatory (-β and -γ) subunits (Stapleton et al., 1996; 1997). AMPK is activated in response to metabolic stresses that increase intracellular ADP/ATP (Oakhill et

al., 2011; Xiao et al., 2011) and AMP/ATP ratios (Hardie et al., 1998; Salt et al., 1998; Winder and Hardie, 1999). These include exercise, hypoxia, hypoglycemia and oxidative stress. Activated AMPK switches off anabolic processes such as protein, fatty acid and cholesterol synthesis and lipolysis to reduce ATP consumption and activates catabolic processes such as fatty acid oxidation and glycolysis to generate ATP (reviewed in (Carling et al., 2012; Hardie et al., 2012)).

In silico analysis of the human kinome (500 enzymes) found a group of protein kinases with significant sequence similarities to the kinase domain of AMPKα1/α2, and these were thus termed 'AMPK-related kinases' (Manning et al., 2002). There are 20 AMPK-related kinases which can be subdivided into 'close relatives' of which there are twelve [BRSK (brain-specific kinases) 1 and 2, NUAK {sucrose-non-fermenting kinase-1 (SNF1)-like kinases} 1 and 2, MARK (microtubule-affinity-regulating kinase) 1, 2, 3 and 4, SIK (Salt-inducible kinase) 1, 2, and 3, MELK (maternal embryonic leucine-zipper kinase)] and 'distant relatives' include the other eight kinases [SNRK (sucrose non-fermenting related kinase), NIM1, TSSK (testis-specific serine kinase) 1, 2, 3 and 4, SSTK (testis-specific serine kinase 6), and HUNK (hormonally up-regulated neu-associated kinase)] (Figure 1.13) (Manning et al., 2002).

Interestingly, AMPKα1/α2 (Hawley et al., 2003; Woods et al., 2003) and twelve of the AMPK-related kinases (BRSK1 and 2, NUAK1 and 2, MARK1, 2, 3 and 4, SIK1, 2, and 3 and SNRK) (Jaleel et al., 2005; Lizcano et al., 2004) are phosphorylated by the Liver kinase B 1 (LKB1) - Ste20-related adaptor protein (STRAD) -mouse protein 25 (MO25) complex on the conserved Thr in the T-loop, which increases their kinase activity (Figure 1.13). Studies in cell-free assays and experiments with LKB1 knock-out mouse embryonic fibroblast (MEF) cells and HeLa cells (which lack LKB1) confirmed the T-loop phosphorylation by this complex (Al-Hakim et al., 2005; Jaleel et al., 2005; Lizcano et al., 2004). Twelve of the 14 AMPK-related kinases with Lys at -2 relative to the T-loop Thr are phosphorylated by LKB1, except MELK and NIM1. AMPK-related kinases that lack Lys at -2 position are not phosphorylated by LKB1 (Figure 1.13). MELK, NIM1

and TSSK1, 2, 3 and 4 autophosphorylate on this residue and have significant kinase activity independent of the LKB1 complex (Jaleel et al., 2005; Lizcano et al., 2004).

There is no evidence to date that AMPK-related kinases are regulated by other AMPK upstream kinases such as CaMKKβ (Bright et al., 2008) and TAK1 {transforming growth factor β (TGFβ)-activated kinase 1)}. However, some AMPK-related kinases including MARK, BRSK, NUAK and SIK isoforms are regulated by additional post-translational events such as phosphorylation and ubiquitylation (reviewed in(Bright et al., 2009)).

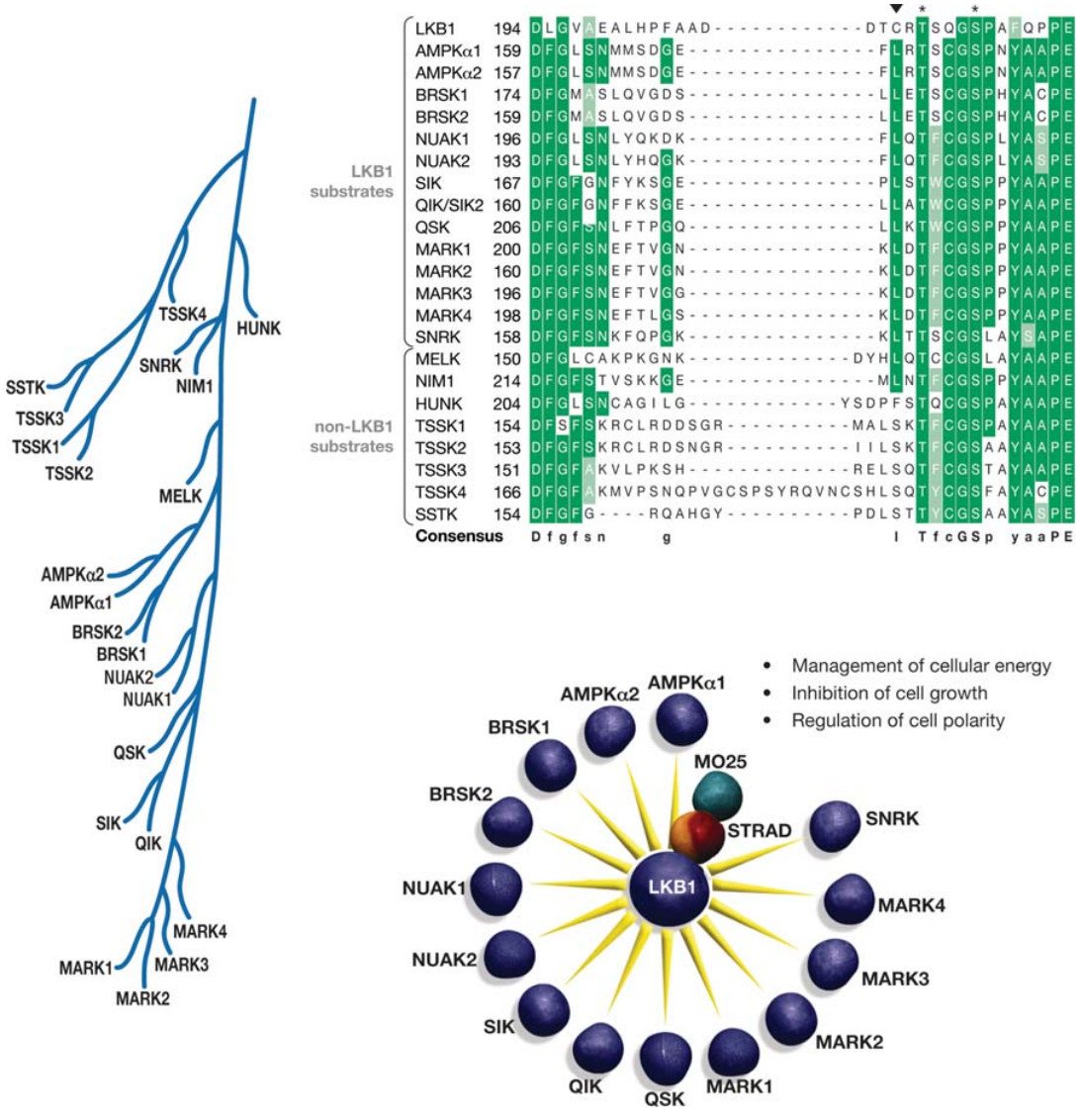

Figure 1.13 AMPK-related kinases

Figure is adapted from Alessi *et* al. (Alessi et al., 2006) AMPK and AMPK-related kinases are shown in a branch of the human kinome dendrogram (left panel) (Manning et al., 2002). Sequence alignment of the activation-loop of all AMPK-related kinases, AMPK and LKB1 is shown (top right). Identical residues are shaded dark green and residues that are conserved in more than 50% sequences are shaded light green. LKB1-regulated Thr and Ser are highlighted using (*). Lys (downward arrow) required for LKB1-mediated

phosphorylation is highlighted (Shaw et al., 2004). Diagram shows AMPK-related kinases that are regulated by LKB1-STRAD-MO25 complex (bottom right).

Out of these 14 LKB1-dependent kinases (Figure 1.13), only AMPKα1 and AMPKα2 are activated under low cellular-energy conditions (i.e. ADP/ATP and/or AMP/ATP ratio increases) or treatment with a cell-permeable AMP-mimetic compound, 5-amino-1-β-D-ribofuranosyl-imidazole-4-carboxamide (AICAR) or phenformin/metformin (Carling et al., 2012; Hardie et al., 2012; Lizcano et al., 2004). This is possibly due to the fact that only AMPKα1/α2 interacts with the regulatory AMPKγ subunit which contains the adenine nucleotide-binding Bateman domains (Carling et al., 2012). However, two other family members, SIK2 (see section 1.5.5.1.2) and NUAK2 are reported to be activated under low-energy conditions, albeit by an unknown mechanism(s). AICAR treatment and glucose deprivation activated NUAK2 in neonatal rat keratinocytes and liver hepatoma cells (Lefebvre et al., 2001; Suzuki et al., 2003), while another study failed to observe similar activation of NUAK2 after AICAR treatment of mouse embryonic fibroblast (Lizcano et al., 2004). Interestingly exercise, another AMPK-activating stimuli, activated NUAK2 in skeletal muscle (Koh et al., 2010).

Little is known regarding the stimuli that direct LKB1 towards any of these AMPK-related kinases. Currently, most widely received model is that LKB1 is constitutively-active and therefore its dependent kinases (except AMPK) are also constitutively phosphorylated (conserved Thr residue in the T-loop) and active in intact cells. It can be also noted that LKB1 is phosphorylated by multiple kinases at different sites, which do not affect its intrinsic activity in cell-free assay, but may indirectly alter *de novo* activity towards its substrates by changes in cellular localisation and/or binding to activating subunits, STRAD-MO25 (Alessi et al., 2006; Xie et al., 2006).

AMPK-related kinases play a role in multiple biological processes including cell proliferations, cell polarity, cancer and metabolism (reviewed in (Bright et al., 2009)). Particularly SIKs have been implicated in regulation of hepatic gluconeogenesis and their biological role and regulation is discussed in the following sections.

1.5 Salt-inducible kinases

1.5.1 Discovery of salt-inducible kinase (SIK)

In 1994, Ruiz and colleagues performed a screening study in an attempt to identify novel protein kinases that may be involved in cell-fate specification in mammalian embryo (Ruiz et al., 1994). They used PCR primers designed to amplify either serine/threonine or tyrosine kinases expressed in embryonic mouse heart and identified 20 putative kinases, of which two (coded as HRT-9 and HRT-20) were predicted to be new. Sequence analysis of the PCR product (termed HRT-20) revealed that it represented a putative serine/threonine kinase most similar to the sucrose non-fermenting kinase (SNF1), yeast homologue of mammalian AMPK, and was therefore termed "myocardial SNF-like kinase" (msk) (Ruiz et al., 1994). A partial cDNA clone was subsequently isolated from an embryonic cDNA library, which contained the entire kinase domain as well as flanking sequences. The authors described that "the entire msk cDNA sequence appears to encode a single open reading frame, however, the msk sequence outside the kinase domain shares no significant homology to SNF1 sequences". However, they did not include complete sequence data in their manuscript (they subsequently deposited the full sequence of msk to NCBI database [NM_010831.2] in October 1999). Ruiz *et* al. observed msk mRNA expression in myocardial cells and their progenitors in the developing heart, but they did not observe msk expression till morphological evidence of heart formation. Thus they concluded that msk does not appear to play a role in myocardial cell-fate specification and may be involved in signalling pathway(s) required for the differentiation of these cells (Ruiz et al., 1994). The msk was subsequebtly indentifeid as SIK.

1.5.2 Identification of SIK1 as a rapidly inducible gene

During the period of 1999-2000, three groups identified SIK as a rapidly inducible gene in response to various manipulations in different cell/tissue types (Feldman et al., 2000; Wang et al., 1999; Xia et al., 2000). Wang and colleagues sought to identify factors that regulate function of

adrenal cortex in response to changes in plasma Na^+/K^+ balance and screened genes that were uniquely induced in rat adrenal gland in response to diet containing 8% NaCl or K^+-loaded water (150 mM KCl) with low Na^+ diet (0.3% NaCl) for 7 days (Wang et al., 1999). A novel cDNA clone, termed salt-inducible kinase (SIK, subsequently termed SIK1 upon identification of SIK2 and SIK3), encoding a polypeptide (776 amino acids) with significant similarity to the SNF1/AMPK family was isolated from adrenal gland of animals fed with Na^+- or K^+-enriched diet (Wang et al., 1999). They also found that adrenocorticotropic hormone (ACTH), a known stimulator of steroidogenesis in adrenal cortex, rapidly (within 30 min) stimulated SIK1 mRNA expression in Y1 mouse adrenocortical cells and also in adrenal glands of ACTH-administered rats following one day treatment (Wang et al., 1999).

Feldman and colleagues were looking for genes in neuronal cells that were preferentially induced by membrane depolarisation, a key cellular event that is known to modulate neuronal plasticity (Feldman et al., 2000). Using PC12 “neuron-like” rat pheochromocytoma cells, they identified a gene product that was induced by KCl, forskolin or calcium ionophore (A23187), but not by neurotrophins or growth factors (i.e. nerve growth factor and epidermal growth factor) and hence provisionally termed it KID-2 (kinase induced by depolarisation-2) (Feldman et al., 2000). However, while their manuscript was under preparation, they realised that an identical cDNA named “SIK” had already been published by Wang *et* al. In addition, they observed using *in situ* hybridisation that SIK mRNA expression was strongly induced in specific regions of the hippocampus and cortex following seizure-induction by systemic kainic acid treatment in rats (Feldman et al., 2000).

Xia and colleagues were studying the genes that were differentially expressed in chicken-embryo fibroblasts transformed by Qin (the forkhead/winged helix transcription factor), the avian homolog of the mammalian forkhead box protein G1 (an essential gene for murine brain development) (Xia et al., 2000). One of the up-regulated Qin targets identified in this analysis was a protein kinase termed QIK (Qin-induced kinase) that displayed high homology to SIK1 cloned by Wang and colleagues. Although this finding raised a hypothesis that QIK might be

involved in transformation, overexpression of QIK in chicken-embryo fibroblasts resulted in only a marginal increase in proliferation (Xia et al., 2000).

It can be noted that all three studies described above confirmed that recombinant SIK1 protein displayed kinase activity in cell-free assays (Feldman et al., 2000; Wang et al., 1999; Xia et al., 2000).

1.5.3 Identification of SIK2 and SIK3

Identification of SIK (SIK1) prompted a search for its closely-related genes in human and mouse genomic sequence databases, which led to identification of SIK2 (Horike, 2003) and SIK3 (Katoh et al., 2004). The SIK1 gene is located on human chromosome 21, whereas both SIK2 and SIK3 genes are localised on chromosome 11 (Horike, 2003). Analysis of primary sequence revealed that all three SIK isoforms share highly homologous N-terminal kinase domain, but their C-terminal regions are less conserved and differ in length (Figure 1.14). Human SIK1 is 783 amino acids long (Uniprot: P57059), whereas SIK2 and SIK3 are 926 (Uniprot: Q9H0K1) and 1263 (Uniprot: Q9Y2K2), respectively. QIK, an avian homologue of SIK, is a 798 amino acid protein. Sequence alignment using the LALIGN software (http://www.ch.embnet.org/software/LALIGN_form.html) revealed that QIK has similarity to SIK1 (64.4%), SIK2 (41.0%) and SIK3 (23.9%). As originally proposed (Ruiz et al., 1994; Xia et al., 2000), QIK appears to be more close to SIK1 than SIK2 at least when judged by the comparison of overall primary sequences. Although SIK3 is described as “QSK” (Lizcano et al., 2004; Manning et al., 2002), I have not been able to trace the origin of this name. SIK is evolutionarily conserved; D. *melanogaster* and C. *elegans* each have SIK homologues, termed dSIK and Kin-29, respectively (Choi et al., 2011; Lanjuin and Sengupta, 2002; Okamoto et al., 2004; Wang et al., 2008).

1.5.4 Expression/tissue distribution of SIK isoforms

SIK1 tissue expression pattern was assessed using a Northen blot analysis of total RNA from rat (Feldman et al., 2000; Lin et al., 2001) and mouse tissue panels (Horike, 2003). They

demonstrated that SIK1 mRNA was ubiquitously expressed and most abundantly present in adrenal glands, ovary, lung, brain, testis and moderately expressed in other tissues including skeletal muscle, heart, liver and adipose. Feldman and colleagues also measured SIK1 mRNA levels in several regions of rat brain and found that they were highly expressed in the cortex, hippocampus and pituitary, and to a lesser extent in the brain stem but not in the cerebellum (Feldman et al., 2000). Recently, SIK1 and SIK2 mRNA expression analysis in various regions of mouse brain using quantitative RT-PCR showed that both SIK1 and SIK2 mRNA were abundantly expressed in cortex (2-3-fold higher than those expressed in adrenal gland) and also in other regions of the brain including cerebellum (Sasaki et al., 2011).

Northern blot (Horike, 2003) and quantitative RT-PCR analysis (Du et al., 2008) of SIK2 mRNA expression in mouse tissues showed that it was most abundantly expressed in both white and brown adipose tissues, and at lower levels in testis, lung, brain, spleen and liver. Du and colleagues also analysed SIK2 protein expression in mouse tissues, which showed a similar pattern to mRNA expression. Authors also analysed SIK2 mRNA expression in human tissues using quantitative RT-PCR, which further confirmed that it was highly expressed in adipose tissue and at lower levels in brain, muscle, testis, kidney and liver (Du et al., 2008). Although one study described that “SIK3 mRNA seemed ubiquitous”, the data was not presented in the manuscript (Katoh et al., 2004). To my knowledge, there is no study so far that has globally assessed tissue-distribution of SIKs and their relative protein expression (in a quantitative way).

1.5.5 Domain structure and regulation of SIK

The SIKs are monomeric and contain an N-terminal kinase domain and a ubiquitin-associated (UBA) domain that lies immediately C-terminal to the kinase domain (Figure 1.14) (Manning et al., 2002).

1.5.5.1 Role of catalytic domain in SIK regulation

1.5.5.1.1 Regulation by LKB1

SIKs share a high homology with AMPK and AMPK-related kinases in their activation-loop (T-loop) of the kinase domain (see section 1.4.1). Hence, Lizcano and colleagues hypothesised that AMPK-related kinases possibly share similar upstream regulation as AMPK. Experiments in cell-free assays, LKB1 knock-out MEF cells and HeLa cells (which lack LKB1) confirmed that similar to AMPK, SIKs were also phosphorylated on the conserved Thr residue in the T-loop by the LKB1-STRAD-MO25 complex (Thr182 for SIK1, Thr175 for SIK2 and Thr221 for SIK3) and that this phosphorylation significantly increased the intrinsic kinase activity of (Lizcano et al., 2004).

Interestingly, LKB1-mediated T-loop phosphorylation of SIK1 and SIK3 was reported to bind 14-3-3, an adaptor to phospho-proteins, and affected their kinase activity and subcellular localisation (Al-Hakim et al., 2005). The *in vitro* kinase activity of SIK1 and SIK3 was significantly reduced when 14-3-3 binding was competed out using excess phosphorylated T-loop peptide and this reduction in kinase activity was rescued with wild-type 14-3-3ζ but not by a 14-3-3ζ [E180K] mutant (unable to interact with phosphopeptides) (Al-Hakim et al., 2005). The authors also studied the effect of 14-3-3 binding on cellular localisation of SIK1 and SIK3 using ectopically expressed GFP-tagged wild-type and T-loop phosphorylation-deficient mutants (T182A, T221A), lacking 14-3-3 binding, in HeLa cells. Wild-type SIK1 was predominantly localised in the nucleus of HeLa cells and at lower levels in the cytoplasm, whereas the T175A SIK1 mutant was completely localised to cytoplasm. Using a similar experimental strategy, 14-3-3 binding was suggested to localise SIK3 to distinctive punctate structures within the cytoplasm of HeLa cells (Al-Hakim et al., 2005). However, a recent report showed that SIK3 had a diffuse cytoplasmic location in HEK293 cells, rather than punctate as previously reported (Berggreen et al., 2012).

While only a trace amount of SIK activity was detected in LKB1-deficient MEF or HeLa cells (Lizcano et al., 2004), LKB1-null mouse skeletal muscle showed significant levels of SIK3 activity

(20-40%) (Al-Hakim et al., 2005; Jeppesen et al., 2013). It is so far unknown whether CaMKKs (alternative up-stream kinase of AMPK) contribute to SIK regulation *in vitro* and *in vivo*. In 3T3-L1 adipocytes, Ca^{2+} ionophore or STO-609 (CaMKK inhibitor) were unable to stimulate or inhibit SIK2, respectively (Gormand et al., 2011; Henriksson et al., 2012). It would be interesting to measure SIK activity in various tissues from CaMKKα/β-null mice and also in response to Ca^{2+}-raising stimuli in various cell systems and determine if CaMKKs contribute to SIK regulation and also to explore if there is/are additional/alternative kinase(s) that can phosphorylate/activate SIK under certain conditions. Currently, how SIKs are switched off at post-translational levels (e.g. through dephosphorylation by phosphatases) is largely unknown.

1.5.5.1.2 Regulation by other AMPK-activating stimuli

Interestingly, SIK2 was also reported to be activated by AMPK-activating stimuli such as AICAR treatment and low-energy conditions such as glucose/serum deprivation of 3T3-L1 adipocytes by unknown mechanism(s) (Du et al., 2008). Although, another study was unable to observe activation of SIK2 using AICAR under similar experimental conditions (Henriksson et al., 2012). AMPK-activating stimuli such as exercise, failed to activate SIK2 and SIK3 in rat skeletal muscle (Sakamoto, 2004), and phenformin failed to activate SIK1, 2 and 3 in HeLa cells and MEF cells (Lizcano et al., 2004).

These studies collectively suggest the need to carefully examine SIK-regulation in various cell types with multiple energy stress stimuli and to identify their mode of activation, direct or indirect. For example, indirect activation via energy stress-regulated enzymes or direct activation through sensing changes in adenine nucleotide levels by nucleotide-binding subunit(s) like AMPKγ. It should also be carefully evaluated if the observed activation of SIK2 in response to energy stress and AICAR was an artifact and derived from contamination of other kinases (e.g. AMPK), given that there is no specific substrate of these kinases for *in vitro* assay and AMPK and SIKs share similar phosphorylation consensus (see below). One idea would be to use AMPK catalytic activity deficient cells (e.g. AMPK-null or AMPKα dominant-negative expressing cells) and measure activity of AMPK-related kinases in response to energy stress.

A) SIK1

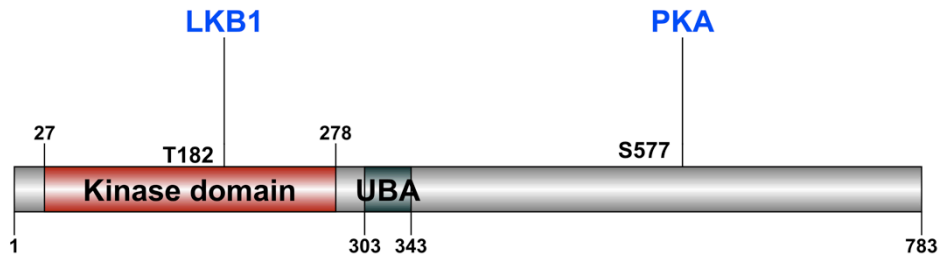

B) SIK2

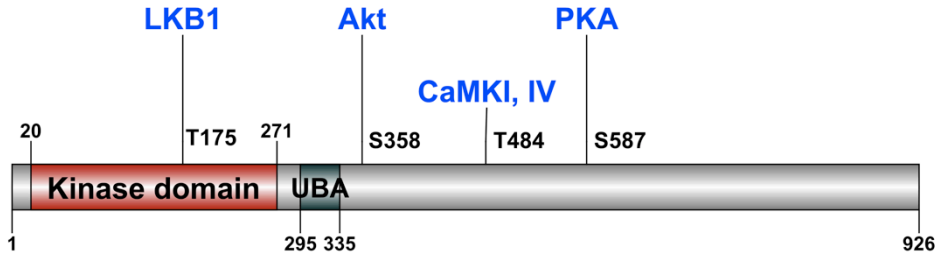

C) SIK3

Figure 1.14 Domain structure and important regulatory phosphorylation sites of human SIKs.

Domain structure of SIK1 (A), SIK2 (B) and SIK3 (C) showing the kinase domain (red) and the ubiquitin-associated (UBA) domain (green). Domain information is from www.uniprot.org. Important regulatory sites along with proposed upstream kinases are shown for all three isoforms.

1.5.5.2 Role of ubiquitin-associated domain in SIK regulation

Sequence analysis identified 10 members of AMPK-related kinases, including all three SIK isoforms, that possess a ubiquitin-associated (UBA) domain immediately C-terminal to their kinase domain (Figure 1.14) (Manning et al., 2002). A series of biochemical analyses by Jaleel *et* al. suggested that the UBA domain plays a unique role in allowing AMPK-related kinases to be phosphorylated and activated by LKB1 (Jaleel et al., 2005). The UBA domain was originally identified by sequence analysis as a domain present in several proteins thought to be involved in the ubiquitin-proteasome pathway, which interacts with ubiquitin or polyubiquitin chains

(Dikic et al., 2009). Jaleel and colleagues were not able to observe detectable interaction between the full-length AMPK-related proteins or their isolated UBA domains and different mono-/poly-ubiquitin species or the ubiquitin-like proteins *in vitro* and in intact cells (Jaleel et al., 2005). Thus they next looked at the role of the UBA domain in controlling the activity of AMPK-related kinases. Interestingly, mutation of most of the conserved residues in the UBA domain of SIK1 and SIK2, including the surface glycine residue, markedly reduced kinase activity and T-loop phosphorylation (Thr182 and Thr175 of human SIK1 and SIK2, respectively) when mutants were ectopically expressed in HEK293 cells (that endogenously express LKB1). Fragments of SIK1 that contained the kinase domain but lacked the UBA domain were nearly devoid of T-loop phosphorylation and activity. They further investigated how mutations in the UBA domains of SIK1 (and also MARK2), expressed as non-phosphorylated forms in E. coli, affected phosphorylation and activation by LKB1 in cell-free assay (Jaleel et al., 2005). When the UBA-domain-conserved glycine residue of these kinases was replaced with alanine, the mutants were barely phosphorylated or activated on treatment with LKB1. Likewise, fragments of SIK1 lacking the UBA domain were not significantly phosphorylated/activated by LKB1. In addition, the authors provide evidence that the UBA domain of SIK1 is required for its punctate nuclear localisation in HEK293 cells (Jaleel et al., 2005).

1.5.5.3 Regulation by Ser577 SIK1 or Ser587 SIK2 phosphorylation

Early studies revealed that SIK1 cellular localisation was modified in response to ACTH or PKA-activators. SIK1 was predominantly localised in the nucleus of non-stimulated Y1 adrenocortical tumour cells and ACTH treatment of these cells caused translocation of SIK1 to the cytoplasm (Katoh et al., 2002; Takemori, 2002). This translocalisation was not seen in PKA signalling-defective kin-7 cells and was rescued by expression of PKA catalytic subunit indicating the involvement of PKA signalling in this process (Takemori, 2002). To verify this notion, various SIK1 mutants harbouring a point mutation in their putative PKA phosphorylation sites (T268A, T475A and S577A) [(R/K) (R/K) X (S/T)] were expressed in Y1 cells. Only the S577A mutant induced a loss of SIK1 nuclear export after ACTH treatment

suggesting that Ser577 phosphorylation by PKA was involved in SIK1 nuclear exportation (Takemori, 2002).

SIK2 was also noted to contain a PKA-dependent phosphorylatable Ser587, a SIK2 equivalent for Ser577 of SIK1 (Horike, 2003). GFP-tagged S587A SIK2 mutant showed increased localisation to the nucleus of non-stimulated 3T3-L1 adipocytes compared to wild-type SIK2 (Horike, 2003). Phosphorylation of this site on SIK1 and SIK2 was later confirmed in various cells including primary hepatocytes following forskolin or cAMP-agonist treatment (Horike, 2003; Katoh et al., 2006; Ravnskjaer et al., 2007; Screaton et al., 2004).

Apart from their influence on cellular localisation, SIK1 S577A mutant was noted to have a significantly greater repressive effect on CRE-reporter activity and CREB-dependent gene expression compared to their wild-type counterpart following ACTH, forskolin or PKA stimulation in Y1 adrenocortical tumour cells and forskolin stimulation of 3T3-L1 cells (Horike, 2003; Katoh et al., 2004; Takemori, 2002; Takemori et al., 2003). Similar results were also observed for the S587A SIK2 mutant in HEK293 cells, 3T3-L1 and T37i brown adipocytes following forskolin stimulation (Horike, 2003; Muraoka et al., 2009; Screaton et al., 2004).

In addition, ectopic expression of the S577A mutant prevented forskolin-mediated CRTC2 nuclear translocation in Y1 adrenocortical tumour and HeLa cells (Katoh et al., 2004; 2006) and S587A SIK2 mutant prevented nuclear translocation of CRTC2 after forskolin treatment of ATYB1 fibroblast cells (Screaton et al., 2004).

Although this PKA-mediated phosphorylation was described in some papers as inhibitory whereas non-phosphorylatable mutants (SIK1 S577A, SIK2 S587A) were constitutively-active, these functions are based on their ability to alter their putative target gene regulation. There is a lack of evidence that SIK phosphorylation of this site alters intrinsic kinase activity when measured after its immunoprecipitation and *in vitro* kinase assays, suggesting that changes in localisation (e.g. subcellular sequestration from substrates) may play some regulatory role.

These studies collectively generated a hypothesis that cAMP activation of PKA promotes phosphorylation of SIK1 and SIK2 on a conserved residue (S577 and S587 respectively), which

causes cytoplasmic translocation of SIK1 and SIK2. These results in repression of SIK1- and SIK2- mediated CRTC2 or CBP/p300 phosphorylation in the nucleus, and thus activation of CRTC2 and CBP/p300. These subsequently lead to increase in CREB-CBP/p300-CRTC2-mediated gene expression.

But this model has not been validated by compelling observations. Firstly wild-type SIK2, which stays in cytoplasm after PKA activation, was also able to inhibit CRE-genes reporter activity to a level similar to wild-type SIK1 (Horike, 2003; Katoh et al., 2004; Screaton et al., 2004). Secondly, chimeric SIK2 (containing the nuclear localisation signal (RK-rich region) of SIK1 predominantly localised to the nucleus, showed suppression of CRE-reporter activity following PKA expression to a similar level as seen in predominantly cytoplasmic wild-type SIK2 (Katoh et al., 2004). Finally, chimeric SIK1 (containing the nuclear export sequence of the HIV-1 rev protein) found predominantly in the cytoplasm, was still able to repress CRE-reporter activity following PKA expression to a level similar to that of the S587A SIK1 (nuclear localised mutant) (Katoh et al., 2004). Therefore, these findings question the importance of nuclear localisation in SIK's capacity to repress CRE-mediated gene expression.

In addition, kinase activity assessment of SIKs following cAMP-elevating agents is not well studied. Some studies have assessed SIK1 kinase activity following ACTH, forskolin or cAMP-agonist treatment of Y1 cells using an *in vitro* kinase assay against a generic substrate GST-Syntide2 as well as SIK1 autophosphorylation (Doi et al., 2002; Katoh et al., 2006; Lin et al., 2001; Takemori, 2002). These studies did not find any significant change in SIK1 kinase activity after these treatments. However, all the studies were conducted with recombinant proteins and lacked in-depth analysis using SIK-specific substrates. In addition, assessment of kinase activity following cAMP-PKA signalling has not been thoroughly assessed for the other SIK isoforms.

SIK1 nuclear shuttling, described in earlier studies, has been observed in different models such as 3T3-L1 cells over-expressing GFP-SIK1 and treated with differentiation mix (Horike, 2003) or HEK293 and HeLa cells over-expressing GFP-SIK1 and treated with forskolin (Al-Hakim et al., 2005; Henriksson et al., 2012; Katoh et al., 2006). In contrast, GFP-SIK2 was predominantly localised to the cytoplasm in un-stimulated cells and remained in cytoplasm of 3T3-L1 adipocytes following treatment with differentiation mix (Horike, 2003), treatment with ACTH in Y1 cells (Katoh et al., 2004) or forskolin in HEK293 cells (Henriksson et al., 2012). To understand the differences between both isoforms, Katoh and collaborator expressed truncated and chimeric forms of SIK1 and SIK2 in Y1 cells treated with or without ACTH. They found that SIK1 possesses an RK-rich region (586-612) that was responsible for its transport across nuclear membrane. However, they also observed that this region was non-functional in SIK2 explaining the difference in behaviour between both isoforms (Katoh et al., 2004).

These studies collectively suggest that molecular regulation of SIKs following cAMP-elevating agents is not clear and requires further research. In addition, there is a lack of evidence of SIK2 regulation in liver by cAMP-PKA signalling-activators, fasting and glucagon.

1.5.5.4 Regulation by Ser358 phosphorylation

While investigating the role of feeding and insulin on CRTC2 in liver, Dentin and colleagues noted that refeeding following overnight fasting in mice and insulin stimulation following forskolin treatment of primary hepatocytes, increased CRTC2 phosphorylation (Dentin et al., 2007). This promoted them to hypothesise that insulin activates SIK2, a known CRTC2 kinase, by Akt-mediated phosphorylation. They noticed that SIK2 contained a single conserved Akt phosphorylation site (RQRRPS) based on their bioinformatic analysis at Ser358 and showed that Akt2 phosphorylated wild-type SIK2 but not the S358A mutant in cell-free assay (Dentin et al., 2007). Further analysis using a generic Akt substrate phospho-motif antibody (raised against a peptide containg the sequence R-X-R-X-X pS/T, X, any amino acids) showed that phosphorylation of recombinant wild-type but not a S358A mutant of SIK2 was observed in HEK293 cells treated with insulin. Interestingly, immunoprecipitated wild-type SIK2, but not

the S358A mutant, had increased autophosphorylation and phosphorylation of recombinant CRTC2 on Ser171 when isolated from HEK293 cells following insulin treatment (Dentin et al., 2007). Similar results of enhanced autophosphorylation of SIK2 following insulin treatment of HEK293 were observed following ^{32}P-labeling of the cells. These results collectively led authors to suggest that Akt2-mediated Ser358 phosphorylation of SIK2 increased its kinase activity towards CRTC2. However, Ser358 phosphorylation was not confirmed directly with Ser358 phospho-specific (site-specific) antibody or by mass spectrometry and authors did not validate these findings in liver/hepatocytes using endogenous SIK2 (Dentin et al., 2007). It is important to note that Ser358 is not conserved in SIK1 and SIK3, therefore this proposed regulation should be SIK2 isoform-specific.

1.5.5.5 Other modes of regulation

Recently, it has been reported that oxygen-glucose deprivation (to mimic ischemic insult *in vivo*) induced the degradation of SIK2 protein concomitantly with dephosphorylation of CRTC1, leading to activation of CREB and its downstream gene targets (Sasaki et al., 2011). The authors proposed that oxygen-glucose deprivation triggers an increase in intracellular Ca^{2+} levels resulting in phosphorylation of SIK2 on Thr484 through CaMKI/IV, leading to SIK2 protein degradation, which subsequently promotes CRTC1 dephosphorylation.

However, the equivalent site on SIK1 (Thr475) was reported to be phosphorylated by PKA in a cell-free assay and was thought to play a role in the stability of SIK1 protein in muscle cells (discussed later in section 1.5.9.2) (Stewart et al., 2013). In addition, monensin (a sodium ionophore) treatment, to mimic intracellular sodium load, of opossum kidney cells was reported to increase SIK1 kinase activity towards phosphatase methylesterase-1 (PME-1) following CaMKI-mediated phosphorylation on Thr322 SIK1, which subsequently led to an increase in Na^+/K^+ ATPase activity (Sjöström et al., 2007). However, this phosphorylation was only shown in cell-free assays and lacked confirmation with a phospho-specific antibody in intact cells (discussed later in section 1.5.9.5). Finally, recombinant SIK2 was acetylated on

Lys53 in HEK293 cells that ectopically expressed CBP. This modification was proposed to reduce SIK2 kinase activity (discussed later in section 1.5.9.8) (Yang et al., 2013).

1.5.5.6 Regulation of SIK expression

In an early study Lin *et* al. demonstrated that ACTH rapidly and transiently stimulates SIK1 mRNA expression in Y1 mouse adrenocortical tumour cells (Lin et al., 2001). To explore the mechanism by which ACTH-dependent increase in SIK1 is regulated, they first examined the effect of actinomycin D, an mRNA synthesis inhibitor, or cycloheximide, a protein synthesis inhibitor, on the expression of SIK1 mRNA in these cells. They observed that actinomycin D completely abolished, whereas cycloheximide enhanced, the ACTH-dependent transcription of the SIK1, and therefore concluded that prior protein biosynthesis is not necessary for the induction of SIK1 transcription (Lin et al., 2001). ACTH activates adenylate cyclase through binding to its specific G-coupled-receptor resulting in the production of cAMP, which stimulates PKA. To demonstrate if cAMP-PKA signalling pathway is responsible for the induction of SIK1 by ACTH, Lin *et* al. used two different PKA activators, forskolin (an activator of adenylate cyclase) and 8-bromo-cAMP (a cell permeable cAMP analogue) on SIK1 expression. Both activators induced SIK1 mRNA expression in Y1 cells, but not in kin-7 cells (a mutant Y1 cell line with defect in cAMP-dependent PKA activity). When PKA signalling was reconstituted via over-expression of PKA catalytic subunit, SIK1 mRNA was induced without ACTH treatment (Lin et al., 2001). These results suggest that PKA signalling is necessary for SIK1 gene transcription at least in mouse adrenocortical tumour cells.

Several lines of evidence report causal effect of enhanced cAMP-PKA signalling in promoting SIK1 expression in various cell systems. These include PC12 pheochromocytoma cells treated with forskolin (Feldman et al., 2000), hepatocytes treated with glucagon (Koo et al., 2005), C2C12 muscle cells treated with forskolin (Berdeaux et al., 2007) and primary pinealocytes {(main constituents of the parenchyme of the pineal gland (pineal body, epiphysis cerebri)} treated with norepinephrine or pineal gland during dark (Kanyo et al., 2009).

Some mechanistic understanding of PKA-mediated increase in SIK1 expression comes from the study by Koo *et* al. They identified two cAMP-responsive element (CRE) motifs present in the SIK1 promoter region (Koo et al., 2005) that show CREB-binding and enhanced recruitment of CRTC2, following forskolin stimulation.

CREB-CRTC2 involvement was further confirmed by the fact that the induction of SIK1 expression in response to forskolin was blocked in primary hepatocytes expressing a dominant-negative CREB mutant and increased by ectopic expression of CRTC2. These results suggest that PKA controls SIK1 expression via an activation of CREB-CRTC2 transcriptional activity (Koo et al., 2005).

So far SIK1 seems to be the only isoform whose expression is induced by PKA activation. This notion is supported by the fact that SIK1, but not SIK2 or SIK3 expression was increased in liver from overnight fasted mice (Koo et al., 2005) or in HeLa cells overexpressing LKB1 treated with forskolin (Katoh et al., 2006). Whether it is due to the absence of a CRE motif in the SIK2 and SIK3 gene promoters is unknown. It has been reported that SIK1 induction rapidly occurs, but is transient upon intracellular cAMP accumulation. This might be due to the consequence of a negative feedback loop as SIK1 inhibits CREB through phosphorylation and nuclear exclusion of CRTC cofactors.

Beside PKA activators, other stimuli/interventions have been shown to induce SIK expression, including membrane depolarisation with KCl in PC12 neuronal cells (Feldman et al., 2000). Since membrane depolarisation/KCl in particular cell types is known to increase intracellular Ca^{2+} levels, it is tempting to speculate that Ca^{2+}-dependent kinases (e.g. CaMK or CaMKK) or -phosphatases (e.g. calcineurin) are involved in the control of SIKs and/or CREB via CRTCs. SIK1 expression can also increase in brain after ischemia (Cheng et al., 2010), cocaine treatment (Dietrich et al., 2012) or in cortical neurons treated with brain-derived neurotrophic factor (BDNF) (Finsterwald et al., 2013). SIK1 expression was also increased in HaCaT (immortal human keratinocyte) cells treated with TGF-β1 (Kowanetz et al., 2008) in a manner dependent on Smad proteins (Lönn et al., 2012).

SIK2 protein content and activity was higher in white adipose tissues from *db/db* mice (Horike, 2003). SIK2 protein content was also increased in liver of *ob/ob* and high-fat diet fed mice but its kinase activity was low (Bricambert et al., 2010). Moreover, SIK2 expression was induced during 3T3-L1 fibroblast differentiation to pre-adipocytes, mainly by dexamethasone present in the differentiation medium (Horike, 2003). In contrast, its expression was reduced in cortical neuron after oxygen-glucose deprivation (Sasaki et al., 2011). SIK3 expression was induced in liver of mice fed with a diet containing high-fat, high-sucrose and also high-cholesterol (Uebi et al., 2012).

1.5.6 Substrate specificity and downstream targets

Table 1-2 SIKs substrates and their phosphorylation sites and proposed function

Kinase responsible (Evidence in literature)	**Substrate and phosphorylation sites**	**Identification method**	***In vitro* kinase assay**	***In vitro* validation with (S/T-A) mutant**	**Cell/*in vivo* validation**	**Proposed Function**
SIK1 and 2 (Dentin et al., 2007; Katoh et al., 2006; Koo et al., 2005; Screaton et al., 2004)	CRTCs Ser171 for CRTC2	Mass spectrometry	Yes	Yes	Yes	Gluconeogenesis
SIK1 (Uebi et al., 2010)	CRTC2 Ser307	Site-directed mutagenesis	Yes	Yes	Yes	Gluconeogenesis
SIKs (Berdeaux et al., 2007; Mihaylova et al., 2011; Walkinshaw et al., 2013)	Class IIa HDACs S246, S467 for HDAC4	Consensus motif for SIKs	Yes	Yes	Yes	Myogenesis, skeletogenesis, neuronal survival
SIK2 (Bricambert et al., 2010; Liu et al., 2008)	p300 S89	Consensus motif for SIKs	Yes	Yes	Yes	Gluconeogenesis, lipogenesis
SIK1 (Yoon et al., 2009)	SREBP-1c S265/S266/S329	Consensus motif for SIKs	Yes	Yes	No	Lipogenesis
SIK1 (Ahmed et al., 2010)	c-Nap1 S2392	Mass spectrometry	Yes	No	No	Cell cycle regulation, Cancer

SIK1 (Sjöström et al., 2007)	PME-1 No sites known	-	Yes	No	No	Na^+/K^+-ATPase activity
SIK1 (Cheng et al., 2009)	p53 S15	Previously identified AMPK site	Yes	Yes		Metastasis, Cancer
SIK1 (Yoshida and Goedert, 2012)	Tau T212, S214, S262 and S356	Screening with phospho-specific antibodies	Yes	Yes		?

Early studies demonstrated that isolated (ectopically expressed) QIK or SIK was unable to phosphorylate widely used Ser/Thr kinase substrates such as histone H1a, H1b and cdc25C recombinant proteins (Feldman et al., 2000; Xia et al., 2000). In contrast, SIK phosphorylated short peptide substrates used to assay CaMK namely Syntide2 (PLARTLSVAGLPKK), but not Autocamtide 2 (KKALRRQETVDAL) (Feldman et al., 2000). In order to determine canonical phosphorylation sequences for SIK, a variety of synthetic peptide substrates were tested. As a result of this, the consensus phosphorylation motif of SIK is described as ([**H**-(**B**-X or X-**B**)-X- X-**S/T-**X-X-X-**H**]., where S/T is phosphorylatable Ser or Thr, and (H) and (B) are hydrophobic and basic residues, respectively (Horike, 2003; Screaton et al., 2004). Furthermore, the described optimal motif is nearly identical to that defined for AMPK using robust peptide screening approaches (Dale et al., 1995; Gwinn et al., 2008). Therefore, this motif is unlikely to be unique to SIK and it can be speculated that other AMPK-related kinases display very similar (short) peptide sequence preference when assayed *in vitro* due to high homology in their catalytic domains (Zagórska et al., 2010).

There are various substrates for SIKs as shown in Table 1-2. Several of these substrates (CRTC, class II HDACs, SREBP1-c, IRS1, p53) are also phosphorylated by AMPK (Cheng et al., 2009; Koo et al., 2005; Takemori et al., 2009; Yoon et al., 2009). It will be interesting to determine if other AMPK substrates are also phosphorylated by SIK kinases and uncover the molecular determinants of substrate selection among these related kinases.

1.5.7 Molecular mechanism of SIK-regulated gene transcription

1.5.7.1 CREB-CBP/p300-CRTC2 dependent gene expression

Because SIK1 was identified as an immediately induced gene/protein found in rat adrenal gland after high-salt diet or ACTH treatment, early studies have focused on the role that SIK1 plays in steroidogenesis, an adrenal gland metabolic pathway regulated by ACTH. Lin *et* al. investigated a possible involvement of SIK1 in steroidogenesis. They observed that SIK1 inhibits expression of StAR (steroidogenic acute regulatory) and CYP11A (cytochrome p450), two proteins belonging to this pathway. Both genes possess a CRE motif in their promoter region which suggests that their expression could be increased by PKA activation (Lin et al., 2001). However in adrenal gland a rise in their expression was observed only 8h following ACTH treatment. This delay corresponded to a period when SIK1 was induced, suggesting a possible repression of these genes by SIK1. In Y1 cells, CYP11A transcription or transcriptional activation of its promoter induced by ACTH or forskolin could be blocked by SIK1 wild-type over-expression, but not by a kinase-inactive mutant (K56M) (Lin et al., 2001).

This suggests that SIK1 kinase activity is required for controlling expression of ACTH-regulated genes. In order to understand which regulatory mechanism was involved in CYP11A expression regulation by SIK1, various truncated versions of CYP11A promoter were inserted in a gene-reporter system and revealed that the region involved in SIK1 repression contained a CRE motif (Doi et al., 2002). Importance of CRE motif in SIK1 repression was confirmed by SIK1's ability to repress expression of a promoter only composed of CRE motif after PKA activation. This suggests that SIK1 is involved in expression of CRE-dependent genes (Doi et al., 2002). It can be noted that CRE gene-reporter repression following PKA activation has been reported for all SIK isoforms: SIK1 (Doi et al., 2002; Takemori, 2002), SIK2 (Horike, 2003; Katoh et al., 2004; Screaton et al., 2004) and SIK3 (Katoh et al., 2006). As CREB is a transcription factor that binds to CRE, Doi and colleagues speculated that SIK1-mediated gene suppression may involve CREB. Use of different truncated forms of CREB revealed that CREB bZIP domain is essential in

mediating SIK1 inhibitory function. They also noted that CREB Ser133 phosphorylation by PKA was unaltered by SIK1 (Doi et al., 2002).

The subsequent discovery of CRTC2 as a CREB-coactivator that exerted its effect by binding to CREB bZIP domain provided a clue to the connection between SIKs and CREB (Conkright et al., 2003; Iourgenko et al., 2003). Interestingly, SIK2 co-immunoprecipitated with CRTC2 and was shown to phosphorylate CRTC2 on Ser171 (Screaton et al., 2004). This phosphorylation was sufficient to promote its cytoplasmic translocation and caused repression of CREB-CRTC2 dependent gene transcription (Screaton et al., 2004).

It is worth noting that in addition to phosphorylation, SIK2 has been shown to repress CRTC2-CREB-dependent gene transcription by reducing acetylation of CRTC2 via SIK2-mediated phosphorylation of hepatic p300 on Ser89 (Bricambert et al., 2010; Liu et al., 2008) (see section 1.3.8.1.1). This provides an alternative mechanism by which SIK-CRTC pathway functions in the regulation of hepatic gene expression.

1.5.7.2 Class IIa HDACs-dependent gene expression

Berdeaux and colleagues were the first to describe the role of SIKs in HDAC-dependent gene expression *in vivo*. They generated a skeletal muscle-specific transgenic mouse model that expressed a dominant-negative mutant of CREB to investigate the role of CREB in myogenesis. These mice displayed a dystrophic phenotype characterised by progressive muscle degeneration and necrosis along with reduced expression of muscle-specific genes regulated by myocyte-specific enhancer factor 2 (MEF2) as well as SIK1, a CREB-regulated gene. Interestingly, authors also observed reduced phosphorylation (and cytoplasmic localisation) of class IIa HDACs, a known MEF2 regulator, which was associated with and inhibited MEF2 activity. Class IIa HDACs contain a consensus SIK phosphorylation motif and were previously shown to be phosphorylated *in vitro* by SIK1 (Screaton et al., 2004; van der Linden et al., 2007). This led Berdeaux and colleagues to hypothesise that reduction in SIK1 expression in these transgenic mice caused a reduction in phosphorylation of HDACs and thus inhibition of MEF2 activity (Berdeaux et al., 2007). Using phospho-specific antibodies and phosphorylation-

deficient mutants of HDACs as well as shRNAi-mediated SIK1 knock-down and skeletal muscle of these transgenic mice, the authors confirmed that SIK1 phosphorylated HDACs on two conserved serine residues (S246 and S467 for HDAC4) which led to their cytoplasmic translocation and alleviation of HDAC-mediated repression of MEF2 transcriptional activity in muscle cells (Berdeaux et al., 2007). Similarly, SIK1 was also found to increase MEF2-reporter activity by inactivating HDAC5 in primary cortical rat neurons (Finsterwald et al., 2013).

A study with overexpressed SIK2 and SIK3 showed that both SIK2 and SIK3 can phosphorylate HDACs in HeLa cells and HEK293 cells, promoting their nuclear export and increasing MEF2 activity (Walkinshaw et al., 2013). Paradoxically, it was noted that SIK-/AMPK-mediated phosphorylation and nuclear export of HDACs in liver reduced gluconeogenic gene expression due to persistent acetylation and inactivation of FoxO1 and 3 (see above section 1.3.2.1) (Mihaylova et al., 2011). It is also important to note that HDACs can be phosphorylated on the same residues as SIKs by CaMKI and II (Linseman, 2003; McKinsey et al., 2000), protein kinase D (Ha et al., 2008) and AMPK (McGee et al., 2008; Takemori et al., 2009).

1.5.7.3 Others

SIK1 was noted to suppress lipogenesis in the liver by phosphorylation of sterol regulatory element-binding protein (SREBP)-1c at Ser265, 266 and 329, thereby reducing SREBP-1c-dependent gene transcription (Yoon et al., 2009). Meanwhile SIK2 suppresses carbohydrate-responsive element–binding protein (ChREBP) 1-dependent lipogenic gene transcription by reducing its acetylation and activation (see below section 1.5.9.3) (Bricambert et al., 2010). SIK2 achieves this by phosphorylating Ser89 on p300 and suppressing its HAT activity towards ChREBP1.

1.5.8 Role of SIK in hepatic gluconeogenesis

Koo and colleagues were the first to link SIK-CREB-CRTC2 signalling pathway to fasting- and glucagon-mediated hepatic gluconeogenic gene regulation (Figure 1.15) (Koo et al., 2005). The authors showed that overexpression of SIK1 in hepatocytes suppressed a forskolin-mediated

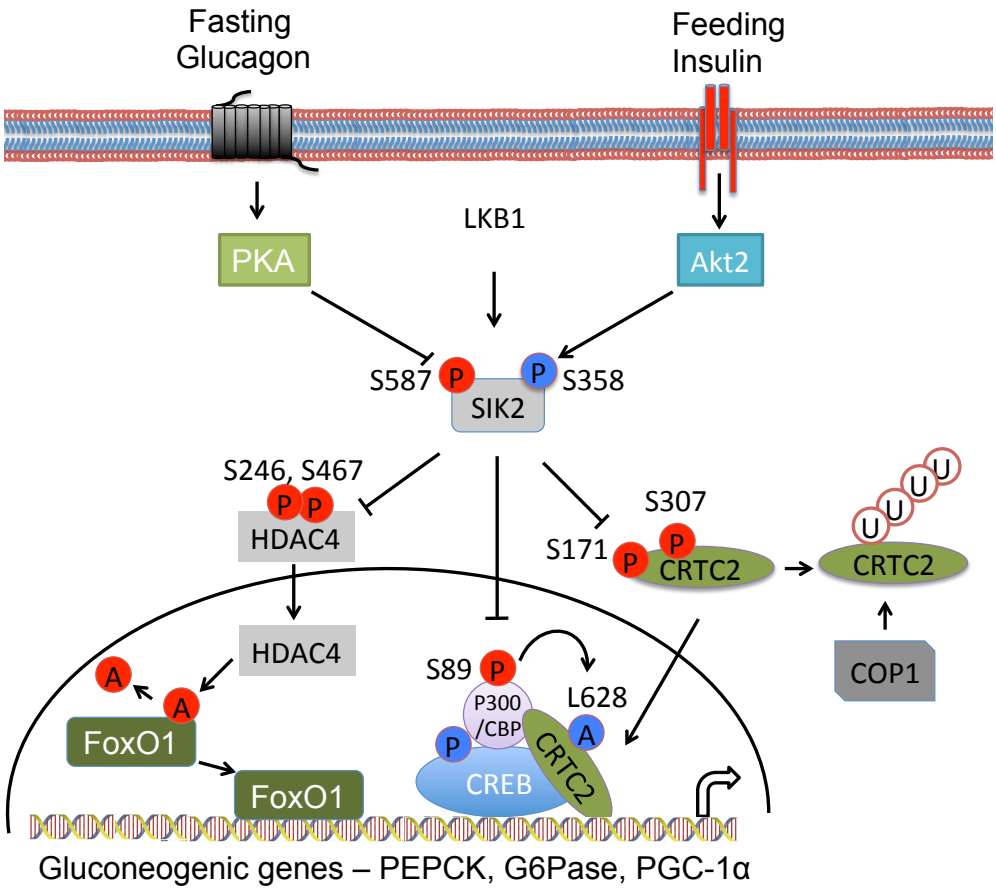

Figure 1.15 Proposed role of SIK2 in hepatic gluconeogenesis.

Based previous literature SIK2 has been proposed to play a key role in the hormonal-regulation of hepatic gluconeogenesis by mediating fasting/glucagon or feeding/insulin effects on FoxO1 or CREB-CBP-CRTC2 pathways. PKA-mediated phosphorylation of Ser587 inhibits SIK2 on these pathways while opposite results are observed with Akt2-mediated phosphorylation of Ser358 on SIK2. Activated-SIK2 during feeding suppresses gluconeogenesis via 1) class IIa HDAC-dependent FoxO1 deacetylation and activation, 2) reduction of CBP-dependent CRTC2 acetylation and degradation 3) and also by direct phosphorylation, cytoplasmic translocation and degradation of CRTC2. Reciprocal actions during fasting increase gluconeogenesis. U, P and A denote ubiquitylation, phosphorylation and acetylation respectively. Red coloured P or A are inhibitory modifications while blue coloured are activatory modifications.

increase in PEPCK gene expression, and that SIK1 phosphorylated CRTC2 on Ser171 in those cells (Koo et al., 2005). Furthermore, this suppression of PEPCK was rescued when a CRTC2 S171A mutant was ectopically overexpressed. ShRNAi-mediated knock-down of SIK1 in primary hepatocytes had the opposite effect of overexpression (SIK1), increased gluconeogenic gene expression and reduced CRTC2 phosphorylation following glucagon treatment. These results were further confirmed *in vivo* following shRNAi-mediated knock-down of SIK1 via adenovirus in liver, which showed increased fasting blood glucose and PEPCK, G6Pase and PGC-1α gene expression (Koo et al., 2005). Meanwhile, transient overexpression of SIK1 in liver reduced fasting blood glucose as well as gluconeogenic gene expression not only in C57BL/6J mice but

also in the diabetic *db/db* mouse model. SIK2 overexpression in liver, similar to SIK1, also suppressed gluconeogenesis in these mice (Koo et al., 2005). It is important to note that the authors did not investigate SIK1 or SIK2 phosphorylation and/or regulation in response to fasting or glucagon in liver and thus the molecular mechanism by which fasting and glucagon inhibit SIK1 and SIK2 activity towards CREB-dependent gluconeogenic genes in the liver remains unknown.

SIK2 (but not SIK1) was also shown to play an important role during feeding and insulin-mediated suppression of gluconeogenesis (Dentin et al., 2007). Authors showed that refeeding following fasting, promoted hepatic CRTC2 Ser171 phosphorylation, nuclear export and COP1-mediated proteasomal degradation, thus suppressing hepatic gluconeogenic gene expression (see above section 1.3.8.1.2 for detail) (Dentin et al., 2007). This refeeding-mediated increase in CRTC2 phosphorylation was thought to be due to an increase in the kinase activity of SIK2 by Akt2-mediated Ser358 SIK2 phosphorylation (Figure 1.15) (see above section 1.5.5.4). However, it is important to note that this study did not assess SIK2 phosphorylation or measure its kinase activity in liver or hepatocytes following insulin or refeeding.

Glucagon reduces Ser89 p300 phosphorylation by inhibiting SIK2, thereby increases CRTC2 acetylation and hepatic gluconeogenic gene expression (Figure 1.15) (see above section 1.3.7.1). In contrast, insulin increases Ser89 p300 phosphorylation by activating SIK2, thereby reducing CRTC2 acetylation and hepatic gluconeogenic gene expression (Bricambert et al., 2010; Liu et al., 2008). In addition to CREB-CBP/p300-CRTC2-dependent gluconeogenic gene expression, SIKs can also phosphorylate class IIa HDACs and suppress FoxO1-dependent gluconeogenic gene expression in the liver (Figure 1.15) (see above section 1.3.2.1). It is important to note that the role of CRTC2 and FoxO acetylation *in vivo* is elusive and controversial (see section 1.3.4, 1.3.8.1.3 for detail)

These studies collectively suggest that SIK2 is a key regulator of hormone-regulated hepatic gluconeogenesis due to its unique ability to modulate both CREB-CBP-/p300-CRTC2- and HDAC-FoxO-mediated hepatic gluconeogenic gene expression (Figure 1.15). At the center of

this mechanism is the phoshoryaltion-dependendent regulation of SIK2. Glucagon/fasting activates PKA promoting Ser587 phosphorylation and inhibition of SIK2, while insulin/feeding activates Akt2 thus promoting Ser358 phosphorylation and stimulation of SIK2 activity. However, this molecular mechanism has not been extensively studied and validated in liver. It was proposed using through contradictory results from non-hepatic cells/tissues studies. Therefore, the precise mechanism behind hormonal-regulation of SIK2 clearly needs further investigation.

1.5.9 Other biological roles of SIKs

1.5.9.1 In vivo knock-out models of SIK/LKB1

Knockout gene	Genetic strategy	Phenotype	Reference
SIK1	Global KO, No information on exact exon deletion, Background - C57BL/6	Only mentioned in materials and methods section of this paper and authors quoted '*The SIK1 WT mice do not show any particular phenotype difference from the SIK1 KO mice or any difference in their reproduction or life span.*'	(Eneling et al., 2012), Section 1.5.9.6
SIK2	Global KO, No information on exact exon deletion, Background - C57BL/6	Ischemic neuronal injury was significantly reduced in the brains of SIK2 KO mice subjected to transient focal ischemia and these mice apparently had no phenotype for body weight control.	(Sasaki et al., 2011) , Section 1.5.9.4
SIK3	Global KO, No information on exact exon deletion, Background - C57BL/6	Malnourished phenotype (i.e., lipodystrophy, hypolipidemia, hypoglycemia, and hyper-insulin sensitivity) accompanied by cholestasis and cholelithiasis.	(Uebi et al., 2012), Section 1.5.9.3
LKB1 muscle specific $LKB1^{fl/fl}Cre^{+/-}$	floxed (fl) allele was exons 5–7 of the LKB1 gene were replaced by a cDNA cassette encoding the remainder of the LKB1 sequence, and	$LKB1^{fl/fl}$ mice showed 90% reduction in expression of LKB1. Muscle specific $LKB1^{fl/fl}Cre^{+/-}$ mice showed reduced AMPK activation and glucose uptake stimulated by AICAR or muscle contraction	(Sakamoto et al., 2005)

	exons 4 of the LKB1 gene. The cDNA cassette was flanked by the loxP Cre excision sequence. Background - C57BL/6		
LKB1 liver specific	8-week-old male mice of $LKB1^{lox/lox}$ genotypes were tail-vein injected with adenovirus expressing Cre recombinase from the cytomegalo-virus promoter. 95% deletion of LKB1 protein in the livers was observed with no signs of deletion in muscle, pancreas, or spleen tissue, as judged by immunoblotting. Background - C57BL/6	Loss of LKB1 function resulted in hyperglycemia with increased gluconeogenic and lipogenic gene expression in LKB1-deficient livers. Adenoviral small hairpin RNA (shRNA) for TORC2 reduced PGC-1α expression and normalised blood glucose levels in mice with deleted liver LKB1 while in vivo metformin failed to reduce hyperglycemia in high fat fed LKB1 knock-out mice.	(Shaw, 2005)
$LKB1^{lox/lox}$	floxed allele was deleted for the *neomycin* resistance gene and contained loxP Cre excision sequence 5' to exon 3 and 3' to exon 6 of LKB1 gene. Background - C57BL/6	No phenotype of $LKB1^{lox/lox}$ mice. $Lkb1^{+/-}$ mice developed intestinal polyps throughout the gastrointestinal tract but no discern dysplastic or adenomatous changes.	(Bardessy et al., 2002)
LKB1 liver specific	$LKB1^{fl/fl}$ were injected with adenovirus Cre-GFP into the penis vein (5 X 10^8 PFU/mouse). $LKB1^{fl/fl}$ mice were obtained from Kei Sakamoto. (Described above, row four) Background - C57BL/6	Primary hepatocytes of these mice showed increased basal and cAMP-stimulated glucose production. However, metformin maintained the suppressive effect on glucose production in LKB1 knock-out hepatocytes.	(Foretz et al., 2010)

1.5.9.2 Myogenesis and skeletogenesis

SIK1 regulation of class IIa HDACs and MEF2 activity is linked to skeletal muscle repair and myogenesis (see section 1.5.7.2) (Berdeaux et al., 2007; Takemori et al., 2009) and may also regulate cardiomyogenesis (Romito et al., 2010). Romito *et* al. employed gene-trap technology to generate an ES (embryonic stem) cell line that expressed the N-terminal portion of SIK1 (1-249) (which lacked kinase activity). These ES cells showed a significant delay in development into beating/functional cardiomyocytes and were associated with a reduced expression of p57, a cyclin-dependent kinase inhibitor. However, the exact molecular mechanism behind this is not clear. It would be interesting to validate these results by generating skeletal-muscle/cardiac-muscle specific SIK1 knock-out mice.

SIK3 was shown to affect skeletogenesis and was required for growth plate maintenance (Sasagawa et al., 2012). Global SIK3-null mice displayed marked skeletal abnormalities mainly in the form of severe inhibition of chondrocyte hypertrophy. SIK3-deficient mice showed dwarfism and were half the weight of wild-type mice. They were born at the expected mendelian frequency but 90% died on the first day after birth (Sasagawa et al., 2012). Suppressed MEF2C activity due to persistent nuclear localisation of HDAC4 secondary to loss of SIK3 was proposed as a possible mechanism for the inhibition of chondrocyte hypertrophy in these mice. In support of this proposed mechanism, it was shown that HDAC4, a crucial repressor of chondrocyte hypertrophy (Vega et al., 2004), remained in the nuclei in SIK3-deficient chondrocytes. Furthermore, transgenic overexpression of SIK3 in chondrocytes of SIK3-null mice, rescued chondrocyte hypertrophy in E16.5 and E18.5 aged mice (Sasagawa et al., 2012). These results collectively suggest that SIK3 plays a key role in chondrocyte regulation.

1.5.9.3 Hepatic lipogenesis

SIK1 and SIK2 both are implicated to suppress hepatic lipogenesis, albeit with different mechanisms. ShRNAi-mediated knock-down of SIK1 in mouse liver tissue and hepatocytes

induced SREBP-1c as well as SERBP-1c-dependent lipogenic genes such as fatty acid synthase (FAS) and acetyl-CoA carboxylase (ACC), while ectopic expression of SIK1 in the liver via adenovirus exhibited opposite effects (Yoon et al., 2009). Investigation into the molecular mechanism underlying these effects led the authors to inspect amino acid sequence of SRBEP-1c for consensus SIK phosphorylation motif, that revealed three putative SIK1 phosphorylation sites namely S265, S266 and S329 on SREBP-1c. Phosphorylation on these sites by SIK1 was confirmed using cell-free assays. This regulation was further assessed using transient-expression of a triple phosphorylation-deficient mutant of SREBP-1c in hepatocytes and liver tissue, which rescued SIK1-mediated suppression of FAS and ACC expression (Yoon et al., 2009).

Bricambert and colleagues noted that shRNAi-mediated knock-down of SIK2 in liver also increased expression of lipogenic genes and resulted in hepatic steatosis (Bricambert et al., 2010). This was associated with p300-mediated ChREBP acetylation predominantly on K672 which increased its transcriptional activity on lipogenic gene promoter. In contrast, SIK2 overexpression in liver suppressed lipogenic gene expression through inactivation of p300 and reduction in ChREBP acetylation. Using phospho-specific antibody and loss and gain of function studies with SIK2, it was shown that SIK2 regulated HAT activity of p300 by Ser89 phosphorylation in liver (Bricambert et al., 2010). Similar to this observation, overexpression of SIK2 suppressed lipogenic genes in primary and in 3T3-L1 adipocytes, while SIK2 knock-down had opposite effects (Du et al., 2008).

SIK3 also seems to contribute to lipogenesis. Along with severe skeletal abnormalities and dwarfism, SIK3-null mice showed reduced fasting blood glucose, hypolipidemia with significant lipodystrophy and small adipocytes (Uebi et al., 2012). These mice were insulin sensitive, had small liver with enlarged gall-bladder and showed significantly increased alanine aminotransferase, alkaline phosphatase and bile acid in liver and blood due to cholestasis and cholelithiasis. The mice were also resistant to high fat-diet-induced weight gain and metabolic changes including lipogenesis but less tolerant to a cholic acid (CA)-containing diet. SIK3-null

mice had a very complex phenotype involving glucose, lipid and bile acid metabolism along with significant skeletal abnormalities making it harder to identify specific molecular mechanisms behind these defects (Uebi et al., 2012). Nonetheless, it highlights the importance of SIK3 in these processes and it would be important to generate conditional (e.g. tissue/cell-specific) knock-out mouse models to determine more specific roles of SIK3 in various cell/tissues systems. Interestingly, a signal nucleotide polymorphism in the SIK3 gene was associated with higher triglyceride levels in an Asian-Indian human cohort (Braun et al., 2012) further highlighting the role of SIK3 in lipid metabolism.

1.5.9.4 Neuronal survival

Sasaki and colleagues suggested a role of the SIK2-CRTC1 pathway in neuronal survival following ischaemic brain injury (Sasaki et al., 2011). It was noted that SIK2 (but not SIK1) was degraded after 3-6 h of oxygen-glucose deprivation in primary cortical neurons and mouse brain. This was associated with dephosphorylation of CRTC1 and higher expression of CREB-CRTC1-dependent pro-survival genes such as BDNF. Experiments using CaMKI and IV dominant-negative mutants, ShRNAi-mediated knock-down and overexpression of CaMK I/IV as well as pharmacological inhibitors of CaMKs, determined that oxygen-glucose deprivation-activated CaMKI and IV phosphorylated SIK2 on Thr484 promoting its degradation thus dephosphorylation and activation of CRTC1. In addition, a phosphorylation-deficient mutant SIK2 (T484A) was resistant to degradation and showed enhanced repression of CRE-activity and prevented nuclear translocation of CRTC1 after oxygen-glucose deprivation in cortical neurons. Finally, *in vivo* role of SIK2 in neuronal survival was confirmed using SIK2-null mice that showed reduced ischaemic lesions and higher expression of CREB-CRTC1-dependent pro-survival genes in the brain in response to transient occlusion of the middle cerebral artery (Sasaki et al., 2011). These data collectively suggest that SIK2-CRTC1 play a role in neuronal survival after ischaemic brain injury and that SIK2 inhibition may protect the brain from ischemic damage.

Interestingly, SIK1 may also affect neuronal survival through a MEF2-dependent mechanism (Finsterwald et al., 2013). BDNF treatment of primary cortical rat neurons induced SIK1 mRNA and protein expression as well as MEF2 activity. SIK1 overexpression increased MEF2 activity in cortical neurons while staurosporine (10 nM) treatment (non-specific SIK1 inhibitor) reduced its activity and was associated with reduced phosphorylation and nuclear accumulation of HDAC5. This led the authors to conclude that BDNF increases neuronal survival by activating SIK1 (Finsterwald et al., 2013).

1.5.9.5 Regulation of Na^+/K^+-ATPase

SIK1 was found to regulate Na^+/K^+-ATPase activity, an enzyme important for intracellular sodium potassium balance, in opposum kidney cells following an increase in intracellular sodium, achieved in this study using sodium ionophore (monensin) treatment (Sjöström et al., 2007). While searching for proteins that were associated with and regulated Na^+/K^+-ATPase activity, authors identified SIK1, PP2A and PME-1 in a co-immunoprecipitation screen conducted using immunoprecipitated GFP-tagged α-subunit of Na^+/K^+-ATPase from kidney cells under basal condition. They noted that wild-type, but not kinase-inactive, SIK1 increased Na^+/K^+-ATPase activity in kidney cells after monensin treatment (Sjöström et al., 2007).

Along with the rise in intracellular sodium, monensin treatment also increased intracellular calcium, while calcium-chelating agents reduced Na^+/K^+-ATPase activity. In addition, monensin treatment of kidney cells also increased autophosphorylation of SIK1, as measured *in vitro* after immunoprecipitation of SIK1 (Sjöström et al., 2007). In contrast, Na^+, Ca^{2+} or monensin did not affect the autophosphorylation of SIK1 in cell-free assay. These led authors to search for an intermediate protein that connected raised cellular Ca^{2+} levels to increased SIK1 activity. Scanning of SIK1 protein sequence identified (IDRQRT^{322}V) a consensus site for CaMKI and CaMKI was shown to phosphorylate SIK1 in cell-free assay.

Furthermore, monensin was noted to increase Na^+/K^+-ATPase activity in kidney cells without affecting its membrane translocation, a classical mechanism of its activation, but by promoting its dephosphorylation by PP2A (protein phosphatase 2A) (Sjöström et al., 2007). Investigation

into this observation led authors to show that SIK1 phosphorylated and thereby inactivated the PP2A inhibitor, PME-1 in cell free assay. This in turn led to activation of PP2A and dephosphorylation of Na^+/K^+-ATPase, thereby increasing its activity. Wild-type SIK1 but not T322A SIK1 increased Na^+/K^+-ATPase activity which led authors to propose that CaMK-mediated Thr322 phosphorylation activated SIK1. However, the study lacked in-depth assessment of SIK1 kinase activity in response to monensin and CaMKI phosphorylation and failed to quantify PME-1 phosphorylation and function in cells using phospho-specific antibodies and phospho-deficient mutants, respectively (Sjöström et al., 2007).

Another study noted that SIK1 activity and expression was increased in renal proximal tubule cells derived from the hypertensive rat model carrying a mutation in α-adducin (F316Y), a ubiquitously expressed heterodimeric cytoskeleton protein which is associated with increased Na^+/K^+-ATPase activity (Stenström et al., 2009). Observations that genetic polymorphism (C-T, rs-3746951) in SIK1 in humans is associated with lower blood pressure and that SIK1 is located in vascular smooth muscle and endothelial cells of human and rat aorta (Popov et al., 2011) may suggest a role of SIK1 in the control of blood pressure.

1.5.9.6 Cancer and cell proliferation

SIK2 was identified in a screen of an ovarian cancer cell line as a candidate gene required for G2 and G2/M cell-cycle progression (Ahmed et al., 2010). Further analysis revealed that SIK2 co-localiased with γ-tubulin in the centrosome and ShRNAi-mediated knock-down of SIK2 resulted in a significant delay in mitotic progression, monopolar spindle and increased sensitivity to taxane-based (mitotic inhibitor) chemotherapeutic agents in the ovarian cancer cell line (Ahmed et al., 2010). Authors also observed that overexpression of wild-type but not kinase-inactive mutant of SIK2 in these cells caused chromosomal splitting, a necessary step for mitosis. These led authors to search protein database for centrosomal proteins that contained putative SIK consensus motif and identify c-Nap1, a centrosome linker protein that was shown to be associated to and phosphorylated by SIK2 in cell free assay. Mass-spectrometry analysis revealed three putative phosphorylation sites on c-NAP1 (S2234, S2392,

and S2394) and phosphorylation of these sites in intact cells was assessed using a non-specific phospho-serine antibody (Ahmed et al., 2010). In addition, observations that wild-type but not kinase-inactive SIK2 displaced c-Nap-1 from chromosomes (a requirement of proper c-Nap1 function) and shRNAi-mediated knock-down of c-Nap1 also induced chromosomal splitting led to the conclusion that SIK2 plays a key role in the initiation of mitosis by regulating c-Nap1. Interestingly, elevated SIK2 mRNA expression was associated with poor outcome in taxane-based (mitotic inhibitor) chemotherapy treatment in human ovarian cancer patients and highlights the role of SIK2 in human cancer (Ahmed et al., 2010).

SIK3 was also implicated to play a role in ovarian cancer. Ovarian cancer cells had significantly reduced tumorigenesis in xenografts when SIK3 was knocked-down, while SIK3 overexpression had opposite effects by promoting G1/S cell progression (Charoenfuprasert et al., 2011). In addition, SIK3 was relatively highly expressed in 55% of human ovarian cancer samples, but was rarely detected in adenomyosis, leiomyoma and normal ovary tissues, thereby showed high specificity (97%) for ovarian cancer which was comparable to the well-known tumor marker CA125 (65%) (Charoenfuprasert et al., 2011). However, the molecular pathways behind this association are not known.

A report on exome and genome sequences of 183 human lung adenocarcinoma tumor/normal DNA pairs identified an in-frame rearrangement of SIK2 (kinase domain duplication, 15 aminoacids upstream of Thr175) as a novel somatic mutation. However, the functional importance of this remains to be elucidated (Imielinski et al., 2012).

A kinome-wide, RNA interference based loss-of-function screen identified SIK1 as a modulator of p53-dependent anoikis (apoptosis induced by cell detachment) in immortalised human mammary epithelial cells expressing a constitutively-activated tumor mutant allele of PIK3 (tHMECs-p) cells (Cheng et al., 2009). ShRNAi-mediated knock-down of SIK1 decreased p53 abundance and increased anchorage-independent growth of the tHMEC-P cancer cell line. These cells showed a higher potential for metastasis when injected into nonobese diabetic-severe combined immunodeficiency (NOD-SCID) mice. Similar changes were also observed

with ShRNAi knock-down of LKB1 in tHMEC-P cancer cells as well as in LKB1-deficient A549 cancer cells (Cheng et al., 2009). Interestingly, all of these changes were recused with SIK1 T175E (constitutively active) but not by kinase-dead mutant of SIK1. Authors also showed that wild-type but not kinase-inactive SIK1 isolated by immunoprecipitation from suspended cells (to activate anoikis) phosphorylated p53 *in vitro* on Ser15 (Cheng et al., 2009), suggesting activation of SIK1 by cell-detachment and possible mechanism of p53 regulation by SIK1. These results highlight the importance of LKB1-SIK1 in anoikis and a role of SIK1 as a tumour suppressor.

SIK1 was also implicated in increased stability of intercellular junctions by reducing the expression of E-cadherin, a marker of epithelial to mesenchymal transition and of tumor invasiveness (Eneling et al., 2012). ShRNAi-mediated knock-down of SIK1 in mouse lung alveolar epithelial (MLE-12) cells increased expression of the transcriptional repressor Snail2 which in turn led to suppression of E-cadherin expression. Opposite results were observed when SIK1 was overexpressed. Lung tissue from SIK1-null mice were noted to have increased expression of Snail2 and reduced E-cadherin expression (Eneling et al., 2012). However, the molecular mechanism behind this effect is not known. Interestingly, SIK1-null mice do not show any significant phenotype (Eneling et al., 2012) but it would be useful to cross these mice to other cancer-prone mouse models to assess anti-metastatic effect of SIK1.

In addition to cell culture data, it was noted that reduced SIK1 mRNA expression was correlated with poor prognosis in two large human breast cancer data-sets (Cheng et al., 2009). In contrast, relatively higher expression of SIK2 and SIK3 was associated with poorer outcome in ovarian cancer (Ahmed et al., 2010; Charoenfuprasert et al., 2011). These data collectively suggest a possibility of isoform-specific role of SIK in cancer but needs further confirmation using simultaneous expression or knock-down of SIKs or studies with SIK inhibitors.

1.5.9.7 Melanogenesis

Ultraviolet light increases melanogenesis by activation of α-melanocyte-stimulating hormone (α-MSH) receptor-PKA signalling which in turn activates CREB-dependent melanogenesis. Overexpression of SIK2 prevented ultraviolet (UV) light-mediated increase in melanin in B16 melanoma cells by suppressing CREB-CRTC2 dependent Mitf (microphthalmia-associated transcription factor) expression which subsequently reduced tyrosinase, an important enzyme for melanin production, while ShRNAi-mediated knock-down of SIK2 increased melanogenesis by reciprocal mechanism (Horike et al., 2010). Treatment of B16 cells with 4'-O-methylfisetin (4'MF), a proposed SIK inhibitor, also showed similar changes in melanogenesis (Kumagai et al., 2011). Interestingly, it was noted that the ultraviolet light-mediated increase in melanogenesis was associated with suppression of SIK2 mRNA and protein in these cells and this caused induction of CREB-CRTC2 dependent Mitf and tyrosinase expression (Horike et al., 2010; Kumagai et al., 2011). Transgenic mice expressing the lethal yellow allele of agouti (A^y/a mice) have yellow hair because of impaired melanogenesis due to defective activation of α-MSH receptor-PKA signalling. Interestingly, SIK2$^{-/+}$/A^y/a chimeric mice showed browning of hair following ultraviolet light stimulation consistent with an inhibitory role of SIK2 in melanogenesis (Horike et al., 2010). However, the exact molecular mechanism behind the suppression of SIK2 expression by ultraviolet light is not known.

1.5.9.8 Autophagy

Recently recombinant SIK2 was shown to be acetylated on Lys53 in HEK293 cells following overexpression of CBP, and deacetylated following overexpression of HDAC6 (Yang et al., 2013). The overexpression of CBP also led to co-localisation of GFP-SIK2 and LC3 (Microtubule-associated protein 1-light chain 3), an autophagosome marker. In addition, an acetylation-mimetic mutant (K53Q), but not acetylation-deficient mutant (K53R), was also co-localised to LC3 (Yang et al., 2013). Interestingly, this mutant had reduced ATP-binding ability *in vitro* and reduced activity towards GST-Syntide2 peptide (non-selective substrate for SIK) *in vitro*. This

led to the hypothesis that SIK2 acetylation reduces its kinase activity and promotes its accumulation in the autophagosome. ShRNAi-mediated knock-down of SIK2 (but not SIK1) reduced autophagosome and lysosome fusion in HEK293 cells suggesting that there may be a function for SIK2 in the autophagosome (Yang et al., 2013). However, all of the experiments in this study were conducted with ectopically-overexpressed protein in a particular cultured cell line, thus the role of endogenous SIK2 acetylation remains to be confirmed.

2 Aims

Recent work has proposed that the members of AMP-activated protein kinase (AMPK)-related kinases, the salt inducible kinases (SIK), play a key role as signalling mediators in the control of insulin- and glucagon-regulated hepatic gluconeogenesis. Among the three SIK isoforms SIK2 has been implicated as a dominant isoform for this role. However, the exact molecular regulation of SIK2 by these hormones is elusive and there is a lack of genetic evidence demonstrating that SIK2 plays an essential role in controlling gluconeogenesis and glucose homeostasis.

Therefore, firstly I aim to investigate glucagon- and insulin-mediated regulation of SIK2 in the liver by assessing the effects of these hormones and hormonal-regulated phosphorylation on various biochemical properties of SIK2 in primary hepatocytes. The role of SIK2 in hepatic gluconeogenesis *in vivo* will be investigated using liver-specific SIK2 knock-out mice in a collaboration with Dr Marc Foretz (Institut Cochin, INSERM, Paris). Finally, I aim to characterise and apply novel SIK inhibitors to investigate the role of SIKs in hepatic gluconeogenesis. Thus I will employ biochemical, genetic and pharmacological approaches to investigate the role of SIKs in the control of hepatic gluconeogenesis.

3 Materials and methods

3.1 Material

3.1.1 Chemicals and instruments

Acetic acid, acetone, ethanol, glycerol, glycine, 4-(2- Hydroxyethyl)piperazine-1-ethanesulfonic acid (Hepes), isopropanol, methanol, orthophosphoric acid, potassium chloride, sodium chloride, sodium ethylenediaminetetraacetic acid (EDTA), sodium ethylene glycol tetraacetic acid (EGTA), sodium fluoride, sodium glycerophosphate, sodium orthovanadate, sucrose and tris (hydroxymethyl) methylamine (Tris) were obtained from BDH (Lutterworth, UK). Tissue culture plates (6, 12, 24 and 96-well), cell-culture dishes and cryovials were from Corning Incorporated (New York, USA). Cell scrapers were from Costar (Cambridge, USA). Dulbecco's modified eagle medium (DMEM), M199 with glutamax, BSA 7.5%, tissue culture grade Dulbecco's phosphate buffered saline (PBS), trypsin/EDTA solution, L-glutamine, sodium pyruvate and penicillin/streptomycin were from Invitrogen (Paisley, UK). Insulin-like growth factor 1 (IGF-1, Cat No. 8917) was from Cell Signaling Technology (CST). Forskolin, MK-2206, wortmannin were from Tocris (Avon, UK). Protein G-sepharose, glutathione-sepharose, enhanced chemiluminescence (ECL) kit, hyperfilm MP were purchased from GE Healthcare (Piscataway, USA). [$Y^{32}P$]-labelled ATP was from PerkinElmer (Massachusetts, USA). Pre-cast NuPAGE Novex SDS (sodium dodecyl sulfate) polyacrylamide 4-12% Bis-Tris gels, NuPAGE MOPS running buffer (20X), 4X NuPAGE LDS (lithium dodecyl sulfate) sample buffer, colloidal blue staining kit and SYBR DNA gel stain were from Invitrogen. Agarose was from Melford Laboratories (Chelsworth, UK). Restriction enzymes, DNA ligase and DNA ladder were from New England Biolabs (Hertfordshire, UK). Photographic developer (LX24) and liquid fixer (FX40) were from Kodak (Liverpool, UK). X-ray films were from Konica Minolta (Tokyo, Japan). Cellophane films, Precision Plus protein markers, iScript cDNA synthesis kit and SsoFast

EvaGreen Supermix were from Bio-Rad (Hertfordshire, UK). 40% (w/v) 29:1 Acrylamide: Bis-Acrylamide solution was from Flowgen Bioscience (Yorkshire, UK). Coomassie protein assay reagent (Bradford reagent) and HRP-conjugated secondary antibodies were from Pierce (Chester, UK). Polyethylenimine (PEI) was from Polysciences (Warrington, USA). Skimmed milk (Marvel) was from Premier Beverages (Stafford, UK). HiSpeed Plasmid Maxi kits and RNeasy Mini kits were from Qiagen (Crawley, UK). Acetonitrile (HPLC grade, Cat No. RH1015) and trifluoroacetic acid (TFA, HPLC grade, Cat No. RP3020) were from Rathburn Chemicals (Walkerburn, UK). Protease inhibitor cocktail tablets were purchased from Roche (Lewes, UK). Anti-HA-agarose, anti-FLAG-agarose, ammonium persulphate (APS), ampicillin, ammonium bicarbonate, benzamidine, bovine serum albumin (BSA), bromophenol blue, dithiothreitol (DTT), dexamethasone, dimethyl sulphoxide (DMSO), glutathione, hydrogen peroxide, iodoacetamide, phenylmethanesulphonylfluoride (PMSF), SDS, sodium tetraborate N, N, N', N'- Tetramethylethylenediamine (TEMED), triethylammonium bicarbonate, Triton X-100, Tween-20, sodium deoxycholate, NP-40, isopropyl β-D-1-thiogalactopyranoside (IPTG), collagenase (from clostridium histolyticum type IV, Cat No. C5138), triidothyronin (Cat No. T2877), dibutyryl-cAMP (Cat No. D0627) and lactate were from Sigma-Aldrich (Poole, UK). Infinity glucose oxidase assay was from Thermo scientific (Essex, UK). Nitrocellulose, P81 paper and 3MM chromatography paper were from Whatman International (Maidstone, UK). Insulin, for injection (100 U/ml) and glucagon (GlucaGen hypo-kit) were from Novo Nordisk (Sussex, UK). AdEasy expression system was from Agilent technologies (Cheshire, UK) and BLOCK-iT expression system was from Invitrogen. Peristaltic pump and platinum-cured silicone tubes (3.2 mm tube bore) were from Watson Marlow (Cornwall, UK). 25 G winged infusion set was from Terumo (Surrey, UK) and Intrafix safe set was from B Braun (Sheffield, UK). Disposable syringe PES filters (0.2 µm) were from Sartorius (Surrey, UK).

3.1.2 Buffers and solutions

Most commonly used buffers are listed below (Table 3-1) and the others are described in the text.

Lysis buffer ensures immediate inhibition of proteases, protein kinases and phosphatases to preserve the *in vivo* state of proteins (and their phosphorylation states) in cell/tissue lysates. Benzamidine and PMSF or complete protease inhibitor tablet prevent the action of metallo, aspartic, cysteine and serine proteases. EGTA and EDTA inhibit metalloproteases and protein kinases that require Ca^{2+} and Mg^{2+}/Mn^{2+} for their action by chelating the respective ions. Sodium fluoride and sodium pyrophosphate inhibit serine and threonine protein phosphatases while sodium orthovanadate inhibits tyrosine phosphatases.

Table 3-1 Buffers and solutions

Buffer/Solutions	Composition
Lysis buffer	50 mM Tris-HCl pH 7.5, 1 mM EGTA, 1 mM EDTA, 0.27 M sucrose, 1% (w/v) Triton X-100, 5 mM sodium pyrophosphate decahydrate and 50 mM sodium fluoride. 1 mM DTT, 1 mM sodium orthovanadate, 0.5 mM PMSF and 1 mM benzamidine are added just before cell lysis. Complete protease inhibitor cocktail tablet was (one tablet/50 ml) used for mouse tissues homogenisation.
Buffer A	50 mM Tris-HCl pH 8.0, 0.1 mM EGTA
PBS	137 mM NaCl, 2.7 mM KCl, 8.1 mM di-sodium hydrogen phosphate, 1.5 mM potassium dihydogen phosphate, pH 7.4
Laemmli sample buffer (4x)	250 mM Tris-HCl, pH 6.8, 8% (w/v) SDS, 40% (w/v) glycerol, 20 mM DTT, 0.008% bromophenol blue
Tris-glycine running buffer	25 mM Tris, 190 mM glycine, 0.1% (w/v) SDS
Transfer Buffer	24 mM Tris, 191 mM glycine, 20% (v/v) methanol
Tris Buffered Saline (TBS)	20 mM Tris-HCl pH 7.5, 150 mM NaCl
TBS-T	20 mM Tris-HCl pH 7.5, 150 mM NaCl, 0.1% (v/v) Tween-20
Colloidal coomassie staining	1% (w/v) coomassie BB G-250, 10% (w/v) ammonium sulphate, 2% (v/v) orthophosphoric acid and 20% (v/v) methanol
TAE	20 mM Tris-HCl pH 7.5, 150 mM NaCl, 0.1% (v/v) Tween-20
Wash buffer	10 mM HEPES pH 7.65, 137 mM NaCl, 7 mM KCl, 0.7 mM sodium phosphate dibasic, 0.1

	mM EDTA
Digestion buffer	10mM Hepes pH 7.65, 137 mM NaCl, 7 mM KCl, 0.7 mM sodium phosphate dibasic, 0.1 mM EDTA, 5 mM $CaCl_2$ and 0.4 mg/ml collagenase A
Exchange buffer	250 mM NaCl, 50 mM Hepes, 0.03% Brij-35, 1 mM DTT, 0.5 mM PMSF
Elution buffer (for BL21 cells)	Exchange buffer plus 10 mM L-glutathione
Elution buffer (for mammalian cells)	0.27 M sucrose, 20 mM L-glutathione, and 1 mM DTT in buffer A, pH re-adjusted to 8.0
Viral storage buffer (2x)	10 mM Tris pH 8.0, 100 mM NaCl, 0.1% (w/v) BSA and 50% (v/v) glycerol
Homogenisation buffer	3 mM imidazole pH 7.4, 0.25 M sucrose, 1 mM EDTA, 1mM EGTA, 50 mM sodium fluoride, 5 mM sodium pyrophosphate decahydrate. 1 mM DTT, 1 mM sodium orthovanadate, 0.5 mM PMSF and 1 mM benzamidine are added just before cell lysis.
RIPA buffer	50 mM Tris-HCl pH 8, 150 mM NaCl, 1 mM EDTA, 50 mM sodium fluoride, 1% (v/v) NP-40, 0.1% (w/v) SDS, 0.5% (w/v) sodium deoxycholate. 1 mM DTT, 1 mM sodium orthovanadate, 0.5 mM PMSF and 1 mM benzamidine are added just before cell lysis.

3.1.3 Antibodies

3.1.3.1 Commercial antibodies

The following commercial antibodies were used for immunoblotting as indicated. Membranes were blocked with 5% skimmed milk, TBS-T for 1h at room temperature followed by incubation with the indicated primary antibodies in 5% BSA, TBS-T overnight at 4°C. These antibodies were used at a dilution recommended by the manufacturers, usually 1:1000.

Table 3-2 Commercial antibodies

Antibody	Animal	Source
SIK1 internal	Rabbit	Santa Cruz (sc-83754)
SIK2 N-terminal	Rabbit	Cell Signaling (#6919)
pSer473 Akt	Rabbit	Cell Signaling (#9271)
pThr308 Akt	Rabbit	Cell Signaling (#9275)
Akt2	Rabbit	Cell Signaling (#2964)
pSer133 CREB	Rabbit	Cell Signaling (#9198)
CREB	Rabbit	Cell Signaling (#9197)
pPKB substrate	Rabbit	Cell Signaling (#9614)
pPKA substrate	Rabbit	Cell Signaling (#9621)
pSer157 VASP	Rabbit	Cell Signaling (#3111)

CRTC2	Rabbit	Calbiochem (ST1099)
CRTC3	Rabbit	Abcam (Ab91654)
pSer171 CRTC2	Rabbit	Cell Signaling
pSer246 HDAC4	Rabbit	Cell Signaling (#3443)
pThr1462 TSC2	Rabbit	Cell Signaling (#3617)
TSC2	Rabbit	Cell Signaling (#3612)
pThr246 PRAS40	Rabbit	Cell Signaling (#2997)
PRAS40	Rabbit	Cell Signaling (#2610)
Inositol 1,4,5-triphosphate (IP3) receptor	Rabbit	Cell Signaling (#1178)
pSer1756 IP3 receptor	Rabbit	Cell Signaling (#3760)
AMPKα	Rabbit	Cell Signaling (#2532)
pThr172 AMPK	Rabbit	Cell Signaling (#2535)
ACC	Rabbit	Cell Signaling (#3662)
pSer79 ACC	Rabbit	Cell Signaling (#3661)
Pan 14-3-3	Rabbit	Santa Cruz (sc-629)
pSer 14-3-3 binding motif	Rabbit	Cell Signaling (#9601)
PEPCK (PECK2)	Rabbit	Cell Signaling (#6924)
GAPDH	Mouse	Abcam (Ab8245)
α-Tubulin	Mouse	Calbiochem (CP06)
HA peroxidase	-	Roche (12013819001)
Flag-M2	Mouse	Sigma (F1804)

3.1.3.2 In-house antibodies

In-house total and phospho-specific antibodies (except SIK2 phospho-specific antibodies) were produced by the antibody production team at Division of Signal Transduction Therapy (DSTT), University of Dundee under the supervision of Dr. James Hastie. SIK2 phospho-specific antibodies were generated by YenZym (San Francisco, USA).

For DSTT antibodies, antisera were raised in sheep by Diagnostics Scotland, Scottish National Blood Transfusion Service (Penicuik, UK). Pre-immune IgG was purified from non-immunised sheep serum using a protein G-sepharose column. All antibodies were affinity purified on a CH-sepharose column that had been covalently coupled to the appropriate antigen. DSTT phospho-specific and total antibodies were generated as follows: first, the peptide immunogen was separately conjugated to BSA and keyhole limpet haemocyanin (KLH). The BSA and KLH immunogen carrier protein conjugates were then injected into sheep along with Freunds' Adjuvant. Sheep were injected with a booster three weeks later and the first bleed was collected after one week. This was repeated twice in order to obtain three separate bleeds.

Each bleed was allowed to clot overnight at 4°C, centrifuged at 1500 *g* for 60 min at 4°C and decanted through glass wool prior to storage at -20°C. For purification, the serum was heated for 20 min at 56°C followed by filtration through a 0.45 µm filter. The anti-serum was diluted 1:1 with 50 mM Tris-HCl pH 7.5 with 2% Triton X-100 and purified on a CH-sepharose column that had been covalently coupled to the appropriate antigen. Elution was carried out using 50 mM glycine pH 2.5 and dialysed overnight into PBS. Total protein antibodies were used at 1 µg/ml in 5% skimmed milk, TBS-T overnight at 4°C. Phospho-specific antibodies were also used at a concentration of 1 µg/ml in the presence of the non-phospho peptide antigen (10 µg/ml) to increase the specificity.

Table 3-3 In-house antibodies

Antibody	Animal No. / Bleed	Immunogen
SIK1 N-terminal	S227B / 3rd	MVIMSEFSADPAGQGQGQQK [residues 1 - 20 of human protein]
SIK1 C-terminal	S227B / 3rd	GDCEMEDLMPCSLGTFVLVQ [residues 764 - 783 of human protein]
SIK1 internal (5-5)	S306D / 3rd	CTSLTQGLKAFRQQLRK [residues 578 - 592 of human potein with an extra cysteine at the N-terminal]
SIK1 internal (5-6)	S306D / 3rd	CKGFLGLNKIKGLARQV [residues 597 - 612 of human protein with an extra cysteine at the N-terminal]
SIK2 (QIK) N-terminal	S236C or S228B / 3rd	MVMADGPRHLQRGPVRVGFYD [residues 1 - 21 of human protein]
SIK2 (QIK) C-terminal	S236C or S228B / 3rd	LFDCEMLDAVDPQHNGYVLVN [residues 906 - 926 of human protein]
SIK3 (QSK) N-terminal	S226B / 3rd	VKRATHLVTKAKVAIKIIDKT [residues 79 - 99 of human protein]
SIK3 (QSK) C-terminal	S226B / 3rd	TDILLSYKHPEVSFSMEQAGV [residues 1349 - 1369 of human protein]
Phospho SIK1 Thr182 (Recognises equivalent T-loop site of SIK2/3)	S235B / 3rd	KSGEPLSpTWCGSPPY [residues 175 - 189 of human SIK1]
VASP	S407B / 1st	GST-HA-VASP [full-length human protein]
PKBα	S742B/ 3rd	His-PKBα [residues 1-147 human PH domain]
GFP	S268B	GST-GFP (2-238) (GST cleaved)
pSer343 SIK2	Rabbit / 1st	LKSHRSpSFPVEQR [residues 337-349 of human SIK2 with an extra cysteine

		at the C-terminal]
pSer484 SIK2	Rabbit / 1st	GQRRHpTLSEVTNQ [residue 479-491 of human SIK2 with an extra cysteine at the N-terminal]
pSer358 SIK2	Rabbit / 7th	DGRQRRPpSTIAEQTV [residues 351-365 of human SIK2] Gift from Dr Olga Göransson (Lund University, Sweden)
pSer577 SIK1 (Recongnises equivalent pSer587 SIK2)	Rabbit	QEGRRApSDTSLT [residues 571–582 of rat SIK1 with an extra cysteine at the N-terminal] Gift from Dr Hiroshi Takemori (National Institute of Biomedical Innovation, Osaka, Japan)
pSer275 CRTC2	Rabbit	Gift from Dr Robert Screaton (Children's Hospital of Eastern Ontario Research Institute, Canada)

3.1.4 Plasmids

Cloning, sub-cloning and PCR involved in the generation of expression plasmids were carried out by Dr Maria Deak (Nestlé Institute of Health Sciences SA, Lausanne, Switzerland) and Dr Mark Peggie (DSTT, University of Dundee, Dundee, UK). A mammalian expression vector under the control of the cytomegalovirus promoter (pCMV5) was used for expression of proteins in mammalian cells. pEBG6P vector was used to express GST-fusion proteins in mammalian cells. pGEX vector was used for expression of GST-fusion proteins in BL21 competent E.Coli which encoded an inducible lac Iq promoter and N-terminal GST tag followed by a precision cleavage site.

Table 3-4 Plasmids

Constructs	Plasmid vector	DSTT Plasmid number
GST-SIK2	pEBG6P	2575
HA-SIK2	pCMV5	1079
HA-T175A SIK2	pCMV5	1239
HA-D160A SIK2	pCMV5	1232
HA-K49A SIK2	pCMV5	39268
HA-S358A SIK2	pCMV5	39307
HA-S343A SIK2	pCMV5	39307
HA-S484A SIK2	pCMV5	39255
HA-S587A SIK2	pCMV5	39244
HA-T96Q SIK2	pCMV5	39561
GST-SIK1	pEBG6P	32734

HA-SIK1	pCMV5	1103
HA-T103Q SIK1	pCMV5	39389
GST-SIK3	pEBG6P	2573
HA-SIK3	pCMV5	1311
HA-T143Q SIK3	pCMV5	39987
GST-CRTC2	pGEX6P	3476
FLAG-CRTC2	pCMV5	31588
FLAG-S171A CRTC2	pCMV5	36569

Recombinant adenoviruses were used for expression of recombinant proteins and gene silencing (short hairpin RNAi, ShRNAi) in primary mouse hepatocytes. AdEasy expression system was used for generating recombinant adenovirus for expression of SIK2 and SIK2 phosphorylation-site mutants (Ser/Thr to Ala). BLOCK-iT RNAi system was used for generating ShRNAi (see sections 3.2.1.11, 3.2.1.12, 3.2.1.13).

Table 3-5 Adenoviral plasmid

Constructs	Plasmid back bone	Adenoviral system	Sequence
GFP- SIK2	pCMV-Shuttle	AdEasy	
GFP-T175A SIK2	pCMV-Shuttle	AdEasy	
GFP-S358A SIK2	pCMV-Shuttle	AdEasy	
GFP-S343A SIK2	pCMV-Shuttle	AdEasy	
GFP-S484A SIK2	pCMV-Shuttle	AdEasy	
GFP-S587A SIK2	pCMV-Shuttle	AdEasy	
GFP-S343A, S358A, S484A SIK2 (3A SIK2)	pCMV-Shuttle	AdEasy	
GFP-S343A, S358A, S484A, S587A SIK2 (4A SIK2)	pCMV-Shuttle	AdEasy	
HA-T96Q SIK2	pCMV-Shuttle	AdEasy	
HA-SIK2 WT	pCMV-Shuttle	AdEasy	Kind gift from Dr Olga Göransson, Lund University, Sweden
CRTC2	pCMV-Shuttle	AdEasy	kind gift from Dr Robert Screaton, University of Ottawa, Canada
ShRNAi SIK1	pENTR-U6	BLOCK-iT	CACCGGCACTTGAGTGAAAAC GAGGTTCAAGAGACCTCGTTT TCACTCAAGTGCC
ShRNAi SIK2	pENTR-U6	BLOCK-iT	CACCGCCTGGACTCTTTGATTG TGTTCAAGAGACACAATCAAA GAGTCCAGGGC
ShRNAi SIK3	pENTR-U6	BLOCK-iT	CACCGTCGGAATATCGTTCATC GTGATTCAAGAGATCACGATG AACGATATTCCGAC
ShRNAi Scrambled	pENTR-U6	BLOCK-iT	CACCGCAACAAGATGAAGAGC

	ACCAATTCAAGAGATTGGTGC TCTTCATCTTGTTG

3.1.5 Primer

The following primers for mouse genes were used for quantitative PCR. All of the primers were obtained from Invitrogen.

Table 3-6 Primers

Gene	Primer direction	Primer sequence
PEPCK-C (*Pck1*)	forward	CCATCACCTCCTGGAAGAACAAG
	reverse	ACCCTCAATGGGTACTCCTTCTG
G6Pase (*G6pc*)	forward	TTAAAGAGACTGTGGGCATCAAT
	reverse	ATCCACTTGAAGACGAGGTTG
β-actin (*Actb*)	forward	CAACGAGCGGTTCCGATG
	reverse	GCCACAGGATTCCATACCCA
HPRT1 (*Hrpt1*)	forward	CCAGCGTCGTGATTAGCGATGATG
	reverse	GAGCACACAGAGGGCCACAATG

3.1.6 Peptide

'Sakamoto'-tide (ALNRTSSDSALHRRR, residues 165 - 176 of human CRTC2 with three additional arginines on the C-terminus) was used as a substrate for SIK *in vitro* kinase assays. Sakamototide is based on the sequence around Ser171 of CRTC2 that is known to be phosphorylated by AMPK and SIK isoforms (Screaton et al., 2004).

3.1.7 Inhibitor

All of the inhibitors were dissolved in DSMO and used in cells as indicated in figure legends.

Table 3-7 Inhibitors

Compound	Target	Source
HG-9-91-01	SIKs	Gift from Dr Nathanael Gray (Harvard University, USA)
KIN112	SIKs	Gift from Dr Nathanael Gray (Harvard University, USA)
MK-2206	Akts	Tocris (Avon, UK)
H-89	PKA	DSTT (In-house)
Wortmannin	PI3K	Tocris (Avon, UK)

3.1.8 Animals

Male wild-type C57BL/6 mice aged 6-8 weeks were obtained from Harlan (UK). Mice were maintained under specific pathogen-free conditions. Routine animal care and welfare was carried out by the staff in the Biological unit, College of Life Sciences (University of Dundee). Mice were *ad libitum* fed standard chow diet (Special diets services, Cat no RM1, 801010). All procedures were carried out in accordance with the University of Dundee and the United Kingdom Home Office regulations.

3.1.8.1 Gene targeting and generation of liver-specific SIK2 knock-out mice.

These mice were generated by Dr Marc Foretz (Institut Cochin, INSERM, Paris). Mice were bred and maintained in Institut Cochin, Paris. All mice were maintained on a standard chow diet (Safe-diets, Cat No A03/R03) or high carbohydrate diet (70% sucrose, Harlan Cat No TD 08247) as indicated.

The SIK2 (*Snf1lk2*) targeting construct was generated from PCR products amplified from the DNA of 129/Sv ES cells by the *pfx* polymerase (Invitrogen). The 5' and 3' homology arms, both 3.4 kb in length, were inserted on either side of a PGK promoter-driven hygromycin selection cassette flanked by FRT sites, into the pL3-FRT-Hygro vector. A 1.1 kb fragment of genomic DNA bearing exon 5, encoding partially the SIK2 catalytic domain including the phosphorylation site Thr175 within the activation loop (corresponding to amino acids 160-201), flanked by loxP sites, was introduced between the hygromycin resistance cassette and the 3' homology arm. Exponentially growing 129/SV CK35 embryonic stem cells (Kress et al., 1998) were electroporated with the linearised target construct DNA and selected on plates containing hygromycin. The targeted clones were identified by PCR across both homology arms, with confirmation by Southern blot analysis. Cell populations expanded from the targeted clones were injected into C57BL6 eight-cell embryos with a laser-assisted micromanipulation system, and animals displaying germline transmission were mated with C57BL/6J mice. The hygromycin resistance cassette flanked by FRT sites was excised by

crossing SIK2$^{lox/+}$ mice with FLP-expressing mice. The resulting heterozygous offspring were backcrossed to at least 4 generations into the C57BL/6J background. Liver disruption of exon 5 flanked by loxP sites was achieved by crossing SIK2-floxed mice with Alfp-Cre transgenic mice to generate SIK2$^{lox/lox}$ (control) and SIK2$^{lox/lox}$-Alfp-Cre (liver KO) mice (Figure 3.1). Routine genotyping was carried out by multiplex PCR on tail DNA with the P1 (5'-gtagtttacattagcacattggtgcctc-3'), P2 (5'- cctagaatgcactctgcaaacactggacac-3') and P3 (5'-tctacatggagggtgtcgcagagctccatg-3') primers, to yield amplification products of 391 bp (WT allele) and 487 bp (floxed allele) with P1/P2 and 708 bp (KO allele) with P1/P3.

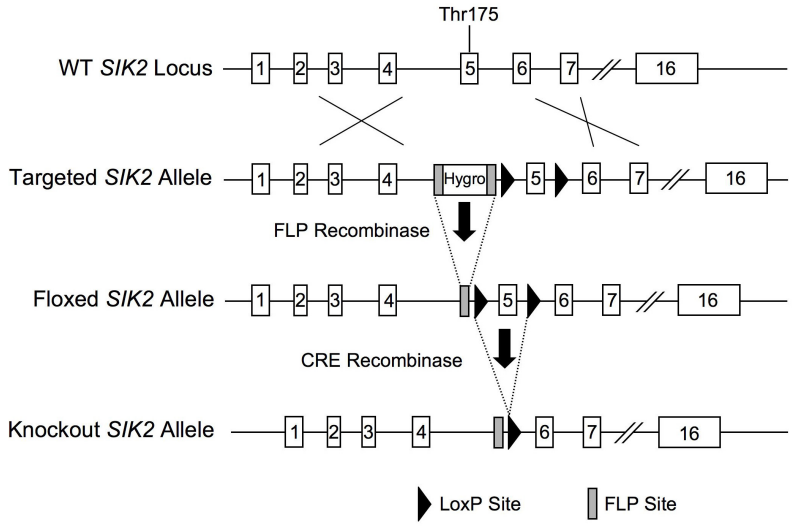

Figure 3.1 Diagram of the generation of liver-specific SIK2 knockout (L-SIK2-KO) mice.

Exon 5 was flanked by loxP sites and a hygromycin resistance cassette flanked by FRT sites was inserted upstream from the 5' loxP site. The hygromycin resistance cassette was excised by the expression of the FLP recombinase in vivo. Liver disruption of exon 5 flanked by loxP sites was achieved by crossing SIK2-floxed mice with Alfp-Cre transgenic mice.

3.1.8.2 Liver-specific LKB1 knock-out mice.

These mice were generated by Dr Marc Foretz. Mice were bred and maintained in Institut Cochin, Paris. Liver-specific LKB1 knock-out mice were generated by crossing LKB1$^{lox/lox}$ mice (kindly provided by Ronald DePinho, Harvard University) with tamoxifen-inducible albumin-Cre-ERT2 mice (Bardessy et al., 2002). Ten-week old LKB1$^{lox/lox}$-Alb-Cre-ERT2 mice were treated either with vehicle containing sunflower oil and ethanol 10% (control) or tamoxifen (Sigma) at 1 mg/mouse injected intraperitoneally in a final volume of 100 µl for 5 consecutive days. Mice

were studied or used for primary hepatocyte isolation 3 weeks after the start of tamoxifen administration.

3.2 Methods

3.2.1 DNA manipulations

3.2.1.1 Transformation of competent E.Coli

The stocks of BL21 and DH5α E.coli were prepared by Dr. Mark Peggie. Approximately 10 ng of DNA was added to 50 µl of E.coli and incubated on ice for 5 min. This Mixture was heat-shocked at 42°C for 45 sec to facilitate the uptake of DNA and incubated on ice for 10 min. 1 ml of super optimal SOCII medium [2% (w/v) peptone, 0.5% (w/v) yeast extract, 10 mM NaCl, 2.5 mM KCl, 10 mM $MgCl_2$, 10 mM $MgSO_4$, 20 mM glucose] was added to the mixture. This was further incubated for 1 h at 37°C in an orbital shaker (200 rpm). 100 µl of this mixture was streaked on Luria-Bertani (LB)-agar plates [1.5% (w/v) agar, 2% (w/v) peptone, 0.5% (w/v) yeast extract, 10 mM NaCl] containing 100 µg/ml of either ampicillin or kanamycin. Plates were inverted and incubated overnight at 37°C.

3.2.1.2 Purification of plasmid DNA from E.Coli

After overnight incubation, a single colony of transformed E.coli was transferred to 3 ml of LB-medium [2% (w/v) peptone, 0.5% (w/v) yeast extract, 10 mM NaCl] with 100 µg/ml of ampicillin or kanamycin and incubated for 8 h (37°C, 220 rpm in an orbital shaker). The culture was then transferred to 150 ml of LB-medium with an appropriate antibiotic and incubated overnight (37°C, 220 rpm in an orbital shaker). The following day, medium was centrifuged at 4°C and 6000 rpm for 15 min to pellet the cells. The DNA was isolated using HiSpeed Plasmid Maxi kit (Qiagen) according to the manufacturer's instructions.

3.2.1.3 Purification of RNA from primary mouse hepatocytes

Primary mouse hepatocytes were plated on 6-well plates at a density of 2.5 x 10^5/well. After indicated treatment, cells were harvested with RNeasy lysis buffer (RNeasy mini kit, Qiagen) and lysates were centrifuged through QIAshredder column. RNA was isolated from the lysates according to the manufacturer's instructions.

3.2.1.4 Determination of DNA and RNA concentration

DNA and RNA concentration were measured by spectrophotometry. Absorbance was measured at 260 nm and 280 nm. At 260 nm an optical density (OD) = 1 corresponds to 50 µg/ml of double-stranded DNA or 40 µg/ml of single-stranded DNA and RNA. The ratio of absorptions at 260 nm to 280 nm provides a measure of the purity of DNA with respect to protein contamination. A preparation of DNA or RNA with a ratio of 1.8 - 2 was considered pure.

3.2.1.5 Restriction enzyme digests of plasmid DNA

Restriction digest of 1 µg DNA was carried out with 1 U of restriction enzyme, 2 µl (10x stock) of appropriate reaction buffer and 0.1 mg/ml of BSA, in a total volume of 20 µl. This mixture was incubated at 37°C for 1 h and analysed via agarose gel electrophoresis.

3.2.1.6 cDNA synthesis

Complementary DNA (cDNA) was generated from 0.6 µg of RNA with 1 µl of iScript reverse transcriptase and 4 µl of 5x reaction buffer (Bio-Rad) in a total of 20 µl reaction volume. The mixture was incubated for 5 min at 25°C followed by 30 min at 42°C and finally for 5 min at 85°C. cDNA was diluted 10 times with DNAase/RNAase free water before any downstream application such as quantitative polymerase chain reaction (qPCR).

3.2.1.7 Quantitative PCR (qPCR)

qPCR was performed with SYBR green (SsoFast EvaGreen supermix) in a 96-well plate with a total reaction volume of 20 µl. The reaction consisted of 5 µl of cDNA, 10 µl of SsoFast

EvaGreen supermix, 0.8 µl (10 µM stock) of forward primer, 0.8 µl (10 µM stock) of reverse primer (final concentration 400 nM) and 3.4 µl of RNAase/DNAase-free water. Plate was sealed with iCycler iQ optical tape and placed on a CFX-96 thermal cycler (Bio-Rad) for the following reaction: 95°C - 30 sec, 95°C - 1 sec, 57°C - 25 sec, 49 repeats of steps 2 - 3, 95°C - 60 sec, 65°C for 60 sec, finally 65 - 95°C with stepwise 0.5°C increments for 5 sec. Melting curves for products were generated automatically from the stepwise increase in temperature. qPCR products were quantified from repeats of step 2 and 3, by monitoring the increase in fluorescent signal intensity. This provided the cycle threshold value (Ct). Ct value is defined by the point at which the fluorescent signal generated during repeat cycles is significantly higher than the base line fluorescence and the increase in fluorescence is exponential. It is inversely proportional to the amount of cDNA present in the sample. Ct was used for the calculations of relative mRNA levels using delta-delta Ct method (Yuan et al., 2006). Target mRNA levels were normalised using measurements of control genes expression such as *Actb* (β-actin) and *Hprt1* (hypoxanthine phosphoribosyltransferase 1).

3.2.1.8 DNA mutagenesis

Mutagenesis was performed by Dr. Mark Peggie and Dr Maria Deak using the QuikChange site-directed mutagenesis method (Papworth et al., 1996) and verified by DNA sequencing.

3.2.1.9 DNA sequencing

Sequencing of either plasmid or PCR product DNA was performed by the Sequencing Service (College of Life Sciences, University of Dundee) using DYEnamic ET terminator chemistry (Amersham BioSciences, Buckinghamshire, UK) on automated DNA sequencers (Applied Biosystems, Warrington, UK). For DNA sequences containing a high GC content (typically > 75%), 10% (v/v) of GC-melt solution (Clontech, Mountain View, USA) was added to the sequencing reaction.

3.2.1.10 Agarose gel electrophoresis

An appropriate amount of agarose (0.5-2% agarose gel) was boiled in 1x TAE buffer. 1x SYBR-safe (Invitrogen) was added and this solution poured into a plastic mold. Electrophoresis was carried out at 90 V for 40-60min.

3.2.1.11 Generation of adenovirus

Generation of recombinant adenovirus was carried out using AdEasy system. Briefly, the gene of interest was cloned into the pCMV shuttle vector. The resultant plasmid (5 µg) was linearised by incubation with *Pme*1 and subsequently transformed into BJ5183 cells by electroporation to generate homologous recombination with the AdEasy-1 virus genome. The BJ5183 cells are competent E.Coli already transformed with adenoviral backbone vector AdEasy-1. AdEasy-1 is an E1 and E3 double-deletion viral vector. This deletion makes the virus replication defective; hence AdEasy-1-derived recombinant adenovirus can only be propagated in E1-expressing packaging cells such as HEK293 or Ad293. Multiple clones from transformed BJ5183 cells were screened for correct homologous recombination by kanamycin resistance and expected appropriate (high) molecular size in agarose gel electrophoresis. Further confirmation of correct recombination was obtained by DNA sequencing and restriction digest analysis. DNA (5 µg) from the confirmed recombinant clone was linearised with *Pac*1 and transfected into the E1-expressing packaging cell line Ad-293 (1x T25 flask, 60% confluence) using PEI as described in section 3.2.2.3. Cells were harvested with a cell scraper after 7-10 days, centrifuged at 500 *g* for 10 min at 4°C and re-suspended in 2 ml PBS. Adenoviruses were extracted from these cells with four cycles of freeze-thaw-vortex. Each cycle comprised of freezing the cells in a dry-ice/methanol bath, thawing in a 37°C water bath and vortexing vigorously (30 sec). Finally, the cell debris were removed by centrifugation at 500 *g* for 10 min at 4°C. The resultant viral lysates were stored in -80°C.

3.2.1.12 Adenovirus amplification and purification

High-titer recombinant adenoviruses were generated from the initial stock of low-titer viral lysates by step-wise amplification in Ad-293 cells and finally purified using cesium chloride (CsCl) banding according to the protocol described by luo and colleagues (Luo et al., 2007). Three rounds of step-wise amplification were performed with increasing number of cells. Viruses were harvested and viral lysates were prepared after each round as described in section 3.2.1.11. For the first round, all the initial stock of viral lysates generated was used to infect 1x T25 flask (80% confluence cells). For the second round 3x T75 flasks (80% confluence cells) were infected with the viral lysates from the 1st round and for the final round 8x T175 flasks (100% confluence cells) were infected with the viral lysates from the 2rd round. Cells from the final round were harvested and resuspended in 8 ml PBS. Viruses were extracted with four freeze-thaw-vortex cycles and cell debris were removed by centrifugation at 7000 *g* for 10 min at 4°C.

Ultra pure CsCl (4.4 g) was added to 8 ml of viral lysates and the solution centrifuged at 176000 *g* for 24 h at 4°C in a polyallomer tube containing a mineral oil cushion. The band of concentrated virus was isolated and diluted with an equal volume of 2x viral storage buffer (Table 3-1). Purified viruses were aliquoted and stored at -80°C.

3.2.1.13 Approximation of viral titer

The approximation of virus titer was determined by spectrophotometry. Optical density (OD) of purified viral stock was measured at 260 nm. To measure OD, 15 µl of virus was added to 15 µl of blank solution [Blank Solution = 1.35 g/ml CsCl mixed with an equal volume of 2x storage buffer] plus 100 µl TE buffer (10 mM Tris-HCl, pH 7.5, 1 mM EDTA) and 0.1% SDS. Mixture was vortexed for 30 sec and centrifuged for 5 min at 13000 rpm before measuring the OD. One OD unit contains ~ 10^{12} viral particles per ml. The ratio of total viral particles to infectious particle is approximately 20:1. This method only provided an estimation of the viral titer.

3.2.2 Cell manipulations

3.2.2.1 General cell culture

HEK293, Ad-293 and HeLa cells were cultured in Dulbecco's Modified Eagle Medium (DMEM) supplemented with 10% (v/v) fetal bovine serum (FBS), 2 mM L-glutamine, 100 U/ml penicillin and 0.1 mg/ml streptomycin. They were maintained in T75 flasks at 50-80% confluence for maximum of 20 passages. The cells were split at 70-80% confluence and plated in a new dish or flask after an appropriate dilution.

3.2.2.2 Infection with adenovirus

Adenoviruses were added to the cells at a defined multiplicity of infection (MOI). One MOI equals to one infectious viral particle per cell. For overexpression studies in primary hepatocytes, the cells were infected with 5 to 50 viral particles per cell (1:5 to 1:50 MOI) for 16 h prior to cell lysis. For gene silencing studies with Ad-ShRNAi, the cells were infected with 1:10 to 1:30 MOI for 48 h prior to cell lysis.

3.2.2.3 Transfection of cells

HEK293 or Ad293 cells were transfected using 25-kD linear PEI. PEI stock (1 mg/ml) was prepared in 20 mM Hepes, pH 7.0 and sterilised by filtration (0.22 µm). Aliquots of PEI were stored at -80°C. 4-6 h prior to transfection, the cells were seeded into 10-cm dishes at 50-60 % confluence (5 x 10^6 cells). 5 µg of DNA was incubated with 20 µg of PEI in 1 ml of serum-free and antibiotic-free DMEM for 30 min at room temperature. This mixture of PEI and DNA was added dropwise to the cells and harvested 36 h post transfection.

3.2.2.4 Treatment with growth factors, hormones or kinase inhibitors

The cells were serum starved overnight before stimulating with hormones, growth factors or kinase inhibitors. Primary mouse hepatocytes were treated with 10 nM insulin or 100 nM glucagon for the time indicated in the figure legends while HEK293 and HeLa cells were treated with 50 ng/ml IGF1 or 10 µM forskolin to stimulate PI3 kinase or PKA pathway respectively. For

inhibitor experiments cells incubated with an equivalent amount of carrier DMSO as a control. The cells were pretreated with kinase inhibitor for the duration indicated in the figure legends (usually 1-2 h) before stimulating with growth factors or hormones.

3.2.2.5 Cell lysis

Medium was aspirated and the cells were rinsed once with ice-cold PBS. The cells were subsequently lysed on ice using ice-cold lysis buffer (Table 3-1). Whole-cell lysate was cleared of insoluble particles by centrifugation at 4°C, 13000 rpm for 10 min. The supernatant was removed and stored at -80°C.

3.2.2.6 Cell fractionation

Differential centrifugation was used to isolate nuclear, membrane and cytoplasmic cellular compartments. Cells were lysed in 200 µl of homogenisation buffer (table xxx) and were passed through a 21 G needle 10 times. Low-speed centrifugation of these homogenates was performed at 1000 *g*, 4°C for 5 min. The resultant pellet contained the nuclear fraction and the supernatant contained the cytoplasmic and membrane fractions of the cells. Nuclear fraction was suspended in 200 µl of RIPA buffer (table xxx) and sonicated twice for 5 sec (amplitude 35%, 2 min interval). The supernatant (200 µl) from low-speed centrifugation was centrifuged at 100000 *g*, 4°C for 1 h to separate the membrane fraction (pellet) and cytoplasmic fraction (supernatant). The membrane fraction was suspended in 200 µl of RIPA buffer and sonicated twice for 5 sec (amplitude 35%, 2 min interval). The supernatant from high-speed centrifugation contained soluble cytoplasmic fraction. Thus, 200 µl of whole-cell homogenates were divided into three equal volumes of membrane, cytoplasmic and nuclear fractions. Hence, this method allowed estimation of abundance of a protein-of-interest between these cellular fractions by maintaining the same volume of buffer to suspend each cellular fraction.

3.2.2.7 Measurement of glucose production in primary hepatocytes

Primary mouse hepatocytes were plated in 12-well plates at a density of 1.25 x 10^5/well. 4 - 6 h later, these cells were serum starved overnight as described in section 3.2.4.1. The next

morning, cells were washed once with 1 ml of PBS (37°C) and 750 µl of G0 medium (DMEM without glucose, 100 U/ml penicillin and 0.1 mg/ml streptomycin, 100 nM dexamethasone, 1 mM sodium pyruvate and 10 mM lactate, pH 7.4) was added per well. The cells were stimulated with kinase inhibitors, 100 µM Bt_2-cAMP or 100 nM glucagon for 8, 12 or 24 h. The culture medium was then collected for measurement of glucose while the hepatocytes were lysed with 100 µl of lysis buffer to measure total protein per well. Glucose in the medium was measured using the Hexokinase / glucose-6-phosphate dehydrogenase (G-6-PDH) method (Altarejos and Montminy, 2011; Chrapkiewicz et al., 1982; Deeg et al., 1980; Dentin et al., 2007; Iynedjian and Hanson, 1977; Johannessen et al., 2004; Koo et al., 2005; Liu et al., 2008). Hexokinase catalyses the phosphorylation of glucose using ATP, producing ADP and glucose-6-phosphate. The resultant, Glucose-6-phosphate is oxidised to 6-phosphogluconate with the reduction of NAD^+ to NADH by G-6-PDH. The amount of NADH formed is proportional to the concentration of glucose in the sample and can be measured by the increase in absorbance at 340 nm.

The assay was performed in 96-well plates by combining 50 µl of cell culture medium with 150 µl of reaction mixture (Infinity Glucose Hexokinase Liquid Stable Reagent, Thermo Scientific). After 15 min at RT, absorbance was measured at 340 nm. The glucose concentration was calculated by calibration against a glucose standard curve generated in the same assay. The final glucose concentration was normalised to the total protein content of the well and the final data was presented as a percentage difference of the basal value (non-treated cells).

3.2.2.8 Immunofluorescence of primary hepatocytes

Primary mouse hepatocytes were fixed on glass coverslips with 3.7% paraformaldehyde after the treatment indicated in figure legends. Cells were washed three times with PBS containing 5% (w/v) BSA followed by incubation with 0.1% NP-40 in PBS for 5 min. Subsequently, cells were blocked with PBS containing 5% (w/v) BSA for 20 min and incubated with primary antibodies as indicated in figure legends (at dilution of 1:500) for 1h at 37°C. Excess antibodies were removed by washing the cells three times with PBS containing 5% (w/v) BSA. This was

followed by a 30 min incubation with secondary antibody (Alexa Fluor 488 anti-rabbit, Invitrogen cat no A11008). Subsequently the cells were washed a further three times with PBS containing 5% (w/v) BSA before mounting the cover slips on a glass slide with mounting media containing DAPI (4',6-diamidino-2-phenylindole) (Invitrogen cat no. P36931). Cells were later analysed with a Nikon Eclipse Ti fluorescent microscope and images were captured using Nikon NIS.Elements BR 3.1 software. The images were cropped using photoshop CS5.1 for subsequent use.

3.2.3 Protein manipulations

3.2.3.1 Purification of GST-fusion proteins from HEK293 cells

HEK293 cells were lysed 36 h post transfection with pEBG vectors coding for GST-SIK isoforms. The recombinant proteins were then purified by affinity chromatography on glutathione-sepharose beads. Lysates were incubated with beads for 1 - 2 h at 4°C, prior to centrifugation at 4°C, 7000 rpm for 1 min. The resultant pellets were washed four times with 0.5 M NaCl supplemented lysis buffer and twice with buffer A (Table 3-1). Finally, GST-fusion proteins were eluted by incubating beads with an equal volume of elution buffer (Table 3-1) for 10 min at room temperature. This was repeated three times to ensure complete elution and supernatants pooled. Purified proteins were snap frozen and stored at -80°C. Protein concentration was estimated by comparing it with known BSA standards on SDS-PAGE followed by colloidal coomassie staining of the gel.

3.2.3.2 Purification of GST-fusion protein from E.Coli

BL21 cells were transformed with pGEX-6P vector and the colonies were selected with ampicillin resistance as described in section 3.2.1.1. A single colony was incubated in 5 ml LB-medium with 100 µg/ml ampicillin over night at 37°C in an orbital shaker (200 rpm). This starter culture was added to 1 L of LB-medium with ampicillin and incubated at 37°C in an orbital shaker (200 rpm) till the OD reached 0.6 - 0.8.

250 µM IPTG was added to the medium (cooled to 15°C) to induce expression of protein and it was incubated at 15°C overnight in an orbital shaker (200 rpm). The next day, medium was centrifuged at 4200 rpm for 25 min at 10°C to pellet the cells. The cells were lysed with 30 ml of lysis buffer (Table 3-1) and proteins were further extracted by sonication for 2 min (amplitude 35%). The lysate was cleared by centrifugation at 25000 *g* for 25 min. The resultant lysate was incubated with glutathione-sepharose beads for 1 h at 4°C. Beads were then washed five times with 250 mM NaCl supplemented lysis buffer and twice with exchange buffer (Table 3-1). Finally, GST-fusion proteins were eluted with equal amount of elution buffer (exchange buffer plus 10 mM L-glutathione) at room temperature for 10 min. This was repeated five-seven times to ensure complete elution and supernatants pooled. Proteins were snap frozen and stored at -80°C. Protein concentration was estimated by comparing it with known BSA standards on SDS-PAGE followed by colloidal coomassie staining of the gel.

3.2.3.3 Quantification of protein concentration

The protein concentration of cell lysates was determined using Bradford method (Bradford, 1976). This method is based on the observation that when coomassie brilliant blue G-250 dye binds to protein in an acidic medium, there is a shift in the absorption maximum from 465 nm to 595 nm and the colour changes from brown to blue. Assays were performed in 96-well plates with 10 µl of 1:20 diluted lysate incubated for 5 min with 200 µl of Bradford reagent. A standard curve was generated using BSA standards in the same assay to calculate protein concentration for the protein lysates from the absorbance value at 595 nm.

3.2.3.4 Immunoprecipitation of recombinant protein.

0.2 - 0.5 mg of lysate from the cells transfected with GST, HA or Flag-tagged proteins was incubated with either 5µl anti-Flag-agarose, glutathione-sepharose or anti-HA-agarose beads for 1 h at 4°C, prior to isolation by centrifugation at 7000 rpm for 1 min. The resultant precipitates were washed twice with 0.5 M NaCl and 1 mM DTT supplemented lysis buffer and

twice with Buffer A supplemented with 1 mM DTT (Table 3-1). Immunoprecipitates were either used for *in vitro* kinase assay or suspended in a laemmli buffer for immunoblot analysis.

3.2.3.5 Immunoprecipitation of endogenous protein.

2 - 3 µg of appropriate antibody or pre-immune IgG (as a control) was incubated with 5 µl of protein G-sepharose for 1 h at 4°C in an orbital shaker. This mixture was then added to 0.5 - 2 mg of lysate and further incubated at 4°C for 1 h prior to isolation by centrifugation. The resultant precipitates were washed and used in downstream applications as described in section 3.2.3.4.

3.2.3.6 SDS Polyacrylamide Gel Electrophoresis (PAGE)

SDS-PAGE is used to separate proteins on the basis of their apparent molecular weight. The anionic detergents, SDS and LDS, bind to the proteins linearising the polypeptide and giving them a negative charge at physiological pH that enables them to be electrophoresed toward an anode. Linearisation means that the speed of migration of the polypeptide through a polyacrylamide gel matrix is a linear function of the logarithm of its molecular weight, with smaller proteins migrating faster than larger proteins through the acrylamide matrix pores.

Lysates or immunoprecipitates were denatured in a laemmli buffer at 70°C for 5 min. Samples (20-40 µg) were loaded onto Tris-glycine gels (6-12%) along with a protein standard and resolved at 100 V for 10 min followed by 150 V for 1 h.

3.2.3.7 Colloidal Coomassie staining of SDS-PAGE gels

SDS-PAGE gels were incubated in fixing solution (10% acetic acid, 40% methanol) for 1 h. Subsequently, the gels were placed in freshly prepared colloidal coomassie staining solution (Table 3-1) and incubated overnight on a gentle shaking platform. The gels were de-stained with several changes of 1% acetic acid solution and scanned on a Li-Cor Odyssey infrared system (LI-COR Biosciences, UK) for imaging and quantification.

3.2.3.8 Immunobloting

The proteins from the SDS-PAGE gels were electrotransfered to a nitrocellulose membrane in a transfer buffer using a Bio-rad mini-transblot system. The membrane was blocked with 5% skimmed milk, TBS-T for 1 h at room temperature followed by incubation with the indicated primary antibodies in 5% skimmed milk or 5% BSA, TBS-T overnight at 4°C. Thereafter, the membrane was washed twice for 10 min with TBS-T followed by incubation with appropriate HRP-conjugated secondary antibody in 5% skimmed milk, TBS-T for 1 h at room temperature. Unbound antibody was removed with two 10 min washes with TBS-T. HRP was activated by addition of ECL to the membrane and the signal was detected by exposing the membrane to X-ray films.

3.2.3.9 Protein Kinase assays with peptide substrates

Quantification of peptide substrate phosphorylation was achieved by measuring the incorporation of radioactive ^{32}P from [$\gamma^{32}P$]-labelled ATP into a substrate peptide. The kinase assays were carried out in a final volume of 50 µl containing 15 µl of protein kinase (purified or immunoprecipitated as described in section 3.2.3.5) and 35 µl of master-mix. The master-mix contained 200 µM of appropriate peptide substrate, 50 mM Hepes, 0.1 mM EGTA, 10 mM magnesium acetate and 0.1 mM [$\gamma^{32}P$]-labelled ATP. Control reactions either lacked purified kinase or contained pre-immune IgG coupled beads. The phosphorylation reactions were initiated by adding master-mix to the protein kinase and incubating on thermomixer at 30°C for the indicated times (usually 20 min). These reactions were terminated by spotting 40 µl of mixture onto a 2 cm^2 P81 phosphocellulose papers (which binds substrates that contain a net basic charge at acidic pH) and immersing them in 75 mM orthophosphoric acid to remove unreacted ATP. P81 papers were washed three times for 10 min with 75 mM orthophosphoric acid and finally in acetone for 5 min. P81 papers were air-dried and the incorporation of ^{32}P into a peptide substrate was determined by Cherenkov counting. Results were expressed in

mU/mg protein where 1 mU equals to 1 pmol of phosphate incorporation into a substrate in one min at 30°C.

3.2.3.10 Protein kinase assays with protein substrate

The assay composition was similar to that described in section 3.2.3.9 except a specified amount of purified full-length protein (usually 0.5 – 1 µg) was used as a substrate instead of peptide in the kinase assay. The assay was carried out as described in section 3.2.3.9 except the termination of phosphorylation reaction was carried out by addition of 1x laemmli buffer. The samples were incubated at 70°C for 5 min and then subjected to SDS-PAGE.

Once the electrophoresis was completed, the gels were colloidal coomassie stained and scanned for future reference. These gels were then placed between two sheets of cellophane and dried in a GelAir Dryer to improve the autoradiographic signal. The dried gels were placed in X-Omat autoradiography cassette and exposed to Hyperfilm MP at -80°C for different length of time. Finally, the gel bands that corresponded to radiographic signals were cut and their ^{32}P incorporation was determined by Cherenkov counting.

3.2.3.11 Immunoprecipitation of HA-SIK2 for mass spectrometry

Primary mouse hepatocytes were infected with Ad-SIK2 at 1:25 MOI for 16 h. These cells were stimulated with 10 nM insulin or 100 nM glucagon for 10 min and lysed with lysis buffer (Table 3-1). HA-SIK2 was immunoprecipitated from 5 mg of lysates with 30 µl of HA-agarose beads as described in section 3.2.3.4. These beads were heated with 1x NuPAGE LDS sample buffer and 10 mM DTT for 5 min at 70°C. Samples were further incubated with 50 mM iodoacetamide for 30 min to alkylate cysteine residues and electrophoresed on NuPAGE 4-12% Bis-Tris gel. This gel was colloidal coomassie stained and HA-SIK2 band was excised and processed as below.

3.2.3.12 Sample preparation for mass spectrometry

The samples were prepared in a laminar flow hood to reduce contamination. The gel pieces were cut and washed for 10 min with 500 µl of water, 50% acetonitrile/water, 0.1 M ammonium bicarbonate (NH_4HCO_3) and 50% acetonitrile/50 mM NH_4HCO_3. Washes were

carried out on a vibrax-shaking platform and all liquid was removed between the washes. The final step was repeated until the gel pieces were colourless. 0.3 ml acetonitrile was added to these gel pieces and removed after 15 min. The gel pieces were dried in a centrifugal-evaporator (Speed-Vac). The protein in the dried gel pieces was digested in 30 µl of 25 mM triethylammonium bicarbonate containing 5 µg/ml of trypsin at 30°C overnight on a shaking platform. Subsequently, an equivalent volume of acetonitrile was added for 15 min. The supernatant was collected in a clean tube and dried using a Speed-Vac. Meanwhile 100 µl 50% acetonitrile/2.5% formic acid was added to the gel pieces, incubated for 15 min. The supernatant was combined with the first dried extract and dried in a Speed-Vac and stored at -20°C.

3.2.3.13 Phosphopeptide mapping by mass spectrometry

Mass spectrometry (MS) analysis was carried out by Dr David Campbell (MRC PPU, University of Dundee, UK). Phosphopeptides and their approximate relative abundances were initially identified by LC-MS-MS mass spectrometry on an Applied Biosystems 4000 QTrap coupled to a Dionex Ultimate 3000 liquid chromatography system. The MS was set up to use a precursor ion scan of m/z 79 in negative ion mode followed by an ion trap high resolution and a high sensitivity MS-MS scan in positive mode (Williamson et al., 2006). Phosphopeptides were also further analysed by LC-MS-MS on a Thermo LTQ-Orbitrap Classic equipped with a nanoelectrospray ion source (Proxeon Biosystems) and coupled to a Proxeon EASY-nLC system. Multi-Stage-Activation was used to provide an MS3 scan of any parent ions showing a neutral loss of 48.9885, 32.6570, 24.4942, allowing for 2+, 3+ and 4+ charge states respectively. The resulting MS3 scan was automatically combined with the relevant MS2 scan prior to data analysis. Results were searched against an in house database containing the SIK sequences using the Mascot algorithm (www.matrixscience.com) to identify peptides. Phosphorylation sites on the peptides were also analysed with Xcalibur software (Thermo Scientific)

3.2.3.14 Sequence alignment

All protein sequence alignments were generated using Jalview 2.4 developed by Geoff Barton Group (University of Dundee, Dundee, UK). The ClustalW Multiple sequence alignment algorithm was used and the sequences were retrieved from UniProt using the indicated accession numbers.

3.2.4 Animal manipulations

Mice were maintained under specific pathogen-free conditions. Routine animal care and welfare was carried out by the staff in the Biological unit, College of Life Science (University of Dundee). All procedures were carried out in accordance with the University of Dundee and the United Kingdom Home Office regulations

3.2.4.1 Primary mouse hepatocytes isolation

Primary mouse hepatocytes were isolated from male 6-10 week old mice.

A bubble-free connection of tubes was prepared to allow perfusion of liver prior to mouse dissection. The first part of this tubing was made of platinum-cured silicone tube (3.2 mm tube bore). One end was submerged in a pre-warmed buffer (37°C) and the other end passed through a peristaltic pump and connected to an intravenous (IV) infusion set containing a drip chamber with 100 µm filter.

The drip chamber acted as a reservoir to prevent air entry into the subsequent tubes as well as a filtering device. The IV set was cut at 60 cm distal to the drip chamber and was connected to a 0.22 µm syringe filter, which was further connected to a 25 G needle (winged with 30 cm tubing length). This needle was used to cannulate inferior vena cava after mouse dissection. This design enabled mouse liver perfusion with sterile buffer in a bubble free environment.

Once the tubing was prepared, a mouse was terminally anaesthetised by an intraperitoneal injection of 100 mg/kg pentobarbital. Liver, inferior vena cava and portal vein were exposed by dissecting the skin and peritoneum. The 25 G needle was inserted into the inferior vena cava, secured with a clamp and perfused with pre-warm wash buffer (10 mM Hepes pH 7.65, 137

mM NaCl, 7 mM KCl, 0.7 mM sodium phosphate dibasic, 0.1 mM EDTA) at a flow rate of 5 ml/min for 10 min. Portal vein was cut immediately after starting the perfusion to create an outlet for the buffer and the superior vena cava was clamped to isolate the hepatic system. After 10 min, the liver was perfused with 50 ml of digestion buffer (10mM Hepes pH 7.65, 137 mM NaCl, 7 mM KCl, 0.7 mM sodium phosphate dibasic, 0.1 mM EDTA, 5 mM $CaCl_2$ and 0.4 mg/ml collagenase A). The digested liver was dissected out of the mouse body and transferred to a tissue culture hood. This liver was gently agitated to disperse the hepatocytes in 50 ml plating medium [M199 with glutamex supplemented with 100 U/ml penicillin, 0.1 mg/ml streptomycin, 0.1% (v/v) BSA, 10% (v/v) FBS, 10 nM insulin, 200 nM triidothyronin, 500 nM dexamethasone]. Hepatocytes were filtered through a 100 µm cell strainer and pelleted at 400 rpm for 2 min. The supernatant was discarded and the pellet was gently resuspended in 25 ml of plating medium. Viability and concentration of the hepatocytes were measured by 0.04% trypan blue staining and counting of the cells using a hemocytometer. Preparations were required to have a cell viability ≥ 90% to be used for experiments. The cells were plated at a density of 1.25 x 10^5 for 12-well plates, 2.5 x 10^5 for 6-well plates or 15 x 10^5 for 10-cm dishes in 1, 2 and 10 ml of plating medium respectively. After 4-6 h of incubation at 37°C and 5% CO_2, the plating medium was replaced with overnight medium (M199 with glutamex supplemented with 100 U/ml penicillin, 0.1 mg/ml streptomycin and 100 nM dexamethasone).

3.2.4.2 Preparation of tissue lysate

Tissues of interest were swiftly collected by surgery following sacrifice of the animal and were immediately snap frozen. Frozen tissues were homogenised during thaw in ice-cold lysis buffer using a Polytron homogeniser (Kinematica, Lucerne, Switzerland) for 15 sec. 20-fold mass excess of lysis buffer was used for the liver, 15-fold mass excess for the heart and 10-fold mass excess for the remaining tissues. Tissue homogenates were cleared by centrifugation at 4°C, 13000 rpm for 10 min. The supernatant was collected, snap frozen and stored at -80°C.

3.2.4.3 Statistical analysis

The number of repeats for every experiment varied and are given in the figure legends, but all the experiments presented in this thesis were performed at least twice. Comparisons of means were carried out with either Student's t-test or One-way ANOVA and error bars indicated standard deviation (SD) or standard error of the mean (SEM) as described in the figure legends. Analysis was conducted with Microsoft Excel or Graphpad Prism software.

4 Generation and characterisation of SIK antibodies and investigation of hormonal-regulation of SIK2 in liver

4.1 Introduction

Recent work has proposed that SIK2 plays a key role as a signalling-mediator in the hormonal-regulation of hepatic gluconeogenesis (Altarejos and Montminy, 2011; Dentin et al., 2007; Koo et al., 2005; Liu et al., 2008), although molecular regulation of SIK isofoms by hormones are poorly understood. Comprehensive understanding of the regulation and roles of SIK isoforms (SIKs) requires validated and isoform-specific antibodies for SIKs. The lack of specificity of commercial antibodies to their intended targets has been demonstrated in various studies, highlighting the need to validate the antibodies before they can be reliably employed (Grimsey et al., 2008; Jensen et al., 2008; Jositsch et al., 2008). Multiple editorials and reviews have strongly supported this notion and have also proposed the following criteria that can be employed to validate an antibody using immunoblotting (Bordeaux et al., 2010; Couchman, 2008; Michel et al., 2009; Saper, 2005).

1) The gold standard criteria to assess the specificity of an antibody is the disappearance of the signal in a gene-targeted knock-out cell/animal of the target protein upon immunoblotting.
2) Significant reduction in the signal upon knock-down (using RNAi technology) of the protein of interest can be used where knock-out cell/animal model is not available.
3) The selectivity of the antibody can be confirmed by immunoblotting target protein vs. related isoforms or subtypes expressed in the same cell line/tissue.

4) For phospho-specific antibody, specificity can be assessed using a respective phosphorylation-defective mutant and also by detecting the signal following a treatment that induces phosphorylation or a lack of signal following treatment with phosphatases.
5) Antibody should be validated in the intact tissue/cell-line from the species intended to be used in the study.

So far SIK2 has been demonstrated to be regulated by phosphorylation on four different residues Thr175, Ser358, Ser587 and Thr484; discussed in detail in section 1.5.5. The proposed PKA-regulated site (Ser587), Akt-regulated site (Ser358) and CaMKI/IV-regulated site (Thr484) were identified retrospectively following an analysis of the SIK2 amino acid sequence for kinase-specific generic consensus motifs (Dentin et al., 2007; Sasaki et al., 2011; Takemori, 2002). So far, most of the studies on the hormonal-regulation of SIK2 were extra-hepatic and lacked consensus on the details of molecular mechanism of regulation. Therefore, rigorous investigation into the hormonal-regulation of SIK2 in the liver/hepatocytes is required.

The objectives of this chapter are as follows:

1) To identify specific and selective antibodies to SIK isoforms that will allow accurate and efficient immunoblotting and immunoprecipitation of endogenous SIK proteins in liver, as well as in other tissues and cell lines.

2) To conduct an unbiased detailed investigation of the phosphorylation of SIK2 using mass spectrometry following glucagon or insulin treatment of primary mouse hepatocytes.

3) To validate that the hormone-regulated SIK2 phosphorylation sites identified in cells are also regulated in intact liver using phospho-specific antibodies.

4.2 Results

4.2.1 Characterisation of SIK antibodies

4.2.1.1 Characterisation of SIK2 antibodies

To study the role of SIK2 in liver, two in-house antibodies were generated in sheep using immunogenic peptides based on N-terminal SIK2 sequence (residues 1 - 21 of human SIK2) and C-terminal SIK2 sequence (residues 906 - 926 of human SIK2), respectively (Figure 4.1). In addition, we purchased a commercial antibody that was raised against a sequence at the N-terminus of human SIK2 (antigen sequence unavailable). SIK1, 2, and 3 have a high sequence homology particularly in the N-terminal domain (Figure 4.1). Therefore, to establish the isoform specificity of SIK2 antibodies, immunoblot analysis was carried out against affinity-purified full-length human GST-SIK isoforms using both in-house as well as the commercial SIK2 antibodies (Figure 4.2A). All of the in-house antibodies were specific for SIK2 with no cross-reactivity towards recombinant SIK1 and SIK3 observed at 1 ng load. Whilst the commercial N-terminal antibody was the most sensitive one as it gave the strongest signal against recombinant GST-SIK2 at 10 ng load, it also detected GST-SIK1 at 100 ng load suggesting some cross reactivity. However, it still exhibited a preference for SIK2 in an order of magnitude. In addition, this antibody readily detected endogenous SIK2 on immunoblot analysis of liver extracts from a $SIK2^{+/+}$ (wild-type) mouse (Figure 4.2C). Although the antibodies were generated against the human SIK2 sequence, this result was not unexpected because there is a very high homology of human immunogen sequences with mouse SIK2 sequence (Figure 4.2B). The complete lack of an equivalent band in the liver extracts of $SIK2^{-/-}$ (knock-out) mice in the same immunoblot analysis clearly demonstrated the high specificity of this commercial antibody for SIK2 (Figure 4.2C). The C-terminal in-house SIK2 antibody weakly detected endogenous SIK2 in cell/tissue extracts (even up to 40 μg protein lysate load), while

the N-terminal in-house antibody failed to detect endogenous SIK2 in the same protein lysate (data not shown). Immunoprecipitation

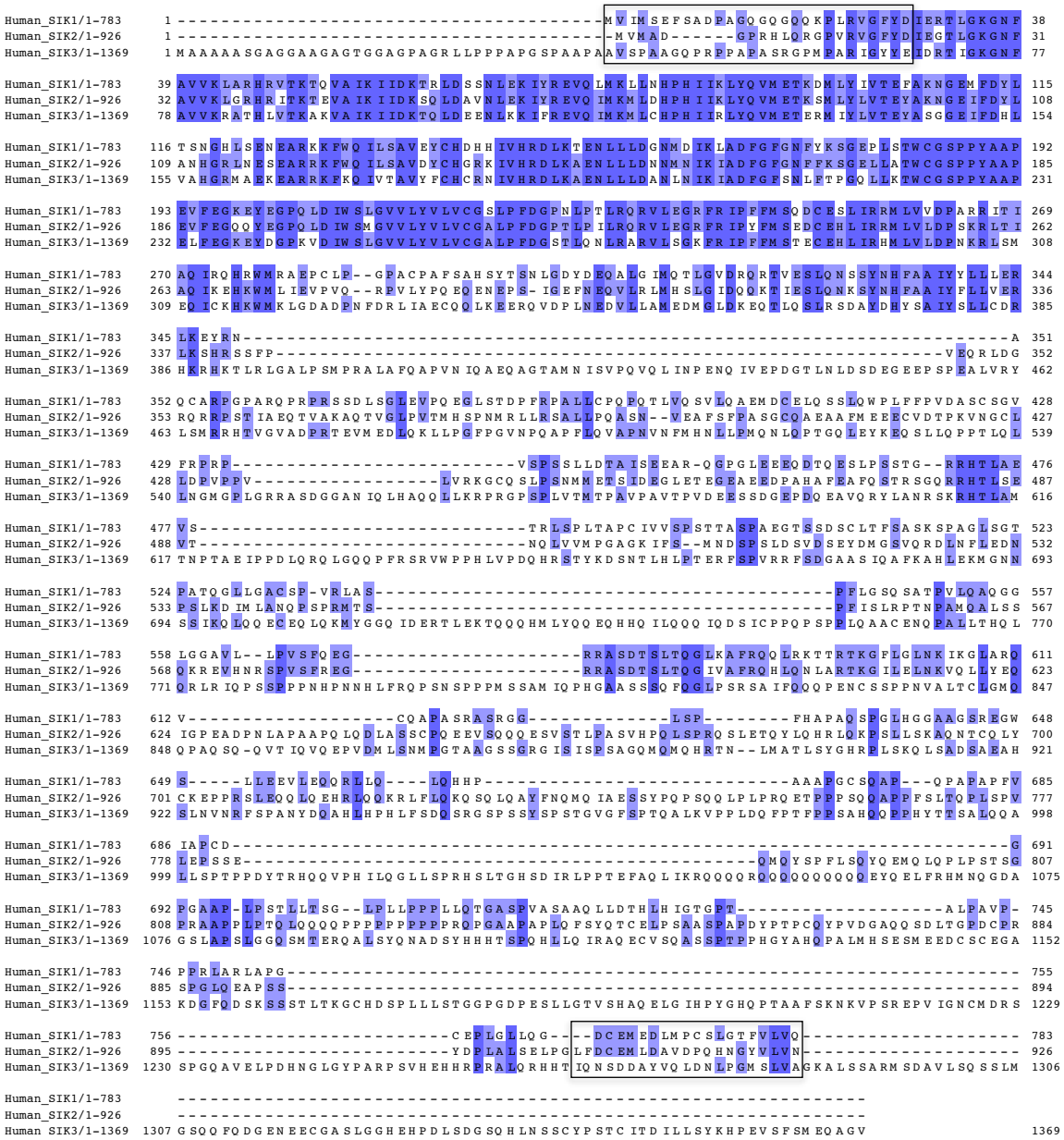

Figure 4.1 Sequence alignment of human SIK isoforms highlighting immunogen sequences of in-house SIK2 antibodies.

Identical residues are shaded in blue. The immunogen sequences are boxed (SIK2 N-terminal in-house antibody, 1 - 21, SIK2 C-terminal in-house antibody, 906 - 926). Human SIK1 and SIK2 sequences were obtained from UniProtKB with the accession numbers P57059 and Q9H0K1, respectively. Human SIK3 sequence was obtained from www.kinase.com. Alignment was performed with Jalview 2.7.

of SIK2 with the C-terminal in-house antibody followed by immunoblot with the N-terminal commercial antibody readily detected a band at an expected molecular mass of SIK2 (~105 kDa), whereas no signal was detected either in immunoprecipitates from SIK2 knock-out

mouse liver extracts or in immunoprecipitates using pre-immune IgG (Figure 4.2C). This confirmed that the detected band was indeed mouse SIK2 protein and validated the C-terminal in-house antibody for endogenous SIK2 immunoprecipitation. Meanwhile, SIK2 kinase activity was measured in the immunoprecipitates of C-terminal antibody from liver extracts to further validate the specificity of the antibody and to ensure it was not an inhibitory molecule. Immunoprecipitates from the wild-type but not SIK2 knock-out mice liver extracts had significant *in vitro* kinase activity (Figure 4.2C). The efficiency of immunoprecipitation was assessed by comparing immunoblots of pre- and post-SIK2 immunoprecipitation supernatants. 2 μg of the SIK2 C-terminal antibody immunoprecipitated more than 50% of endogenous SIK2 from 1 mg of hepatocyte protein lysate (Figure 4.2D).

A

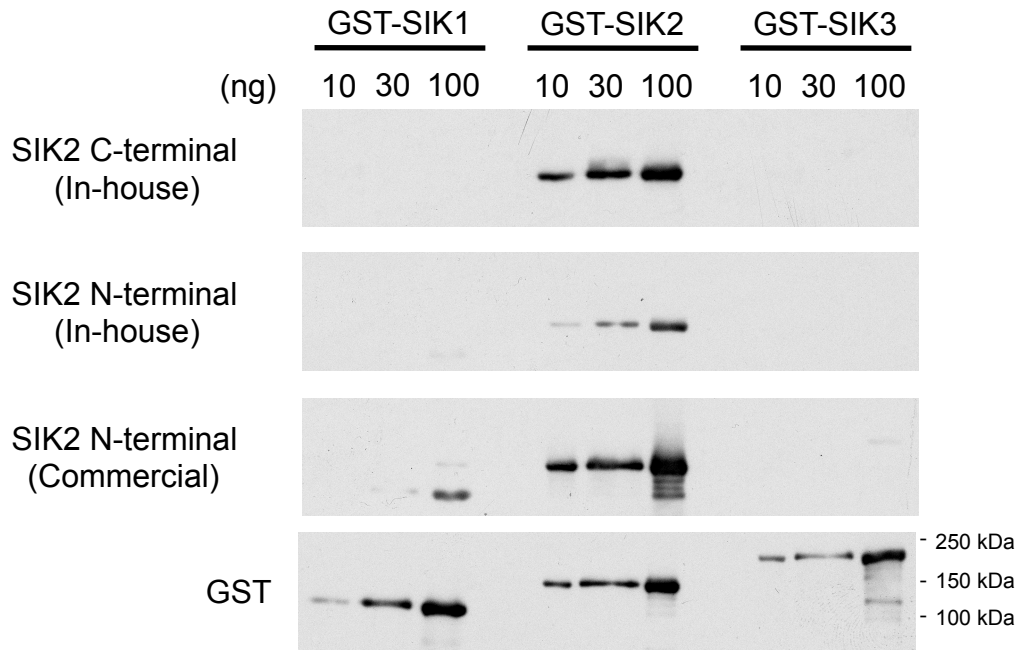

B

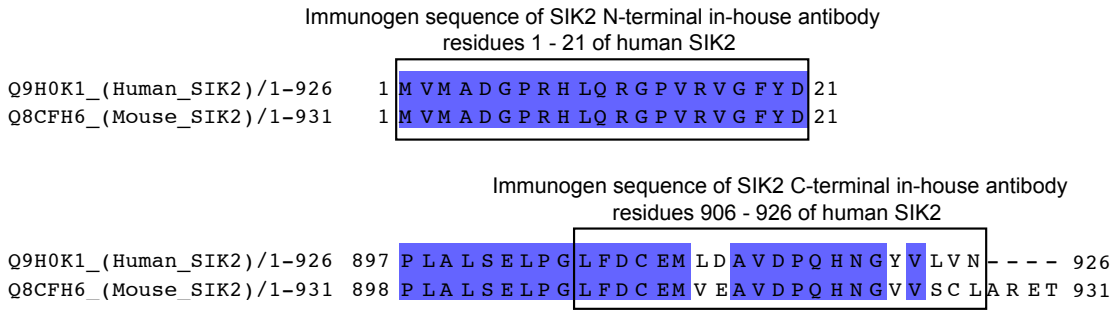

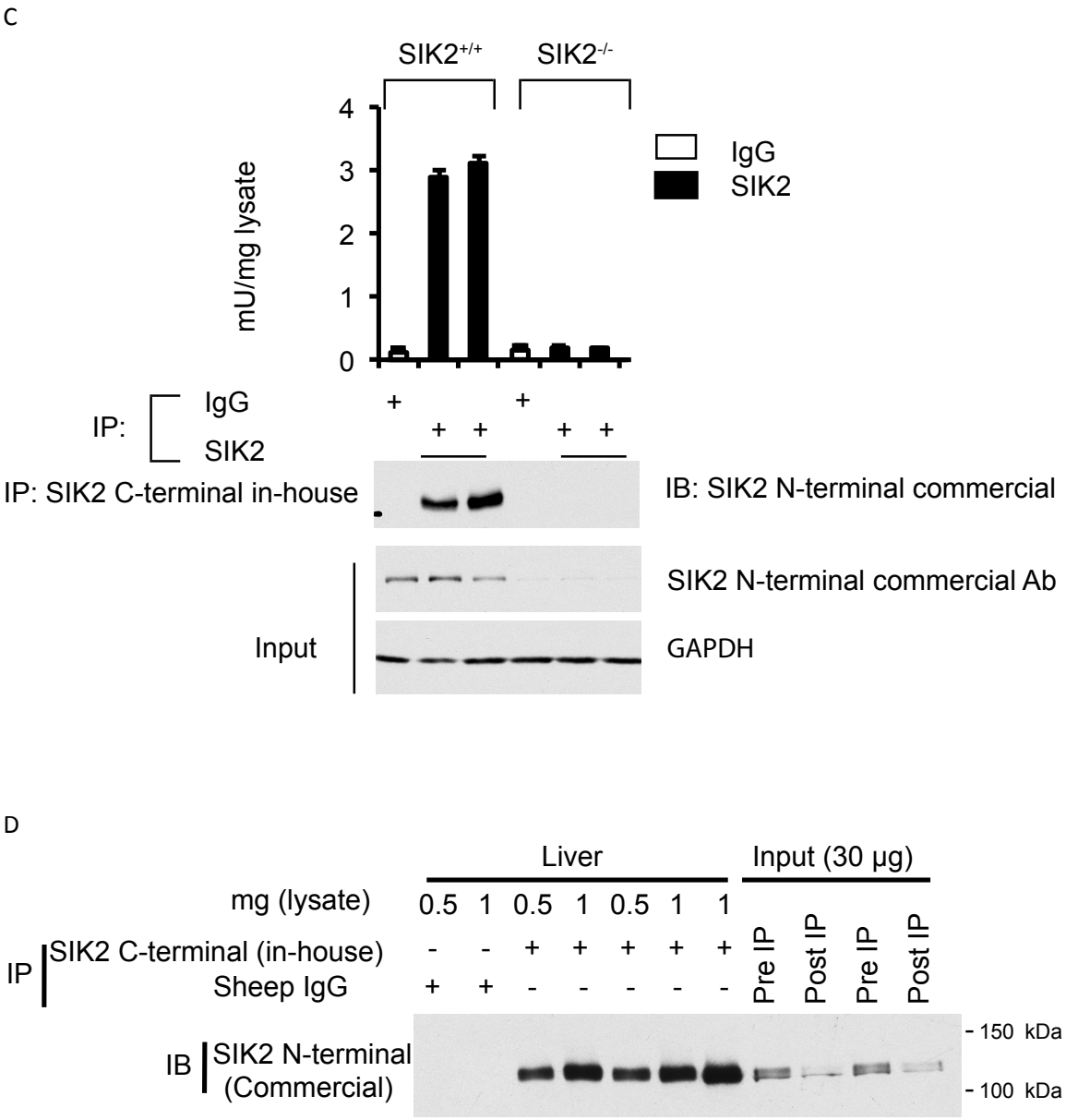

Figure 4.2 Characterisation of SIK2 antibodies.

A) Increasing amounts of affinity-purified full-length GST-SIK1, 2, 3 (expressed in HEK293 cells) were immunoblotted with 1 µg/ml of the indicated SIK2 antibodies and a GST antibody as a loading control. Results are representative of two independent experiments. **B)** Immunogen sequences of SIK2 N-terminal (1 - 21 residues, top panel) and C-terminal (906 - 926 residues, bottom panel) in-house antibodies are boxed within an alignment of the human and mouse SIK2 sequences using Jalview 2.7. Identical residues are shaded in blue, and it was the human sequence that was used as immunogen. **C)** Endogenous SIK2 was immunoprecipitated from 0.5 mg liver homogenates from $SIK2^{+/+}$ or liver-specific $SIK2^{-/-}$ mice using 2 µg of SIK2 C-terminal in-house antibody (Ab) or pre-immune IgG coupled to protein G-sepharose. The resultant immunoprecipitates were subjected to either *in vitro* kinase assay in triplicate for 20 min using 200 µM 'SAKAMOTO'-tide as substrate (data is presented as mean ± SD; n=3, each column represent separate mouse liver) or were immunoblotted with the commercial SIK2 N-terminal antibody. 40 µg of homogenates were loaded as input and immunoblotted for SIK2 and GAPDH as a loading control. The lysates for this experiment were received from Dr Marc Foretz (Institut Cochin - INSERM, France). **D)** Endogenous SIK2 was immunoprecipitated from the indicated amount of wild-type mouse liver homogenates as described in C and immunoblotted with the commercial SIK2 N-terminal antibody. 30 µg of pre-immunoprecipitation (Pre IP) and SIK2 depleted post-immunoprecipitation (Post IP) homogenates were loaded to assess efficiency of IP.

4.2.1.2 Characterisation of SIK3 antibodies

To study the role of SIK3 in liver, two in-house antibodies were generated in sheep against immunogenic peptides based on N-terminal SIK3 sequence (residues 79 - 99 of human SIK3) or C-terminal SIK3 sequence (residues 1349 - 1369 of human SIK3) (Figure 4.3). Cross-reactivity of these antibodies towards SIK1 and SIK2 was assessed by immunoblot analysis using increasing amounts of affinity-purified full-length human GST-SIK isoforms (Figure 4.4A). The N-terminal SIK3 antibody showed higher sensitivity but lacked the selectivity for SIK3 as it detected SIK2 and SIK1 at 100 ng load. In contrast, the C-terminal antibody was selective for SIK3 with no cross-reactivity to SIK1 or SIK2. Despite significant homology between the human and mouse SIK3 sequence for the immunogen sequence used to generate the N-terminal SIK3 antibody (Figure 4.4B), it failed to detect endogenous mouse SIK3 in the primary mouse hepatocyte lysates (Figure 4.4C). In contrast, immunoblotting of the same primary mouse hepatocyte lysates with the C-terminal SIK3 antibody readily detected a band at the expected molecular mass (~150 kDa) of SIK3 (Figure 4.4C). Most importantly, the intensity of this band was significantly reduced in immunoblots of lysates from hepatocytes where SIK3 was selectively depleted via shRNAi, suggesting that the antibody was indeed specific for the SIK3 isoform. The C-terminal SIK3 antibody was able to immunoprecipitate endogenous SIK3 from primary mouse hepatocytes (Figure 4.4C and D). Immunoprecipitation followed by immunoblotting readily detected a band at the expected molecular mass of SIK3, whereas no signal was detected in immunoprecipitates using pre-immune IgG. In addition, immunoprecipitates of SIK3 from primary hepatocytes showed significant *in vitro* kinase activity, whereas the kinase activity of immunoprecipitates from primary hepatocytes where SIK3 had been depleted was profoundly reduced by ~70% (Figure 4.4C). Together, these observations suggest that the C-terminal antibody selectively recognises endogenous SIK3 protein. Finally, the efficiency of immunoprecipitation was assessed by comparing immunoblots of lysates pre- and post-SIK3 immunoprecipitation which showed that 2 µg of the SIK3 C-terminal antibody immunoprecipitated up to 90% of SIK3 from 1 mg of hepatocyte protein lysate (Figure 4.4D).

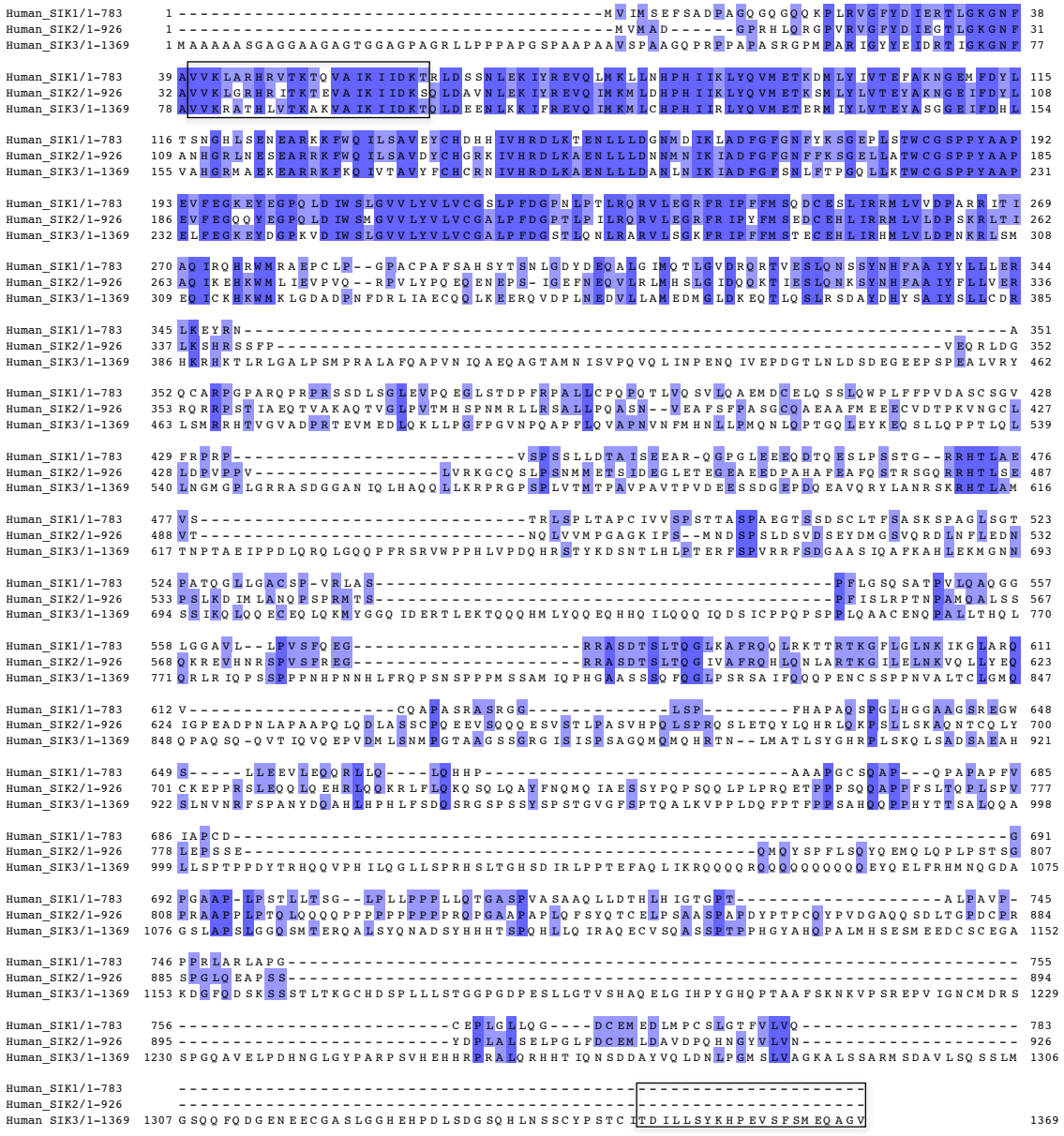

Figure 4.3 Sequence alignment of human SIKs highlighting immunogen sequences of in-house SIK3 antibodies.

Identical residues are shaded in blue. The immunogen sequences are boxed (SIK3 N-terminal in-house antibody, 79 - 99 residues of human SIK3, SIK3 C-terminal in-house antibody, 1349 - 1369 residues of human SIK3). Human SIK1 and SIK2 sequences were obtained from UniProtKB with the accession numbers P57059 and Q9H0K1, respectively. Human SIK3 sequence was obtained from www.kinase.com. Alignment was performed with Jalview 2.7.

A

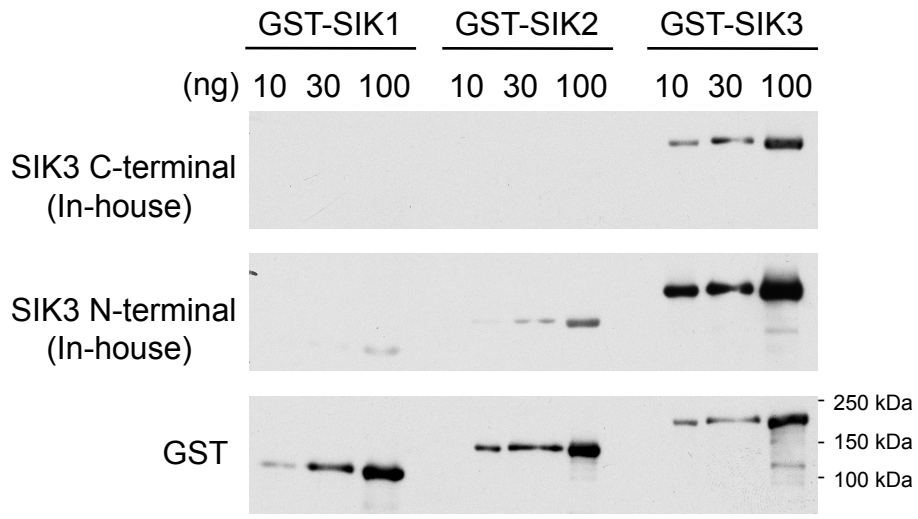
GST-SIK1
GST-SIK2
GST-SIK3
(ng) 10 30 100 10 30 100 10 30 100
SIK3 C-terminal (In-house)
SIK3 N-terminal (In-house)
GST
250 kDa
150 kDa
100 kDa

B

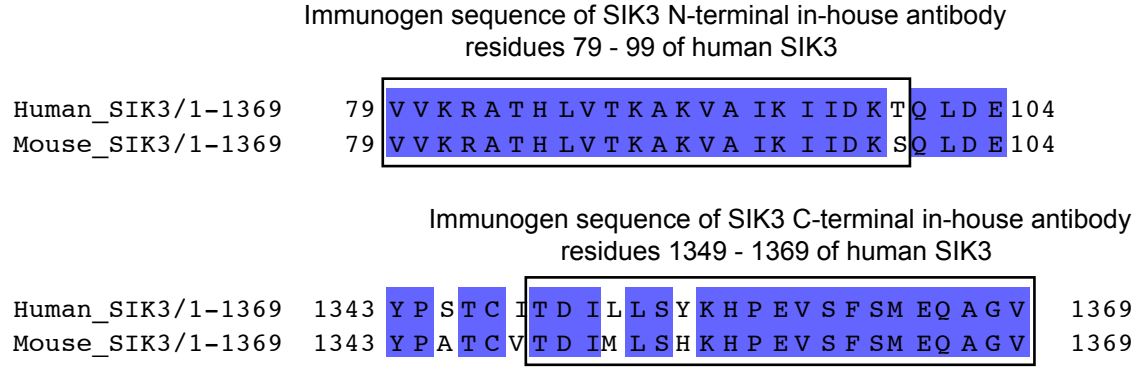
Immunogen sequence of SIK3 N-terminal in-house antibody
residues 79 - 99 of human SIK3
Human_SIK3/1-1369 79 VVKRATHLVTKAKVAIKIIDKTQLDE 104
Mouse_SIK3/1-1369 79 VVKRATHLVTKAKVAIKIIDKSQLDE 104
Immunogen sequence of SIK3 C-terminal in-house antibody
residues 1349 - 1369 of human SIK3
Human_SIK3/1-1369 1343 YPSTCITDILLSYKHPEVSFSMEQAGV 1369
Mouse_SIK3/1-1369 1343 YPATCVTDIMLSHKHPEVSFSMEQAGV 1369

C

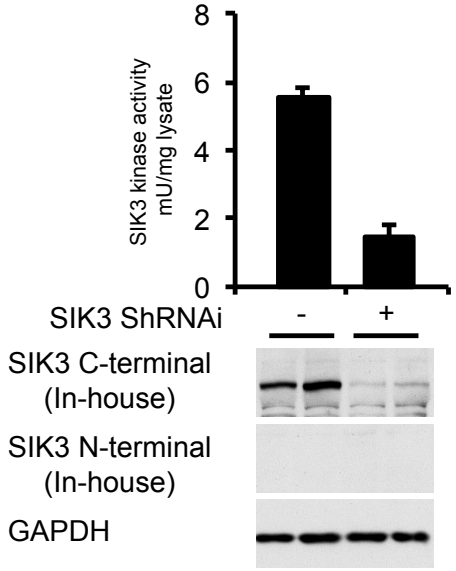
SIK3 kinase activity mU/mg lysate
8
6
4
2
0
SIK3 ShRNAi - +
SIK3 C-terminal (In-house)
SIK3 N-terminal (In-house)
GAPDH

D

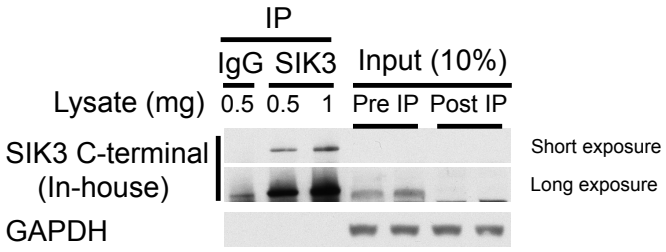
IP
IgG SIK3
Input (10%)
Lysate (mg) 0.5 0.5 1
Pre IP Post IP
SIK3 C-terminal (In-house)
Short exposure
Long exposure
GAPDH

Figure 4.4 Characterisation of SIK3 antibodies.

A) Increasing amounts of affinity-purified full-length GST-SIK1, 2, 3 (expressed in HEK293 cells) were immunoblotted with 1 µg/ml of the indicated SIK3 antibodies and a GST antibody as a loading control. Results are representative of two independent experiments. **B)** Immunogen sequences of SIK3 N-terminal (79 - 99 residues, top panel) and C-terminal (1349 - 1369 residues, bottom panel) in-house antibodies are boxed within an alignment of human and mouse SIK3 sequences using Jalview 2.7. Identical residues are shaded in blue and it was the human sequence that was used as immunogen. **C)** Primary mouse hepatocytes were infected with recombinant adenoviral vector SIK3 ShRNAi or scrambled ShRNAi at 1:30 MOI for 48 h prior to cell lysis. 40 µg of these lysates were immunoblotted with 1 µg/ml of the indicated SIK3 in-house antibodies and a GAPDH antibody as a loading control. Results are representative of three independent experiments. Endogenous SIK3 was immunoprecipitated from 0.5 mg of these lysates using 2 µg of SIK3 C-terminal antibody coupled to protein G-sepharose and were subjected to *in vitro* kinase assay in triplicate as described in **Figure 4.2**. Data is presented as mean ± SD, n=3 independent experiments. **D)** Endogenous SIK3 was immunoprecipitated from the indicated amount of primary hepatocyte lysates using 2 µg of SIK3 C-terminal in-house antibody or pre-immune IgG coupled to protein G-sepharose and were immunoblotted with the same SIK3 antibody. 10% of pre-immunoprecipitation (Pre IP) and SIK3 depleted post-immunoprecipitation (Post IP) lysates were loaded to assess efficiency of IP. Results are representative of two independent experiments.

4.2.1.3 Characterisation of SIK1 antibodies

Analysis of human SIK isoform sequences (Figure 4.5) as well as a comparison between human and mouse SIK1 sequences (Figure 4.6A), four immunogenic peptides identified for the generation of in-house antibodies specific for SIK1. These were based on sequence at the N-terminus (residues 1 - 20), the C-terminus (residues 764 - 783), and two towards internal sequences (5-5) [residues 578 - 592] and (5-6) [residues 597 - 612] of human SIK1. All of these immunogen sequences showed high sequence homology between human and mouse SIK1 (Figure 4.6A).

The specificity of these antibodies were analysed using protein lysates from primary mouse hepatocytes treated with or without Bt_2-cAMP, a cell-permeable cAMP analogue, along with lysates from hepatocytes where SIK1 had been depleted using shRNAi (Figure 4.6B).

Antibodies purified from the third bleed of the sheep injected with SIK1 internal (5-5) or SIK1 C-terminal immunogens were able to detect a band at the expected molecular mass of SIK1 of ~85 kDa, but only in the cells treated with Bt_2-cAMP. In contrast, no signal was detected in the lysates from cells where SIK1 had been depleted, implying that the observed signal was indeed derived from SIK1 protein. The sensitivity of the other antibodies were either relatively weak

or not affected by knock-down of SIK1. VASP, a cytoskeletal protein known as PKA substrate, was used as a marker of efficacy of the Bt_2-cAMP treatment and GAPDH as a loading control.

Next the ability of the C-terminal and internal (5-5) SIK1 antibodies to immunoprecipitate endogenous SIK1 was assessed. As shown in Figure 4.6C, immunoprecipitation of SIK1 with either of these antibodies followed by immunoblotting with a commercial SIK1 antibody detected a band at the expected molecular mass of SIK1 and only in Bt_2-cAMP-treated lysates. This signal was significantly reduced in the immunoprecipitates generated from SIK1 knock-down lysates, while no signal was detected in immunoprecipitates using pre-immune IgG. This provides evidence that the antibodies are specific for SIK1. Even though the SIK1 immunoblot signal was relatively weak when isolated from lysates generated in unstimulated cells, these immunoprecipitates still contained significant *in vitro* SIK1 kinase activity (Figure 4.6C). Furthermore, consistent with the immunoblotting data, the SIK1 kinase activity of the immunoprecipitates from Bt_2-cAMP-treated cell lysates was 10-fold higher compared to immunoprecipitates from unstimulated cell lysates. Finally, the SIK1 kinase activity was significantly reduced in immunoprecipitates generated from cells where SIK1 had been depleted (both unstimulated and Bt_2-cAMP-treated cells) confirming that the kinase activity of the immunoprecipitates was indeed due to endogenous SIK1 protein (Figure 4.6C).

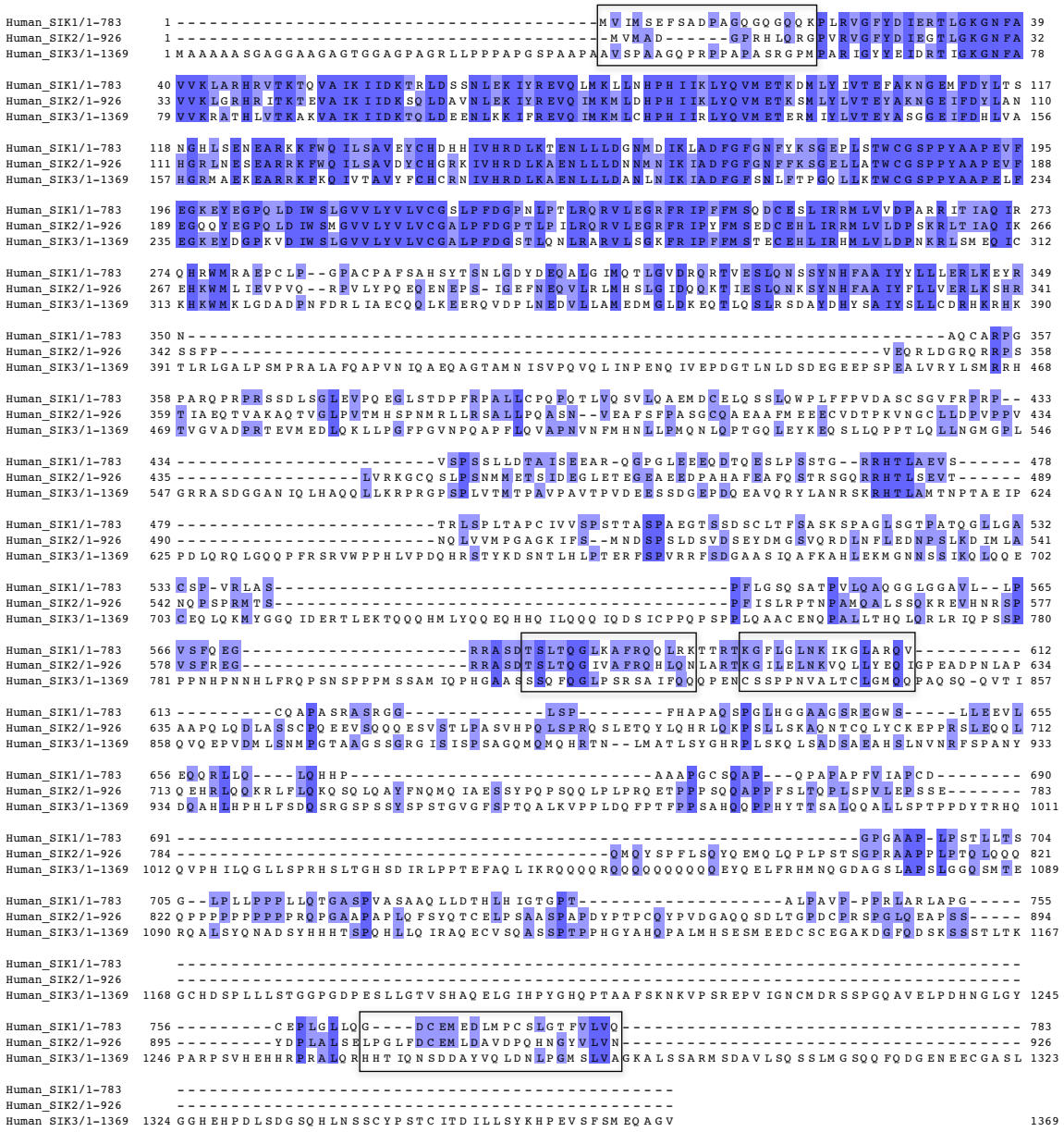

Figure 4.5 Sequence alignment of human SIK isoforms highlighting immunogen sequences of in-house SIK1 antibodies.

Identical residues are shaded in blue. The immunogen sequences are boxed (SIK1 N-terminal in-house antibody, 1 - 20 residues of human SIK1, SIK1 internal (5-5) in-house antibody, 578 - 592 residues of human SIK1, SIK1 internal (5-6), 597 - 612 residues of human SIK1 and SIK1 C-terminal in-house antibody, 764 - 783 residues of human SIK1). Human SIK1 and SIK2 sequences were obtained from UniProtKB with the accession numbers P57059 and Q9H0K1, respectively. Human SIK3 sequence was obtained from www.kinase.com. Alignment was performed with Jalview 2.7.

A

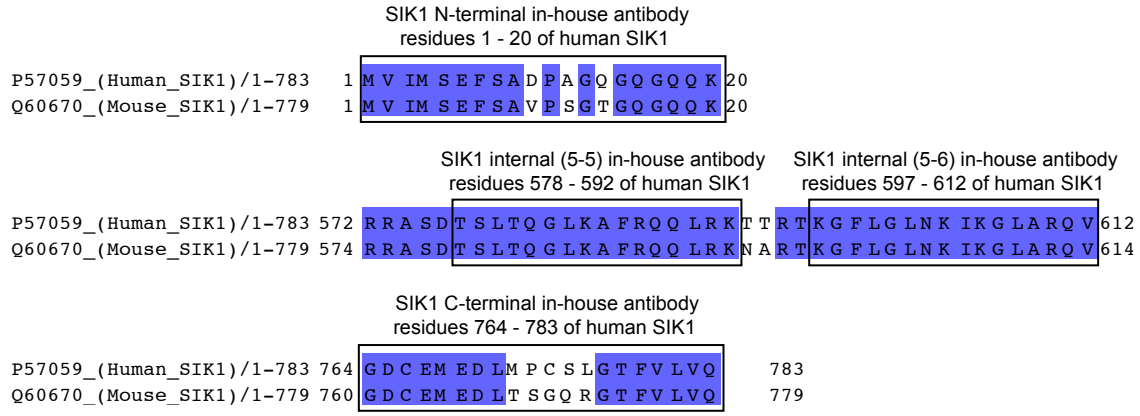
SIK1 N-terminal in-house antibody
residues 1 - 20 of human SIK1
P57059_(Human_SIK1)/1-783 1 M V IM S E F S A D P A G Q G Q G Q Q K 20
Q60670_(Mouse_SIK1)/1-779 1 M V IM S E F S A V P S G T G Q G Q Q K 20
SIK1 internal (5-5) in-house antibody
residues 578 - 592 of human SIK1
SIK1 internal (5-6) in-house antibody
residues 597 - 612 of human SIK1
P57059_(Human_SIK1)/1-783 572 R R A S D T S L T Q G L K A F R Q Q L R K T T R T K G F L G L N K I K G L A R Q V 612
Q60670_(Mouse_SIK1)/1-779 574 R R A S D T S L T Q G L K A F R Q Q L R K N A R T K G F L G L N K I K G L A R Q V 614
SIK1 C-terminal in-house antibody
residues 764 - 783 of human SIK1
P57059_(Human_SIK1)/1-783 764 G D C E M E D L M P C S L G T F V L V Q 783
Q60670_(Mouse_SIK1)/1-779 760 G D C E M E D L T S G Q R G T F V L V Q 779

B

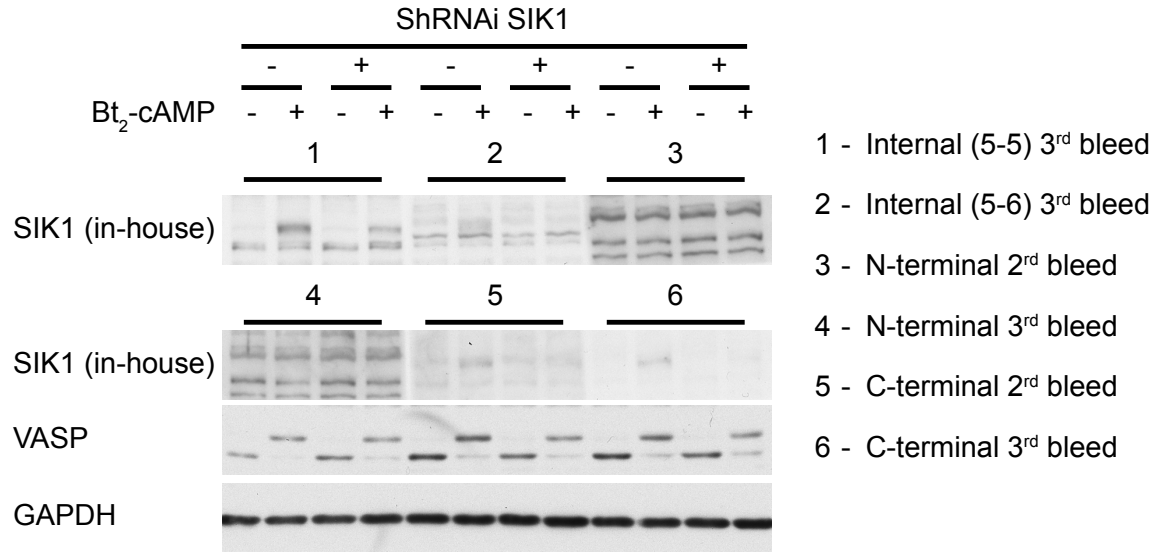
ShRNAi SIK1
- + - + - +
Bt2-cAMP - + - + - + - + - + - +
1 2 3
SIK1 (in-house)
4 5 6
SIK1 (in-house)
VASP
GAPDH
1 - Internal (5-5) 3rd bleed
2 - Internal (5-6) 3rd bleed
3 - N-terminal 2rd bleed
4 - N-terminal 3rd bleed
5 - C-terminal 2rd bleed
6 - C-terminal 3rd bleed

C

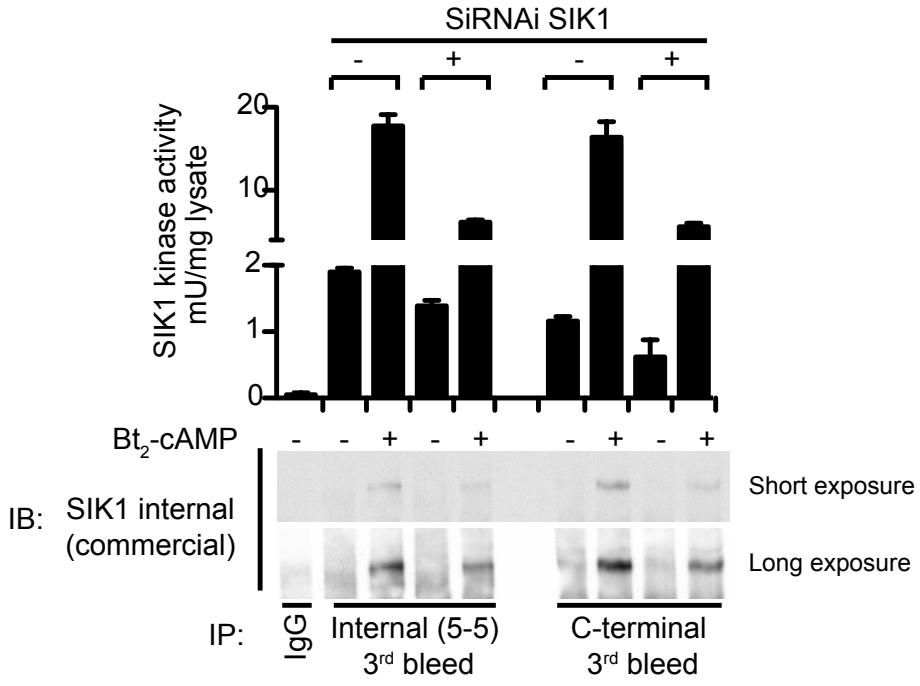
SiRNAi SIK1
- + - +
SIK1 kinase activity
mU/mg lysate
20
10
2
1
0
Bt2-cAMP - - + - + - + - +
IB: SIK1 internal
(commercial)
Short exposure
Long exposure
IP: IgG Internal (5-5)
3rd bleed
C-terminal
3rd bleed

Figure 4.6 Characterisation of SIK1 antibodies.

A) Immunogen sequences of human SIK1 N-terminal, C-terminal, internal (5-5) and internal (5-6) are boxed within an alignment of human and mouse SIK1 sequences using Jalview 2.7. Identical residues are shaded blue and it was the human sequence that was used as immunogen. **B)** Primary mouse hepatocytes were infected with recombinant adenoviral vector SIK1 ShRNAi or scrambled ShRNAi at 1:30 MOI for 48 h. These hepatocytes were stimulated with 100 µM Bt_2-cAMP for the last 5 h prior to cell lysis. 40 µg of these lysates were immunoblotted with 1 µg/ml of the indicated SIK1 in-house antibodies, with a VASP antibody to confirm the activation of PKA by Bt_2-cAMP and a GAPDH antibody as a loading control. Results are representative of three independent experiments. **C)** Endogenous SIK1 was immunoprecipitated from 1 mg of lysates from the same experiment using 2 µg of the indicated in-house antibodies or pre-immune IgG coupled to protein G-sepharose. The precipitates were subjected to either *in vitro* kinase assay in triplicate as described in **Figure 4.2** (data is presented as mean ± SD; n=3 independent experiments) or were immunoblotted with a commercial SIK1-internal (Santa Cruz) antibody.

4.2.2 Expression of SIK2 and SIK3 protein in mouse tissues

4.2.2.1 Protein expression of SIK2 in various mouse tissues

Having validated the antibodies for individual SIK isoforms, these were applied to investigate the expression of SIK isoforms in mouse tissues. First, SIK2 tissue distribution was studied by immunoblot analysis of a panel of mouse tissue extracts (alongside HEK293 cell lysate, Figure 4.7A). SIK2 was present in most tissues with the notable exception of kidney. It was most abundantly expressed in adipose tissue but also enriched in brain, testis, adrenal gland and HEK293 cells. These findings were further validated by immunoprecipitation of endogenous SIK2 from lysates prepared from the same mouse tissue panel using the C-terminal SIK2 antibody, followed by immunoblot using the commercial SIK2 antibody (Figure 4.7B).

A

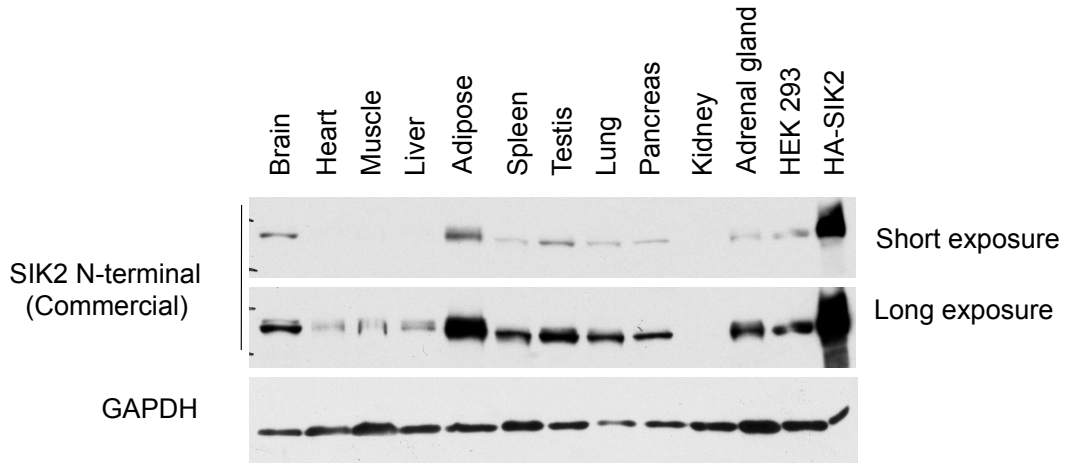

B

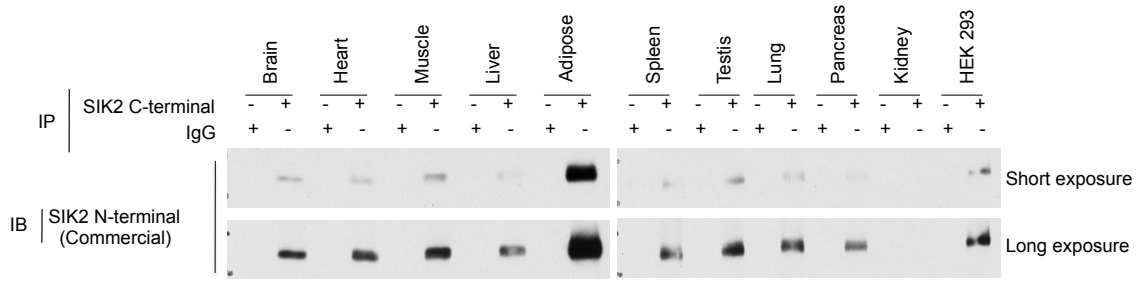

Figure 4.7 Expression of SIK2 protein in various mouse tissues.

Indicated tissues were collected from C57BL/6 mice and homogenates prepared as described in Materials and Methods. **A)** 30 µg of homogenates of the indicated tissues (and HEK293 cells) were immunoblotted using the SIK2 commercial antibody and a GAPDH antibody as a loading control. 10 µg of lysate from HEK293 cells expressing of HA-SIK2 was loaded as a positive control. **B)** SIK2 was immunoprecipitated from 0.5 mg of tissue homogenates as indicated using 2 µg of the SIK2 C-terminal Ab. In each case pre-immune sheep IgG coupled to protein G-sepharose was included as a negative control. Immunoprecipitates were analysed by immunoblotting using the SIK2 N-terminal commercial Ab. Results are representative of experiments performed on tissues from at least three different mice.

4.2.2.2 Protein expression of SIK3 in various mouse tissues

SIK3 tissue expression pattern was investigated in the same manner as that for SIK2 (described above 4.2.2.1) using the SIK3 C-terminal in-house antibody (Figure 4.8A). SIK3 was expressed in most tissues, being most abundant in brain (and HEK293 cells). As observed with SIK2, SIK3 was not detected in the kidney and was also relatively weakly expressed in skeletal muscle and lung. These findings were further validated by immunoprecipitation of endogenous SIK3 proteins from lysates prepared from the same mouse tissue panel using the SIK3 C-terminal antibody followed by immunoblot with the same antibody (Figure 4.8B).

A

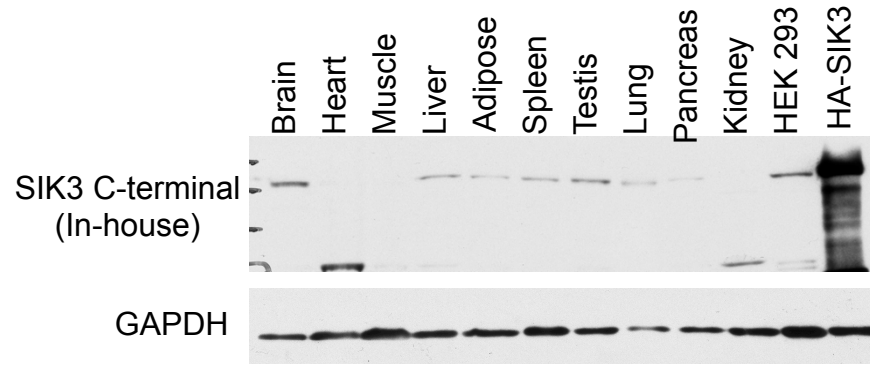

B

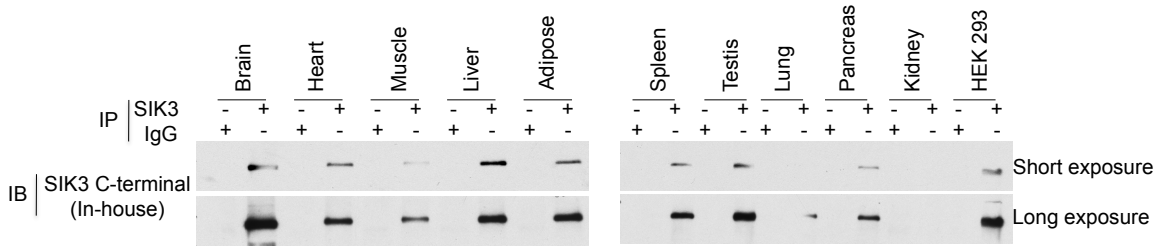

Figure 4.8 Expression of SIK3 protein in various mouse tissues.

Indicated tissues were collected from C57BL/6 mice and homogenates prepared as described in Materials and Methods. **A)** 30 µg of homogenates of the indicated tissues (and HEK293 cells) were immunoblotted using the SIK3 C-terminal in-house antibody and a GAPDH antibody as a loading control. 10 µg lysate from HEK293 cells expressing HA-SIK3 was loaded as a positive control. **B)** SIK3 was immunoprecipitated from 0.5 mg homogenates as indicated using 2 µg of the SIK3 C-terminal in-house antibody. In each case pre-immune sheep IgG coupled to protein G-sepharose was included as a negative control. Immunoprecipitates were analysed by immunoblotting using the SIK3 C-terminal in-house antibody. Results are representative of experiments performed on tissues from at least three different mice.

4.2.3 Hormonal-regulation of SIK2 in liver

4.2.3.1 SIK2 phosphopeptide mapping by mass spectrometry

SIK2 is phosphorylated on multiple sites, including Ser358 by Akt2, Ser587 by PKA and constitutive-phosphorylation on Thr175 by LKB1-STRAD-MO25 complex (see section 1.5.5.1.1). The research leading to identification of these sites had been initiated by the presence of minimum kinase consensus motifs following a bioinformatics analysis. Therefore, I decided to take a more unbiased approach and perform global phosphopeptide mapping of recombinant SIK2 in primary mouse hepatocytes following glucagon or insulin treatment (Figure 4.9). Recombinant HA-tagged SIK2 was expressed in primary mouse hepatocytes using an adenoviral vector. HA-SIK2 was immuno-purified from the cells that had been exposed to either glucagon or insulin, in-gel digested with trypsin and the released peptides were analysed by Liquid Chromatography–Mass Spectrometry (LC–MS) on a LTQ-orbitrap classic mass spectrometer system. As a result, five phosphopeptides were identified after the analysis using Xcalibur Qual software (Thermo Fisher Scientific, USA). All of the phosphopeptides had

significantly higher intensity in glucagon-treated cells, but surprisingly, none of these were affected by insulin treatment of cells (Figure 4.9B). This implied that glucagon has a much more significant effect than insulin on SIK2 phosphorylation in primary hepatocytes. Detailed analysis of these phosphopeptides using MASCOT software (Matrix Science, USA) revealed five different phosphorylation sites, namely Ser343, Ser358, Ser379, Ser484, and Ser587 (Figure 4.9) Importantly, LC-MS analysis coverage of HA-SIK2 sequence was exceptionally high at around 90% for all three conditions (Figure 4.10), reducing the risk of unidentified phosphorylation sites. In order to investigate whether the remaining 10% of SIK2 contained any potential PKA- or Akt-regulated phosphorylation sites, the SIK2 sequence was scanned for PKA or Akt consensus motifs using Scansite 2.0 (http://scansite.mit.edu/) (Figure 4.11) (Obenauer, 2003). The sequence was scanned with 'low stringency' level to achieve higher sensitivity and to reduce the possibility of missing out any potential sites. All the predicted PKA and Akt sites were covered by the LC-MS analysis except for the sequence surrounding Thr42, which was identified as a potential PKA phosphorylation motif. However, the prediction software generated a relatively high score (0.5981) and a very high percentile (3.645%) for this potential PKA motif (Figure 4.11). A higher score dictates higher divergence from the perfect consensus PKA site which scores 0.0, while a higher percentile suggests lower selectivity for PKA, as highly selective sites will have a percentile less than 0.2% (Obenauer, 2003). Importantly, the LC-MS analysis of regions outside the coverage area did not identify any additional phosphorylation sites with similar scores and percentiles than the sites identified in my LC-MS study (Thr359, Ser674 and Ser688). These results suggest that Thr42 is unlikely to be regulated by PKA.

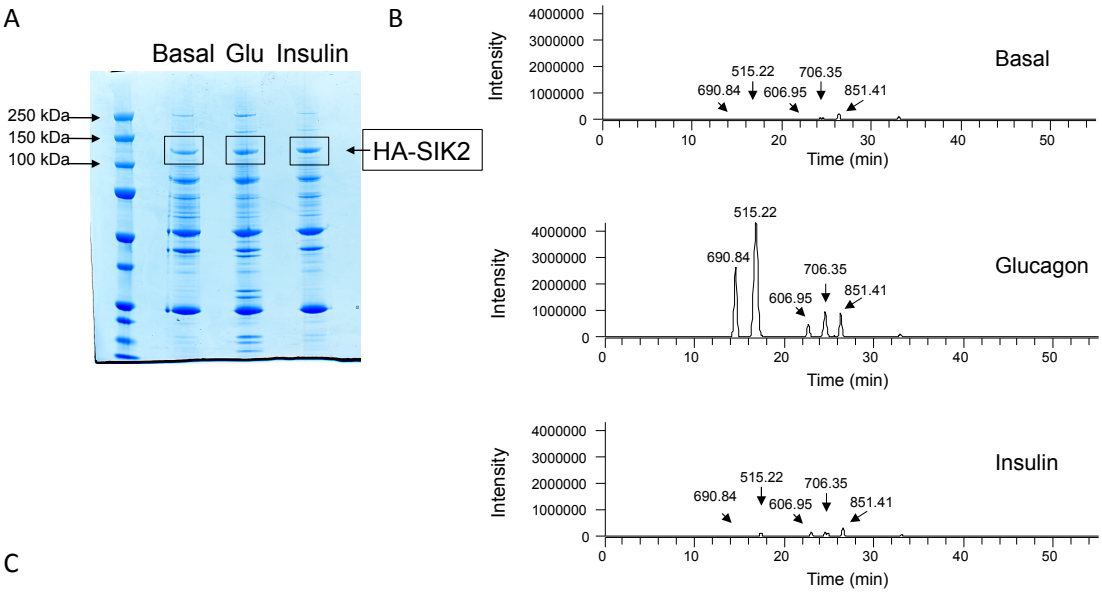

M/z	Peptide	Phospho site
690.84	R.RP**S**TIAEQTVAK.A	Ser358
515.22	R.S**S**FPVEQR.L	Ser343
606.95	K.AQTVGLPVTMH**S**PNMR.L	Ser379
706.35	R.RH**T**LSEVTNQLVVMPGAGK.I	Thr484
851.41	R.RA**S**DTSLTQGIVAFR.Q	Ser587

Figure 4.9 Phosphopeptide mapping of SIK2 with LC-MS.

A) Recombinant HA-SIK2 was expressed in primary mouse hepatocytes using adenoviral infection (1:20 MOI) 16 h prior to stimulation with 100 nM glucagon or 10 nM insulin for 10 min. HA-SIK2 was immunoprecipitated from 5 mg of lysates with HA-agarose beads and the precipitates were subjected to SDS-PAGE followed by colloidal coomassie staining of the gel. Bands corresponding to HA-SIK2 (highlighted in boxes) were excised, in-gel digested with trypsin and analysed using liquid chromatography mass spectrometry (LC-MS) as described in Materials and Methods. HA-SIK2 adenoviral construct was kindly donated by Dr Olga Göransson, Lund University, Sweden. **B)** Graphs show the absolute extracted ion currents for SIK2 phosphopeptides from control (upper panel), glucagon-treated (middle panel) and insulin-treated samples (lower panel) along with respective M/z values. **C)** Table illustrates the sequences of the phosphopeptides identified, M/z values and respective phosphorylated residues (bold and underlined) of SIK2.

A

```
  1 MYPYDVPDYA VMADGPRHLQ RGPVRVGFYD IEGTLGKGNF AVVKLGRHRI
 51 TKTEVAIKII DKSQLDAVNL EKIYREVQIM KMLDHPHIIK LYQVMETKSM
101 LYLVTEYAKN GEIFDYLANH GRLNESEARR KFWQILSAVD YCHGRKIVHR
151 DLKAENLLLD NNMNIKIADF GFGNFFKSGE LLATWCGSPP YAAPEVFEGQ
201 QYEGPQLDIW SMGVVLYVLV CGALPFDGPT LPILRQRVLE GRFRIPYFMS
251 EDCEHLIRRM LVLDPSKRLT IAQIKEHKWM LIEVPVQRPV LYPQEQENEP
301 SIGEFNEQVL RLMHSLGIDQ QKTIESLQNK SYNHFAAIYF LLVERLKSHR
351 SSFPVEQRLD GRQRRPSTIA EQTVAKAQTV GLPVTMHSPN MRLLRSALLP
401 QASNVEAFSF PASGCQAEAA FMEEECVDTP KVNGCLLDPV PPVLVRKGCQ
451 SLPSNMMETS IDEGLETEGE AEEDPAHAFE AFQSTRSGQR RHTLSEVTNQ
501 LVVMPGAGKI FSMNDSPSLD SVDSEYDMGS VQRDLNFLED NPSLKDIMLA
```

551 NQPSPRMTSP FISLRPTNPA MQALSSQKRE VHNRSPVSFR EGRRASDTSL
601 TQGIVAFRQH LQNLARTKGI LELNKVQLLY EQIGPEADPN LAPAAPQLQD
651 LASSCPQEEV SQQQESVSTL PASVHPQLSP RQSLETQYLQ HRLQKPSLLS
701 KAQNTCQLYC KEPPRSLEQQ LQEHRLQQKR LFLQKQSQLQ AYFNQMQIAE
751 SSYPQPSQQL PLPRQETPPP SQQAPPFSLT QPLSPVLEPS SEQMQYSPFL
801 SQYQEMQLQP LPSTSGPRAA PPLPTQLQQQ QPPPPPPPPP PRQPGAAPAP
851 LQFSYQTCEL PSAASPAPDY PTPCQYPVDG AQQSDLTGPD CPRSPGLQEA
901 PSSYDPLALS ELPGLFDCEM LDAVDPQHNG YVLVN

B

1 MYPYDVPDYA VMADGPRHLQ RGPVRVGFYD IEGTLGKGNF AVVKLGRHRI
51 TKTEVAIKII DKSQLDAVNL EKIYREVQIM KMLDHPHIIK LYQVMETKSM
101 LYLVTEYAKN GEIFDYLANH GRLNESEARR KFWQILSAVD YCHGRKIVHR
151 DLKAENLLLD NNMNIKIADF GFGNFFKSGE LLATWCGSPP YAAPEVFEGQ
201 QYEGPQLDIW SMGVVLYVLV CGALPFDGPT LPILRQRVLE GRFRIPYFMS
251 EDCEHLIRRM LVLDPSKRLT IAQIKEHKWM LIEVPVQRPV LYPQEQENEP
301 SIGEFNEQVL RLMHSLGIDQ QKTIESLQNK SYNHFAAIYF LLVERLKSHR
351 SSFPVEQRLD GRQRRPSTIA EQTVAKAQTV GLPVTMHSPN MRLLRSALLP
401 QASNVEAFSF PASGCQAEAA FMEEECVDTP KVNGCLLDPV PPVLVRKGCQ
451 SLPSNMMETS IDEGLETEGE AEEDPAHAFE AFQSTRSGQR RHTLSEVTNQ
501 LVVMPGAGKI FSMNDSPSLD SVDSEYDMGS VQRDLNFLED NPSLKDIMLA
551 NQPSPRMTSP FISLRPTNPA MQALSSQKRE VHNRSPVSFR EGRRASDTSL
601 TQGIVAFRQH LQNLARTKGI LELNKVQLLY EQIGPEADPN LAPAAPQLQD
651 LASSCPQEEV SQQQESVSTL PASVHPQLSP RQSLETQYLQ HRLQKPSLLS
701 KAQNTCQLYC KEPPRSLEQQ LQEHRLQQKR LFLQKQSQLQ AYFNQMQIAE
751 SSYPQPSQQL PLPRQETPPP SQQAPPFSLT QPLSPVLEPS SEQMQYSPFL
801 SQYQEMQLQP LPSTSGPRAA PPLPTQLQQQ QPPPPPPPPP PRQPGAAPAP
851 LQFSYQTCEL PSAASPAPDY PTPCQYPVDG AQQSDLTGPD CPRSPGLQEA
901 PSSYDPLALS ELPGLFDCEM LDAVDPQHNG YVLVN

C

1 MYPYDVPDYA VMADGPRHLQ RGPVRVGFYD IEGTLGKGNF AVVKLGRHRI
51 TKTEVAIKII DKSQLDAVNL EKIYREVQIM KMLDHPHIIK LYQVMETKSM
101 LYLVTEYAKN GEIFDYLANH GRLNESEARR KFWQILSAVD YCHGRKIVHR
151 DLKAENLLLD NNMNIKIADF GFGNFFKSGE LLATWCGSPP YAAPEVFEGQ
201 QYEGPQLDIW SMGVVLYVLV CGALPFDGPT LPILRQRVLE GRFRIPYFMS
251 EDCEHLIRRM LVLDPSKRLT IAQIKEHKWM LIEVPVQRPV LYPQEQENEP
301 SIGEFNEQVL RLMHSLGIDQ QKTIESLQNK SYNHFAAIYF LLVERLKSHR
351 SSFPVEQRLD GRQRRPSTIA EQTVAKAQTV GLPVTMHSPN MRLLRSALLP
401 QASNVEAFSF PASGCQAEAA FMEEECVDTP KVNGCLLDPV PPVLVRKGCQ
451 SLPSNMMETS IDEGLETEGE AEEDPAHAFE AFQSTRSGQR RHTLSEVTNQ
501 LVVMPGAGKI FSMNDSPSLD SVDSEYDMGS VQRDLNFLED NPSLKDIMLA
551 NQPSPRMTSP FISLRPTNPA MQALSSQKRE VHNRSPVSFR EGRRASDTSL
601 TQGIVAFRQH LQNLARTKGI LELNKVQLLY EQIGPEADPN LAPAAPQLQD
651 LASSCPQEEV SQQQESVSTL PASVHPQLSP RQSLETQYLQ HRLQKPSLLS
701 KAQNTCQLYC KEPPRSLEQQ LQEHRLQQKR LFLQKQSQLQ AYFNQMQIAE
751 SSYPQPSQQL PLPRQETPPP SQQAPPFSLT QPLSPVLEPS SEQMQYSPFL
801 SQYQEMQLQP LPSTSGPRAA PPLPTQLQQQ QPPPPPPPPP PRQPGAAPAP
851 LQFSYQTCEL PSAASPAPDY PTPCQYPVDG AQQSDLTGPD CPRSPGLQEA
901 PSSYDPLALS ELPGLFDCEM LDAVDPQHNG YVLVN

Figure 4.10 Sequence coverage of HA-SIK2 in phosphopeptide mapping by LC-MS

The sequence that was covered in Orbitrap LC-MS analysis by peptides with Mascot scores of > 20 (where a score **>** 20 indicates identity or extensive homology ($p<0.05$)) is highlighted in bold and red. Sequence coverage of HA-SIK2 was 88% from unstimulated cells (A) and from both glucagon (B) or insulin (C) treated cells**.**

Protein Kinase A		
Site	Score	Percentile
T484	0.2802	0.061 %

Protein Kinase A		
Site	Score	Percentile
S358	0.3085	0.110 %

Protein Kinase A		
Site	Score	Percentile
T261	0.3539	0.228 %

Protein Kinase A		
Site	Score	Percentile
S587	0.4093	0.462 %

Protein Kinase A		
Site	Score	Percentile
S343	0.4940	1.061 %

Protein Kinase A		
Site	Score	Percentile
T359	0.5126	1.295 %

Protein Kinase A		
Site	Score	Percentile
S674	0.5502	2.023 %

Protein Kinase A		
Site	Score	Percentile
T42	0.5981	3.645 %

Protein Kinase A		
Site	Score	Percentile
S688	0.6143	4.392 %

Akt Kinase		
Site	Score	Percentile
T484	0.5454	0.480 %

Akt Kinase		
Site	Score	Percentile
T359	0.6571	2.100 %

Akt Kinase		
Site	Score	Percentile
S358	0.6666	2.340 %

Akt Kinase		
Site	Score	Percentile
S343	0.6865	2.927 %

Akt Kinase		
Site	Score	Percentile
S503	0.6917	3.098 %

Akt Kinase		
Site	Score	Percentile
S587	0.7142	3.928 %

Akt Kinase		
Site	Score	Percentile
S590	0.7295	4.635 %

Figure 4.11 Scansite 2.0 analysis of Human SIK2 sequence for PKA and Akt1 motif.

Human SIK2 (UniProtKB accession number Q9H0K1) was analysed using Scansite 2.0 (Massachusetts Institute of Technology, USA, http://scansite.mit.edu/) for PKA and Akt1 consensus phosphorylation motif. Scores start at 0.000 if the sequence optimally matches the given motif, and the scores increase for sequences as they diverge from the optimal match.

LC-MS identified four phosphorylation sites on SIK2 that were regulated by glucagon, the next step was to develop phospho-specific antibodies and validate the phosphorylation on these sites in cell-based systems and *in vivo*. Phospho-specific antibodies were custom-generated commercially (against Ser343, Thr484), generated in-house by the DSTT (Thr175) or provided by our external collaborators (Ser358 and Ser587). Figure 4.12 shows sequence-alignment of human SIK1, 2, and 3 detailing the immunogen sequences used to generate the phospho-specific antibodies. Thr484 and Thr175 are the only phosphorylation sites that are conserved amongst all three SIK isoforms. In addition, immunogen sequences used to generate all phospho-specific antibodies were identical between human and mouse SIK2, except one conservative amino acid difference (Ser to Thr) in the sequence surrounding pThr175 (Figure 4.13). Therefore these antibodies were anticipated to recognise the appropriate phosphorylated sites in both human and mouse SIK2.

To characterise the phospho-specific antibodies, immunoblot analysis was conducted using lysates from primary hepatocytes that expressed recombinant GFP-SIK2 (wild-type) and were treated with or without glucagon (Figure 4.14A). The phosphorylation site-specificity of each antibody was assessed by immunoblotting lysates from the glucagon-treated hepatocytes that expressed phosphorylation-defective GFP-SIK2 mutants (Ser/Thr to Ala) (Figure 4.14A).

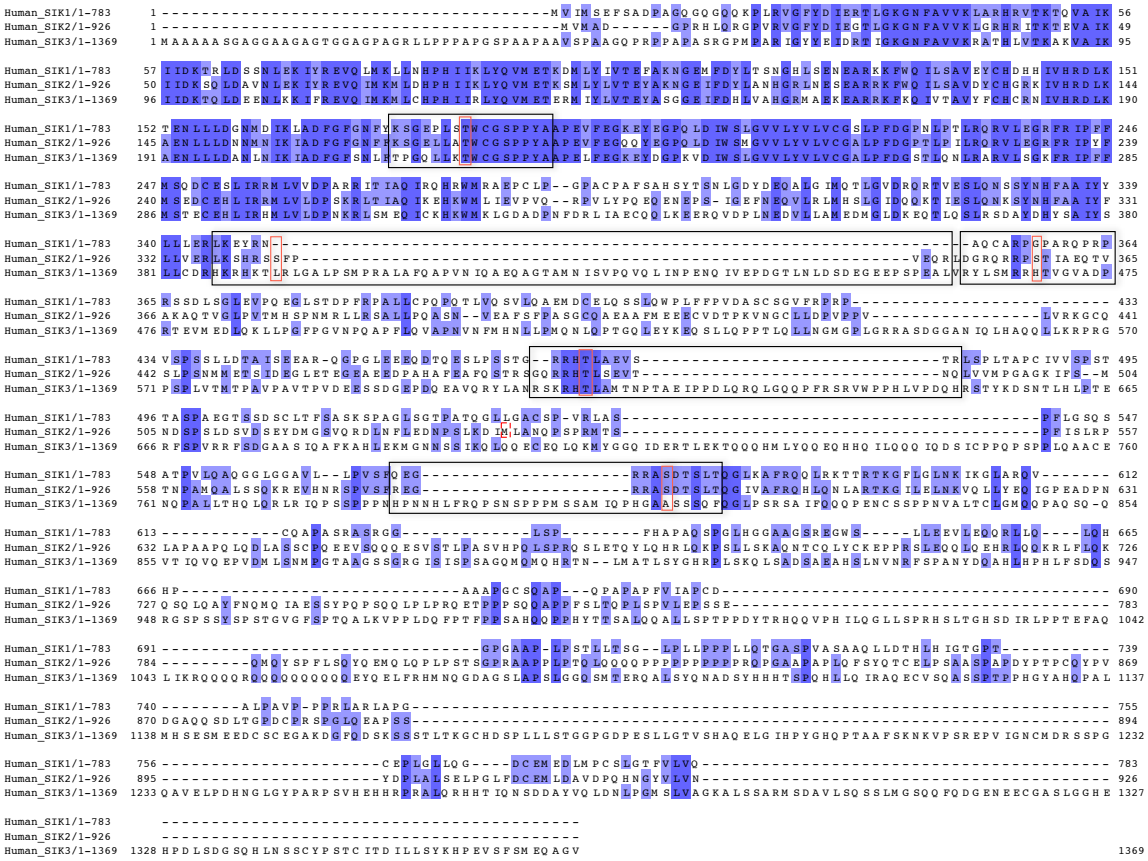

Figure 4.12 Sequence alignment of human SIKs highlighting immunogen sequences of SIK2 phospho-specific antibodies.

Identical residues are shaded blue and phosphorylation sites are highlighted with red rectangles. The immunogen sequences of the peptides used to generate the pThr182 SIK1 antibody (residues 175 - 189 of human SIK1), pSer343 SIK2 antibody (residues 337 - 349 of human SIK2), pSer358 SIK2 antibody (residues 351 - 365 of human SIK2), pThr484 SIK2 antibody (residues 479 - 491 of human SIK2) and pSer577 SIK1 antibody (residues 571 - 582 of rat SIK1) are boxed. The pThr182 SIK1 antibody also recognises the equivalent sites on SIK2 (pThr175) and SIK3 (pThr221). The pSer577 SIK1 antibody also recognises the equivalent site on SIK2 (pSer587). Therefore an antibody is available to detect phosphorylation of all 5 sites on SIK2. Antibodies against pSer343, pThr484 and pThr175 of SIK2 were generated in-house while antibodies against pSer587 and pSer358 of SIK2 were gifts from Dr Hiroshi Takemori (National Institute of Biomedical Innovation, Osaka, Japan) and Dr Olga Göransson (Lund University, Sweden) respectively.

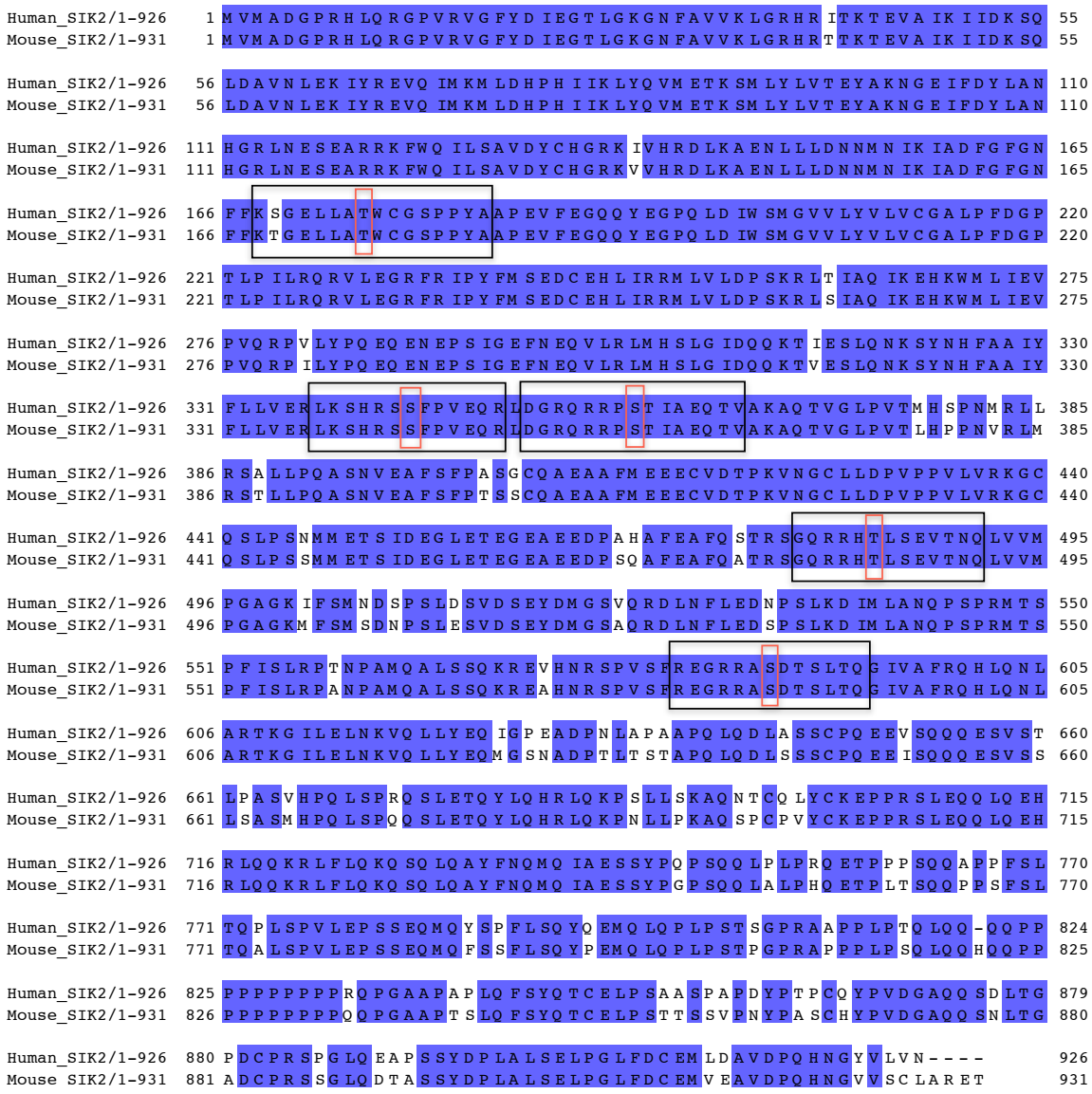

Figure 4.13 Sequence alignment of human and mouse SIK2 highlighting immunogen sequences for SIK2 phospho-specific antibodies.

Identical residues are shaded blue and phosphorylation sites are highlighted in red rectangles. First, second and third boxed regions show immunogen sequences used to generate the pThr175, pSer343 and pSer358 SIK2 antibodies respectively. The fourth and fifth boxed regions show immunogen sequences used to generate the pThr484 and pSer587 SIK2 antibodies respectively.

A

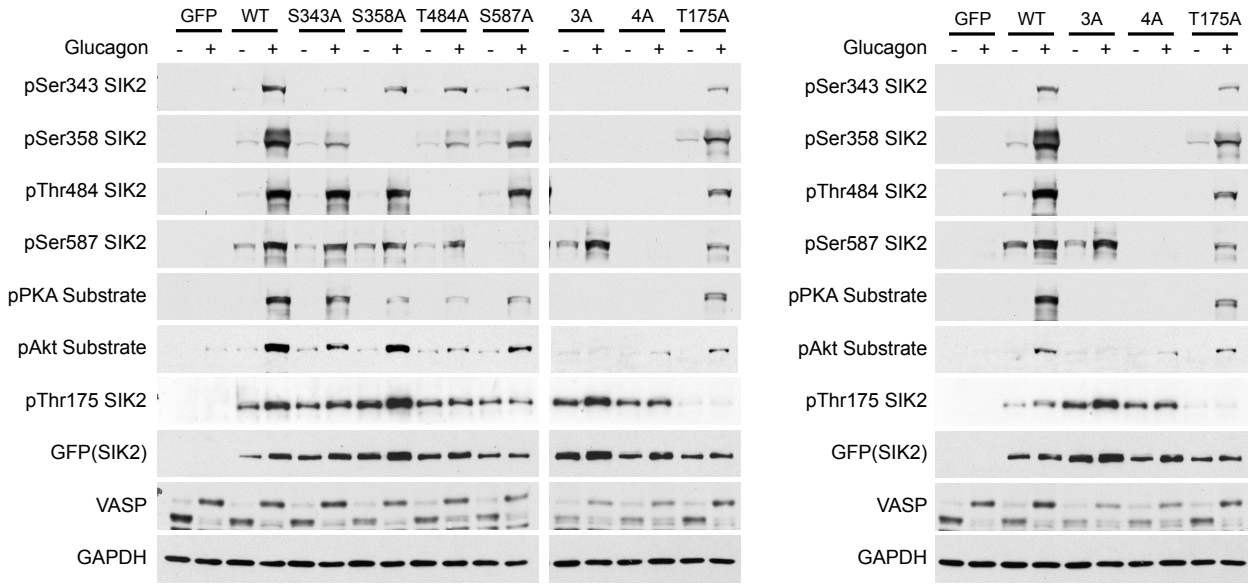

B

PKA substrate phosphorylation motif	R-R-X-pS/T-X
SIK2 (337-345, pS343)	L-K-S-H-R-S-pS -F-P
SIK2 (352-360, pS358)	G-R-Q-R-R-P-pS -T-I
SIK2 (378-486, pT484)	S-G-Q-R-R-H-pT -L-S
SIK2 (581-589, pS587)	R-E-G-R-R-A-pS -D-T
Akt substrate phosphorylation motif	R-X-R-X-X-pS/T-X

Figure 4.14 Characterisation of SIK2 phospho-specific antibodies.

A) Primary mouse hepatocytes were infected (1:20 MOI) with adenoviral vectors expressing SIK2 wild-type or the indicated SIK2 phosphorylation-site mutants including 3A (S343A, S358A and T484A together), 4A mutant (3A and S587A together) and the kinase-inactive T-loop mutant T175A. Primary hepatocytes infected with Ad-GFP were included as a control. After 16 h the hepatocytes were stimulated for 10 min with 100 nM glucagon prior to cell lysis. The lysates were subjected to immunoblotting with the indicated phospho-specific SIK2 antibodies, with a pPKA substrate antibody, with a VASP antibody to confirm the PKA activation by glucagon and with a GAPDH antibody as a loading control. Lysates were also immunoblotted with a pAkt substrate antibody to assess the cross-reactivity to the pPKA substrate antibody. Results are representative of three independent experiments. **B)** Indicated human SIK2 amino acid sequence encompassing phosphorylation sites are aligned with the PKA and Akt consensus substrate phosphorylation motif (highlighted in blue colour).

All of the phospho-specific antibodies, except the pThr175 antibody, exclusively detected a band at the expected molecular mass of GFP-SIK2 in lysates isolated from cells following glucagon stimulation, supporting the phosphopeptide mapping results (Figure 4.14A). For all phospho-specific antibodies, no signal was detected with the lysates from cells expressing each respective phosphorylation-defective mutant, once more confirming the site-specificity

of these antibodies**.** In addition, the pPKA substrate antibody (raised against a peptide sequence based on the consensus PKA phosphorylation site) detected a band in the hepatocytes expressing wild-type protein and this response was only lost in lysates isolated from cells expressing a 3A or 4A mutant. This suggested that the pPKA antibody recognised the glucagon-mediated phosphorylation of at least three different sites (Ser343, Ser358 and Thr484) of SIK2.

Crucially, the pAkt substrate antibody (raised against a peptide sequence based on the consensus Akt phosphorylation site) detected all four phosphorylation sites following glucagon treatment. This cross-reactivity may be explained by the observation that the sequences around Ser358 and other phosphorylation sites (Ser343, Thr484 and Ser587) of SIK2 actually provide a preferred consensus motif for both PKA and Akt (Figure 4.14B). It was further reflected in Scansite 2.0 analysis of SIK2 sequence for PKA and Akt motifs which identified all four sites as potential PKA and Akt sites (Figure 4.14C). However, the scores and percentiles for Ser343, Ser358, Thr484 and Ser587 sites were significantly favourable for PKA than Akt suggesting that PKA was a preferred kinase for these sites. Finally, mutations of any or all (4A) of the glucagon-induced phosphorylation sites had no effect on T-loop phosphorylation (Thr175) of SIK2 (Figure 4.14A) and phosphorylation on Thr175 was similar in both untreated and glucagon-treated cells (Figure 4.14A).

4.2.3.2 Hormonal-regulation of SIK2 phosphorylation in primary mouse hepatocytes

To confirm above findings with endogenous SIK2 in a more physiological setting, the hormonal-regulation of SIK2 was assessed with validated phospho-specific antibodies in primary mouse hepatocytes. Endogenous SIK2 was immunoprecipitated from cell lysates generated from glucagon- or insulin-treated primary hepatocytes and subjected to immunoblot analysis with the Ser343, Ser358 and Thr484 phospho-specific antibodies (Figure 4.15). As with recombinant SIK2, all three sites on the endogenous protein were

phosphorylated following glucagon treatment of the cells. In contrast, insulin treatment of

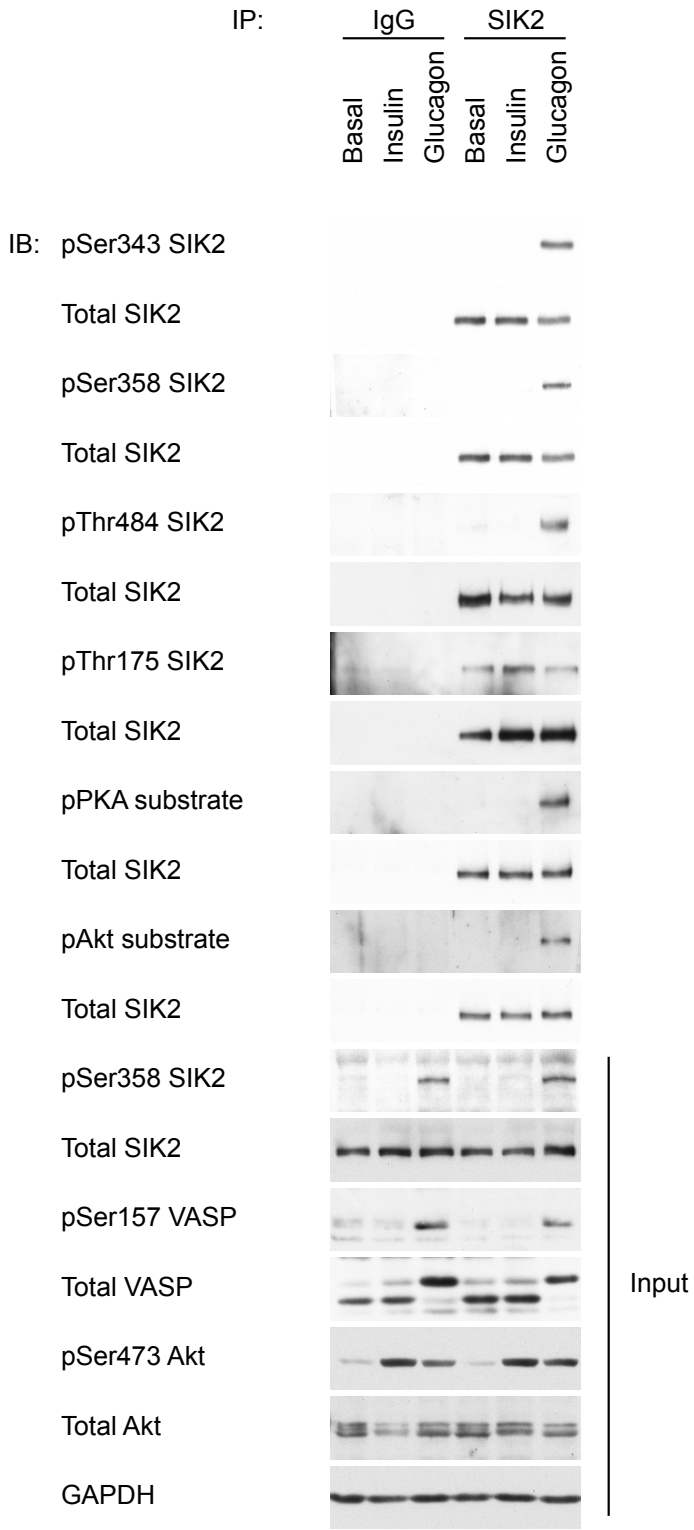

Figure 4.15 SIK2 phosphorylation in primary mouse hepatocytes.

Primary hepatocytes were stimulated with either 100 nM glucagon or 10 nM insulin for 10 min prior to cell lysis. Endogenous SIK2 was immunoprecipitated from 1 mg of cell lysate using 2µg of the SIK2 antibody or pre-immune IgG as a control. The resultant precipitates (and 40 µg of lysates as input) were immunoblotted with the indicated antibodies. The pSer473 Akt and VASP antibodies were used to confirm the stimulation by insulin and PKA activation by glucagon respectively, while the GAPDH antibody was used as a loading control. Results are representative of three independent experiments.

primary hepatocytes had no effect on phosphorylation of these sites on SIK2. Once more, SIK2 phosphorylation was detected with the pPKA substrate antibody but only in glucagon treated cells. There was no effect of insulin treatment on the phosphorylation recognised by pPKA substrate antibody. Consistent with the results of overexpressed SIK2, a pAkt substrate antibody detected SIK2 phosphorylation in lysates from glucagon-treated cells but crucially not from insulin-treated cells (Figure 4.15). In addition, neither glucagon nor insulin treatment altered Thr175 phosphorylation of SIK2 in hepatocytes. Similar findings were observed using HEK293 cells, where endogenous SIK2 was phosphorylated on Ser343, Ser358 and Thr484 following treatment of the cells with the cAMP-elevating agent (forskolin) but not by IGF-1 treatment (Appendix 1 and Appendix 3).

4.2.3.3 SIK2 phosphorylation in vivo

To confirm that the data obtained in primary hepatocytes was indicative of SIK2 phosphorylation *in vivo*, immunoblot analysis of liver extracts generated from mice following 16-h fasting (stimulation of endogenous glucagon secretion) or 16-h fasting followed by 4-h refeeding (stimulation of endogenous insulin secretion) was performed (Figure 4.16). Immunoblotting of immunoprecipitated SIK2 from these liver extracts confirmed that Ser343, Ser358 and Thr484 were phosphorylated following fasting but not after refeeding, which was consistent with the data from glucagon- or insulin-treated primary mouse hepatocytes.

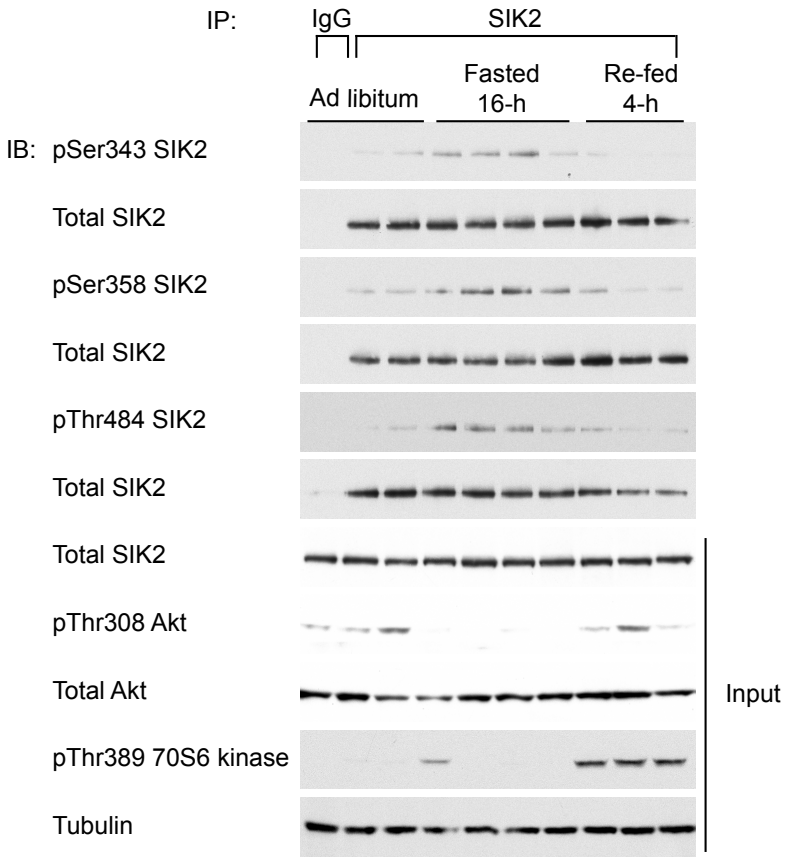

Figure 4.16 SIK2 phosphorylation *in vivo*.

Liver extracts were generated from C57BL/6 male mice (8-10 week-old) that had been subjected to *ad libitum* feeding, 16-h fasting or 16-h fasting followed by 4-h refeeding. Liver homogenates were prepared as described in Materials and Methods. Endogenous SIK2 was immunoprecipitated from 1 mg of homogenates using the SIK2 antibody while pre-immune IgG was used as a negative control. The precipitates (along with 40 µg of lysates as an input) were immunoblotted with the indicated phospho-specific SIK2 antibodies. The pThr308 Akt and pThr389 p70S6 kinase antibodies were used to confirm the effect of fasting or refeeding on insulin/nutrient stimulation of the liver and the tubulin antibody was used as a loading control. Each lane represents homogenates from independent mouse liver.

4.2.3.4 SIK2 Ser358 phosphorylation in liver

Previous reports had proposed that SIK2 Ser358 phosphorylation was regulated by insulin through the PI3K-Akt pathway (see section 1.5.5.4 for details). In contrast, my studies (see section 4.2.3) using phosphopeptide mapping of recombinant HA-SIK2 and immunoblotting of endogenous SIK2 in primary mouse hepatocytes and HEK293 cells as well as *in vivo*, found that Ser358 phosphorylation was enriched only after fasting or in response to cAMP-elevating agents such as glucagon or forskolin treatment but not with refeeding, insulin or IGF-1 treatment. To investigate this discrepancy further the SIK2 Ser358 phospho-specific antibody was used to analyse SIK2 phosphorylation in primary hepatocytes isolated from SIK2 wild-type or knock-out mice and Akt2 wild-type or knock-out mice, treated with glucagon or Bt_2-cAMP

(Figure 4.17, Figure 4.18). SIK2 Ser358 phosphorylation was detected following glucagon or Bt_2-cAMP treatment in wild-type hepatocytes but was absent in SIK2 knock-out hepatocytes, confirming the specificity of the Ser358 antibody for SIK2 (Figure 4.17). More importantly, SIK2 was phosphorylated on Ser358 in response to Bt_2-cAMP treatment but not following insulin treatment of primary hepatocytes obtained from both the wild-type and the Akt2 knock-out mice (Figure 4.18). These results indicated that insulin did not induce Ser358 phosphorylation and that the presence of Akt2 and its activity were not required for the glucagon induction of Ser358 phosphorylation on SIK2.

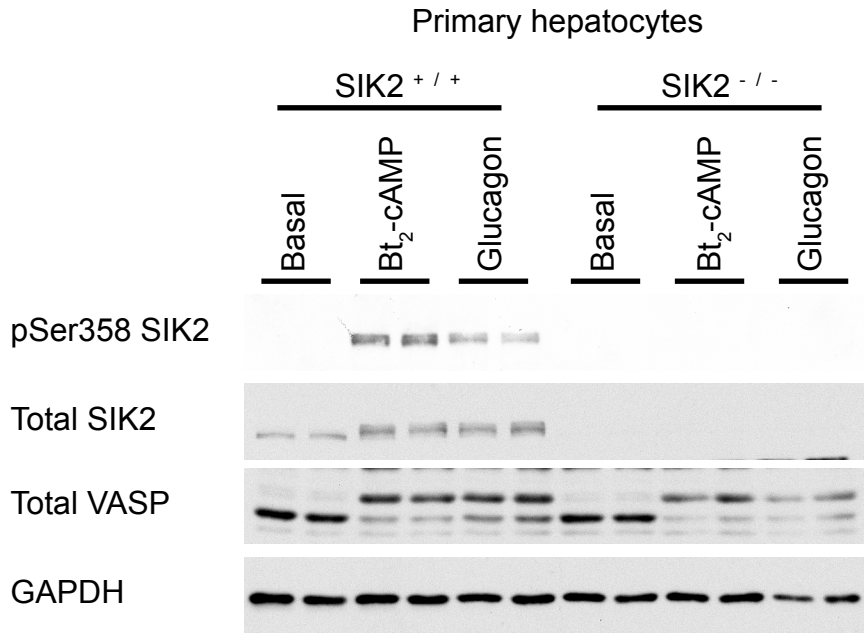

Figure 4.17 Validation of pSer358 SIK2 antibody employing SIK2 knock-out primary hepatocytes.

Primary hepatocytes were isolated from two $SIK2^{+/+}$ and liver-specific $SIK2^{-/-}$ mice, and then stimulated with either 100 µM Bt_2-cAMP or 100 nM glucagon for 10 min. The resultant lysates were immunoblotted with the indicated antibodies, with a VASP antibody to confirm PKA activation by Bt_2-cAMP or glucagon and a GAPDH antibody as a loading control. The lysates for this experiment were received from Dr Marc Foretz (Institut Cochin - INSERM, France). Each lane represents lysate from independent mouse.

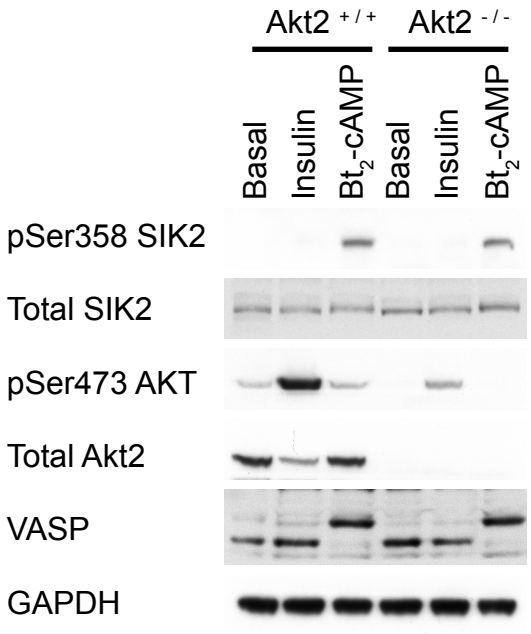

Figure 4.18 Ser358 SIK2 phosphorylation in Akt2 knock-out primary hepatocytes.

Primary mouse hepatocytes were isolated from Akt2$^{+/+}$ and liver-specific Akt2$^{-/-}$ mice and then stimulated with 10 nM Insulin or 100 μM Bt2-cAMP for 10 min prior to cell lysis. The lysates were immunoblotted with the indicated SIK2 antibodies, and the Akt2 antibody to confirm the absence of Akt2 (in the knock-out mice). The pSer473 Akt and VASP antibodies were used to confirm the stimulation by insulin and PKA activation by glucagon respectively, while the GAPDH antibody was used as a loading control. The lysates for this experiment were received from Dr Morris Birnbaum (University of Pennsylvania, USA). Results representative of three independent experiments.

To further explore the potential role of insulin signalling pathway components in the regulation of SIK2 Ser358 phosphorylation, immunoblot analysis was conducted on primary mouse hepatocytes incubated with the Akt inhibitor (MK-2206) (Al-Hakim et al., 2005; Hirai et al., 2010) or the PI3K inhibitor (wortmannin). Once again Ser358 was only phosphorylated following glucagon treatment of the cells and not after insulin treatment (Figure 4.19A). Treatment of the cells with MK-2206 or wortmannin had no effect on Ser358 phosphorylation. Similarly, insulin or MK-2206 and wortmannin had no effect on SIK2 phosphorylation when immunoblotted with pPKA or pAkt substrate antibodies (Figure 4.19B). As stated, the SIK2 sequence surrounding phosphorylation sites has high homology with the consensus PKA and Akt substrate phosphorylation motifs (Figure 4.14B), and this probably explains the ability of these antibodies to identify SIK2 phosphorylation following glucagon treatment. However, the data indicated that insulin, PI3K and Akt do not regulate any sites on SIK2 detected by either of these antibodies under experimental conditions tested in the current study.

In contrast, glucagon-induced phosphorylation of SIK2 at Ser358 was significantly reduced by H-89 (a PKA inhibitor) treatment of the cells (Figure 4.20). PKA inhibition in the cells was confirmed with a significant reduction in phosphorylation of inositol 1,4,5-triphosphate receptor (IP3R), a known PKA substrate, and also the reduction in dephosphorylation of CRTC2 as judged by band mobility shift. These data demonstrate that PKA mediates Ser358 phosphorylation in response to glucagon treatment of hepatocytes.

To assess the effects on SIK2 phosphorylation of longer exposure to these hormones, immunoblot analysis was carried out on lysates prepared from primary hepatocytes treated with glucagon or insulin for 10, 20 or 40 min (Figure 4.21). Once again the SIK2 phosphorylation on Ser358 only occurred following glucagon treatment of the cells but not following insulin treatment.

A

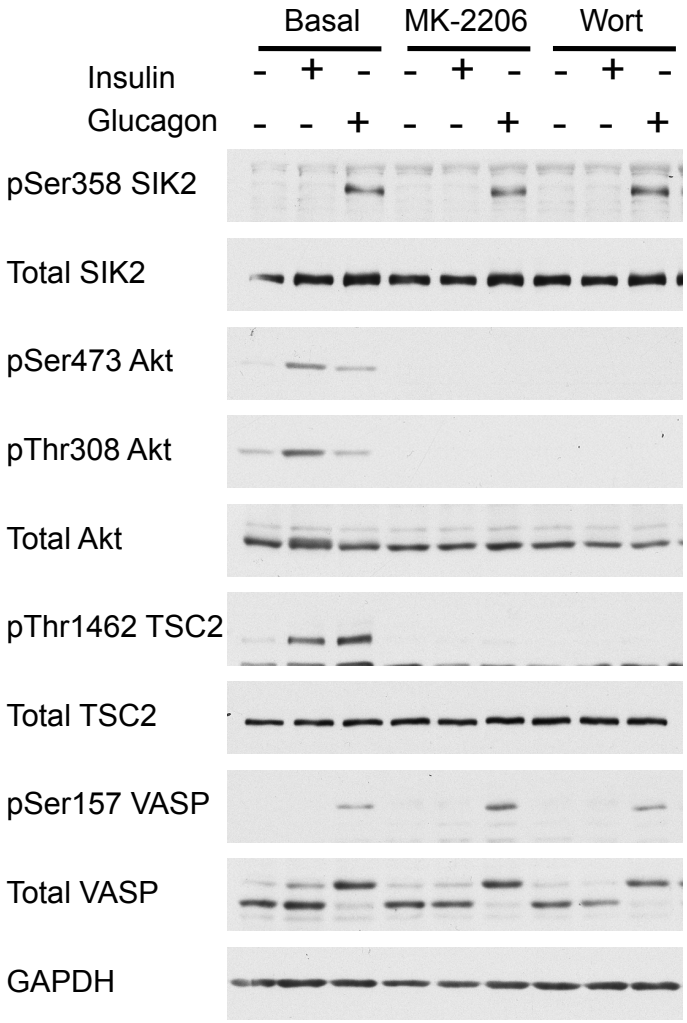

B

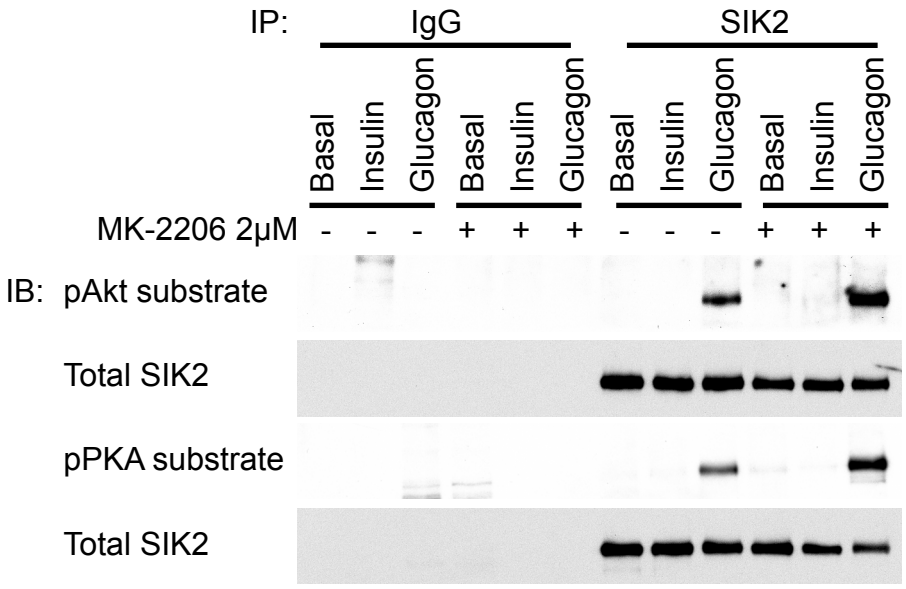

Figure 4.19 Effect of Akt and PI3K inhibitors on Ser358 SIK2 phosphorylation.

A) Primary mouse hepatocytes were pre-treated with 2 μM MK-2206 or 0.1 μM wortmannin (wort) for 1 h followed by stimulation with 100 nM glucagon or 10 nM insulin for 10 min. Lysates were immunoblotted with the indicated antibodies. Phospho-Akt and -TSC2 antibodies were used to confirm the effects of the inhibitors while the VASP antibody was used to confirm the activation of PKA by glucagon. **B)** Endogenous SIK2 was immunoprecipitated from 0.5 mg of the indicated lysates using the SIK2 antibody or a pre-immune IgG as negative control. These were then immunoblotted with the pPKA and pAkt substrate antibodies. Results are representative of three independent experiments.

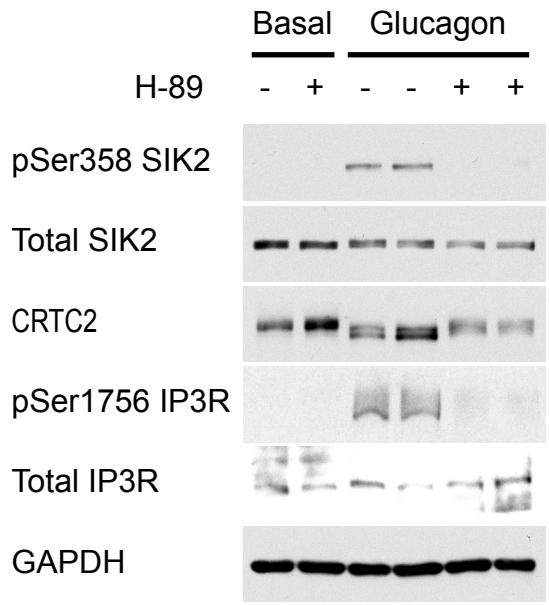

Figure 4.20 Effect of PKA inhibition on glucagon-induced Ser358 SIK2 phosphorylation in primary hepatocytes.

Primary mouse hepatocytes were pre-treated with 25 μM H-89 for 1 h followed by 100 nM glucagon treatment for 10 min prior to cell lysis. Lysates were immunoblotted for pSer358 SIK2 antibody, and with the CRTC2, pSer1756 inositol 1,4,5-triphosphate receptor (IP3R) antibodies to confirm the effects of inhibitor while the GAPDH antibody as a loading control. Results are representative of three independent experiments.

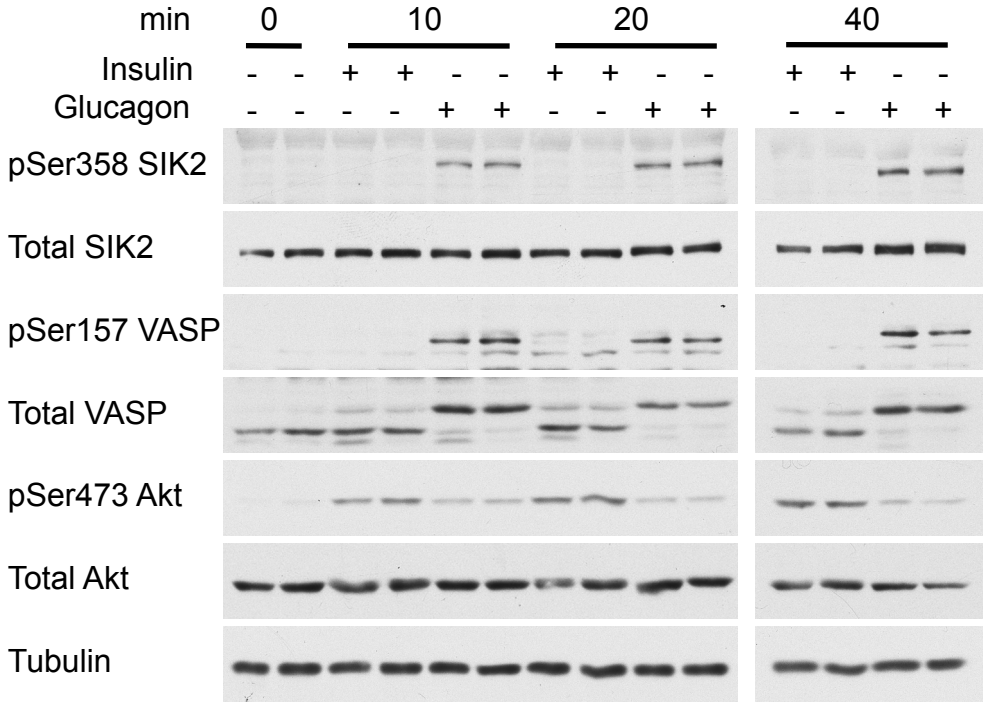

Figure 4.21 Longer-duration treatment of glucagon and insulin in primary hepatocytes.

Primary mouse hepatocytes were incubated with 100 nM glucagon or 10 nM insulin for the indicated times prior to cell lysis. Lysates were immunoblotted with the indicated antibodies. pAkt and VASP antibodies were used to confirm the stimulation by insulin and glucagon while the tubulin antibody was used as a loading control. Results are representative of three independent experiments.

4.2.4 Discussion

Phosphopeptide mapping identified that incubation of primary hepatocytes with glucagon promoted phosphorylation at five sites (Ser343, Ser358, Ser379, Thr484 and Ser587) in SIK2, whereas in stark contrast insulin treatment did not induce significant production of any phosphopeptides (Figure 4.9). Further analysis of mass spectrometry data with Proteome Discoverer software (Thermo Scientific, USA) failed to confirm Ser379 as a significant phosphorylation site and therefore it was not further investigated. In addition, phosphopeptide mapping did not identify Thr175 phosphorylation on SIK2 as the data analysis software (Xcalibur Qual and Proteome Discoverer) could not conclusively identify the phosphorylated residue in the peptide fragment that encompassed Thr175 (generated by in-gel trypsin digest) due to its long length (K*SGELLA**T**WCGSPPYAAPEVFEGQQYEGPQLDIWSMGVVLYVLVCGALPFDGPTLPILR*Q, * denotes

trypsin cleavage sites, residues 169 - 226). However, the constitutive-phosphorylation of SIK2 on Thr175 in the liver and HEK293 cells was confirmed using a phospho-specific antibody (Figure 4.15), supporting the previous results of Lizcano *et* al. Lizcano and colleagues showed, in cell-free assays and in LKB1 knock-out mouse embryonic fibroblast (MEF) as well as in LKB1-lacking HeLa cells, that SIKs were catalytically-inactive until phosphorylated by the LKB1-STRAD-MO25 complex at a well conserved T-loop threonine residue in their kinase domains (Thr175 for SIK2) (Lizcano et al., 2004). This was later confirmed in muscle tissue using muscle-specific LKB1 knock-out mice (Al-Hakim et al., 2005).

Investigation of hormonal-regulation of SIK2 phosphorylation in liver using carefully characterised and validated phospho-specific antibodies confirmed that SIK2 was indeed phosphorylated on at least four sites, Ser343, Ser358, Thr484, and Ser587 following glucagon treatment of primary hepatocytes (Figure 4.15) and also forskolin treatment of HEK293 cells (Appendix 1). Importantly, none of these sites were induced in response to insulin treatment of primary hepatocytes or IGF-1 treatment of HEK293 cells. Consistent with the results in primary hepatocytes, SIK2 Ser343, Ser358 and Thr484 phosphorylation were induced in liver by overnight fasting *in vivo*, which increases hepatic gluconeogenesis and glucagon secretion, but not by refeeding which promotes insulin secretion and as a consequence suppresses gluconeogenesis (Figure 4.16).

Ser358 phosphorylation induction following glucagon treatment was not altered by inhibition of the PI3K-Akt pathway using MK-2206 (an allosteric inhibitor of Akt) or wortmannin (PI3K inhibitor) and was observed in Akt2 knock-out primary hepatocytes (Figure 4.18, Figure 4.19). In contrast, SIK2 Ser358 phosphorylation in cells was significantly reduced by PKA inhibition using H-89, suggesting that glucagon requires PKA activity to increase phosphorylation of SIK2 on Ser358 (Figure 4.20). These results are contradictory to the previously published work of Dentin *et* al. (Dentin et al., 2007). They reported that insulin induces SIK2 phosphorylation on Ser358 in liver in an Akt-dependent fashion. However this identification of Ser358 as a potential Akt phosphorylation site in SIK2 was primarily based on the presence of the

minimum kinase consensus motif for Akt phosphorylation rather than unbiased phosphopeptide mapping. The authors used cell-free assays and experiments with recombinant wild-type and S358A SIK2 expressed in HEK293 cells to provide evidence that Akt could phosphorylate Ser358. Noticeably, Dentin and colleagues based most of their conclusions on the use of a generic phospho-Akt substrate motif antibody rather than generating/using a site-specific phospho-antibody to Ser358. Interestingly, the sequence around Ser358 and other phosphorylation sites (Ser343, Thr484 and Ser587) of SIK2 actually conforms to a preferred consensus motif for both PKA and Akt (Figure 4.14). Indeed I demonstrated that the Akt and PKA phospho-motif antibodies both readily detected SIK2 phosphorylation in primary hepatocytes following glucagon stimulation, which persisted even when Akt was inhibited using MK-2206, and importantly insulin treatment of primary hepatocytes did not induce phosphorylation of endogenous SIK2 at sites recognised by either of these antibodies (Figure 4.19). In addition, site-directed mutagenesis of SIK2 confirmed that both of these antibodies recognised all four phosphorylation sites (Figure 4.14). This argues that the cross-reactivity of this antibody may partly explain the discrepancy and erroneous conclusion of Dentin and colleagues. Indeed in support of my work another study in 3T3-L1 cells and primary rat adipocytes also found that Ser358 was phosphorylated after various cAMP-elevating treatments (β-adrenergic receptor agonist CL 316,243 and forskolin), but not after insulin treatment (Henriksson et al., 2012).

Recently, MacKenzie and colleagues using a phospho-proteomics approach in a mouse macrophage cell line (RAW264.7) found that SIK2 became phosphorylated on Ser343 following prostaglandin (PGE_2) or PGE_2 plus lipopolysaccharide (LPS) stimulation (MacKenzie et al., 2013). The authors did not validate this finding in a more physiological system, but they did use the phospho-specific antibody that I had validated to indicate that forskolin treatment of HEK293 cells promoted Ser343 phosphorylation on overexpressed SIK2. PGE_2 and LPS treatment of macrophages increases intracellular cAMP levels thereby activating PKA (similar to glucagon treatment of liver (Jiang and Zhang, 2003)), which may suggest a common

pathway to Ser343 phosphorylation in these two very different cell systems. However, further studies with more specific PKA inhibitors (when available as H-89 is not highly specific) and/or genetic manipulation (e.g. introduction of dominant-negative PKA catalytic subunit) are needed to confirm the above hypothesis.

SIK2 was phosphorylated on Thr484 following glucagon treatment of primary hepatocytes or fasting in intact mouse liver. Interestingly, this site was reported to be phosphorylated in mouse primary cortical neurons following induction of increase in intracellular [Ca^{2+}] and in brain following transient oxygen-glucose-deprivation of mice (Sasaki et al., 2011). In both cases Ca^{2+}/calmodulin-dependent protein kinases (CaMK) I/IV were activated and were proposed to mediate phosphorylation of SIK2 on Thr484. Glucagon treatment of primary hepatocytes can also increase intracellular calcium and activate CaMKII (Wang et al., 2012). However, this activation was proposed to be downstream of PKA-mediated phosphorylation of IP3R that promoted Ca^{2+} release from the endoplasmic reticulum (Ozcan et al., 2012; Wang et al., 2012). In addition, in cell-free assays, PKA was found to directly phosphorylate SIK1 on Thr475, the equivalent site to Thr484 of SIK2 (Stewart et al., 2013). Based on these studies, SIK2 Thr484 phosphorylation in liver following glucagon or overnight fast is likely to be mediated by cAMP-PKA signalling. However, further studies using specific PKA or CaMK inhibitors (when available) and/or their dominant-negative mutants in wild-type primary hepatocytes or CaMKIIγ-null hepatocytes are needed to confirm the protein kinase(s)/phosphatase(s) responsible for Thr484 phosphorylation/dephosphorylation following glucagon or fasting in the liver.

I was unable to conclusively detect significant/consistent phosphorylation of endogenous SIK2 on Ser587 by immunoblot analysis of either whole-cell lysates or immunoprecipitated SIK2 from primary hepatocytes (data not shown). However, immunoblot analysis did detect Ser587 phosphorylation on overexpressed SIK2 after glucagon treatment of primary mouse hepatocytes and following forskolin treatment of HEK293 cells (Figure 4.14). These results support previous studies which found that Ser587 was phosphorylated in response to cAMP-

elevating agents (i.e. forskolin) or overexpression of recombinant PKA in various cell lines (Horike, 2003; Ravnskjaer et al., 2007; Screaton et al., 2004).

Moreover, a recent study with SIK3 in 3T3-L1 adipocytes (Berggreen et al., 2012) and SIK1 phosphopeptide mapping in primary hepatocytes following glucagon treatment (K.Patel, K.Sakamoto, and D.Campbell, data not shown) suggested that similar to SIK2, both SIK1 and SIK3 are phosphorylated on multiple residues following cAMP-PKA signalling, while insulin treatment did not induce detectable phosphorylation of SIK1 in primary hepatocytes when assessed using phosphopeptide mapping. These results collectively indicate that all three SIK isoforms are regulated by glucagon through multiple phosphorylation but are less likely to be regulated by insulin.

My studies have characterised and validated selective SIK1, 2 and 3 antibodies as well as SIK2 phospho-specific antibodies for endogenous SIK proteins in mouse tissues and in a cultured human cell line (HEK293) based on stringent experimental criteria (Bordeaux et al., 2010; Couchman, 2008; Michel et al., 2009; Saper, 2005). This provides confidence that these antibodies are suitable for the study of the expression, role and regulation of SIKs in the liver (and other cell/tissue systems) with accuracy and reliability.

These validated antibodies allowed, for the first time, analysis of the protein expression pattern for SIK2 and SIK3 across various mouse tissues. This information may help to further investigate the regulation and physiological importance of these isoforms in different mouse tissues. The data is actually in good agreement with the mRNA expression pattern previously reported for SIK2 and SIK3 (Horike, 2003; Katoh et al., 2004). Interestingly, there appears to be very little, if any, SIK2 or SIK3 in mouse kidney (Figure 4.7, Figure 4.8). This is somewhat unexpected as gluconeogenesis occurs in both liver and kidney. It is possible that SIK2 and 3 are specifically expressed in particular region/cell types in kidney, which were diluted and remained undetectable in the total kidney tissue extracts or that the SIK1 is the dominant SIK isoform in the kidney. I was unable to assess the protein expression of SIK1 in tissue due to poor sensitivity/reliability of the SIK1 antibodies in unstimulated cells/tissues. However, SIK1

mRNA was found in the kidney albeit at a lower level compared to brain and adrenal gland (Horike, 2003). It would also be important to validate the relative protein expression patterns of SIKs in human tissue extracts (e.g. adipose, muscle, liver).

In summary, the data in this chapter supports a role for phosphorylation of four different sites on SIK2 (Ser343, Ser358, Th484 and Ser587) in the regulation of SIK2 by fasting and glucagon. Importantly re-feeding and insulin treatment did not regulate SIK2 phosphorylation in the liver. Glucagon induction of PKA is the likely mechanism that promotes phosphorylation of SIK2 at these sites, however further studies as described above are needed to confirm this hypothesis. In addition, it remains possible that these hormones may regulate SIK2 by mechanisms independent of phosphorylation but this remains to be proven.

5 Role of phosphorylation in the regulation of SIK2 functions

5.1 Introduction

Previous studies proposed that SIK2 is phosphorylated on multiple residues including constitutively on Thr175 which is essential for its intrinsic kinase activity (Lizcano et al., 2004), on Ser358 which is proposed to increase the intrinsic kinase activity of SIK2 (Dentin et al., 2007), on Ser587 by PKA following induction of cAMP-signalling in various cell lines (reviewed in (Berdeaux, 2011)) and on Thr484 by CaMKI/IV following oxygen-glucose deprivation in neurons and intact brain (Sasaki et al., 2011). The role for these site-specific phosphorylations on SIK2 regulation is discussed in detail in section 1.5.5.

Additional studies have proposed that fasting and glucagon antagonise SIK2 repression of CREB-dependent gene transcription by Ser587 phosphorylation, potentially by promoting its cytoplasmic translocation/retention and reduced phosphorylation and nuclear retention of CRTC2 (Screaton et al., 2004). However, this requires more detailed investigation as there is a lack of evidence on the effect of phosphorylation of Ser587 or glucagon on intrinsic kinase activity of SIK2. In addition, this proposed regulation is derived from experiments in non-hepatic cells/tissues and the studies have reported contradictory results (see section for detail 1.5.5.3). Moreover, results described in Chapter 4 suggest that glucagon induces additional phosphorylations on SIK2 in liver questioning whether Ser587 is even the principle regulatory phosphorylation site.

In summary, studies so far have identified multiple modes of potential regulation of SIK2, but have lacked clarity and validation on the effect of phosphorylation on intrinsic activity of endogenous SIK2 or its cellular localisation in more physiologically relevant models and its importance in hormone-regulated hepatic gluconeogenesis. Hence the mechanism by which

cAMP-agonists or -elevating agents regulate SIK2 activity and downstream CREB-dependent gene transcription requires more detailed investigation.

Thus, the objectives of this chapter are as follows;

1) To investigate the effects of glucagon or insulin on SIK2 kinase activity, intracellular localisation and complex formation (protein-protein interaction).
2) To investigate the importance of SIK2 phosphorylation at each glucagon-regulated site on kinase activity, intracellular localisation and complex formation (protein-protein interaction) properties of SIK2.

5.2 Results

5.2.1 Kinase activity of SIK2 in primary mouse hepatocytes and liver

Measurement of endogenous SIK2 kinase activity in mouse primary hepatocytes showed that there was a significant inherent SIK2 kinase activity detectable when immunoprecipitated from unstimulated cells and assayed *in vitro* using 'SAKAMOTO'-tide (ALNRTSSDSALHRRR, residues 165-176 of human CRTC2 with three additional arginines (underlined) on the C-terminus) as a substrate (Figure 5.1). Although glucagon or insulin induced significant SIK2 phosphorylation (Figure 4.21), this did not cause any detectable/significant changes in its kinase activity (Figure 5.1).

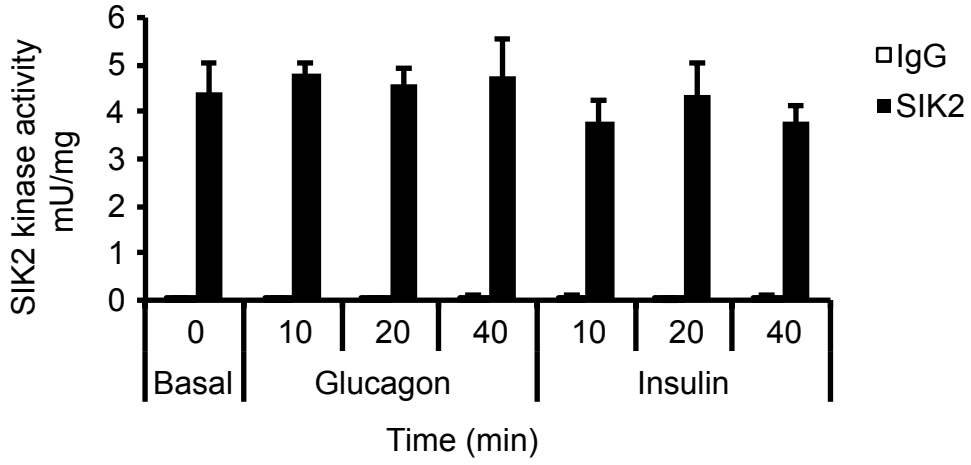

Figure 5.1 SIK2 kinase activity in primary mouse hepatocytes.

Primary hepatocytes were treated with 100 nM glucagon or 10 nM insulin for the indicated time prior to cell lysis. Stimulation for respective signalling pathway (insulin or glucagon) was confirmed by immunoblotting (**Figure 4.21**). Endogenous SIK2 was immunoprecipitated from 0.5 mg of cell lysate with 2 µg of the C-terminal in-house antibody or pre-immune IgG as a negative control. The immunoprecipitates were subjected to *in vitro* kinase assay for 20 min using 200 µM 'SAKAMOTO'-tide as substrate (as described in Material and Methods section). Assay was conducted in triplicate. Data is presented as mean ± SD, n=3 independent experiments.

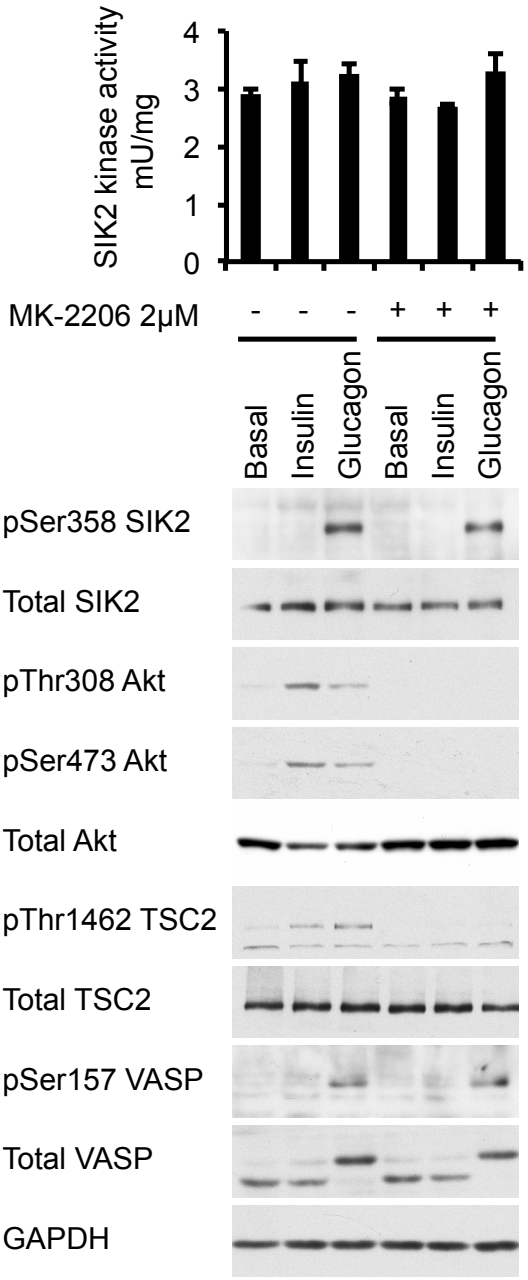

Figure 5.2 Hormone-stimulated SIK2 kinase activity in primary mouse hepatocytes in the presence or absence of Akt inhibitor.

Primary hepatocytes were pre-treated with 2 µM MK-2206 (a specific Akt inhibitor) for 1 h followed by 100 nM glucagon or 10 nM insulin treatment for 10 min (MK-2206 was present during hormone treatments). The lysates were immunoblotted with the indicated antibodies. The pAkt and pTSC2 antibodies were used to confirm the effects of insulin and MK-2206 and the pVASP and total VASP antibodies were used to confirm PKA activation by glucagon. Endogenous SIK2 was immunoprecipitated from 0.5 mg of these lysates and was subjected to *in vitro* kinase assay in triplicate using 200 µM 'SAKAMOTO'-tide as substrate. Data is presented as mean ± SD, n=3 independent experiments.

To clarify whether the basal SIK2 kinase activity was regulated by Akt-PI3K signalling, MK-2206, an allosteric Akt inhibitor (Hirai et al., 2010), was added to the primary mouse hepatocytes followed by stimulation with glucagon or insulin. Insulin stimulation activates PI3K and the generation of the second messenger phosphatidylinositol 3,4,5-trisphosphate [PtdIns(3,4,5)P_3] (Mora et al., 2004). This binds to the pleckstrin homology (PH) domain of Akt, inducing a conformational change that enables PDK1 (phosphoinositide-dependent kinase-1) to phosphorylate and activate Akt which in turn phosphorylates multiple downstream substrates including TSC2 (tuberous sclerosis 2) (Taniguchi et al., 2006). As shown in Figure 5.2, MK-2206 ablated insulin-stimulated phosphorylation of Akt and its substrate TSC2, while insulin or MK-2206 had no effect on PKA-mediated phosphorylation on VASP. The basal and stimulated (with glucagon or insulin) SIK2 activity was not affected by inhibition of Akt with MK-2206 in primary mouse hepatocytes (Figure 5.2).

In parallel, the kinase activity of immunoprecipitated SIK2 was measured in liver extracts generated from mice following 16-h fasting (to stimulate endogenous glucagon secretion) or 16-h fasting followed by 4-h refeeding (to stimulate endogenous insulin secretion). Similar to the results in primary hepatocytes, significant SIK2 kinase activity was detected in the liver extracts from fed *ad libitum* mice, while neither fasting nor refeeding had any impact on SIK2 kinase activity (Figure 5.3), despite significant SIK2 phosphorylation following fasting (Figure 4.16).

SIK2 kinase activity was further measured using full-length bacterially expressed/purified GST-CRTC2 protein as substrate to rule out the possibility that the hormonal-regulation was not apparent when measured using the synthetic short peptide substrate 'SAKAMOTO'-tide (Figure 5.4). The immunoprecipitated endogenous SIK2 from primary mouse hepatocyte lysates had similar basal activity towards GST-CRTC2, and this was not affected by glucagon treatment of the cells (Figure 5.4). All of this CRTC2 phosphorylation could be blocked using a SIK inhibitor (HG-9-91-01) *in vitro* (Figure 5.4) (Clark et al., 2012).

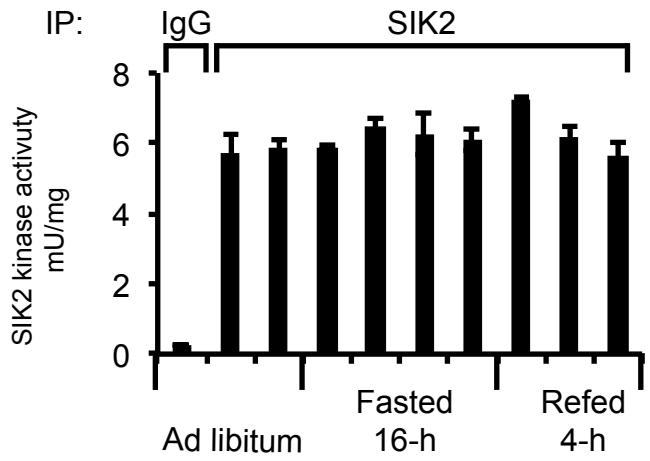

Figure 5.3 SIK2 kinase activity in liver of fasted and refed mice.

Homogenates were generated from livers derived from C57BL/6 male mice (8-10 week-old) that had been subjected to fed *ad libitum*, 16-h fasting (overnight) or 16-h fasting followed by 4-h refeeding. Confirmation that SIK2 phosphorylation responded to fasting and refeeding is shown in (**Figure 4.16**). Endogenous SIK2 was immunoprecipitated from 0.5 mg of these liver homogenates using the C-terminal SIK2 antibody or pre-immune IgG as a negative control. The precipitates were subjected to *in vitro* kinase assay as described in **Figure 5.1**. Data is presented as mean ± SD, n=3 technical replicate. Each column represents independent mouse liver homogenates.

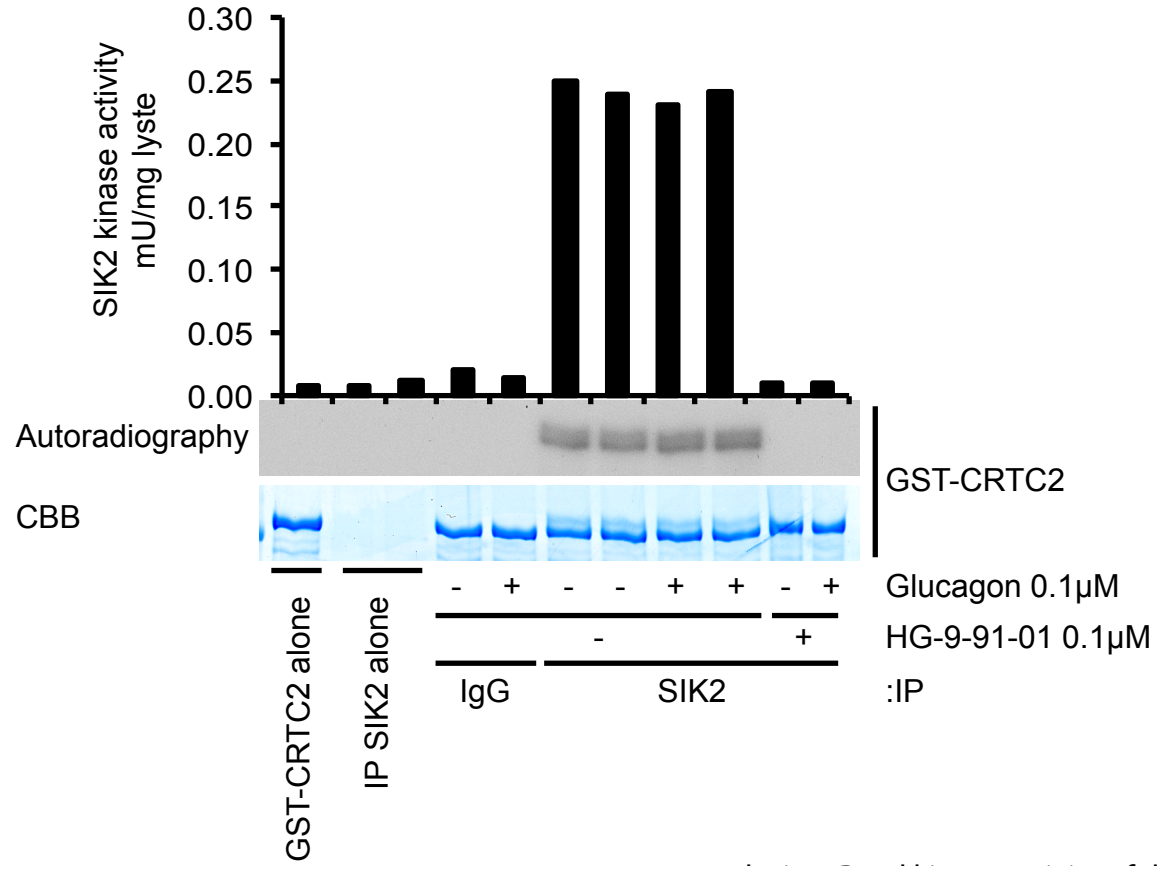

Figure 5.4 *In vitro* SIK2 kinase activity measured with full-length CRTC2 as substrate.

Primary hepatocytes were treated with 100 nM glucagon for 10 min prior to cell lysis. Endogenous SIK2 was immunoprecipitated from 1 mg of these lysates and subjected to an *in vitro* kinase assay using 1 μg of full-length GST-human CRTC2 (bacterially expressed) as substrate. The final assay mixtures were electrophoresed (SDS-PAGE) and the gel was stained with coomassie brilliant blue (CBB) and dried for autoradiography. Subsequently, the GST-CRTC2 bands were excised and the radioactivity (^{32}P) incorporated into the substrate was measured by Cerenkov counting. Additional SIK2

immunoprecipitates were pre-treated with 0.1 µM HG-9-91-01 (SIK inhibitor) for 10 min prior to assay. Pre-immune IgG (IP) was included as a negative control. Results are representative of two independent experiments.

5.2.2 Analysis of the kinase activity of phosphorylation-defective mutants of SIK2

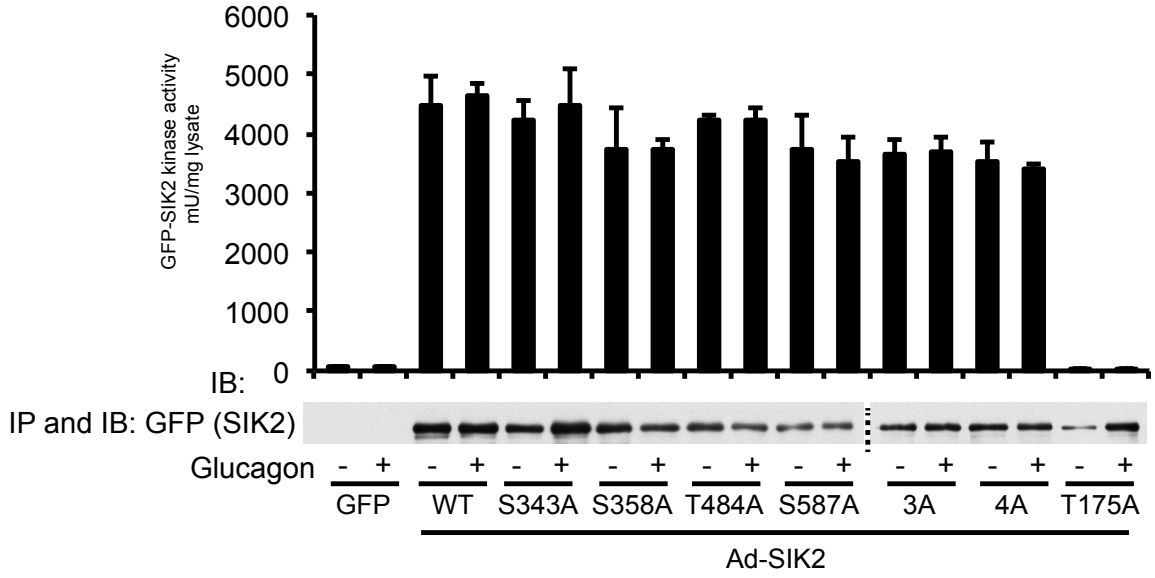

Figure 5.5 Kinase activity of SIK2 wild-type and phosphorylation-defective mutants with or without glucagon treatment.

GFP, GFP-SIK2 wild-type (WT) or the indicated GFP-SIK2 mutants were expressed in primary hepatocytes using adenoviral vectors (1:10 MOI) 16 h prior to 100 nM glucagon treatment for 10 min. GFP-SIK2 was immunoprecipitated from 50 µg of lysates with GFP-agarose beads and subjected to either *in vitro* kinase assay in duplicate with 200 µM of 'SAKAMOTO'-tide or immunoblotting. The SIK2 3A recombinant protein included S343A, S358A and T484A mutations, while 4A mutant had these mutations plus S587A mutation. Data is presented as mean ± SD, n=3 independent experiments.

The data in Chapter 4 demonstrated that phosphorylation of SIK2 is enhanced on four different residues (Ser343, Ser358, Thr484 and Ser587) following glucagon treatment of hepatocytes. To assess whether these phosphorylations (either individually or in combination) impacted on inherent kinase activity, GFP-tagged wild-type or phosphorylation-defective mutants (Ser/Thr to Ala) of SIK2 were ectopically-expressed in mouse primary hepatocytes using adenoviral vectors (as described in section 3.2.2.2). As with endogenous SIK2, the *in vitro* kinase activity of recombinant wild-type GFP-SIK2 was not altered following glucagon treatment (Figure 5.5). In addition, the activity of each phosphorylation-defective mutant (S343A, S358A, T484A and S587A) exhibited similar specific activity to that of wild-type SIK2

and there was no difference between basal and glucagon-treated cells (Figure 5.5). Furthermore, the kinase activities of GFP-SIK2 (3A or 4A), where SIK2 was mutated on three (3A) or all four (4A) different glucagon-promoted phosphorylation sites (S343A, S358A, T484A or S343A, S358A, T484A and S587A), were similar to that of wild-type SIK2. Once more, glucagon treatment had no effect on their *in vitro* kinase activity following immunoprecipitation (Figure 5.5). In contrast, mutation of the T-loop Thr175 of SIK2 (T175A) generated a SIK2 that lacked intrinsic kinase activity (Figure 5.5) as expected (Lizcano et al., 2004). Therefore, we concluded here that the phosphorylation of SIK2 in response to glucagon does not modulate SIK2 intrinsic activity.

5.2.3 SIK2 autophosphorylation

Experiments so far did not investigate the effects of glucagon-/forskolin-mediated phosphorylation on SIK2 kinase activity when measured against peptide (Figure 5.5) or full-length protein substrate (Figure 5.4). Numerous protein kinases have been shown to autophosphorylate and a previous report indicated that SIK2 autophosphorylation increased following Ser358 phosphorylation (Dentin et al., 2007) prompting us to investigate the effect of SIK2 phosphorylation on its ability to autophosphorylate. HA-SIK2 wild-type and phosphorylation-defective mutants were expressed in HEK293 cells prior to stimulation with or without forskolin to increase intra-cellular cAMP concentration and consequently activate the PKA pathway (Figure 5.6). Immunoprecipitated HA-SIK2 was then incubated with Mg^{2+}-[γ-^{32}P] ATP and subjected to SDS-PAGE and autoradiography (Figure 5.6). The wild-type SIK2 underwent significant autophosphorylation with no change in the extent of autophosphorylation after forskolin treatment. Similarly, the phosphorylation-defective SIK2 single point mutants (S343A, S358A, T484A or S587A) showed a similar level of autophosphorylation to that seen with wild-type SIK2. There was no autophosphorylation of the kinase-inactive mutants (T175A and D260A), confirming the phosphorylation of wild-type SIK2 was not due to a contaminating kinase(s) in the immunoprecipitate. These results suggest

that point mutation on S343A, S358A, T484A or S587A has no impact on the autophosphorylation of SIK2 (Figure 5.6).

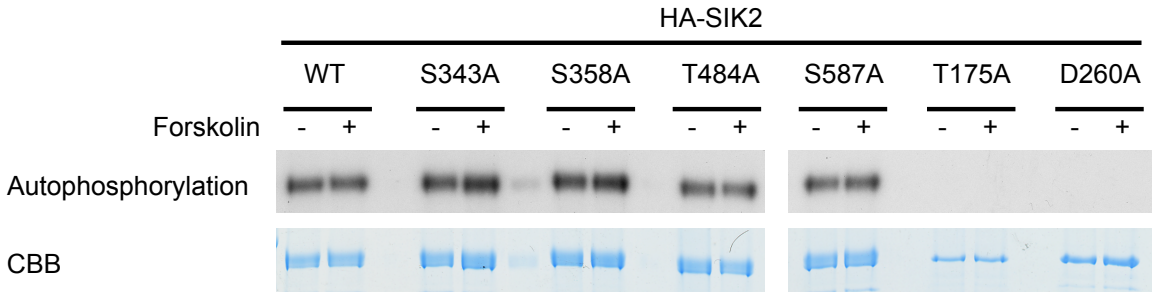

Figure 5.6 *In vitro* autophoshorylation of SIK2 wild-type and phospho-defective mutants.

Wild-type (WT) or the indicated HA-SIK2 mutants were expressed in HEK293 cells for 36 h prior to treatment with 10 µM forskolin for 10 min. HA-SIK2 was immunoprecipitated from 0.5 mg lysates using HA-agarose beads and was then incubated with Mg^{2+}-[γ-^{32}P] ATP *in vitro*. The resultant mixtures were electrophoresed (SDS-PAGE) using tris-glycine gels. The gels were stained with coomassie brilliant blue (CBB) and dried before autoradiography. Kinase inactive mutants of SIK2 T175A and D260A were used as negative controls. Data is representative of two independent experiments.

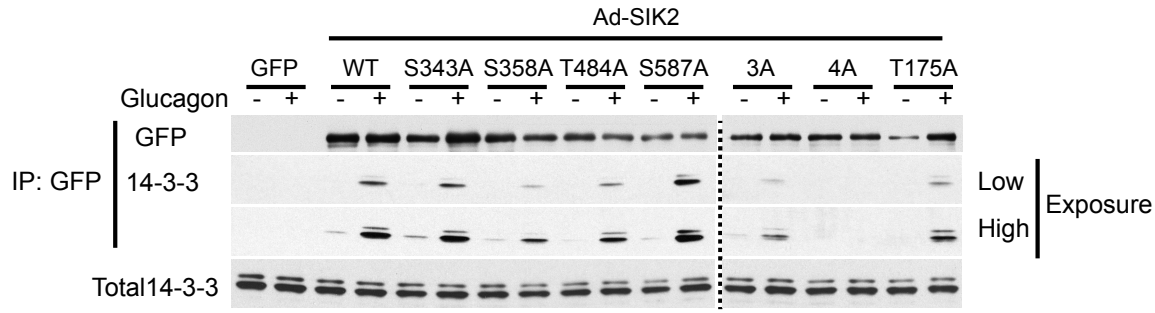

Figure 5.7 SIK2 interactions with 14-3-3 proteins.

GFP, GFP-SIK2 WT or the indicated GFP-SIK2 mutants were expressed in primary hepatocytes using adenoviral vectors (1:10 MOI) 16 h prior to 100 nM glucagon treatment for 10 min. GFP-SIK2 was immunoprecipitated from 50 µg of lysates with GFP-agarose beads and subjected to immunoblotting and detection of 14-3-3 binding using pan-14-3-3 antibody. The SIK2 3A protein included S343A, S358A and T484A mutations, while 4A mutant had these mutations plus S587A mutation. Data is representative of two independent experiments.

5.2.4 14-3-3 binding

14-3-3 isoforms are dimeric adapter proteins that bind to phospho-serine/-threonine residues of their target proteins and have been implicated in multiple cellular processes such as cell growth and metabolism (Tinti et al., 2012). The 14-3-3 binding can affect the activity, function or cellular location of its target proteins by either blocking the functional domain, creating conformational change or by providing a scaffold for further interactions (Tinti et al., 2012). Therefore, 14-3-3 binding in wild-type and phosphorylation-deficient SIK2 mutants was investigated in primary mouse hepatocytes. Lysates were prepared from cells after treatment

with or without glucagon (Figure 5.5). GFP-SIK2 bound to 14-3-3 was only detected following glucagon treatment, suggesting that glucagon-mediated phosphorylation is likely to be responsible for SIK2-14-3-3 interaction (Figure 5.5). Further investigation using phosphorylation-defective mutants of SIK2 showed that mutation of Ser358 to Ala partially disrupted the 14-3-3 binding, while the 4A GFP-SIK2 mutant completely abolished 14-3-3 binding. These data indicated that all four glucagon-mediated phosphorylation sites (S343A, S358A, T484A and S587A) participate to some extent in 14-3-3 binding. Importantly, the T-loop T175A mutant bound 14-3-3 to a similar extent to that of wild-type SIK2 (Figure 5.5), unlike SIK1 and 3 where T-loop phosphorylation served as a principle-binding site for 14-3-3 (Al-Hakim et al., 2005).

5.2.5 Sub-cellular location of SIK2 in primary mouse hepatocytes

Immunofluorescence (with an anti-SIK2 primary antibody) demonstrated that both endogenous SIK2 and adenovirally-overexpressed recombinant SIK2 were predominantly localised in the cytoplasm of not only unstimulated primary mouse hepatocytes but also in the cytoplasm following 10 min of glucagon treatment (Figure 5.8). SIK2 was diffusely localised in cytoplasm and did not appear (by visual examination under microscope) to accumulate in any specific regions of the cells. These findings were further supported by cell fractionation experiments (Figure 5.9A), where SIK2 was shown to be localised in the cytoplasm before and after glucagon treatment. In addition, H-89 treatment of the cells to inhibit cAMP-PKA signalling and SIK2 phosphorylation had no effect on the cytoplasmic location of SIK2 (Figure 5.9A). Similar findings were observed up to 60 min following stimulation of primary hepatocytes with glucagon and H-89 treatment (Figure 5.9B).

Consistently, all phosphorylation-defective SIK2 mutants were found in the cytoplasm of the cells before or after the exposure to glucagon (Figure 5.8). Most noteworthy, the SIK2 4A mutant (that completely lacked 14-3-3 binding as shown Figure 5.7) was also located in the cytoplasm in the absence or presence of glucagon. It should be noted that for these

experiments anti-SIK2 antibody was used for GFP-tagged SIK2, since due to low-level expression (MOI 1:1) of GFP-SIK2 (that was intentionally used in these experiments to minimise experimental artifacts due to excess overexpression) it was not possible to detect significant GFP fluorescence.

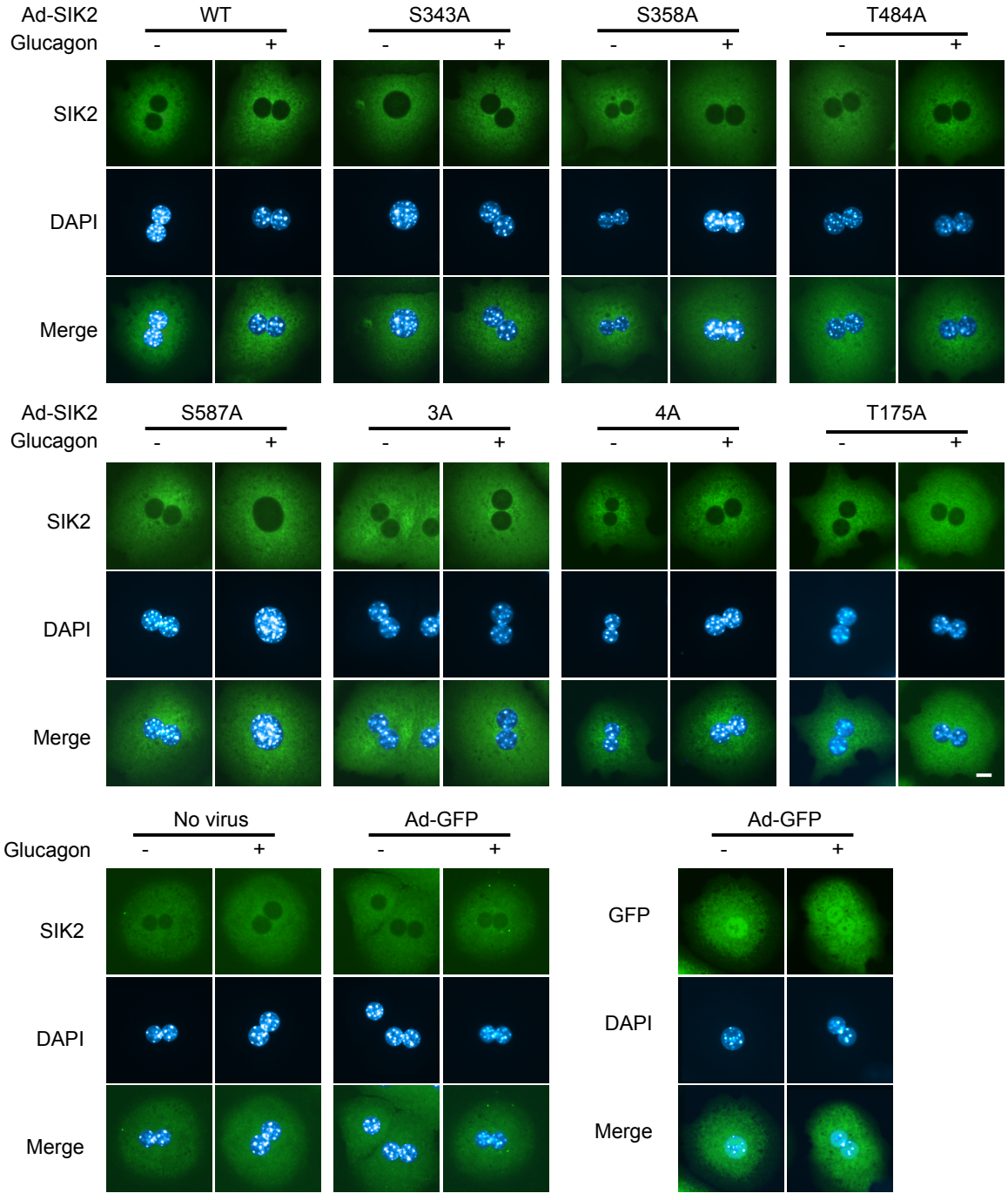

Figure 5.8 Analysis of SIK2 cellular localisation by immunofluorescence.

Primary hepatocytes were infected with the indicated SIK2 adenoviral constructs (Ad-SIK2) or Ad-GFP (control) for 16 h (1:1 MOI) followed by 100 nM glucagon stimulation for 10 min. Subsequently, cells were fixed with 3.7% paraformaldehyde and immunostained with anti-SIK2 to visualise SIK2 or DAPI to visualise the nuclei. Images were captured with a fluorescence microscope (Nikon Eclipse Ti) using Nikon NIS-Elements BR 3.1 software. Images were cropped using Adobe Photoshop CS5.1. Scale bar is 10 µm in length. Data is representative of three independent experiments.

A

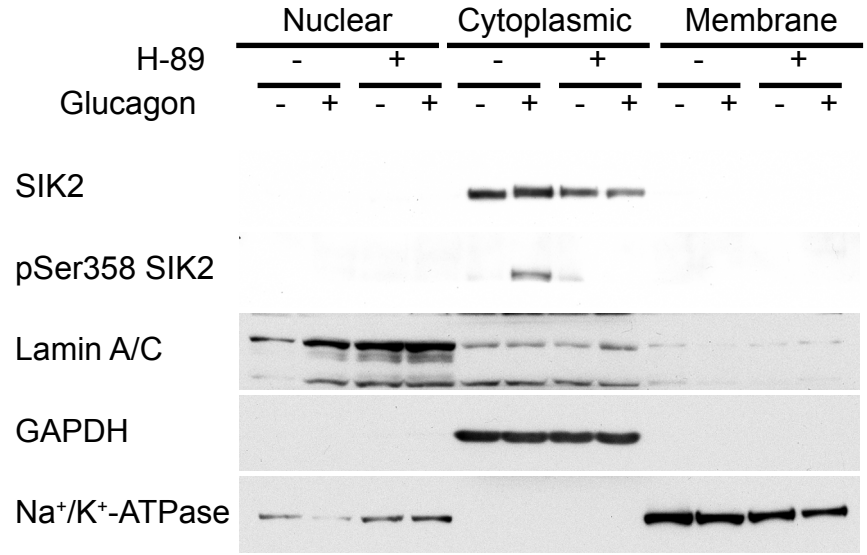

B

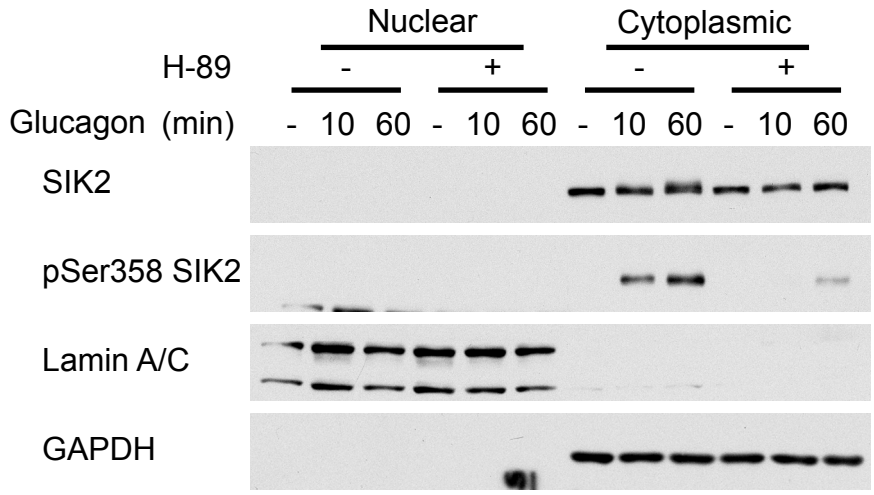

Figure 5.9 Analysis of SIK2 cellular localisation by cell fractionation.

A) Primary hepatocytes were pre-treated with 25 µM H-89 for 1 h followed by 100 nM glucagon for 10 min. Subsequently, the cells were lysed and lysates were fractionated to generate nuclear, cytoplasmic and membrane compartments as described in Materials and Methods. The fractions were immunoblotted with the indicated antibodies. The Lamin A/C, GAPDH and Na^+/K^+-ATPase antibodies were used to validate nuclear, cytoplasmic and membrane fractions respectively. **B)** Primary hepatocytes were pre-treated with 25 µM H-89 for 1 h followed by 100 nM glucagon for 10 or 60 min. The lysates were analysed as above. Results are representative of two independent experiments.

5.2.6 Effects of SIK2 phosphorylation-defective mutants on SIK2 substrate phosphorylation in primary hepatocytes.

Glucagon treatment induces a reduction in the phosphorylation on SIK2 substrates such as CRTC2 and class IIa HDACs in intact cells (Berdeaux et al., 2007; Dentin et al., 2007; Koo et al., 2005; Mihaylova et al., 2011). In contrast, results presented in this thesis so far have shown that glucagon-mediated phosphorylation had no effect on SIK2 intrinsic activity or cellular localisation (Figure 5.2, Figure 5.8). This raises the question as to whether glucagon induced changes in the phosphorylation of SIK2 substrates in cells are dependent on SIK2 phosphorylation. To this end, SIK2 substrate phosphorylation was assessed in intact hepatocytes that ectopically-expressed SIK2 phosphorylation-defective mutants (Figure 5.10). CRTC2 and CRTC3 undergo increased mobility on SDS-PAGE (indicative of dephosphorylation) when lysates are isolated from glucagon-treated control lysates (GFP alone). Glucagon-induced mobility of these proteins was similar in lysates from cells expressing SIK2 wild-type or individual phosphorylation-defective SIK2 mutants. In contrast, this glucagon-induced band-shift was absent in lysates isolated from cells expressing the 3A or 4A SIK2 mutants. Similar observations were also noted with HDAC4, an alternative SIK substrate, visualised using the phospho-specific Ser264 HDAC4 antibody. There was a lack of reduction in signal in glucagon-treated 3A- and 4A-mutant-expressing lysates. Taken together, these results suggested that glucagon-induced dephosphorylation of SIK2 substrates (at least CRTC2/3 and HDACs) might be mediated directly via SIK2 regulation and all four glucagon-regulated sites were important for this effect.

Figure 5.10 SIK2 substrate phosphorylation in hepatocytes expressing SIK2 wild-type or phosphorylation-defective mutants.

GFP, GFP-SIK2 wild-type (WT) or the indicated GFP-SIK2 mutants were expressed in primary hepatocytes using adenoviral vectors (1:10 MOI) 16 h prior to 100 nM glucagon treatment for 10 min. The lysates were immunoblotted with the indicated antibodies. The recombinant SIK2 3A protein included S343A, S358A and T484A mutations, while 4A mutant had these mutations plus S587A mutation. Results are representative of three independent experiments.

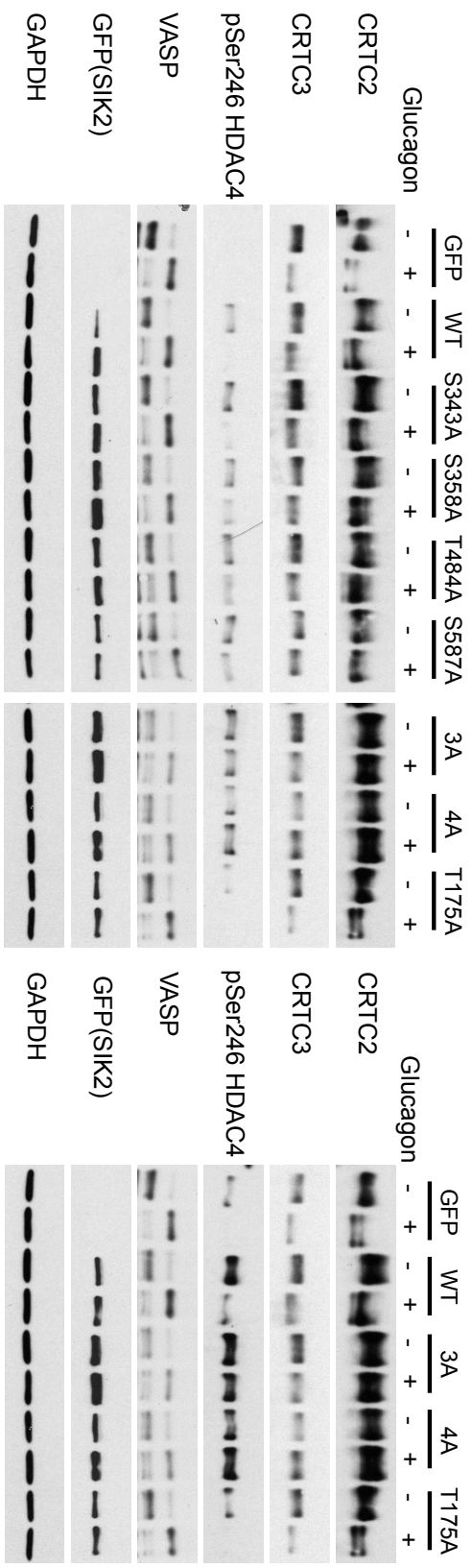

5.2.7 Analysis of SIK2 complexes by size exclusion chromatography

SIK2 binds to 14-3-3 in a phosphorylation-dependent manner (Figure 5.7) and this may serve as a scaffold to interact with other proteins. To investigate the effect of glucagon on potential protein-protein interactions of SIK2, whole-cell lysates of primary mouse hepatocytes were subjected to non-denaturing size-exclusion chromatography and the resultant fractions were immunoblotted with SIK2 antibodies (Figure 5.11). SIK2 was detected in fractions eluted at the expected molecular mass of SIK2 (~100 kDa) and also in fractions eluted at molecular mass of ~600 kDa (Figure 5.11). Noticeably, following glucagon treatment of the cells, SIK2 was only detected in the fractions of expected molecular mass of SIK2 (Figure 5.11). SIK2 phosphorylated at Ser358 was only detected in the glucagon-treated cells.

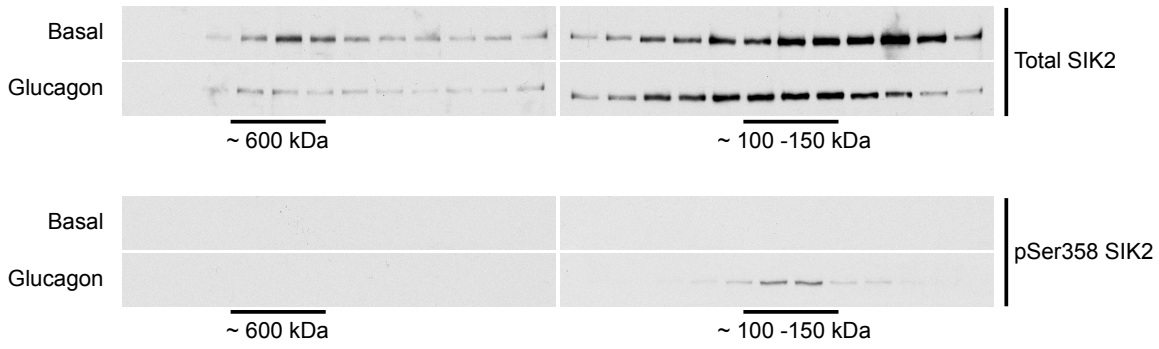

Figure 5.11 Molecular size detection of hepatic SIK2 using size-exclusion chromatography.

Primary hepatocytes were treated with or without 100 nM glucagon for 10 min. The lysates were subjected to size-exclusion chromatography on a HiLoad 16/60 Superdex 200 pg column and alternate fractions were immunoblotted with the indicated SIK2 antibodies. Blots are representative of three independent experiments.

5.3 Discussion

In vitro kinase activity following immunoprecipitation of endogenous or recombinant protein is routinely used to assess the inherent specific-activity of the enzyme (Hastie et al., 2006). As phosphorylation status is maintained during this isolation, it provides a measure of the direct effects of phosphorylation on enzyme activity (Hastie et al., 2006). I assessed the effect of hormone-induced SIK2 phosphorylation prior to isolation (using glucagon or forskolin treatment of cells for up to 40 min, or by overnight fasting *in vivo*) and compared the activity of phosphorylation site mutants (single, triple or quadruple) with wild-type SIK2. In every case

there was no measurable impact of phosphorylation at these glucagon-regulated residues on SIK2 specific activity assessed in cell-free assays (Figure 5.1, Figure 5.2, Figure 5.3, and Figure 5.5). Insulin treatment of cells, refeeding *in vivo* or inhibition of the key insulin-regulated PI3K-Akt pathway using MK-2206 had no effect on the kinase activity of SIK2 (Figure 5.2, Figure 5.3). Similar findings were observed when SIK2 activity was assessed using a peptide substrate or full-length GST-CRTC2 (as more physiologically-relevant protein substrate) (Figure 5.4). In addition, SIK2 autophosphorylation did not change following cAMP-elevating agent (forskolin) treatment in HEK293 cells (Figure 5.6). Together these data demonstrate in a compelling way that the inherent activity of SIK2 is not altered by glucagon or insulin treatment of primary hepatocytes, by fasting or refeeding *in vivo* liver or by phosphorylation of any or all of the glucagon-regulated phosphorylation sites at least when assessed *in vitro* (Figure 5.12). This is in agreement with previous findings in primary adipocytes, where SIK2 activity was unchanged following c-AMP-elevating (CL 316,243 β-adrenergic receptor agonist) treatment and the authors reached a similar conclusion using a different peptide substrate ('HDAC5'-tide: PLRKTASEPNLKRRR, residues 253-267 of human HDAC5) as well as HDAC5 protein (1-550 of human protein) to measure the kinase activity of SIK2 (Henriksson et al., 2012).

The results presented in this chapter are in direct contrast to those of Dentin *et* al. who proposed that Ser358 phosphorylation increases SIK2 kinase activity in liver following insulin exposure through an Akt-dependent mechanism (Dentin et al., 2007). To assess the effect of insulin on kinase activity of SIK2, they immunoprecipitated recombinant SIK2, wild-type or S358A, from HEK293 cells treated with or without insulin (60 min) and measured its activity using immunoprecipitated SIK2 in cell-free assay by either *in vitro* autophosphorylation assay or *in vitro* assay using full-length CRTC2 as a substrate (Dentin et al., 2007). Their results showed increased SIK2 autophosphorylation (^{32}P autoradiography) and CRTC2 phosphorylation (when measured using Ser171 CRTC2 phospho-specific antibody) in immunoprecipitated SIK2 from the cells expressing wild-type SIK2 treated with insulin, compared to untreated cells, but not with S358A mutant expressing cells.

Contrary to their results, I did not observe any change in the ability of SIK2 to autophosphorylate following forskolin treatment of HEK293 cells expressing recombinant wild-type or phosphorylation-defective mutants of SIK2 (including a S358A mutant), despite this treatment inducing phosphorylation of Ser358 (Figure 5.6, Figure 5.4). Unlike Dentin *et* al., the experiments described in this chapter were conducted in a more physiological system and included analysis of endogenous SIKs. The lack of information on duration of kinase assay, detailed kinase assay protocol and quantitative measurement on ^{32}P incorporation in CRTC2 (majority of all the key data was shown in supplementary section with little experimental details), makes it difficult to comment further on the results of Dentin *et* al. (Dentin et al., 2007). Moreover, I have provided compelling evidence that Ser358 is not actually phosphorylated following insulin treatment of primary hepatocytes or in liver of refed mice (Figure 4.16, Figure 4.18, Figure 4.19).

These findings collectively demonstrate that the hormone glucagon does not seem to regulate intrinsic SIK2 phosphotransferase activity through phosphorylation in mouse primary hepatocytes and liver tissue. However, the current results cannot completely rule out the possibility that this lack of change in the *in vitro* kinase activity of the immunoprecipitated SIK2 could be due to loss of co-factor(s) or interacting proteins during the isolation processes (e.g. cell lysis, immune-complex washing procedures) and may not truly reflect "*in vivo*" activity status of SIK2.

Glucagon treatment is reported to reduce phosphorylation of SIK2 substrates in intact cells (Dentin et al., 2007; Koo et al., 2005; Mihaylova et al., 2011), but the lack of effect on SIK2 kinase activity led us to investigate whether phosphorylation of SIK2 may alter its intracellular localisation or protein binding properties and thus affect its access to substrates. The results presented here showed that SIK2 phosphorylation in response to glucagon did not change the cytoplasmic location of endogenous SIK2 or recombinant SIK2 in primary hepatocytes, despite 14-3-3 binding (Figure 5.8, Figure 5.9). In addition, all phosphorylation-defective mutants

either individually or together (3A, 4A mutant), including kinase-inactive mutants were cytoplasmic, regardless of exposure to glucagon or 14-3-3 binding (Figure 5.8, Figure 5.12).

Similar but less comprehensive results were reported by Henriksson and colleagues who found that GFP-tagged SIK2 wild-type and mutants (S587A and S358A) were all localised in the cytoplasm when expressed in HEK293 cells (Henriksson et al., 2012). In contrast, Horike and colleagues reported that a GFP-tagged S587A SIK2 mutant was localised to the nucleus and cytoplasm compared to wild-type SIK2 which was predominantly localised to the cytoplasm of 3T3 L1 pre-adipocytes (Horike, 2003). This discrepancy in the subcellular localisation of S587A mutant is difficult to explain, but it may suggest a cell-specific regulation of subcellular localisation of SIK2. Interestingly, chimeric SIK2 (containing nuclear localisation signal (RK-rich region) of SIK1) which localised to the nucleus, showed similar suppression of a CRE-reporter activity to the cytoplasmic localised wild-type SIK2 following PKA activation of adrenocortical tumour cells (Katoh et al., 2004). Similarly, chimeric SIK1 (containing the nuclear export sequence of HIV-1 rev protein) that localised to the cytoplasm showed similar suppression of CRE-reporter activity to that seen with the nuclear localised S587A SIK1 mutant following PKA activation of adrenocortical tumour cells (Katoh et al., 2004). These results together suggest that cytoplasmic translocation/retention is unlikely to be the key mechanism by which SIK2 transcriptional function is regulated by glucagon.

In addition to kinase activity and cellular localisation, SIK2 protein expression is not regulated *in vivo* by fasting (Figure 4.16) or in primary hepatocytes by 12-h exposure to glucagon (Figure 6.5), which thus reduces the possibilities of proteasomal degradation, transcription regulation or instability of protein as mechanisms of regulation of SIK2 by glucagon.

The above results collectively raise a possibility that the SIK2 regulation by glucagon may not significantly contribute towards dephosphorylation of known SIK2 substrates (e.g. CRTC2, class IIa HDACs) in intact cells. For example, the dephosphorylation in response to glucagon may be mediated by a protein phosphatase(s) rather than by inhibiting SIK2. This notion may be

supported by a recent finding that glucagon activated protein phosphatase 2 B/calcineurin and caused dephosphorylation of CRTC2 in the liver following an increase in intracellular Ca^{2+} in an IP3R-dependent manner (Wang et al., 2012). Wang and colleagues used a calcineurin inhibitor (cyclosporin A), transient overexpression and shRNAi-mediated knock-down of calcineurin in liver/primary hepatocytes to demonstrate that calcineurin binds and dephosphorylates CRTC2 on Ser171 and Ser275 sites following glucagon/fasting and increases gluconeogenic gene expression.

However, the lack of dephosphorylation of CRTC2, 3 and HDAC4 following glucagon stimulation of intact hepatocytes expressing a phosphorylation-defective SIK2 (3A or 4A mutant) argues that glucagon-mediated phosphorylation of SIK2 is important and contributes to dephosphorylation of SIK2 substrates in intact cells (Figure 5.10). However, the exact mechanism of this effect is not clear from the current studies. Interestingly, preliminary work using non-denaturing size-exclusion chromatography revealed that SIK2 was a part of a large molecular mass complex in unstimulated hepatocytes (Figure 5.11). This suggests an intriguing possibility that SIK2 may form a complex that regulates substrate phosphorylation and following glucagon-mediated phosphorylation this complex may be disrupted. Further studies to identify complex components using proteomics and investigation into the effect of phosphorylation-deficient mutants of SIK2 on complex formation will be needed to validate this hypothesis.

In summary, glucagon- or fasting-induced phosphorylation of SIK2 in liver did not affect its intrinsic kinase activity or cellular location but induced binding to 14-3-3. All four phosphorylation sites (Ser343, Ser358, Thr484 and Ser587) are important for glucagon-regulation of SIK2 function and not just Ser587 as previously considered (Figure 5.12). In addition, preliminary data suggests that glucagon disrupts the formation of a large molecular mass SIK2 containing complex which deserves further investigation as the potential mode of glucagon repression of SIK2's activity towards its substrates.

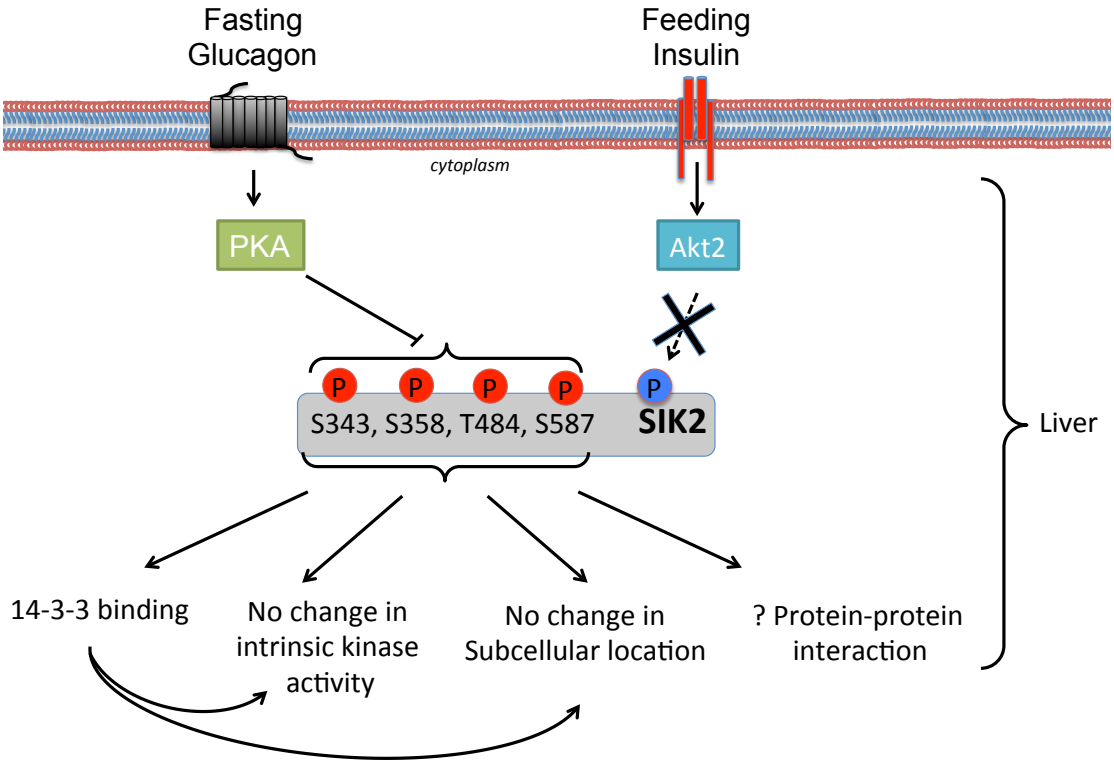

Figure 5.12 Hormonal-regulation of SIK2 in liver.

6 The role of SIKs in hepatic gluconeogenesis

6.1 Introduction

The results from previous chapters establish that the regulation of SIK2 by phosphorylation in the liver is not restricted to one site, Ser587, but actually involves at least up to four phosphorylation events (Ser343, Ser358, Thr484 and Ser587) following glucagon treatment in mouse liver/hepatocytes. Neither glucagon treatment of primary hepatocytes nor induction of these four phosphorylation events have any detectable effects/changes on the intrinsic kinase activity or subcellular localisation of SIK2, but may affect its interactome, which may contribute to the change in SIK2 regulation of CREB-dependent transcription following glucagon. In addition, contrary to a previous report (Dentin et al., 2007), insulin stimulation of hepatocytes or refeeding (after overnight fast) does not affect SIK2 activity or phosphorylation in the liver (chapter 5). Together these results question the importance of SIK2 as a major mediator of hormone-regulated hepatic gluconeogenesis as previously proposed.

To establish the role of SIK2 in hepatic gluconeogenesis *in vivo*, a liver-specific SIK2 knock-out mouse (L-SIK2 KO) was generated by our collaborator Dr Marc Foretz (Institut Cochin, Paris).

A

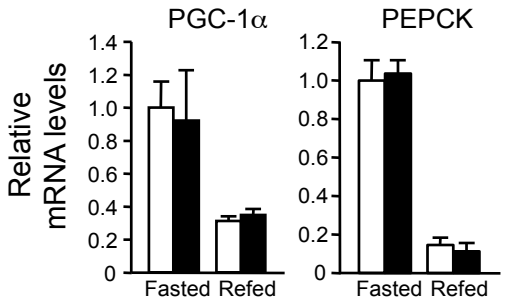

B

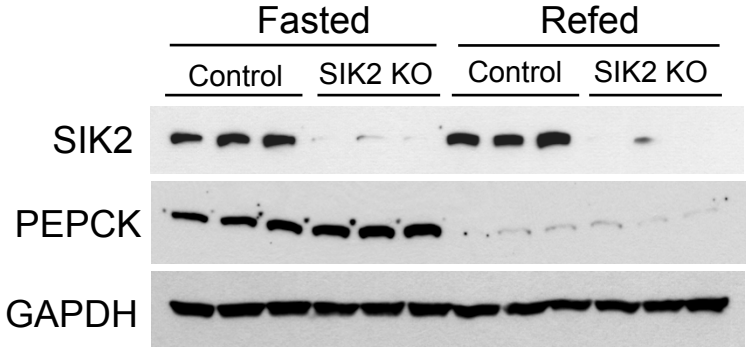

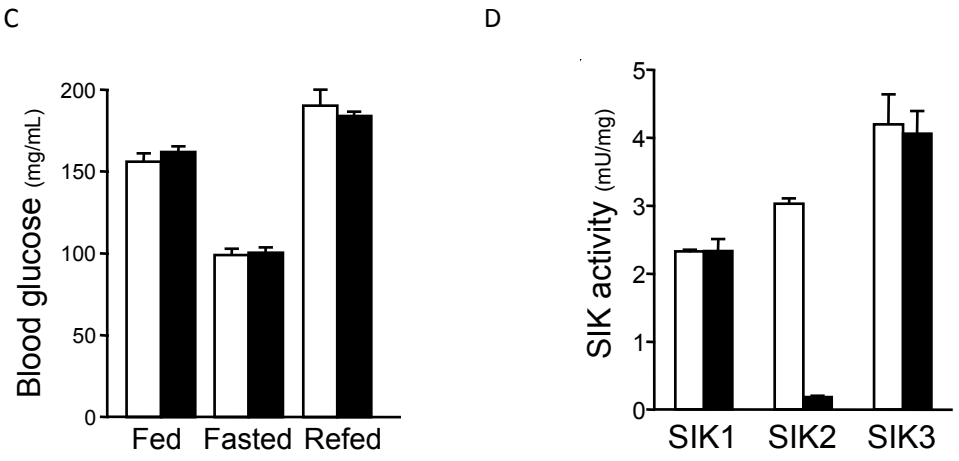

Figure 6.1 Hepatic gluconeogenesis in liver-specific SIK2 KO mice.

A, B) liver extracts were generated from control (white bars) and L-SIK2-KO mice (black bars) following 18-h fasting (fasted) or 24-h fast followed by an overnight refeeding with a high carbohydrate diet (refed). **A)** Relative mRNA level of PGC-1α and PEPCK was measured by quantitative PCR from these extracts. n = 6 for each group. All values are presented as means ± SEM. **B)** liver extracts were also immunoblotted using a SIK2, PEPCK and GAPDH antibody. Data are representative of 9 mice per group. **C)** Blood glucose levels of control (white bars) and L-SIK2-KO (black bars) mice fed ad libitum (fed), fasted for 18-h (fasted) or refed overnight with a high carbohydrate diet following a 24-h fast (refed). n = 6-12 for each group. **D)** Kinase activity of SIK1, 2 and 3 in liver extracts generated from fed *ad libitum* (fed) control (white bars) and L-SIK2 KO (black bars) mice. SIK1, 2 and 3 were immunoprecipitated with respective isoform specific antibodies from 1 mg of liver extracts in triplicate and subjected to *in vitro* kinase assay against 200 μM 'SAKAMOTO'-tide. Data is presented as mean ± SD, n=3 independent mouse. Dr Marc Foretz carried out all of these experiments except the data in (D) that was generated by myself.

To investigate the effect of SIK2 deficiency on hepatic gluconeogenic genes *in vivo*, Dr Foretz measured PEPCK and PGC-1α mRNA and PEPCK protein levels in liver after 18-h fast or 24-h fast followed by an overnight (*ad libitum*) feeding of L-SIK2 KO mice (Figure 6.1). Strikingly, the lack of SIK2 in the liver had no influence on fasting- or feeding-mediated changes in the levels of PEPCK mRNA and protein or PGC-1α mRNA expression in both fasted and fed states (Figure 6.1A, B). Moreover, SIK2 deficiency in the liver had no effect on fasted (for 18 h) or fed blood glucose levels (Figure 6.1C). These results were not due to compensatory increased in expression of other SIK isoforms as both SIK1 and SIK3 showed similar kinase activity between wild-type and L-SIK2 KO liver (Figure 6.1D). To further investigate the effect of cAMP-mediated gluconeogenesis in SIK2-null mice, primary hepatocytes from L-SIK2-null mice were treated with cell-permeable cAMP analogue (Bt_2-cAMP) and PEPCK, G6Pase and PGC-1α mRNA expression, PEPCK protein levels and glucose production were measured (Figure 6.2). Similar

to *in vivo* results, SIK2-null hepatocytes had unaltered PEPCK, G6Pase and PGC-1α mRNA expression (Figure 6.2A) and PEPCK protein levels after Bt_2-cAMP treatment (Figure 6.2B). In addition, SIK2-null hepatocytes showed significant increase in glucose production after Bt_2-cAMP treatment, which was similar to control cells (Figure 6.2C). Finally, Immunoblot analysis of CRTC2 from SIK2-null hepatocytes showed unaltered mobility of CRTC2 (phosphorylation) in basal condition and showed similar downward band-shift (dephosphorylation) to control cells following Bt_2-cAMP treatment (Figure 6.2B). This was surprising as SIK2 has been proposed as the dominant isoform responsible for phosphorylation of CRTC2 in liver, thus loss of SIK2 should have prompted dephosphorylation of CRTC2 in the absence of stimuli (Altarejos and Montminy, 2011; Dentin et al., 2007; Koo et al., 2005). However, it will be important to confirm this result using the Ser171 CRTC2 phospho-specific antibody, a known SIK2-mediated phosphorylation site.

A

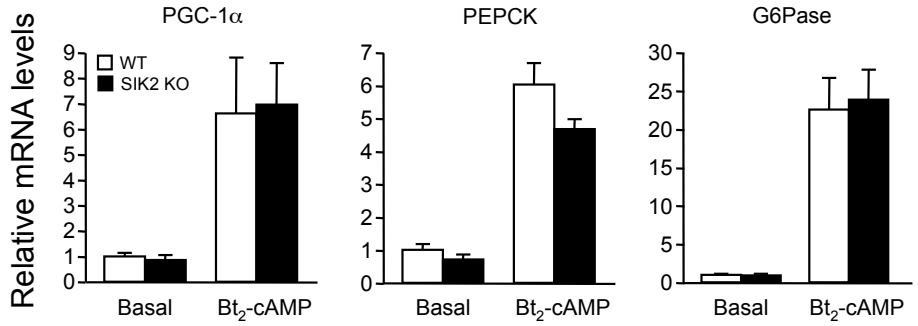

B

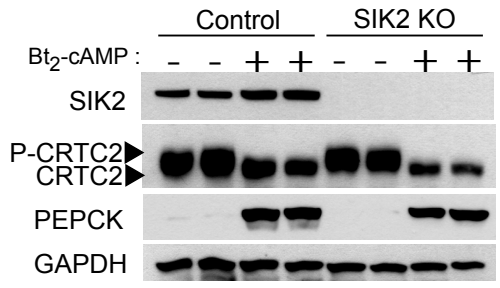

C

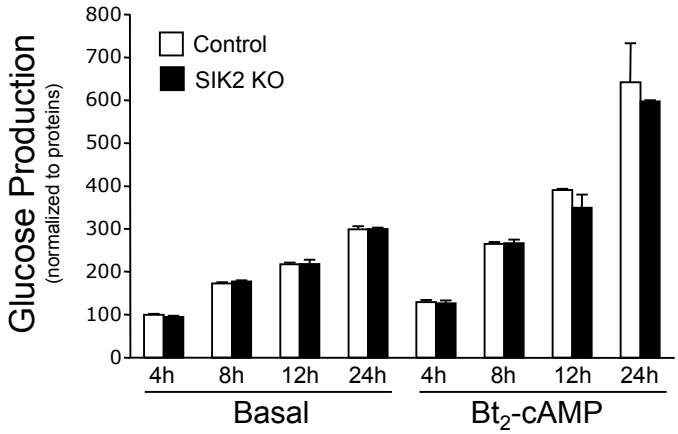

Figure 6.2 Hepatic gluconeogenesis in L-SIK2 knock-out hepatocytes.

A) Glucose production was measured in the culture medium of primary hepatocytes isolated from control or liver SIK2-deficient (SIK2 KO) mice after indicated duration of treatment with or without 100 µM Bt_2-cAMP. Glucose production was normalised to protein content and expressed as a percentage of glucose production by control hepatocytes incubated for 4 hr in the absence of Bt_2-cAMP. Data is presented as mean ± SD, n=3 independent experiments. B, C) Primary hepatocytes isolated from control and liver SIK2-deficient (SIK2 KO) mice and treated with or without 100 µM Bt_2-cAMP for 8 h. Lysates were either subjected to qPCR **(B)** to measure relative mRNA levels of PEPCK, G6Pase and PGC-1α. Data is presented as mean ± SEM, n=3. or immunoblot analysis with the indicated antibodies **(C).**

These results collectively suggest that SIK2 is either dispensable, or the lack of SIK2 is compensated by basal level of other SIK isoforms suggesting a potential redundancy among SIKs for hepatic gluconeogenesis. Alternatively, they raise a critical question as to whether SIKs (or SIK2 at least) are fundamentally important regulators of hepatic gluconeogenesis.

To fully delineate the role of SIKs in hepatic gluconeogenesis would require complete ablation of all SIK-isoform activity in the liver. To achieve this, either pharmacological inhibition (pan SIK inhibitor) or simultaneous knock-out of all SIK isoforms in the liver to prevent compensation/redundant effect is required. Recently two novel small-molecule ATP-competitive pan SIK inhibitors (HG-9-91-01 and KIN112) were generated by Prof Nathanael Gray (Harvard University, Boston, USA) and these inhibitors have been characterised/validated by Prof Philip Cohen's group (MRC PPU, Dundee, UK) in a study on the role of SIKs in innate immunity (Clark et al., 2012). Prof Gray was kind enough to supply these compounds for validation and application in my studies in the liver.

SIKs have been implicated in the regulation of the CRTC2-CREB (Koo et al., 2005; Liu et al., 2008) and the class IIa HDACs-FoxO (Mihaylova et al., 2011) signal transduction pathways in hepatic gluconeogenesis where CRTCs and HDACs are substrates of SIKs (see section 1.5.6). These pathways therefore provide potential readouts for endogenous SIK activity in the cells, and hence for the efficacy of SIK inhibition or genetic silencing/depletion. Glucagon promotes the dephosphorylation and nuclear translocation of CRTC2, contributing to an up-regulated transcription of gluconeogenic genes. Therefore, it is not only possible to investigate the efficacy of SIK inhibition using CRTC2, but also to test the importance of the SIK-CRTC2 regulation in control of hepatic gluconeogenesis. One would expect SIK inhibition with HG-9-91-01 or KIN112, similar to glucagon, to promote dephosphorylation and nuclear translocation of CRTC2, and thus increase gluconeogenic gene transcription, and glucose production in primary hepatocytes.

Thus, the aims of this chapter are as follows.

1) To characterise the efficacy, selectivity and specificity of SIK inhibitors in cell-free and -based assays (primary mouse hepatocytes and HEK293 cells).
2) To investigate the role of SIKs in the control of hepatic gluconeogenesis by applying SIK inhibitors to primary mouse hepatocytes.

6.2 Results

6.2.1 Characterisation of SIK inhibitors *in vitro*

All *in vitro* characterisation data was generated by DSTT, University of Dundee, UK (www.kinase-screen.mrc.ac.uk) and published recently by Clark *et* al. (Clark et al., 2012).

Despite their high homology, SIKs are the only AMPK-related kinases that contain a small amino acid residue (threonine) at the 'gatekeeper' site creating a small hydrophobic pocket, while others contain a large amino acid such as methionine or leucine (Zhang et al., 2009). KIN112 and HG-9-91-01 were specifically designed to target the ATP-binding site and this adjacent small hydrophobic pocket to enhance the selectivity for SIKs (Clark et al., 2012).

To assess the selectivity of HG-9-91-01 and KIN112, IC_{50} values were obtained against AMPK and AMPK-related kinases (Table 6-1). HG-9-91-01 was more potent than KIN112 against the SIKs (1-10 nM and 10-60 nM respectively), but both possessed highest potency against SIK1 followed by SIK2 and were least potent against SIK3 in cell-free assays. Noticeably, HG-9-91-01 and KIN112 had substantial selectivity towards the SIKs compared to the other members of the AMPK-related kinase family (Table 6-1). AMPK, MARK1, 2, 3 and 4, NUAK1, and the BRSK1 and 2 exhibited >1000 times higher IC_{50} values for both compounds compared to SIK1. NUAK2 was the only other kinase tested with an IC_{50} lower than 1 μM (145 nM for HG-9-91-01), but it is significantly (>100 fold) higher than that for SIK1.

HG-9-91-01 and KIN112 were further tested against 140 protein kinases *in vitro* to assess the selectivity (Figure 6.3). SIK2 and SIK3 kinase activities were both inhibited >90% by 1 μM HG-9-91-01 (Figure 6.3), while KIN112 reduced SIK2 activity by >80% at 1 μM, and SIK3 by around 60% at this concentration (Figure 6.3). These compounds had relatively good selectivity for SIKs, however a few kinases mostly tyrosine kinases such as Src family members (Src, Lck, and Yes), BTK, and FGF and Ephrin receptors, were inhibited to a similar extent to the SIKs at 1 μM concentration. This is likely due to the fact, they all have the same small amino acid in their 'gatekeeper site' as SIKs (Figure 6.3) (Clark et al., 2012). Crucially, HG-9-91-01 and KIN112 did

not inhibit the upstream kinases of AMPK and AMPK-related kinases such as LKB1 which has an IC_{50} more than 1000 fold higher than SIKs, while CaMKKβ and TAK1 were inhibited only 16% and 11% by HG-9-91-01, and 16% and 0% by KIN112 respectively.

Therefore based on these data, these compounds (especially HG-9-91-01) were considered as selective pan SIK inhibitors.

6.2.2 Characterisation of SIK inhibitors in primary hepatocytes

Encouraged by the results from *in vitro* studies (as described above), I went ahead to further characterise these two inhibitors in primary mouse hepatocytes. HDAC4 and CRTC2 are the reported substrates of SIKs, phosphorylated on Ser246 and Ser171 respectively, and significant phosphorylation of both the substrates has been reported in unstimulated cells (Berdeaux et al., 2007; Screaton et al., 2004). Therefore we decided to use changes in phosphorylation of HDAC4 and CRTC2 as a read-out for changes in the endogenous/*de novo* SIK activity in intact cells.

Table 6-1 IC50 (nM) for AMPK-related kinases, AMPK and LKB1 for HG-9-91-01 and KIN112.
Data was obtained from DSTT(University of Dundee, UK).

	KIN112	HG-9-91-01
LKB1	>10000	>10000
AMPKα1/α2	>10000	4500
MARK1	>10000	3300
MARK2	>10000	1600
MARK3	>10000	1900
MARK4	>10000	1300
SIK1	10	0.92
SIK2	22	6.6
SIK3	60	9.6
NUAK1	>10000	4280
NUAK2	2100	145
BRSK1	>10000	>10000
BRSK2	>10000	8800
MELK	2000	2500

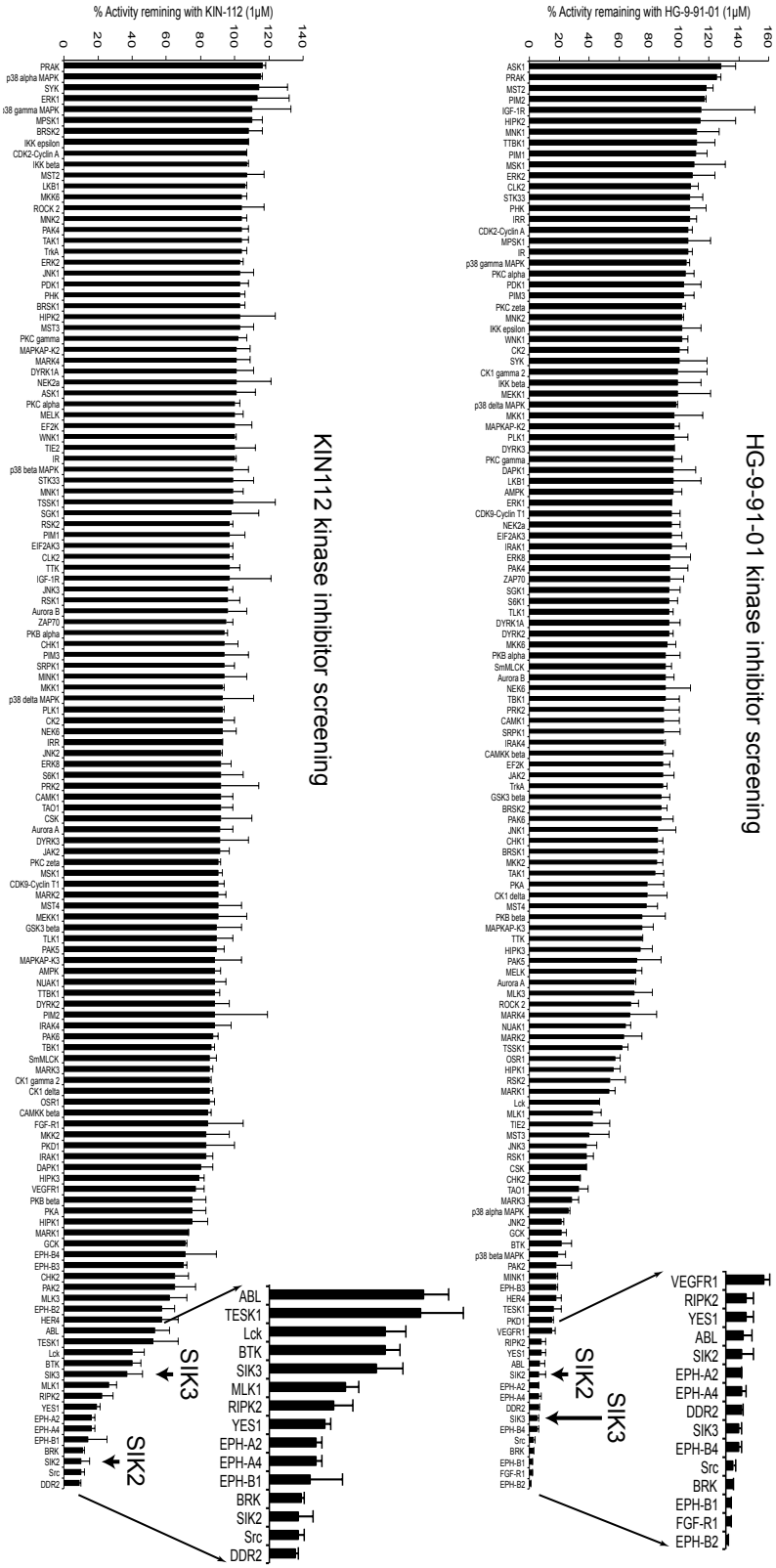

Figure 6.3 Kinase inhibitor screening for HG-9-91-01 and KIN112.

Kinase inhibitor screening was conducted against a panel of 140 known kinases *in vitro* with 1 μM HG-9-91-01 (upper panel) and 1 μM KIN112 (lower panel) by DSTT, University of Dundee, UK (www.kinase-screen.mrc.ac.uk). Data is reported as the percent of activity remaining in the presence of the inhibitor relative to the activity measured in the absence of inhibitor. SIK2 and SIK3 were highlighted and showed in the inset picture. Data is expressed as mean ± SD, n=2 technical replicates.

In order to investigate the optimum concentration of inhibitors required to achieve effective SIK inhibition in cell-based assays, lysates were generated from primary mouse hepatocytes following treatment with increasing amounts of KIN112 or HG-9-91-01 (Figure 6.4A). The phosphorylation of CRTC2 leads to slower migration on SDS-PAGE whereas dephosphorylation leads to faster migration (Screaton et al., 2004). Both KIN112 and HG-9-91-01 treatment of cells led to increase in a faster migrating (lower) band (less phosphorylated form) of CRTC2, with a reciprocal reduction in the slower migrating (upper) band (more phosphorylated form) (Figure 6.4A). Similarly, there was also a dose-dependent reduction in pSer246 HDAC4 with both of the compounds (Figure 6.4A). Consistent with the results seen in the *in vitro* assay, KIN112 was a relatively weaker SIK inhibitor with only partial reduction in CRTC2 and HDAC4 phosphorylation even at 10 μM (Figure 6.4A).

The inhibitory effects of HG-9-91-01 on SIKs were measured in primary hepatocytes with overexpressed CRTC2. Immunoblot analysis showed a dose-dependent reduction in pSer171 CRTC2 and pSer246 HDAC4 in HG-9-91-01-treated cells (Figure 6.4B) and the complete loss of substrate phosphorylation required 4 μM HG-9-91-01. Similar effect on reduction in phosphorylation of Ser246 of HDAC4 and Ser171 of CRTC2, as well as the band shift of total CRTC2 (indicative of dephosphorylation) was seen with glucagon treatment (Figure 6.4B). Glucagon treatment (100 nM) not only caused dephosphorylation but also nuclear translocation/retention of CRTC2 (Koo et al., 2005; Wang et al., 2012). Therefore, we questioned whether 4 μM HG-9-91-01 treatment, that achieved comparable CRTC2 dephosphorylation, would affect localisation of CRTC2 in the same way as glucagon. To address this, immunofluorescence of endogenous CRTC2 was carried out following HG-9-91-01 treatment. CRTC2 was translocated from the cytoplasm to the nucleus following HG-9-91-01 treatment of primary hepatocytes and once again it was comparable to glucagon treatment (Figure 6.4 C). These results collectively suggested that 4 μM HG-9-91-01 treatment for 1 h

would generate a similar inhibition of SIK in primary mouse hepatocytes to that obtained with glucagon treatment.

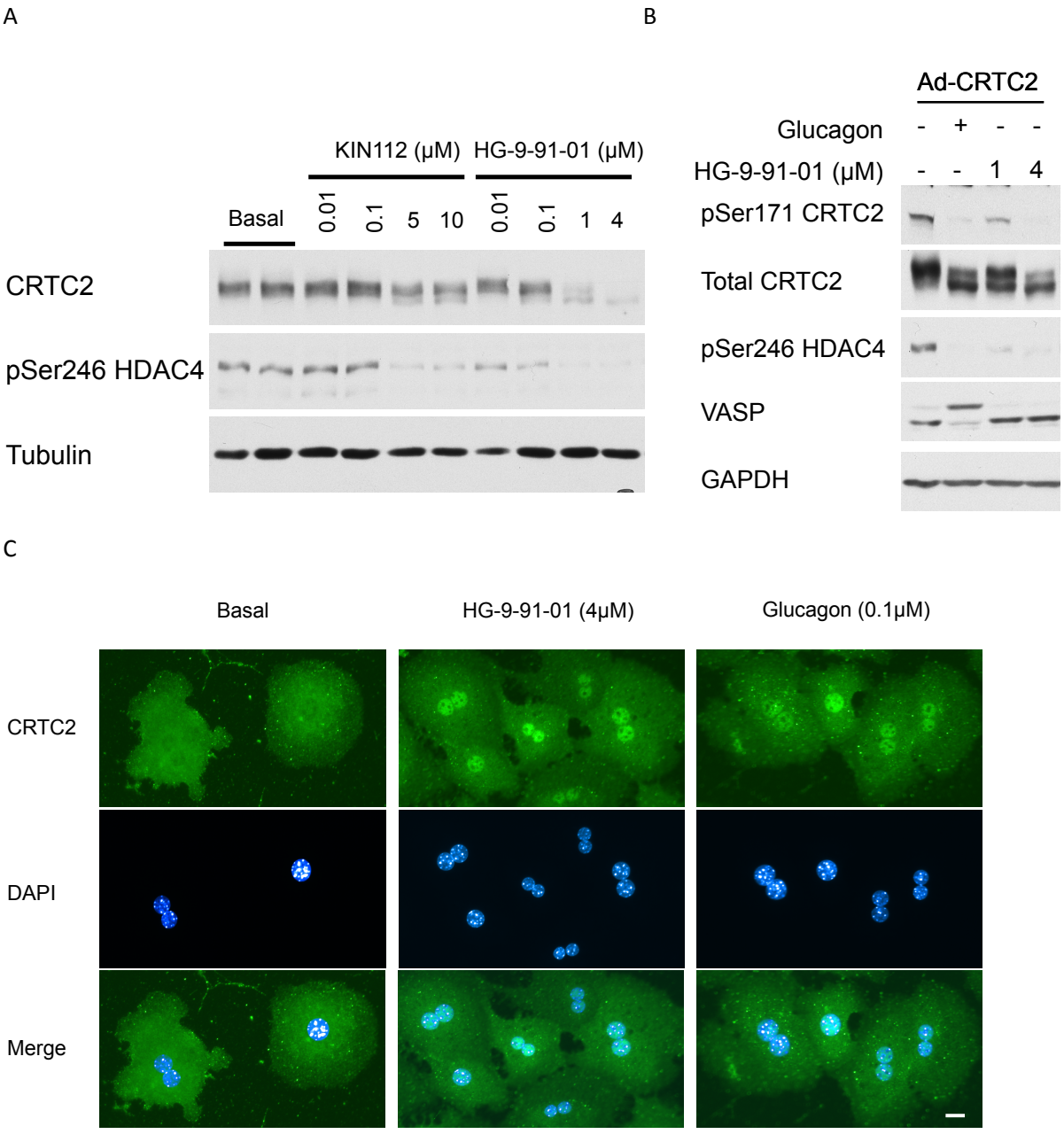

Figure 6.4 Characterisation of SIK inhibitors in primary hepatocytes.

A) Primary hepatocytes were treated with increasing amounts of SIK inhibitors, KIN112 or HG-9-91-01, for 1 h prior to cell lysis. Lysates were immunoblotted with the indicated antibodies. The total CRTC2 and pSer246 HDAC4 antibodies were used to assess the effect of the inhibitors and the tubulin antibody was used as loading control. **B)** Flag-CRTC2 was expressed in primary hepatocytes (1:5 MOI) by an adenoviral vector for 16 h followed by HG-9-91-01 (1 μM or 4 μM) treatment for 1 h, or 0.1 μM glucagon treatment for 15 min (positive control) prior to cell lysis. Lysates were immunoblotted with the indicated antibodies. The VASP antibody was used to confirm PKA activation by glucagon and the GAPDH antibody was used as loading control. **C)** Primary hepatocytes were treated with 4 μM HG-9-91-01 for 1 h and 0.1 μM glucagon for 10 min. Subsequently cells were fixed with 3.7% paraformaldehyde and immunostained using CRTC2 antibody and stained with DAPIfor nuclear visualisation. Images were captured with fluorescence microscope (Nikon Eclipse Ti) using Nikon NIS-Elements BR 3.1 software. Images were cropped using Adobe Photoshop CS5.1. Scale bar is 10 μm in length. All above results are representative of three independent experiments.

6.2.3 Effects of SIK inhibition on hepatic gluconeogenesis

Having identified the optimum concentration of HG-9-91-01 for SIK inhibition that achieved dephosphorylation and nuclear translocation of CRTC2 comparable to glucagon in primary hepatocytes, the effects of HG-9-91-01 on hepatic gluconeogenesis were investigated by measuring PEPCK protein and mRNA expression, G6Pase mRNA expression, as well as glucose production (i.e. the physiological outcome of gluconeogenesis). Glucagon treatment was used in the same experiments as a positive control.

Figure 6.5A shows the immunoblot analysis of the lysates from hepatocytes that were treated with increasing amounts of HG-9-91-01 for 4, 8 or 12 h. As shown in the previous experiment (Figure 6.4), robust CRTC2 dephosphorylation (judged by band shift) was only apparent with 4 µM HG-9-91-01 (Figure 6.5A).

A

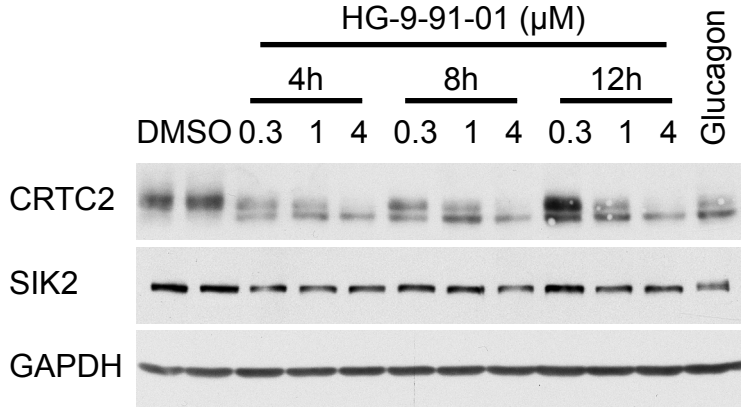

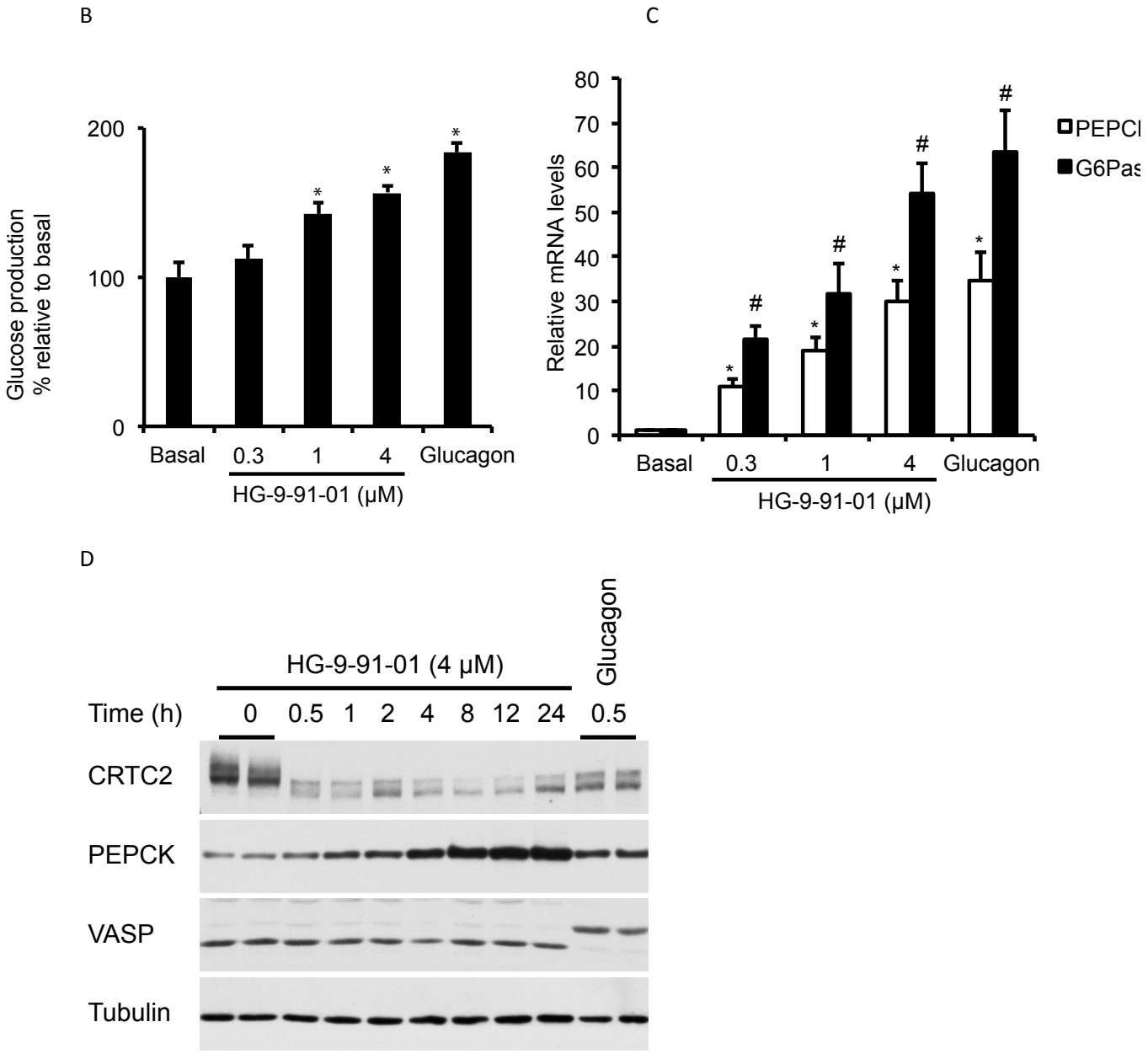

Figure 6.5 Effects of HG-9-91-01 on hepatic gluconeogenesis.

A) Primary hepatocytes were treated with indicated concentrations of HG-9-91-01 for 4, 8 or 12 h prior to cell lysis. Lysates were subjected to immunoblotting with the indicated antibodies. Primary hepatocytes were also treated with 0.1 μM glucagon for 12 h and included in the experiment as positive control. **B)** Cell culture medium (12-h treatment) from the same experiment was used to analyse glucose production (in triplicate) as described in Materials and Methods. Glucose production was normalised to total cellular protein content and presented as percentage of glucose production by hepatocytes without treatment (Basal). 0.1 μM glucagon treatment for 12 h was used as positive control. Data is presented as mean ± SD, n=3 independent experiments. *p < 0.001 basal versus 1 μM HG-9-91-01, 4 μM HG-9-91-01 or glucagon. **C)** Relative mRNA levels of PEPCK and G6Pase were measured from primary hepatocytes in triplicate using qPCR after 8-h treatment of indicated amount of HG-9-91-01 or 0.1 μM glucagon treatment. The mRNA levels were expressed as fold increase from non-treated hepatocytes (Basal). Data is presented as mean ± SD, n=3 independent experiments. Glucagon treatment was used as positive control. * p < 0.001 basal versus each treatment for PEPCK mRNA, # p < 0.0001 basal versus each treatment for G6Pase mRNA. **D)** Primary hepatocytes were treated with 4 μM HG-9-91-01 for the indicated duration or 0.1 μM glucagon for 0.5 h prior to cell lysis. Lysates were subjected to immunoblot analysis with the indicated antibodies. Glucagon-treated lysates were included as positive control. The CRTC2 and PEPCK antibodies were used to confirm the effect of the inhibitor. The VASP antibody was used to confirm PKA activation by glucagon and the tubulin antibody was used as loading control. Results are representative of three independent experiments.

Importantly, SIK2 expression was not affected by HG-9-91-01 (Figure 6.5A). There was a dose-dependent increase in glucose production with the HG-9-91-01 treatment (Figure 6.5B). Despite similar effects on CRTC2, the 4 μM HG-9-91-01 treatment could not fully induce glucose production similar to the levels observed with glucagon treatment (Figure 6.5B). Similarly, PEPCK and G6Pase mRNA levels increased in HG-9-91-01-treated hepatocytes (Figure 6.5C) but did not reach the glucagon-mediated increase in PEPCK and G6Pase mRNA expression. The effects of HG-9-91-01 on PEPCK protein expression were analysed using extracts generated from primary mouse hepatocytes that were treated with HG-9-91-01 at various time points for up to 24 h (Figure 6.5D). CRTC2 was robustly dephosphorylated within 30 min of HG-9-91-01 treatment and persisted for up to 24 h (Figure 6.5D). PEPCK protein expression increased with time from 1 h, reaching a plateau level between 12-24 h of hepatocyte treatment (Figure 6.5D).

Furthermore, glucose production was significantly increased in primary hepatocytes following incubation with the structurally distinct SIK inhibitor KIN112 (Figure 6.6A). 10 μM KIN112 treatment of primary hepatocytes increased glucose production, CRTC2 and CRTC3 dephosphorylation and PEPCK protein expression (Figure 6.6A). Glucagon-induced glucose production and PEPCK expression was higher than that achieved with KIN112 in primary hepatocytes (Figure 6.6A). In addition, KIN112 showed lower efficacy in inducing glucose production than HG-9-91-01, which was consistent with *in vitro* and cell-based assays results (as described above). These results confirm that HG-9-91-01 is a more potent SIK inhibitor than KIN112 (Figure 6.6B).

The combination of glucagon and HG-9-91-01 treatment of hepatocytes had an additive effect on glucose production which was significantly higher than individual treatment with either glucagon or HG-9-91-01 (Figure 6.7A). The possible molecular mechanism behind this additive effect was investigated by measuring the phosphorylation of glucagon-regulated signalling

molecules implicated in hepatic gluconeogenesis (Figure 6.7B). As expected glucagon induced phosphorylation of CREB, PFKFB1 and IP3R, known PKA substrates implicated in the control of hepatic gluconeogenesis (Miller et al., 2013). In contrast, HG-9-91-01 had no effect on the phosphorylation of these proteins (Figure 6.7B). Combined treatment with HG-9-91-01 and glucagon did not further enhance phosphorylation of these proteins (CREB, PFKFB1 and IP3R) compared to glucagon alone (Figure 6.7B). However, it did have an additive effect on the dephosphorylation of CRTC2, which could be an explanation for the additive effect on glucose production (Figure 6.7). Together these results provide evidence that SIK inhibition may increase glucose production in primary mouse hepatocytes in concert with reducing CRTC2 phosphorylation and inducing expression of the gluconeogenic genes such as PEPCK and G6Pase.

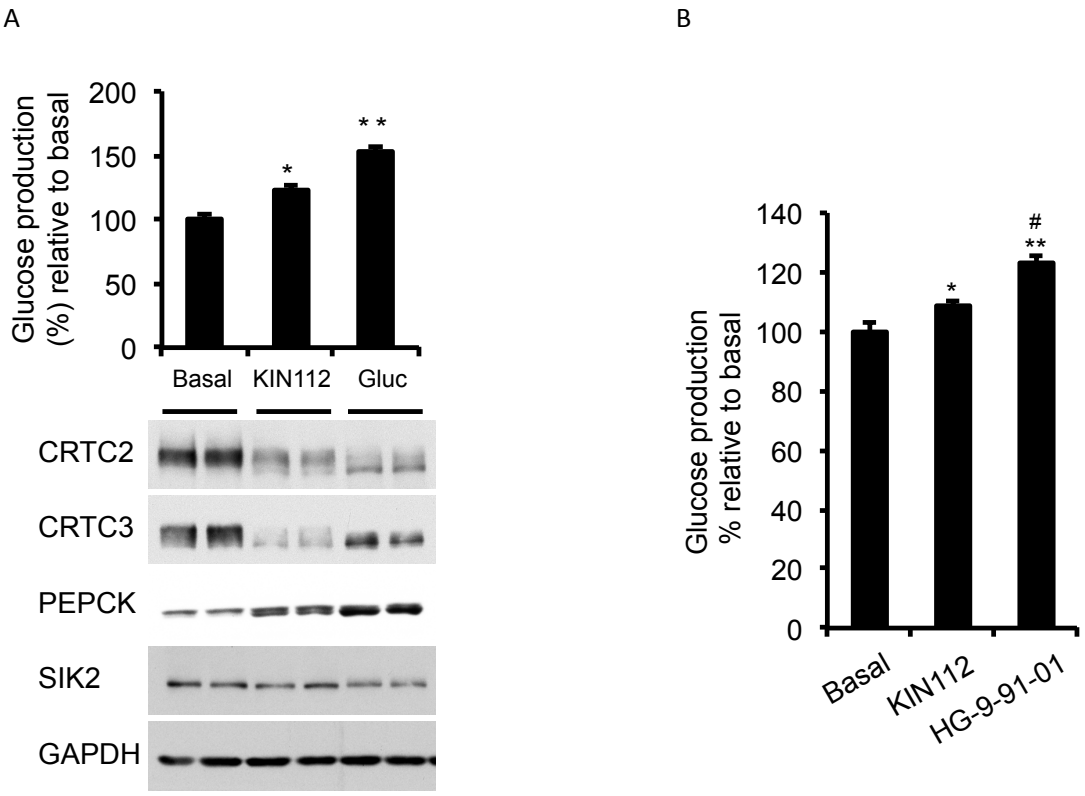

Figure 6.6 Effect of KIN112 on CRTC2/3 phosphorylation and hepatic gluconeogenesis.

A) Primary hepatocytes were treated with 10 µM KIN112 (SIK inhibitor) or 0.1 µM glucagon (Gluc) for 12 h. Subsequently culture medium was used for measurement of glucose production (upper panel) while cells were lysed for immunoblotting (lower panels). Glucose production was normalised to total protein content and presented as a percentage of glucose production by hepatocytes without treatment (Basal). Lysates were immunoblotted with the indicated antibodies. Glucagon treatment was used as positive control. Data is presented as mean ± SD, n=3 independent experiments. *$p < 0.01$ basal versus KIN112, **$p < 0.001$ basal versus glucagon**. B)** Glucose production was measured from primary hepatocytes after

12 h treatment with 10 µM KIN112 or 4 µM HG-9-91-01. Data is presented as mean ± SD, n=6 *p < 0.005 basal versus Kin112, **p < 0.001 basal versus HG-9-91-01, #p < 0.001 KIN112 versus HG-9-91-01.

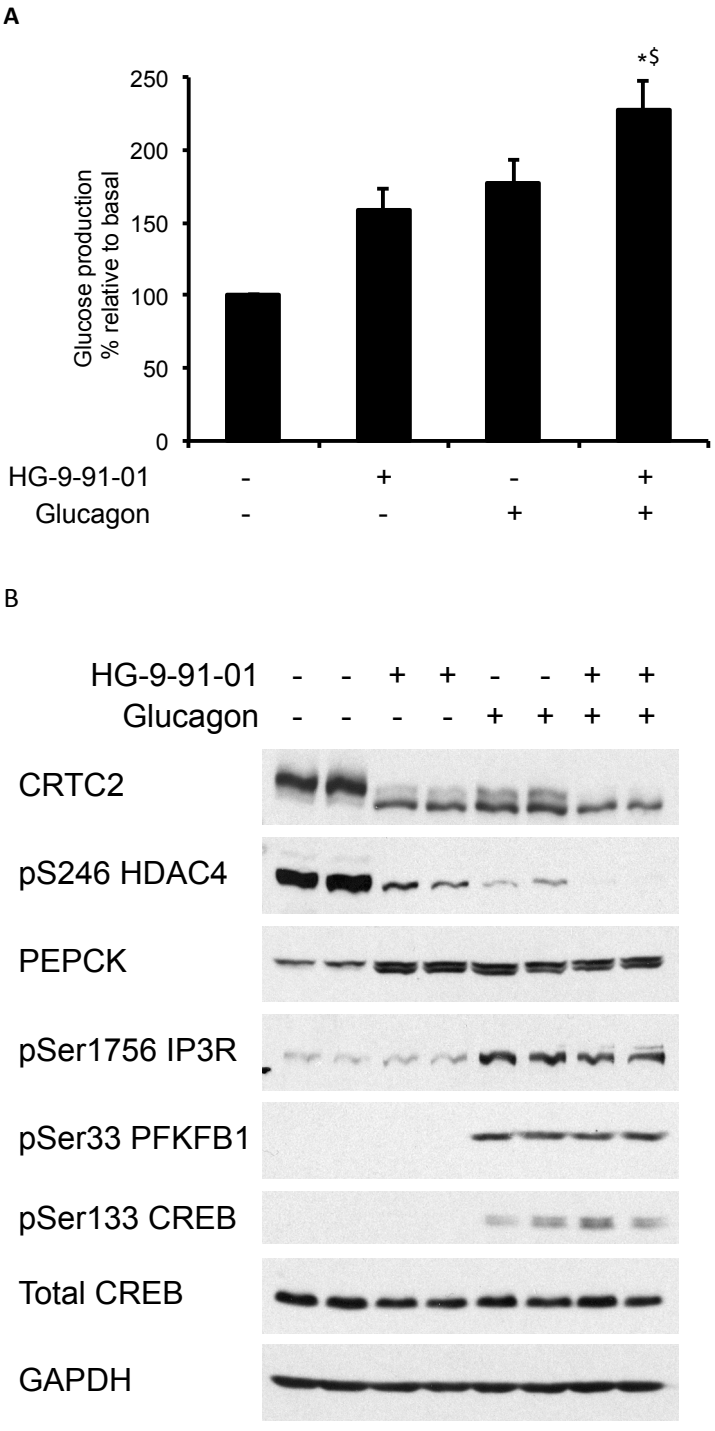

Figure 6.7 Effect of combination treatment of HG-9-91-01 and glucagon in primary hepatocytes.

A) Glucose production was measured from primary hepatocytes that were treated with 4 µM HG-9-91-01 and/or 0.1 µM glucagon for 8h. Glucose production was normalised to total protein content and presented as percentage of glucose production by hepatocytes without treatment (Basal). Data is presented as mean ± SD, n=3 independent experiments. *p < 0.001 HG-9-91-01 versus HG-9-91-01 plus glucagon for each time point, $p < 0.002 glucagon versus HG-9-91-01 plus glucagon for each time point. **B)** Lysates from the same experiments were immunoblotted with the indicated antibodies. The 6-

phosphofructo-2-kinase/fructose-2, 6-bisphosphatase (PFKFB1), CREB and Inositol 1,4,5-triphosphate receptor (IP3R) phospho-specific antibodies were used to confirm PKA activation by glucagon. Results are representative of three independent experiments.

6.2.4 Validation of SIK inhibitor selectivity

In order to confirm that the effects of the SIK inhibitors on hepatic gluconeogenesis were indeed due to SIK inhibition and not due to 'off-target' effects, we applied SIK inhibitors to the cell model expressing drug-resistant SIK mutants and to the genetic models where SIKs were catalytically-inactive.

6.2.4.1 SIK inhibitor validation with drug-resistant mutant in intact cells

6.2.4.1.1 Characterisation of drug-resistant mutant

A useful approach to establish that the observed effects of a compound that inhibits a kinase of interest is not an 'off-target' effect, is to show that the inhibitor action disappears when a drug-resistant (DR) mutant kinase is expressed in place of the wild-type kinase (Cohen, 2010). Clark *et* al. showed that mutation of the gatekeeper threonine to glutamine (amino acid with long side-chain) made SIKs 1000-fold less sensitive to HG-9-91-01 (Clark et al., 2012). Therefore, SIK1 T103Q, SIK2 T96Q and SIK3 T143Q should serve as DR mutants.

The kinase activity and T-loop phosphorylation of these DR mutants in comparison to wild-type enzymes was assessed. Wild-type and DR mutants for SIK1, 2 and 3 showed similar intrinsic kinase activity *in vitro* (to their respective wild-type enzymes) when expressed in HEK293 cells (Figure 6.8A). T-loop phosphorylation of wild-type and DR mutants of each SIK isoform was similar (Figure 6.8A, B). More importantly, there was no significant difference in the band shift for CRTC2 observed between forskolin-treated cells expressing wild-type SIKs and the ones expressing DR mutants (Figure 6.8B). This demonstrates that the DR mutants are not only active, but also responsive to inhibition by cAMP-elevating agents such as forskolin and that there is no significant difference in these properties between DR mutants and wild-type enzymes. In contrast, no change was observed in the phosphorylation of either CRTC2 or HDAC4 following KIN112 or HG-9-91-01 treatment in the cells expressing DR mutants (Figure

6.8B). Hence, these mutants are resistant to the inhibitors at optimised concentration and therefore indicate that CRTC2 phosphorylation is mediated by SIKs.

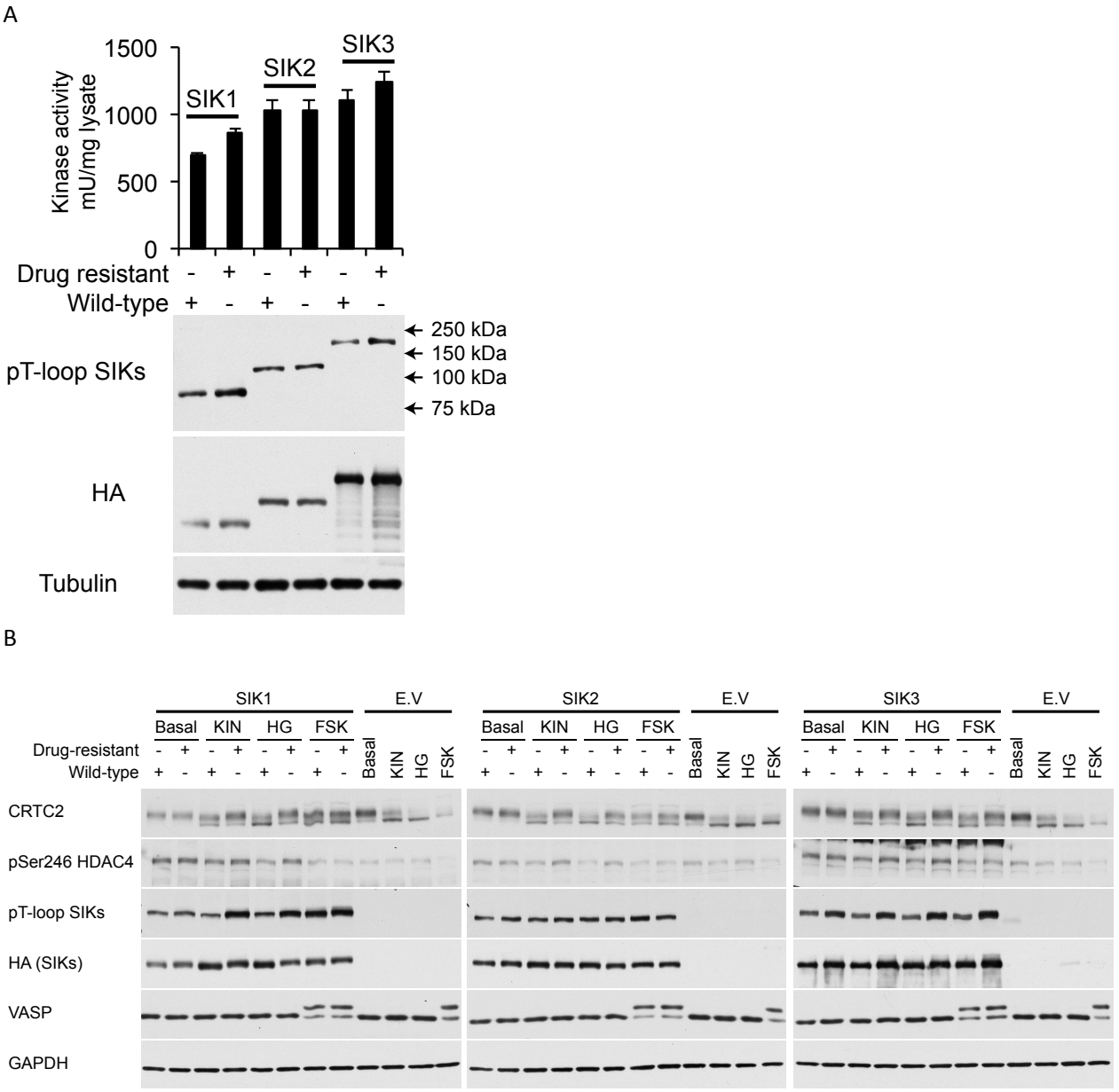

Figure 6.8 SIK drug-resistant mutants in HEK293 cells.

HA-empty-vector (without SIKs), HA-SIK wild-type or HA-SIK drug-resistant mutants (SIK1 T103Q, SIK2 T96Q and SIK3 T146Q) were expressed in HEK293 cells for 36 h followed by 1-h treatment with 10 µM KIN112 (KIN) or 1 µM HG-9-91-01 (HG) and 10 min stimulation with 10 µM forskolin (FSK) (as positive control) prior to cell lysis. **A, B)** Lysates were immunoblotted with the indicated antibodies and HA-SIKs were immunoprecipitated and subjected to *in vitro* kinase assay **(A).** Data is presented as mean ± SD, n=3 independent experiments. The pT-loop SIK antibody recognises the phosphorylation of an equivalent residue on SIK1 (T182), SIK2 (T175) and SIK3 (T221). The VASP antibody was used to confirm PKA activation by FSK and the GAPDH antibody was used as loading control. Results are representative of three independent experiments.

SIK2 has been proposed as a dominant isoform that play a key role in hepatic gluconeogenesis (Altarejos and Montminy, 2011). Hence the SIK2 DR mutant (T96Q) was further characterised

in a more physiological setting of primary hepatocytes where the constructs expressing either GFP (control), wild-type or T96Q mutant were introduced via adenoviral vectors (Figure 6.9). Similar to the results in HEK293 cells (Figure 6.8), there was no discrepancy in the kinase activity of immunoprecipitated SIK2 proteins and T-loop phosphorylation between wild-type and DR mutant of SIK2 (Figure 6.9A). Consistent results were also observed with glucagon-induced CRTC2 and CRTC3 dephosphorylation and SIK2 phosphorylation on Ser343, Ser358 and Thr484 (Figure 6.9B). Endogenous CRTC2 and CRTC3 showed a downward band-shift (dephosphorylation) in control lysates (GFP-expressing hepatocytes) and in lysates from cells expressing SIK2 wild-type following HG-9-91-01 treatment (Figure 6.9B). Strikingly, the dephosphorylation of CRTCs no longer occured following HG-9-91-01 treatment of the cells expressing the SIK2 DR mutant (Figure 6.9B).

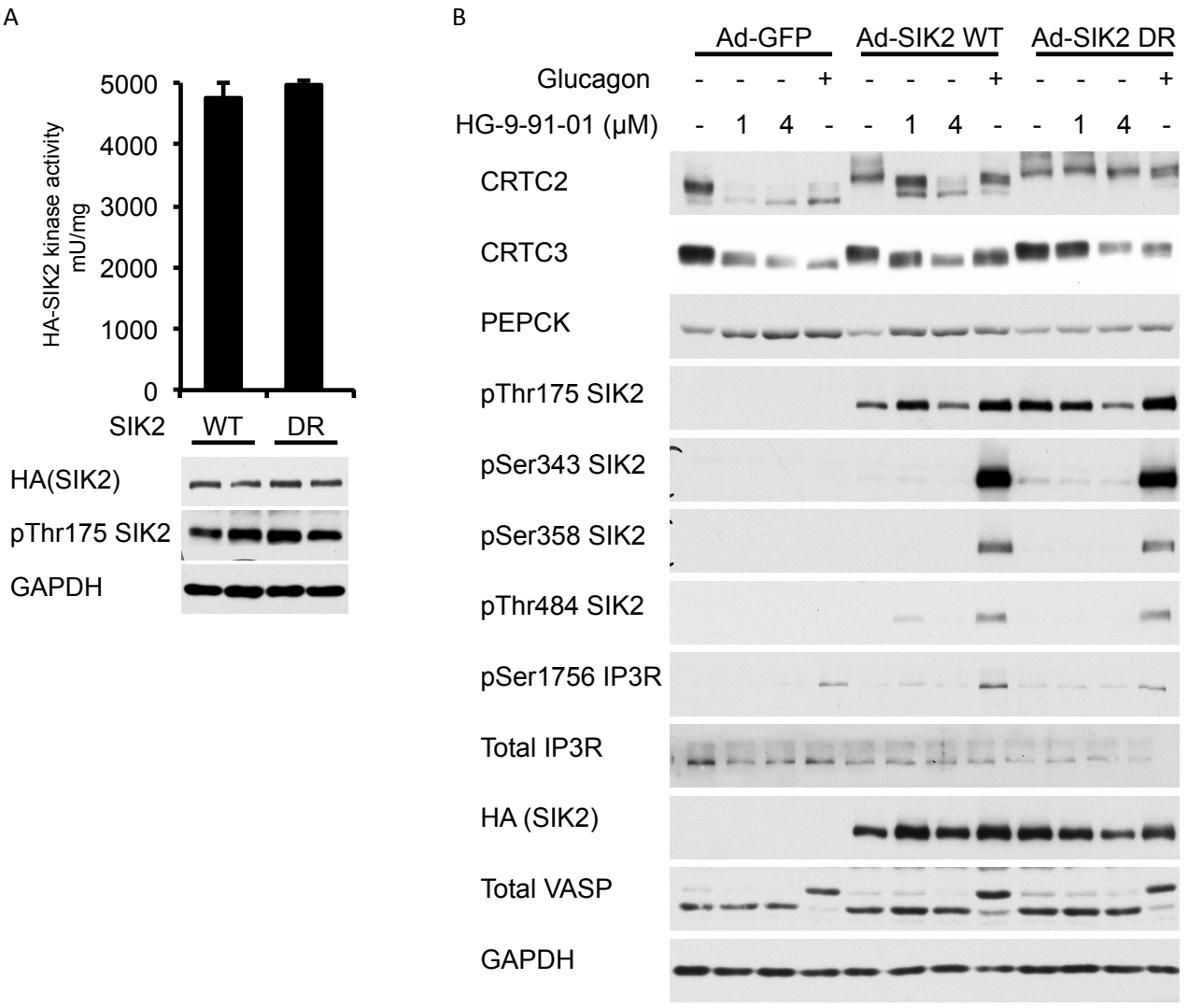

C

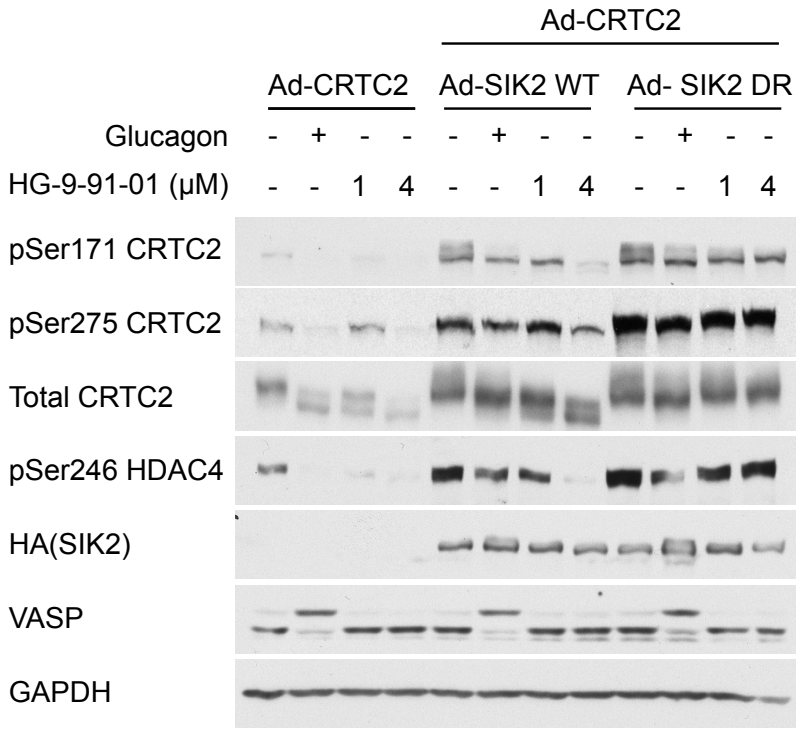

D

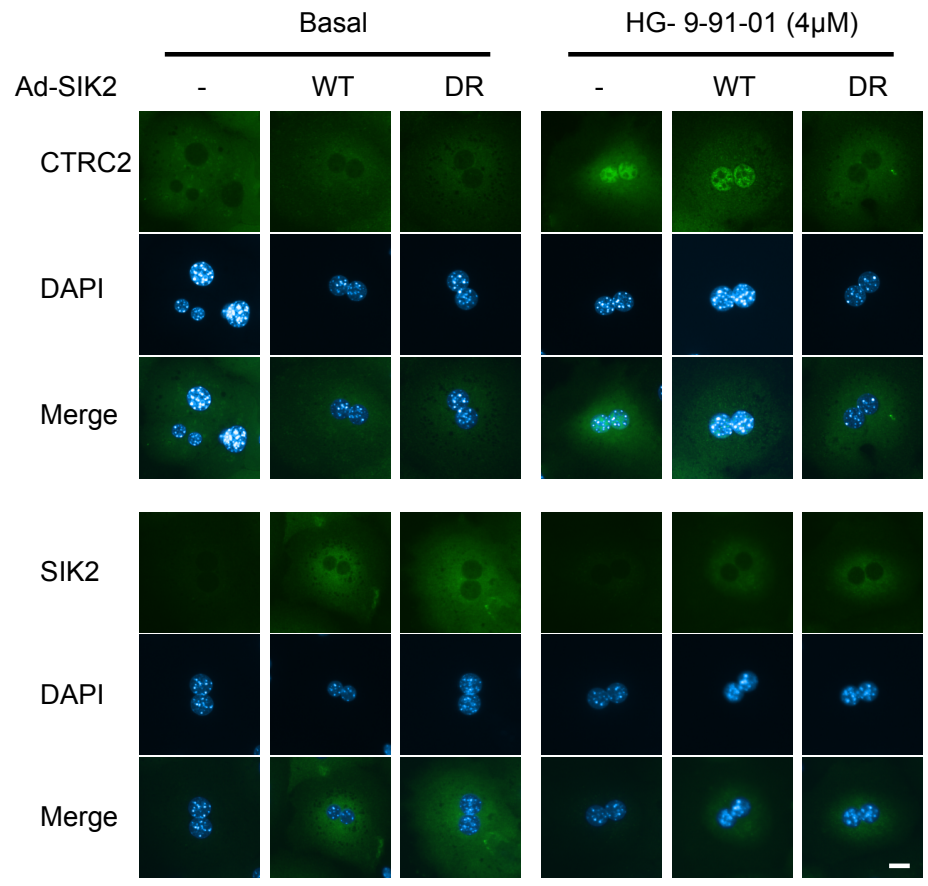

Figure 6.9 Characterisation of SIK2 drug-resistant mutant in primary hepatocytes.

A) HA-tagged SIK2 wild-type (WT) or T96Q drug-resistant (DR) mutant were expressed in primary mouse hepatocytes for 16 h using adenoviral vectors (1:5 MOI) prior to cell lysis. HA-SIK2 was

immunoprecipitated from 100 µg lysates and kinase activity was assayed with 200 µM 'SAKAMOTO'-tide. Data is presented as mean ± SD, n=3 independent experiments. Lysate were also immunoblotted with the indicated antibodies. **B)** Primary hepatocytes were infected for 24 h (1:5 MOI) with HA-SIK2 wild-type (Ad-SIK2 WT), HA-SIK2 T96Q drug-resistant mutant (Ad-SIK2 DR) or Ad-GFP (as infection control) adenoviruses (Ad) prior to cell lysis. The cells were treated for last 12 h with 1 µM HG-9-91-01, 4 µM HG-9-91-01 or 0.1 µM glucagon and lysates were subjected to immunoblotting with the indicated antibodies. **C)** Primary hepatocytes were infected with the indicated adenovirus for 16 h (1:5 MOI) followed by 1 h treatment of the indicated amount of HG-9-91-01 or 10 min treatment or 0.1 µM glucagon (as positive control) prior to cell lysis. Lysates were immunoblotted with indicated antibodies. The VASP antibody was used to confirm PKA activation by glucagon and the GAPDH antibody was used as loading control. **D)** Primary hepatocytes were infected (1:2 MOI) with HA-SIK2 adenovirus (Ad-SIK2) WT or DR mutant for 16 h followed by 4 µM HG-9-91-01 treatment for 1 h before fixing the cells. The cells were immunostained with the indicated antibodies. The DAPI dye was used for nuclear staining. Images were captured with a fluorescence microscope (Nikon Eclipse Ti) using Nikon NIS-Elements BR 3.1 software. The images were cropped using Adobe Photoshop CS5.1. Scale bar is 10 µm in length**.** All above results are representative of three independent experiments.

In addition, PKA activation measured with phosphorylation of IP3R and VASP was similar in the glucagon-treated cells of control (GFP-), SIK2 WT- or DR-mutant expressing hepatocytes and HG-9-91-01 treatment had no effect on these phosphorylations (Figure 6.9B).

The antibodies recognising site-specific phosphorylation of either CRTC2 (Ser171) or HDAC4 (Ser246) were applied to further confirm the drug-resistant property of the SIK2 T96Q mutant (Figure 6.9C). There was a dose-dependent reduction in phosphorylation of these SIK substrates in response to HG-9-91-01 in the SIK2 WT-expressing cells and this response was greatly reduced in SIK2 DR-expressing cells (Figure 6.9C). Importantly, substrate dephosphorylation in response to glucagon was similar in cells expressing either SIK2 WT or DR mutant (Figure 6.9C).

Apart from SIKs, MARK2 (one of the AMPK-related kinases) has also been shown to phosphorylate CRTC2 *in vitro,* albeit on a different residue (Ser275) and it was observed that the exposure of islets to high-glucose (20 mM), but not forskolin treatment, caused dephosphorylation of this site (Jansson et al., 2008). SIK and MARK2 also have a high degree of homology in their kinase domain. These data raise the possibility that HG-9-91-01-mediated dephosphorylation of total CRTC2 is not only contributed by SIK inhibition but also, at least partially if not completely, by the inhibition of MARK2. However, this possibility is less likely as the IC_{50} of HG-9-91-01 for MARK1, 2, 3 and 4 was 1000-fold higher compared to SIK *in vitro* (Table 6-1). To support the *in vitro* data, inhibition of MARK2 in intact cells was further

investigated by immunoblotting with an anti-phospho Ser275 CRTC2 antibody (MARK2 site (Jansson et al., 2008)). Surprisingly, glucagon and HG-9-91-01 treatment reduced this phosphorylation in control hepatocytes (Figure 6.9C) and overexpression of SIK2 WT increased phosphorylation of Ser275, and this was reduced by glucagon or HG-9-91-01 treatment (Figure 6.9C). In contrast, Ser275 phosphorylation of CRTC2 was not reduced by HG-9-91-01 in SIK2 DR mutant-expressing cells (Figure 6.9C). These findings may suggest that glucagon via SIK can also induce phosphorylation of CRTC2 on Ser275 in liver.

Endogenous CRTC2 was translocated to the nucleus following HG-9-91-01 treatment (Figure 6.4). Hence the drug-resistant property of SIK2 T96Q was assessed using CRTC2 cellular localisation in response to HG-9-91-01 (Figure 6.9D). CRTC2 translocated to the nucleus in response to HG-9-91-01 treatment in both control and SIK2 WT-expressing hepatocytes, whereas it remained in the cytoplasm of SIK2 DR-expressing hepatocytes following HG-9-91-01 treatment (Figure 6.9D).

These results collectively confirmed and validated SIK2 T96Q as a drug-resistant mutant in cell-based assays of primary hepatocytes and that mutation of Thr96Glu had no deleterious effect on intrinsic kinase activity of SIK2 or its regulation by glucagon.

6.2.4.1.2 Effects of drug-resistant SIK2 mutant on HG-9-91-01-mediated alteration of hepatic gluconeogenesis

The validated SIK2 DR mutant was expressed in primary hepatocytes to confirm the HG-9-91-01-mediated increase in gluconeogenesis, indicated by the increase in glucose production and mRNA expression of PEPCK and G6Pase, is specifically due to SIK inhibition rather than an 'off-target' effect.

First, glucose production was measured following HG-9-91-01 or glucagon treatment of primary hepatocytes that expressed either recombinant GFP (negative control), SIK2 WT or DR mutants (Figure 6.10A). HG-9-91-01 treatment of cells overexpressing SIK2 WT protein showed significantly increased glucose production (Figure 6.10A), whereas HG-9-91-01 had little or no effect on glucose production in SIK2 DR mutant-expressing hepatocytes. Glucose production in

response to glucagon treatment was similar (albeit lower compared to control hepatocytes) in SIK2 WT and DR mutant-expressing hepatocytes (Figure 6.10A). Similarly, PEPCK protein and mRNA levels as well as G6Pase mRNA expression were significantly increased in SIK2 WT- but not SIK2 DR mutant-expressing cells following HG-9-91-01 treatment (Figure 6.9B).

These results suggest that HG-9-91-01 mediaed increase in hepatic glucose production may be mediated by inhibition of SIKs.

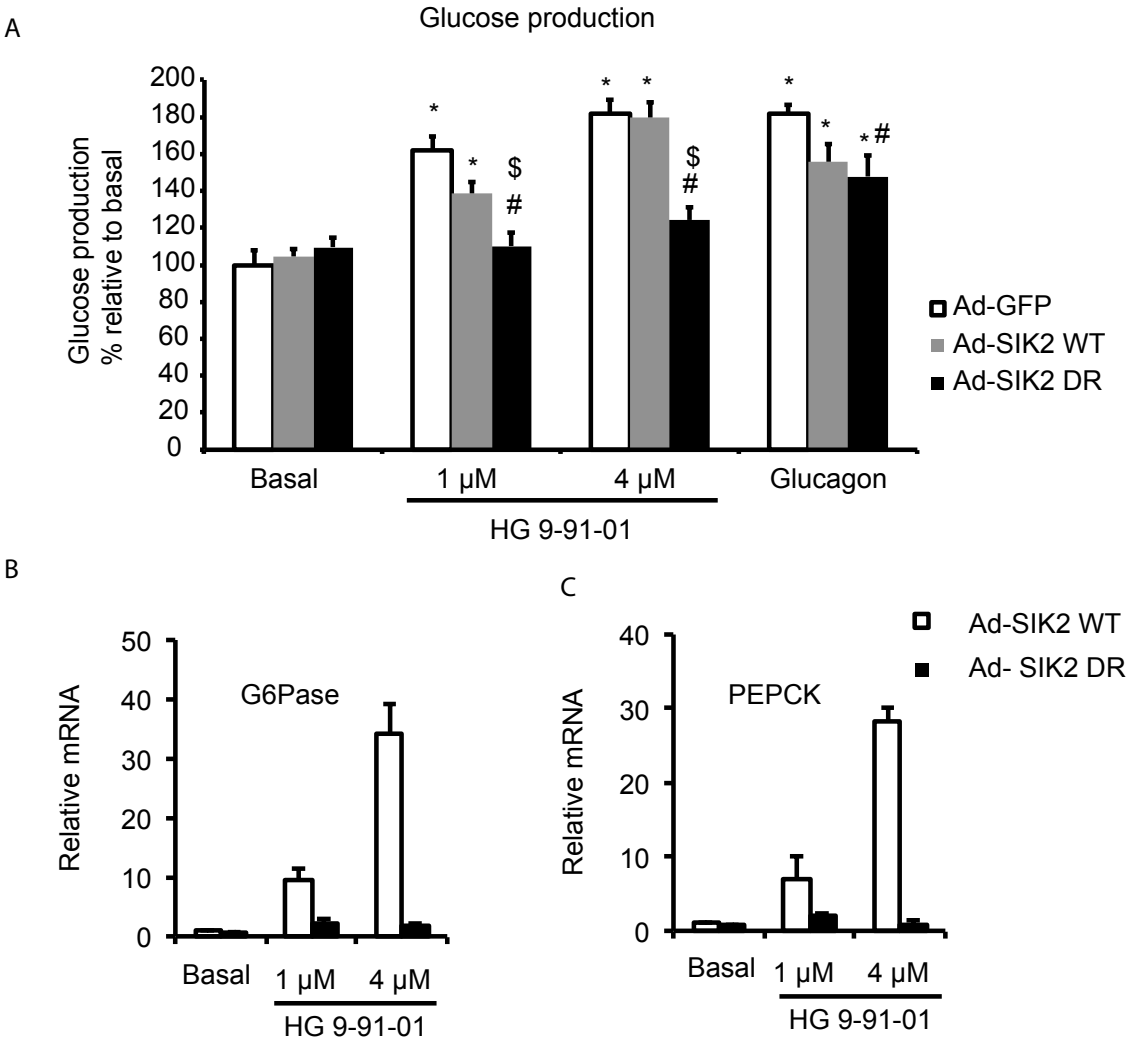

Figure 6.10 Effects of HG-9-91-01 on hepatic gluconeogenesis in primary hepatocytes expressing SIK2 WT or drug-resistant mutant.

Primary hepatocytes were infected for 24 h (1:5 MOI) with HA-SIK2 wild-type (Ad-SIK2 WT), HA-SIK2 T96Q drug-resistant mutant (Ad-SIK2 DR) or Ad-GFP (as infection control) adenoviruses. **A)** The cells were treated for the last 12 h of infection with 1 μM HG-9-91-01, 4 μM HG-9-91-01 or 0.1 μM glucagon and the culture medium was used to measure glucose production in triplicate. Glucose production was normalised to total protein content and presented relative to hepatocytes without treatment (Basal). Data is presented as mean ± SD, n=3 independent experiments. *p < 0.001 basal versus each treatment in Ad-GFP and in Ad-SIK2 WT group, basal versus glucagon in Ad-SIK2 DR group. $ p < 0.01 HG-9-91-01 treatment in SIK2 WT versus SIK2 DR and # p < 0.05 basal versus HG-9-91-01 treatment in Ad-SIK2 DR,

glucagon treatment in SIK2 WT versus SIK2 DR. **B, C)** The cells were treated for the last 8 h of infection with 1 or 4 µM HG-9-91-01. Relative mRNA levels of PEPCK or G6Pase were measured using qPCR. The mRNA levels were expressed as fold increase from non-treated hepatocytes. Data is presented as mean ± SD, n=3 independent experiments.

6.2.4.2 SIK inhibitor validation using LKB1 ineffective cells/tissues

Apart from the use of DR mutants, the specificity of kinase inhibitors to their intended targets can be ascertained by demonstrating a lack of actions of the inhibitors in cells/tissues where the kinase targets are genetically inactivated (Cohen, 2010). This can be achieved for the SIK isoforms by employing HeLa cells that lack LKB1 or alternatively in LKB1 knock-out mouse liver. Both of these systems lack the LKB1-MO25-STRAD complex, required for the constitutive T-loop phosphorylation of SIKs and essential for intrinsic SIK activity (Lizcano et al., 2004).

6.2.4.2.1 LKB1 knock-out mice

SIK2 was immunoprecipitated from liver extracts generated from $LKB1^{+/+}$ (8-10 weeks old, vehicle-treated $LKB1^{lox/lox}$ Albumin-$CreER^{T2}$ mice) or $LKB1^{-/-}$ (8-10 weeks old, tamoxifen treated $LKB1^{lox/lox}$ Albumin-$CreER^{T2}$ mice) mice and subjected to an *in vitro* kinase assay (Figure 6.11A). SIK2 isolated from the $LKB1^{+/+}$ liver had significant kinase activity while SIK2 isolated from the $LKB1^{-/-}$ liver showed significantly reduced SIK2 activity (almost baseline/background) (Figure 6.11A). Consistent with this the phosphorylation of Thr175 of SIK2 was absent in the LKB1 knock-out liver. Furthermore, lack of LKB1 activity in the knock-out liver was also confirmed by immunoblotting the *bone fide* LKB1 target AMPKα (phospho-Thr172) (Figure 6.11A). LKB1 knock-out liver had dramatically lower phosphorylation on Thr172 of AMPKα compared to LKB1 wild-type liver (Figure 6.11A). These results ascertained that SIKs were catalytically inert in LKB1 knock-out liver and validated this model for further experiments with HG-9-91-01 to evaluate its effects on hepatic gluconeogenesis.

A

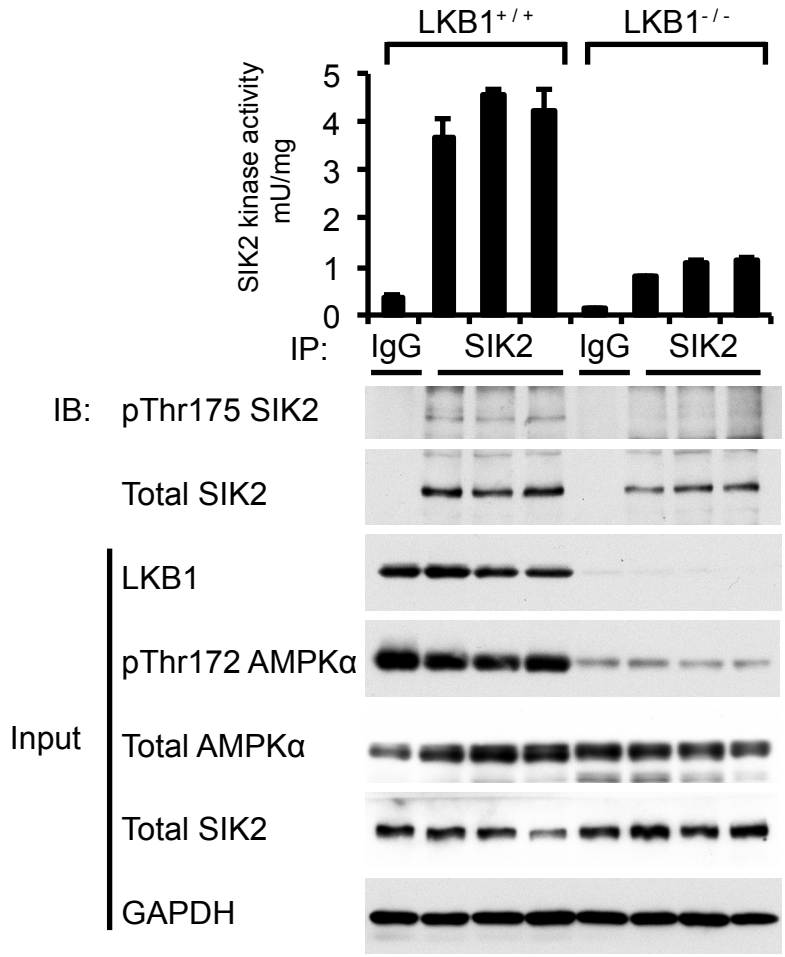
LKB1+/+
LKB1-/-
SIK2 kinase activity mU/mg
0
1
2
3
4
5
IP:
IgG
SIK2
IgG
SIK2
IB:
pThr175 SIK2
Total SIK2
Input
LKB1
pThr172 AMPKα
Total AMPKα
Total SIK2
GAPDH

B

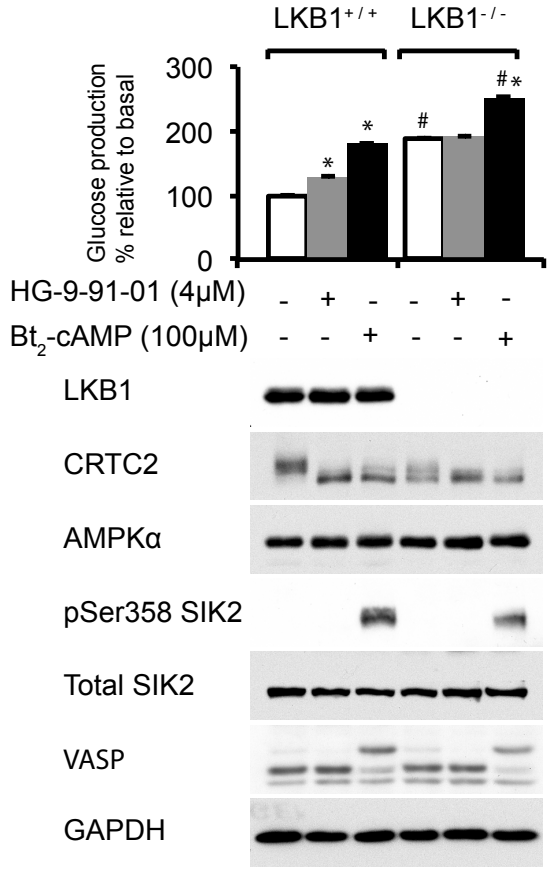
LKB1+/+
LKB1-/-
Glucose production
% relative to basal
0
100
200
300
*
*
#
#*
HG-9-91-01 (4μM)
- + - - + -
Bt2-cAMP (100μM)
- - + - - +
LKB1
CRTC2
AMPKα
pSer358 SIK2
Total SIK2
VASP
GAPDH

Figure 6.11 Effect of HG-9-91-01 on glucose production in LKB1-null hepatocytes.

A) Endogenous SIK2 was immunoprecipitated from 1 mg liver extracts of three $LKB1^{+/+}$ or $LKB1^{-/-}$ mice using the C-terminal in-house SIK2 antibody or pre-immune IgG and subjected to either *in vitro* kinase assay in triplicate or immunoblot analysis. Pre-immune IgG was used as negative control. Data is presented as mean ± SD, n=3 independent mouse. 40 µg of the same liver extracts were included in immunoblot analysis as input. **B)** Glucose production from primary hepatocytes of $LKB1^{+/+}$ or $LKB1^{-/-}$ mice was measured following 4 µM HG-9-91-01 or 100 µM Bt_2-cAMP treatment for 8 h. Lysates from the same experiment were immunoblotted with the indicated antibodies. The VASP antibody was used to confirm PKA activation by glucagon and the GAPDH antibody was used as loading control. The lysates of primary hepatocytes and liver of $LKB1^{+/+}$ (vehicle-treated $LKB1^{lox/lox}$ Albumin-CreERT2 mice) and $LKB1^{-/-}$ (tamoxifen treated $LKB1^{lox/lox}$ Albumin-CreERT2 mice) were generated by Dr Marc Foretz, Institut Cochin, Paris. Dr Marc Foretz also conducted the glucose production assay. Data is presented as mean ± SD, n=3 independent experiments. * $p < 0.01$ basal versus each treatment in $LKB1^{+/+}$ and basal versus glucagon in $LKB1^{-/-}$, # $p < 0.001$ basal $LKB1^{+/+}$ versus basal $LKB1^{-/-}$, glucagon $LKB1^{+/+}$ versus glucagon $LKB1^{-/-}$.

Next, we tested the response of the primary hepatocytes isolated from LKB1 wild-type and knock-out mice to either HG-9-91-01 or Bt_2-cAMP. Dr Marc Foretz generated the lysates for this experiment while I carried out immunoblot analysis. There was much lower basal phosphorylation of CRTC2 in LKB1 knock-out hepatocytes compared to wild-type cells (Figure 6.11B). In contrast to the wild-type hepatocytes, the CRTC2 band only had a minor increase in mobility in lysate from the HG-9-91-01 or Bt_2-cAMP treated LKB1-null hepatocytes (Figure 6.11B). The ability of HG-9-91-01 to promote dephosphorylation of CRTC2 was significantly reduced in hepatocytes lacking LKB1 (and hence with negligible SIK activity). However, it should be noted that tamoxifen inducible knock-out of a gene in adult mice may not be always complete particularly in liver due to insufficient Cre-recombinase expression (Davey, 2006; Hayashi and McMahon, 2002). Therefore it is likely that very minimal remaining phosphorylation of CRTC2 in control lysate of LKB1 knock-out hepatocytes was due to residual LKB1 in the liver and may explain the modest dephosphorylation with SIK inhibitors.

Consistent with this result, LKB1 knock-out hepatocytes produced much higher level of glucose (almost 2-fold) compared to wild-type cells (Figure 6.11B). This level of glucose production was not further increased by HG-9-91-01 treatment but was significantly increased by glucagon treatment (Figure 6.11B). The absolute level of glucose production in response to glucagon was much higher in the LKB1 knock-out hepatocytes than in the wild-type hepatocytes. This data indicates a key role of LKB1-SIKs in repressing hepatic glucose production. Similar to the

results of LKB1 knock-out hepatocytes, HG-9-91-01 and KIN112 treatment did not alter CRTC2 phosphorylation in HeLa cells where SIKs are catalytically-inactive due to the absence of LKB1 (Appendix 4).

6.2.4.3 Effects of HG-9-91-01 in AMPK knock-out primary hepatocytes

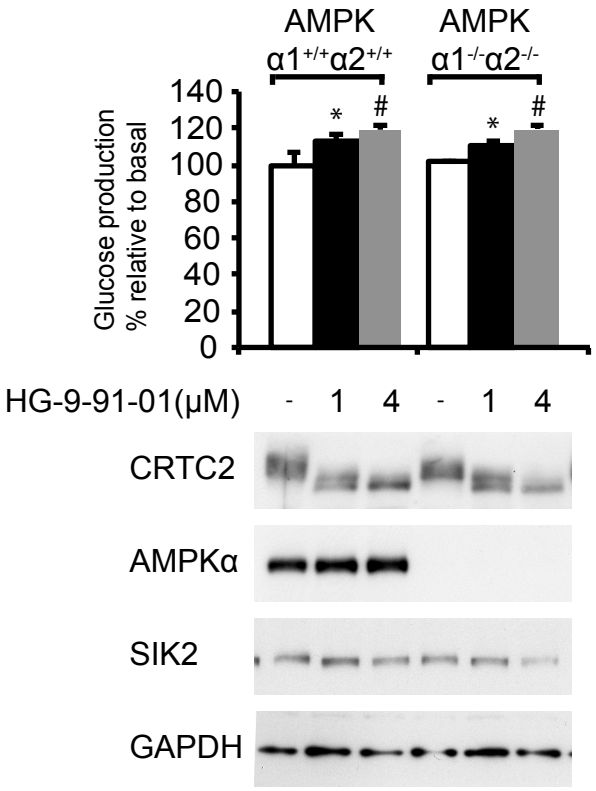

Figure 6.12 Effect of HG-9-91-01 on gluconeogenesis in AMPKα1$^{-/-}$α2$^{-/-}$ knock-out hepatocytes.

Primary hepatocytes from wild-type (AMPKα1$^{+/+}$α2$^{+/+}$) and knock-out (AMPKα1$^{-/-}$α2$^{-/-}$) mice were treated with the indicated amount of HG-9-91-01 for 8 h prior to cell lysis. Immunoblot analysis was conducted with the indicated antibodies and glucose was measured in culture medium. Glucose production was normalised to total protein content and presented as percentage of glucose production by non-treated hepatocytes. Data is presented as mean ± SD, n=3 independent experiments. *$p < 0.01$ basal versus 1 μM HG-9-91-01 treatment in both genotypes and and # $p < 0.001$ basal versus 4 μM HG-9-91-01 treatment in both genotypes. The lysates of primary hepatocytes of AMPKα1/α2 wild-type and knock-out mice were generated by Dr Marc Foretz, Institut Cochin, Paris. Dr Marc Foretz also conducted the glucose production assay.

AMPK is reported to phosphorylate CRTC2 on same residue (Ser171) as SIKs *in vitro* (Koo et al., 2005) and also phosphorylates class IIa HDACs on the same residues as SIKs (Berdeaux et al., 2007; Mihaylova et al., 2011). Despite the high homology of the kinase domain between AMPK and SIKs (Lizcano et al., 2004), HG-9-91-01 has more than a 1000-fold greater potency against SIKs than AMPK in cell-free assay (Table 6-1). However, due to the reported regulation of

CRTC2 and class IIa HDACs by AMPK and its proposed ability to influence gluconeogenesis, it remained plausible that part of the effect of this compound on hepatic gluconeogenesis could be mediated by AMPK. Therefore, the effects of HG-9-91-01 on hepatic gluconeogenesis were investigated in primary hepatocytes genetically lacking both AMPKα catalytic isoforms (α1 and α2) (Figure 6.12). Both wild-type and AMPKα1$^{-/-}$α2$^{-/-}$ knock-out hepatocytes showed identical basal as well as HG-9-91-01- and glucagon-induced glucose production and CRTC2 dephosphorylation (Figure 6.12).

These results collectively suggested that the ability of HG-9-91-01 to increase hepatic glucose production was not dependent on AMPK and further confirmed the selectivity of HG-9-91-01 for SIKs.

6.3 Discussion

This is the first study that characterised and validated the effect of selective SIK inhibitors (HG-9-91-01 and KIN112) in primary hepatocytes. Previous studies have used relatively (or more precisely "largely") non-specific kinase inhibitors, such as staurosporine (Berdeaux et al., 2007; Hashimoto et al., 2008; Katoh et al., 2006; Liu et al., 2008; Ravnskjaer et al., 2007; Uebi et al., 2010), compound C (Sasaki et al., 2011) or 4'-O-methylfisetin (Kumagai et al., 2011) to pharmacologically reduce SIK activity in intact cells. Although staurosporine was shown to inhibit SIK activity in cell-based assays (Katoh et al., 2006), it is one of the most promiscuous kinase inhibitors. Indeed it had the poorest selectivity when compared to 37 other protein kinase inhibitors against 317 protein kinases (Karaman et al., 2008). Similarly, compound C which was initially proposed as an AMPK-selective inhibitor (Zhou et al., 2001) has a huge range of kinase targets with many exhibiting as potent response as SIKs (Bain et al., 2007; Vogt et al., 2011). Neither compound C (Sasaki et al., 2011) nor 4'-O-methylfisetin (Kumagai et al., 2011) were confirmed as SIK-specific by the use of DR mutants, SIKs-null/silenced or LKB1-deficient cells/tissues and there was no evidence of cell-based validation using phospho-specific antibodies against known SIK substrates (e.g. CRTCs and HDACs). Furthermore 4'-O-

methylfisetin, identified using kinase inhibitor screening against SIK2, failed to increase basal CRE-reporter in cell culture models even at 25 μM and lacked assessment of selectivity against panel of protein kinases (including AMPK and AMPK-related kinases). Thus these inhibitors do not meet the criteria proposed by Cohen *et* al. for use in intact cells (Cohen, 2010) (described in page 175, 182). In contrast, HG-9-91-01 and KIN112 meet all such criteria and show evidence for high selectivity and potency towards SIK.

Application of these reagents in the analysis of SIK function in physiologically-relevant cells may allow us to define the regulation and role of SIK isoforms in the control of hepatic glucose production. The known SIK targets CRTC2, CBP and class IIa HDACs are associated with the control of glucose production as well as the regulation of expression of gluconeogenic genes, PEPCK and G6Pase (Koo et al., 2005; Liu et al., 2008; Mihaylova et al., 2011). HG-9-91-01 treatment in primary hepatocytes significantly increased glucose production, mRNA expression of PEPCK and G6Pase and protein expression of PEPCK concordant with changes in CRTC2 (and CRTC3) and HDAC4 phosphorylation (Figure 6.5).

These effects were shown to be dependent on SIK activity by:

i) expressing inhibitor-resistant SIKs which eliminated all the measured effects of HG-9-91-01

ii) showing that the compounds had little or no effect on glucose production, SIK substrate phosphorylation or gluconeogenic gene expression in the cell systems where SIK activity was depleted (LKB1-null hepatocytes and HeLa cells) and finally by

iii) showing that two structurally different SIK inhibitors (HG-9-91-01 and KIN112) had similar effect on gluconeogenesis.

Therefore, the results presented in this chapter suggest possible role of SIK in glucose production and PEPCK and G6Pase gene expression in mouse hepatocytes. Data presented in this chapter also indicate that inhibition of SIK activity is not the only mechanism underlying glucagon-induced hepatic glucose production; indeed it may mediate ~60% of the response. Glucagon also increases hepatic glucose production by regulating 6-phosphofructo-2-

kinase/fructose-2,6-bisphosphatase (Kurland and Pilkis, 1995), CREB Ser133 phosphorylation (Herzig et al., 2001) and the recently described IP3R-calcineurin (Wang et al., 2012) and CaMK-FoxO pathways (Ozcan et al., 2012). The lack of effect on these pathways by SIK inhibition suggests that glucagon regulation of these pathways is likely to be independent of SIKs and likely to explain the more robust effect of glucagon compared to SIK inhibitors on hepatic glucose production (Figure 6.7).

However, this does not explain the additive effects of a combination of HG-9-91-01 and glucagon on glucose production (Figure 6.7). Fasting/glucagon increased SIK1 mRNA and protein expression using the CREB-CRTC2 pathway thus creating a negative feedback loop for glucose production (Koo et al., 2005). It is possible that the combination of SIK inhibitor and glucagon removes this negative feedback loop and hence explains the additive effect on glucose production and CRTC2 phosphorylation (Figure 6.7). This needs to be confirmed with further experiments using SIK1 knock-out hepatocytes.

It is important to note that HG-9-91-01 and KIN112 also potently inhibit several tyrosine kinases such as Src family members (Src, Lck, and Yes), BTK, and FGF and Ephrin receptors that have been implicated in cell proliferation or growth factor signalling (Figure 6.3). Therefore, caution is needed when studying signalling pathways involving these kinases and it is important to validate the results using multiple controls (i.e. drug-resistant mutants).

The results in this chapter may provide an explanation for the observation that LKB1-null mice have raised fasting glycaemia with increased hepatic gluconeogenic gene expression (Mihaylova et al., 2011; Shaw, 2005). Interestingly, shRNAi-mediated acute knock-down of CRTC2 (Shaw, 2005) or class IIa HDACs (Mihaylova et al., 2011) in liver significantly reduced fasting hyperglycaemia and gluconeogenic gene expression in these mice. However, previous work had not been able to dissect the individual contribution of the LKB1 substrates that regulate CRTC2 (e.g. AMPK, SIKs and MARK2) or class IIa HDACs (AMPK and SIKs), to this phenotype (Lin and Accili, 2011).

The results in this chapter show that: 1) LKB1 knock-out hepatocytes have raised glucose production, which was not further increased by HG-9-91-01 treatment (Figure 6.11), 2) HG-9-91-01-induced hepatic glucose production was not altered in AMPKα1/α2-null mice (Figure 6.12) and 3) Other AMPK-related kinases including MARK isoforms exhibit 100-1000 fold higher HG-9-91-01 IC_{50} compared to SIKs (Table 6-1).

Moreover, Foretz and colleagues showed that liver-specific AMPKα1/α2-null mice had normal fasting and fed glucose *in vivo* and hepatocytes from these mice had unaltered cAMP-stimulated gluconeogenic gene expression and glucose production (Foretz et al., 2010), whereas global MARK2-null mice showed normal fasting glucose and had unaltered basal and clamp (hyperinsulinaemic-euglycaemic clamp) hepatic glucose production *in vivo* compared to wild-type mice (Hurov et al., 2007).

Therefore, collectively these observations suggest that the higher glucose production in the LKB1 knock-out liver is may be due to inactivation of SIKs which not only increases glucose production via enhancement of the CREB-CRTC2 pathway but also by the HDAC-FoxO pathway (Figure 6.13).

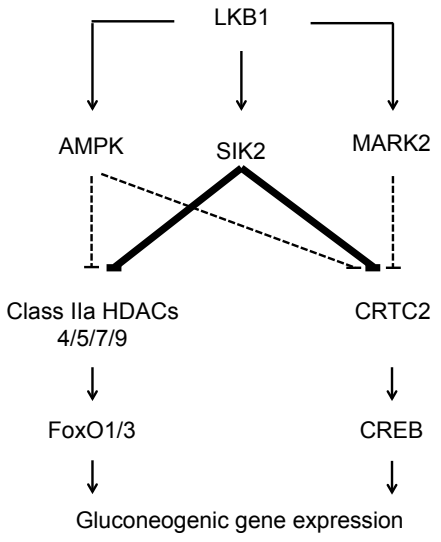

Figure 6.13 LKB1-dependent signalling in regulation of hepatic gluconeogenesis

In collaboration with Dr Marc Foretz, we have now shown that the regulation of hepatic glucose production in resting and cAMP-stimulated states is normal in SIK2-null hepatocytes (Figure 6.2). Moreover, liver-specific SIK2-null mice have normal glycaemic profiles in fasted

and fed states (Figure 6.1). Therefore, the significant increase in hepatic gluconeogenesis in the cells exposed to SIK inhibitors, that reduce activity of all three SIK isoforms, may suggest a degree of redundancy in the SIK-mediated regulation of hepatic glucose production (i.e. individual SIK isoforms might be dispensable for normal regulation of hepatic gluconeogenesis).

This is a novel and important finding, which is contrary to the previous reports that claimed SIK2 as the major regulator of hepatic gluconeogenesis (Altarejos and Montminy, 2011; Dentin et al., 2007; Koo et al., 2005; Liu et al., 2008). This notion of SIK redundancy could be appropriately investigated using a triple knock-out mouse model, however, this may be difficult to achieve and may well be lethal because SIK3-null mice showed significant skeletal muscle abnormality and 90% mice died within the first day after birth (Sasagawa et al., 2012; Uebi et al., 2012). ShRNAi-mediated knock-down of SIKs is another approach to investigate the notion but the possibility of off-target effects and insufficient knock-down with minimal effects on substrate phosphorylation would make this approach less robust for the proof of redundancy of the SIK isoforms (Appendix 5).

This study cannot exclude the contribution of isoforms other than CRTC2 to hepatic glucose production and gluconeogenic gene expression following SIK inhibition. Recent studies with CRTC2-null mice have raised a question regarding *in vivo* contribution of CRTC2 in regulation of hepatic gluconeogenesis (see section 1.3.8.1.3 for detail) and generate a possibility of redundancy among the CRTC isoforms based on the following observations: 1) overexpression of CRTC1 in primary hepatocytes augmented forskolin-promoted glucose production similar to CRTC2 (Koo et al., 2005), 2) All the isoforms shared similar modes of regulation by cAMP and calcium signalling (Bittinger et al., 2004; Conkright et al., 2003; Iourgenko et al., 2003; Takemori et al., 2007) and were able to increase steroidogenesis with equal efficiency in cultured cells (Takemori et al., 2007), 3) SIKs can also phosphorylate CRTC1 and 3 with equal efficiency as CRTC2 (Katoh et al., 2006) and 4) the only reason that CRTC2 has been extensively studied in the liver is because it is claimed to be the most abundant isoform in the liver (Koo et

al., 2005). Therefore, further studies are ongoing in collaboration with Prof Morris Birnbaum (University of Pennsylvania, USA) to study the potency of SIK inhibitors in liver-specific CRTC2-null mice to address this issue of redundancy in CRTC isoforms.

6.4 Overall Conclusion:

Insulin and glucagon regulate hepatic gluconeogenesis by modulating multiple signal transduction pathways. My investigation of SIK2 regulation by hormones in liver revealed that SIK2 was phosphorylated on multiple residues following glucagon stimulation but not following insulin stimulation. Surprisingly, these hormonal treatments had no effect on the intrinsic kinase activity or cellular location of SIK2 in liver. In addition, liver-specific SIK2 knock-out mice showed unaltered hepatic gluconeogenesis. Thus results in this thesis challenge the current dogma that SIK2 is the dominant isoform to regulate gluconeogenesis and that this isoform is a common target for insulin and glucagon signaling which regulate its activity in opposing fashion (Figure 6.14). Surprisingly, significant increase in hepatic glucose production and gluconeogenic gene expression following novel SIK inhibitors (HG-9-91-01 and KIN112) treatment of primary hepatocytes may indicate a novel insulin-independent pathway in which, under basal conditions, SIK isoforms collectively keep hepatic gluconeogenesis off, most likely by phosphorylating and inactivating CRTCs and class IIa HDACs, which in turn reduce expression of key enzymes required for glucose production (Figure 6.14). Importantly, these studies also suggest that SIK2 is not the only or the dominant SIK isoform that regulates hepatic gluconeogenesis.

Thus, my studies propose a non-hormonal dimension of gluconeogenesis control, in which LKB1-SIKs collectively work together as a molecular gate-keeper to continually suppress gluconeogenesis until it is stimulated by glucagon or fasting. However, further studies using liver-specific SIK triple knock-out mice and/or more specific SIK inhibitors are needed to confirm these findings.

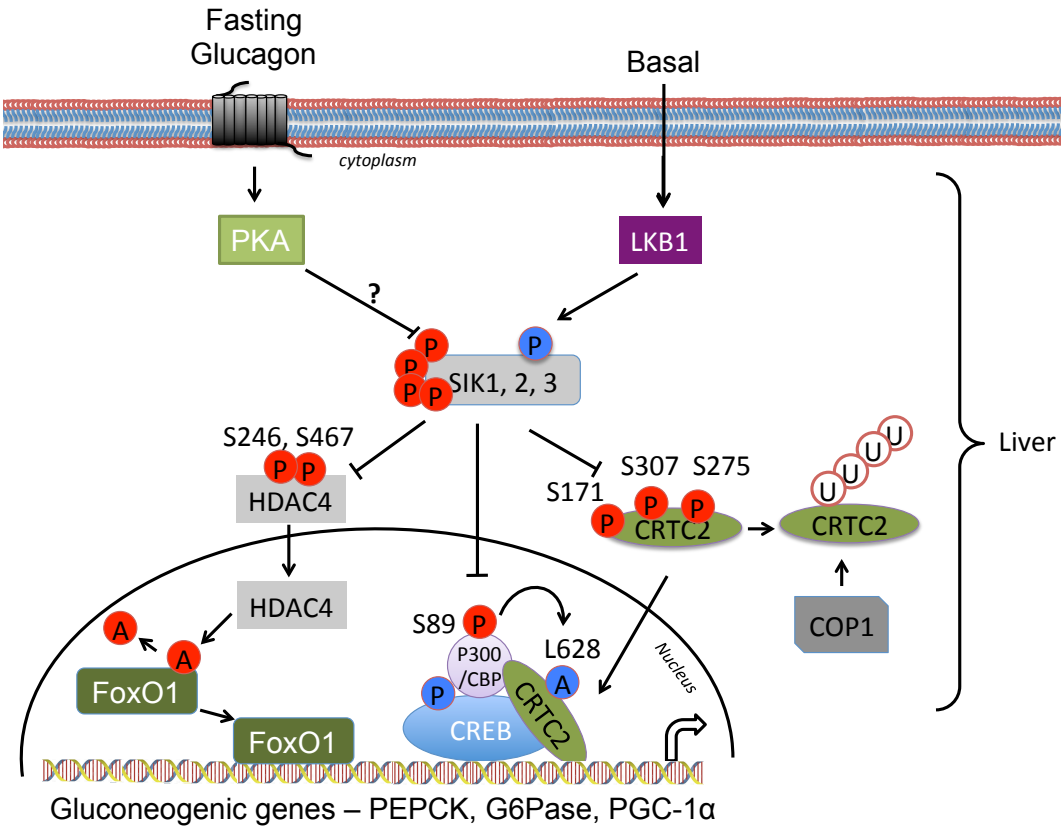

Figure 6.14 Role of SIKs in hepatic gluconeogenesis based on the results of this thesis

7 References

Agius, L. (2007). New hepatic targets for glycaemic control in diabetes. Best Practice & Research Clinical Endocrinology & Metabolism *21*, 587–605.

Ahmed, A.A., Lu, Z., Jennings, N.B., Etemadmoghadam, D., Capalbo, L., Jacamo, R.O., Barbosa-Morais, N., Le, X.F., Vivas-Mejia, P., and Lopez-Berestein, G. (2010). SIK2 is a centrosome kinase required for bipolar mitotic spindle formation that provides a potential target for therapy in ovarian cancer. Cancer Cell *18*, 109–121.

Al-Hakim, A.K., Goransson, O., Deak, M., Toth, R., Campbell, D.G., Morrice, N.A., Prescott, A.R., and Alessi, D.R. (2005). 14-3-3 cooperates with LKB1 to regulate the activity and localization of QSK and SIK. J. Cell. Sci. *118*, 5661–5673.

Alessi, D.R., Sakamoto, K., and Bayascas, J.R. (2006). LKB1-dependent signaling pathways. Annu. Rev. Biochem. *75*, 137–163.

Altarejos, J.Y., and Montminy, M. (2011). CREB and the CRTC co-activators: sensors for hormonal and metabolic signals. Nature Publishing Group *12*, 141–151.

Altomonte, J., Richter, A., Harbaran, S., Suriawinata, J., Nakae, J., Thung, S.N., Meseck, M., Accili, D., and Dong, H. (2003). Inhibition of Foxo1 function is associated with improved fasting glycemia in diabetic mice. Am. J. Physiol. Endocrinol. Metab. *285*, E718–E728.

Arany, Z., Sellers, W.R., Livingston, D.M., and Eckner, R. (1994). E1A-associated p300 and CREB-associated CBP belong to a conserved family of coactivators. Cell *77*, 799–800.

Aronoff, S.L., Berkowitz, K., Shreiner, B., and Want, L. (2004). Glucose metabolism and regulation: beyond insulin and glucagon. Diabetes Spectrum *17*, 183–190.

Attwood, P.V. (1993). Locus of action of acetyl CoA in the biotin-carboxylation reaction of pyruvate carboxylase. Biochemistry *32*, 12736–12742.

Authier, F., and Desbuquois, B. (2008). Glucagon receptors. Cell. Mol. Life Sci. *65*, 1880–1899.

Bain, J., Plater, L., Elliott, M., Shpiro, N., Hastie, C.J., Mclauchlan, H., Klevernic, I., Arthur, J.S.C., Alessi, D.R., and Cohen, P. (2007). The selectivity of protein kinase inhibitors: a further update. Biochem J *408*, 297.

Banks, A.S., Kim-Muller, J.Y., Mastracci, T.L., Kofler, N.M., Qiang, L., Haeusler, R.A., Jurczak, M.J., Laznik, D., Heinrich, G., Samuel, V.T., et al. (2011). Dissociation of the Glucose and Lipid Regulatory Functions of FoxO1 by Targeted Knockin of Acetylation-Defective Alleles in Mice. Cell Metabolism *14*, 587–597.

Banks, A.S., Kon, N., Knight, C., Matsumoto, M., Gutierrez-Juarez, R., Rossetti, L., Gu, W., and Accili, D. (2008). SirT1 Gain of Function Increases Energy Efficiency and Prevents Diabetes in Mice. Cell Metabolism *8*, 333–341.

Bannister, A.J., and Kouzarides, T. (1996). The CBP co-activator is a histone acetyltransferase.

Basu, R., Chandramouli, V., Dicke, B., Landau, B., and Rizza, R. (2005). Obesity and type 2 diabetes impair insulin-induced suppression of glycogenolysis as well as gluconeogenesis.

Diabetes *54*, 1942–1948.

Belov, A.A., and Mohammadi, M. (2013). Molecular Mechanisms of Fibroblast Growth Factor Signaling in Physiology and Pathology. Cold Spring Harbor Perspectives in Biology *5*, a015958–a015958.

Benayoun, B.R.N.A., Caburet, S., and Veitia, R.A. (2011). Forkhead transcription factors: key players in health and disease. Trends in Genetics *27*, 224–232.

Berdeaux, R. (2011). Metabolic regulation by salt inducible kinases. Frontiers in Biology *6*, 231–241.

Berdeaux, R., Goebel, N., Banaszynski, L., Takemori, H., Wandless, T., Shelton, G.D., and Montminy, M. (2007). SIK1 is a class II HDAC kinase that promotes survival of skeletal myocytes. Nat Med *13*, 597–603.

Berggreen, C., Henriksson, E., Jones, H.A., Morrice, N., and Goransson, O. (2012). cAMP-elevation mediated by β-adrenergic stimulation inhibits salt-inducible kinase (SIK) 3 activity in adipocytes. Cellular Signalling *24*, 1863–1871.

Biggs, W.H., Meisenhelder, J., Hunter, T., Cavenee, W.K., and Arden, K.C. (1999). Protein kinase B/Akt-mediated phosphorylation promotes nuclear exclusion of the winged helix transcription factor FKHR1. Proc. Natl. Acad. Sci. U.S.a. *96*, 7421–7426.

Bittinger, M.A., McWhinnie, E., Meltzer, J., Iourgenko, V., Latario, B., Liu, X., Chen, C.H., Song, C., Garza, D., and Labow, M. (2004). Activation of cAMP Response Element-Mediated Gene Expression by Regulated Nuclear Transport of TORC Proteins. Current Biology *14*, 2156–2161.

Bokar, J.A., Roesler, W.J., Vandenbark, G.R., Kaetzel, D.M., Hanson, R.W., and Nilson, J.H. (1988). Characterization of the cAMP responsive elements from the genes for the alpha-subunit of glycoprotein hormones and phosphoenolpyruvate carboxykinase (GTP). Conserved features of nuclear protein binding between tissues and species. J. Biol. Chem. *263*, 19740–19747.

Bordeaux, J., Welsh, A., Agarwal, S., Killiam, E., Baquero, M., Hanna, J., Anagnostou, V., and Rimm, D. (2010). Antibody validation. Biotech. *48*, 197–209.

Bouskila, M., Hunter, R.W., Ibrahim, A.F.M., Delattre, L., Peggie, M., van Diepen, J.A., Voshol, P.J., Jensen, J., and Sakamoto, K. (2010). Allosteric Regulation of Glycogen Synthase Controls Glycogen Synthesis in Muscle. Cell Metabolism *12*, 456–466.

Bradford, M.M. (1976). A rapid and sensitive method for the quantitation of microgram quantities of protein utilizing the principle of protein-dye binding. Anal. Biochem. *72*, 248–254.

Braun, T.R., Been, L.F., Singhal, A., Worsham, J., Ralhan, S., Wander, G.S., Chambers, J.C., Kooner, J.S., Aston, C.E., and Sanghera, D.K. (2012). A replication study of GWAS-derived lipid genes in Asian Indians: the chromosomal region 11q23.3 harbors loci contributing to triglycerides. PLoS ONE *7*, e37056.

Bricambert, J., Miranda, J., Benhamed, F., Girard, J., Postic, C., and Dentin, R. (2010). Salt-inducible kinase 2 links transcriptional coactivator p300 phosphorylation to the prevention of ChREBP-dependent hepatic steatosis in mice. J. Clin. Invest. *120*, 4316–4331.

Bright, N.J., Carling, D., and Thornton, C. (2008). Investigating the Regulation of Brain-specific Kinases 1 and 2 by Phosphorylation. Journal of Biological Chemistry *283*, 14946–14954.

Bright, N.J., Thornton, C., and Carling, D. (2009). The regulation and function of mammalian AMPK-related kinases. Acta Physiol (Oxf) *196*, 15–26.

Brunet, A., Bonni, A., Zigmond, M.J., Lin, M.Z., Juo, P., Hu, L.S., Anderson, M.J., Arden, K.C., Blenis, J., and Greenberg, M.E. (1999). Akt promotes cell survival by phosphorylating and inhibiting a Forkhead transcription factor. Cell *96*, 857–868.

Carling, D., Thornton, C., Woods, A., and Sanders, M.J. (2012). AMP-activated protein kinase: new regulation, new roles? Biochem J *445*, 11–27.

Carter, M.E., and Brunet, A. (2007). FOXO transcription factors. Current Biology *17*, R113–R114.

Cassuto, H. (2005). Glucocorticoids Regulate Transcription of the Gene for Phosphoenolpyruvate Carboxykinase in the Liver via an Extended Glucocorticoid Regulatory Unit. Journal of Biological Chemistry *280*, 33873–33884.

Chan, H.M., and La Thangue, N.B. (2001). p300/CBP proteins: HATs for transcriptional bridges and scaffolds. J. Cell. Sci. *114*, 2363–2373.

Charoenfuprasert, S., Yang, Y.-Y., Lee, Y.-C., Chao, K.-C., Chu, P.-Y., Lai, C.-R., Hsu, K.-F., Chang, K.-C., Chen, Y.-C., Chen, L.-T., et al. (2011). Identification of salt-inducible kinase 3 as a novel tumor antigen associated with tumorigenesis of ovarian cancer. Oncogene *30*, 3570–3584.

Charron, M.J., Brosius, F.C., Alper, S.L., and Lodish, H.F. (1989). A glucose transport protein expressed predominately in insulin-responsive tissues. Proc. Natl. Acad. Sci. U.S.a. *86*, 2535–2539.

Chen, D., Bruno, J., Easlon, E., Lin, S.J., Cheng, H.L., Alt, F.W., and Guarente, L. (2008). Tissue-specific regulation of SIRT1 by calorie restriction. Genes & Development *22*, 1753–1757.

Cheng, H., Liu, P., Wang, Z.C., Zou, L., Santiago, S., Garbitt, V., Gjoerup, O.V., Iglehart, J.D., Miron, A., Richardson, A.L., et al. (2009). SIK1 Couples LKB1 to p53-Dependent Anoikis and Suppresses Metastasis. Science Signaling *2*, ra35–ra35.

Cheng, J., Uchida, M., Zhang, W., Grafe, M.R., Herson, P.S., and Hurn, P.D. (2010). Role of salt-induced kinase 1 in androgen neuroprotection against cerebral ischemia. Journal of Cerebral Blood Flow &Amp; Metabolism *31*, 339–350.

Cherrington, A.D. (1999). Banting Lecture 1997. Control of glucose uptake and release by the liver in vivo. Diabetes *48*, 1198–1214.

Choi, S., Kim, W., and Chung, J. (2011). Drosophila Salt-inducible Kinase (SIK) Regulates Starvation Resistance through cAMP-response Element-binding Protein (CREB)-regulated Transcription Coactivator (CRTC). Journal of Biological Chemistry *286*, 2658–2664.

Chopra, A.R., Kommagani, R., Saha, P., Louet, J.-F., Salazar, C., Song, J., Jeong, J., Finegold, M., Viollet, B., DeMayo, F., et al. (2011). Cellular Energy Depletion Resets Whole-Body Energy by Promoting Coactivator-Mediated Dietary Fuel Absorption. Cell Metabolism *13*, 35–43.

Chrapkiewicz, N.B., Beale, E.G., and Granner, D.K. (1982). Induction of the messenger ribonucleic acid coding for phosphoenolpyruvate carboxykinase in H4-II-E cells. Evidence for a nuclear effect of cyclic AMP. J. Biol. Chem. *257*, 14428–14432.

Chrivia, J.C., Kwok, R.P., Lamb, N., Hagiwara, M., Montminy, M.R., and Goodman, R.H. (1993).

Phosphorylated CREB binds specifically to the nuclear protein CBP. Nature *365*, 855–859.

Clark, K., MacKenzie, K.F., Petkevicius, K., Kristariyanto, Y., Zhang, J., Choi, H.G., Peggie, M., Plater, L., Pedrioli, P.G.A., McIver, E., et al. (2012). Phosphorylation of CRTC3 by the salt-inducible kinases controls the interconversion of classically activated and regulatory macrophages. Proc. Natl. Acad. Sci. U.S.a. *109*, 16986–16991.

Cohen, P., and Frame, S. (2001). The renaissance of GSK3. Nature Reviews Molecular Cell Biology *2*, 769–776.

Cohen, P. (2010). Guidelines for the effective use of chemical inhibitors of protein function to understand their roles in cell regulation. Biochem J *425*, 53–54.

Conkright, M.D., Canettieri, G., Screaton, R., Guzman, E., Miraglia, L., Hogenesch, J.B., and Montminy, M. (2003). TORCs. Molecular Cell *12*, 413–423.

Couchman, J.R. (2008). Commercial Antibodies: The Good, Bad, and Really Ugly. Journal of Histochemistry and Cytochemistry *57*, 7–8.

Daitoku, H., Hatta, M., Matsuzaki, H., Aratani, S., Ohshima, T., Miyagishi, M., Nakajima, T., and Fukamizu, A. (2004). Silent information regulator 2 potentiates Foxo1-mediated transcription through its deacetylase activity. Proc. Natl. Acad. Sci. U.S.a. *101*, 10042–10047.

Daitoku, H., Sakamaki, J.-I., and Fukamizu, A. (2011). Regulation of FoxO transcription factors by acetylation and protein–protein interactions. BBA - Molecular Cell Research *1813*, 1954–1960.

Dale, S., Wilson, W.A., Edelman, A.M., and Hardie, D.G. (1995). Similar substrate recognition motifs for mammalian AMP-activated protein kinase, higher plant HMG-CoA reductase kinase-A, yeast SNF1, and mammalian calmodulin-dependent protein kinase I. Febs Lett *361*, 191–195.

Davey, R.A. (2006). Current and future approaches using genetically modified mice in endocrine research. AJP: Endocrinology and Metabolism *291*, E429–E438.

De Cesare, D., Fimia, G.M., and Sassone-Corsi, P. (1999). Signaling routes to CREM and CREB: plasticity in transcriptional activation. Trends Biochem. Sci. *24*, 281–285.

Deeg, R., Kraemer, W., and Ziegenhorn, J. (1980). Kinetic determination of serum glucose by use of the hexokinase/glucose-6-phosphate dehydrogenase method. J. Clin. Chem. Clin. Biochem. *18*, 49–52.

Defronzo, R.A. (2004). Pathogenesis of type 2 diabetes mellitus. Medical Clinics of North America *88*, 787–835.

Dentin, R., Liu, Y., Koo, S.-H., Hedrick, S., Vargas, T., Heredia, J., Yates, J.R., and Montminy, M. (2007). Insulin modulates gluconeogenesis by inhibition of the coactivator TORC2. Nature *449*, 366–369.

Dietrich, J.-B., Takemori, H., Grosch-Dirrig, S., Bertorello, A., and Zwiller, J. (2012). Cocaine induces the expression of MEF2C transcription factor in rat striatum through activation of SIK1 and phosphorylation of the histone deacetylase HDAC5. Synapse *66*, 61–70.

Dikic, I., Wakatsuki, S., and Walters, K.J. (2009). nrm2767. 1–13.

Doi, J., Takemori, H., Lin, X.-Z., Horike, N., Katoh, Y., and Okamoto, M. (2002). Salt-inducible kinase represses cAMP-dependent protein kinase-mediated activation of human cholesterol side chain cleavage cytochrome P450 promoter through the CREB basic leucine zipper domain. J. Biol. Chem. *277*, 15629–15637.

Dong, X.C., Copps, K.D., Guo, S., Li, Y., Kollipara, R., DePinho, R.A., and White, M.F. (2008). Inactivation of Hepatic Foxo1 by Insulin Signaling Is Required for Adaptive Nutrient Homeostasis and Endocrine Growth Regulation. Cell Metabolism *8*, 65–76.

Du, J., Chen, Q., Takemori, H., and Xu, H. (2008). SIK2 can be activated by deprivation of nutrition and it inhibits expression of lipogenic genes in adipocytes. Obesity (Silver Spring) *16*, 531–538.

Eberhard, C.E., Fu, A., Reeks, C., and Screaton, R.A. (2013). CRTC2 is required for beta cell function and proliferation. Endocrinology.

Eijkelenboom, A., and Burgering, B.M.T. (2013). nrm3507. Nature Reviews Molecular Cell Biology *14*, 83–97.

Eneling, K., Brion, L., Pinto, V., Pinho, M.J., Sznajder, J.I., Mochizuki, N., Emoto, K., Soares-da-Silva, P., and Bertorello, A.M. (2012). Salt-inducible kinase 1 regulates E-cadherin expression and intercellular junction stability. The FASEB Journal.

Erion, D.M., Kotas, M.E., McGlashon, J., Yonemitsu, S., Hsiao, J.J., Nagai, Y., Iwasaki, T., Murray, S.F., Bhanot, S., Cline, G.W., et al. (2013). CREB-regulated transcription coactivator 2 (CRTC2) promotes glucagon clearance and hepatic amino acid catabolism to regulate glucose homeostasis. Journal of Biological Chemistry.

Erion, D.M., Ignatova, I.D., Yonemitsu, S., Nagai, Y., Chatterjee, P., Weismann, D., Hsiao, J.J., Zhang, D., Iwasaki, T., Stark, R., et al. (2009). Prevention of Hepatic Steatosis and Hepatic Insulin Resistance by Knockdown of cAMP Response Element-Binding Protein. Cell Metabolism *10*, 499–506.

Exton, J.H., and Park, C.R. (1967). Control of gluconeogenesis in liver. I. General features of gluconeogenesis in the perfused livers of rats. J. Biol. Chem. *242*, 2622–2636.

Feldman, J.D., Vician, L., Crispino, M., Hoe, W., Baudry, M., and Herschman, H.R. (2000). The salt-inducible kinase, SIK, is induced by depolarization in brain. J. Neurochem. *74*, 2227–2238.

Finsterwald, C., Carrard, A., and Martin, J.-L. (2013). Role of Salt-Inducible Kinase 1 in the Activation of MEF2-Dependent Transcription by BDNF. PLoS ONE *8*, e54545.

Fischle, W., Dequiedt, F., Hendzel, M.J., Guenther, M.G., Lazar, M.A., Voelter, W., and Verdin, E. (2002). Enzymatic activity associated with class II HDACs is dependent on a multiprotein complex containing HDAC3 and SMRT/N-CoR. Molecular Cell *9*, 45–57.

Foretz, M., Hébrard, S., Leclerc, J., Zarrinpashneh, E., Soty, M., Mithieux, G., Sakamoto, K., Andreelli, F., and Viollet, B. (2010). Metformin inhibits hepatic gluconeogenesis in mice independently of the LKB1/AMPK pathway via a decrease in hepatic energy state. J. Clin. Invest. *120*, 2355–2369.

Foulkes, N.S., Borrelli, E., and Sassone-Corsi, P. (1991). CREM gene: use of alternative DNA-binding domains generates multiple antagonists of cAMP-induced transcription. Cell *64*, 739–749.

Fowler, M.J. (2007). Diabetes: Magnitude and mechanisms. Diabetes Care *25*, 25–28.

Frescas, D. (2005). Nuclear Trapping of the Forkhead Transcription Factor FoxO1 via Sirt-dependent Deacetylation Promotes Expression of Glucogenetic Genes. Journal of Biological Chemistry *280*, 20589–20595.

Gastaldelli, A., Toschi, E., Pettiti, M., Frascerra, S., Quiñones-Galvan, A., Sironi, A.M., Natali, A., and Ferrannini, E. (2001). Effect of physiological hyperinsulinemia on gluconeogenesis in nondiabetic subjects and in type 2 diabetic patients. Diabetes *50*, 1807–1812.

Gerich, J.E., Meyer, C., Woerle, H.J., and Stumvoll, M. (2001). Renal gluconeogenesis: its importance in human glucose homeostasis. Diabetes Care *24*, 382–391.

Gonzalez, G.A., Yamamoto, K.K., Fischer, W.H., Karr, D., Menzel, P., Biggs, W., Vale, W.W., and Montminy, M.R. (1989). A cluster of phosphorylation sites on the cyclic AMP-regulated nuclear factor CREB predicted by its sequence. Nature *337*, 749–752.

Gonzalez, G.A., and Montminy, M.R. (1989). Cyclic AMP stimulates somatostatin gene transcription by phosphorylation of CREB at serine 133. Cell *59*, 675–680.

Goodman, R.H., and Smolik, S. (2000). CBP/p300 in cell growth, transformation, and development. Genes & Development *14*, 1553–1577.

Gormand, A., Henriksson, E., Ström, K., Jensen, T.E., Sakamoto, K., and Goransson, O. (2011). Regulation of AMP-activated protein kinase by LKB1 and CaMKK in adipocytes. J. Cell. Biochem. *112*, 1364–1375.

Granner, D., Andreone, T., Sasaki, K., and Beale, E. (1983). Inhibition of transcription of the phosphoenolpyruvate carboxykinase gene by insulin.

Grimsey, N.L., Goodfellow, C.E., Scotter, E.L., Dowie, M.J., Glass, M., and Graham, E.S. (2008). Specific detection of CB1 receptors; cannabinoid CB1 receptor antibodies are not all created equal! Journal of Neuroscience Methods *171*, 78–86.

Gwinn, D.M., Shackelford, D.B., Egan, D.F., Mihaylova, M.M., Mery, A., Vasquez, D.S., Turk, B.E., and Shaw, R.J. (2008). AMPK Phosphorylation of Raptor Mediates a Metabolic Checkpoint. Molecular Cell *30*, 214–226.

Ha, C.H., Wang, W., Jhun, B.S., Wong, C., Hausser, A., Pfizenmaier, K., McKinsey, T.A., Olson, E.N., and Jin, Z.G. (2008). Protein Kinase D-dependent Phosphorylation and Nuclear Export of Histone Deacetylase 5 Mediates Vascular Endothelial Growth Factor-induced Gene Expression and Angiogenesis. Journal of Biological Chemistry *283*, 14590–14599.

Haase, T.N., Ringholm, S., Leick, L., Bienso, R.S., Kiilerich, K., Johansen, S., Nielsen, M.M., Wojtaszewski, J.F., Hidalgo, J., Pedersen, P.A., et al. (2011). Role of PGC-1 in exercise and fasting-induced adaptations in mouse liver. AJP: Regulatory, Integrative and Comparative Physiology *301*, R1501–R1509.

Haeusler, R.A., Kaestner, K.H., and Accili, D. (2010). FoxOs Function Synergistically to Promote Glucose Production. Journal of Biological Chemistry *285*, 35245–35248.

Hai, T.W., Liu, F., Coukos, W.J., and Green, M.R. (1989). Transcription factor ATF cDNA clones: an extensive family of leucine zipper proteins able to selectively form DNA-binding heterodimers. Genes & Development *3*, 2083–2090.

Hanson, R. (2003). Glyceroneogenesis revisited. Biochimie *85*, 1199–1205.

Hanson, R.W., and Patel, Y.M. (1994). Phosphoenolpyruvate carboxykinase (GTP): the gene and the enzyme. Adv Enzymol Relat Areas Mol Biol *69*, 203–281.

Hardie, D.G., Carling, D., and Carlson, M. (1998). The AMP-activated/SNF1 protein kinase subfamily: metabolic sensors of the eukaryotic cell? Annu. Rev. Biochem. *67*, 821–855.

Hardie, D.G., Ross, F.A., and Hawley, S.A. (2012). AMP-Activated Protein Kinase: A Target for Drugs both Ancient and Modern. Chemistry & Biology *19*, 1222–1236.

Hashimoto, Y.K., Satoh, T., Okamoto, M., and Takemori, H. (2008). Importance of autophosphorylation at Ser186 in the A-loop of salt inducible kinase 1 for its sustained kinase activity. J. Cell. Biochem. *104*, 1724–1739.

Hastie, C.J., McLauchlan, H.J., and Cohen, P. (2006). Assay of protein kinases using radiolabeled ATP: a protocol. Nat Protoc *1*, 968–971.

Hawley, S.A., Boudeau, J., Reid, J.L., Mustard, K.J., Udd, L., Mäkelä, T.P., Alessi, D.R., and Hardie, D.G. (2003). Complexes between the LKB1 tumor suppressor, STRADα/β and MO25α/β are upstream kinases in the AMP-activated protein kinase cascade. J Biol *2*, 28.

Hayashi, S., and McMahon, A.P. (2002). Efficient Recombination in Diverse Tissues by a Tamoxifen-Inducible Form of Cre: A Tool for Temporally Regulated Gene Activation/Inactivation in the Mouse. Developmental Biology *244*, 305–318.

He, L., Sabet, A., Djedjos, S., Miller, R., Sun, X., Hussain, M.A., Radovick, S., and Wondisford, F.E. (2009). Metformin and insulin suppress hepatic gluconeogenesis through phosphorylation of CREB binding protein. Cell *137*, 635–646.

Henriksson, E., Jones, H.A., Patel, K., Peggie, M., Morrice, N.A., Sakamoto, K., and Goransson, O. (2012). The AMP activated protein kinase (AMPK) -related kinase Salt-inducible Kinase (SIK) 2 is Regulated by cAMP via Phosphorylation at Ser358 in Adipocytes. Biochem J.

Herzig, S., Long, F., Jhala, U.S., Hedrick, S., Quinn, R., Bauer, A., Rudolph, D., Schutz, G., Yoon, C., Puigserver, P., et al. (2001). CREB regulates hepatic gluconeogenesis through the coactivator PGC-1. Nature *413*, 179–183.

Hirai, H., Sootome, H., Nakatsuru, Y., Miyama, K., Taguchi, S., Tsujioka, K., Ueno, Y., Hatch, H., Majumder, P.K., Pan, B.S., et al. (2010). MK-2206, an Allosteric Akt Inhibitor, Enhances Antitumor Efficacy by Standard Chemotherapeutic Agents or Molecular Targeted Drugs In vitro and In vivo. Molecular Cancer Therapeutics *9*, 1956–1967.

Hoeffler, J.P., Meyer, T.E., Yun, Y., Jameson, J.L., and Habener, J.F. (1988). Cyclic AMP-responsive DNA-binding protein: structure based on a cloned placental cDNA. Science *242*, 1430–1433.

Horike, N. (2003). Adipose-specific Expression, Phosphorylation of Ser794 in Insulin Receptor Substrate-1, and Activation in Diabetic Animals of Salt-inducible Kinase-2. Journal of Biological Chemistry *278*, 18440–18447.

Horike, N., Kumagai, A., Shimono, Y., Onishi, T., Itoh, Y., Sasaki, T., Kitagawa, K., Hatano, O., Takagi, H., Susumu, T., et al. (2010). Downregulation of SIK2 expression promotes the melanogenic program in mice. Pigment Cell Melanoma Res *23*, 809–819.

Hosaka, T., Biggs, W.H., Tieu, D., Boyer, A.D., Varki, N.M., Cavenee, W.K., and Arden, K.C. (2004). Disruption of forkhead transcription factor (FOXO) family members in mice reveals their functional diversification. Proc. Natl. Acad. Sci. U.S.a. *101*, 2975–2980.

Huang, S., and Czech, M.P. (2007). The GLUT4 Glucose Transporter. Cell Metabolism *5*, 237–252.

Hummler, E., Cole, T.J., Blendy, J.A., Ganss, R., Aguzzi, A., Schmid, W., Beermann, F., and Schutz, G. (1994). Targeted mutation of the CREB gene: compensation within the CREB/ATF family of transcription factors. Proc. Natl. Acad. Sci. U.S.a. *91*, 5647–5651.

Hurov, J.B., Huang, M., White, L.S., Lennerz, J., Choi, C.S., Cho, Y.R., Kim, H.J., Prior, J.L., Piwnica-Worms, D., Cantley, L.C., et al. (2007). Loss of the Par-1b/MARK2 polarity kinase leads to increased metabolic rate, decreased adiposity, and insulin hypersensitivity in vivo. Proc. Natl. Acad. Sci. U.S.a. *104*, 5680–5685.

Imielinski, M., Berger, A.H., Hammerman, P.S., Hernandez, B., Pugh, T.J., Hodis, E., Cho, J., Suh, J., Capelletti, M., Sivachenko, A., et al. (2012). Mapping the hallmarks of lung adenocarcinoma with massively parallel sequencing. Cell *150*, 1107–1120.

Inoue, H., Ogawa, W., Asakawa, A., Okamoto, Y., Nishizawa, A., Matsumoto, M., Teshigawara, K., Matsuki, Y., Watanabe, E., Hiramatsu, R., et al. (2006). Role of hepatic STAT3 in brain-insulin action on hepatic glucose production. Cell Metabolism *3*, 267–275.

Inoue, Y. (2004). Disruption of Hepatic C/EBP Results in Impaired Glucose Tolerance and Age-dependent Hepatosteatosis. Journal of Biological Chemistry *279*, 44740–44748.

Iourgenko, V., Zhang, W., Mickanin, C., Daly, I., Jiang, C., Hexham, J.M., Orth, A.P., Miraglia, L., Meltzer, J., Garza, D., et al. (2003). Identification of a family of cAMP response element-binding protein coactivators by genome-scale functional analysis in mammalian cells. Proc. Natl. Acad. Sci. U.S.a. *100*, 12147–12152.

Iyer, N.G., 214 zdag, H., and Caldas, C. (2004). p300/CBP and cancer. Oncogene *23*, 4225–4231.

Iynedjian, P.B., and Hanson, R.W. (1977). Increase in level of functional messenger RNA coding for phosphoenolpyruvate carboxykinase (GTP) during induction by cyclic adenosine 3“: 5-”monophosphate. J. Biol. Chem. *252*, 655–662.

Jaleel, M., McBride, A., Lizcano, J.M., Deak, M., Toth, R., Morrice, N.A., and Alessi, D.R. (2005). Identification of the sucrose non-fermenting related kinase SNRK, as a novel LKB1 substrate. Febs Lett *579*, 1417–1423.

James, D.E., Strube, M., and Mueckler, M. (1989). Molecular cloning and characterization of an insulin-regulatable glucose transporter. Nature *338*, 83–87.

Jansson, D., Ng, A.C.-H., Fu, A., Depatie, C., Azzabi, Al, M., and Screaton, R.A. (2008). Glucose controls CREB activity in islet cells via regulated phosphorylation of TORC2. Proc. Natl. Acad. Sci. U.S.a. *105*, 10161–10166.

Jensen, B.C., Swigart, P.M., and Simpson, P.C. (2008). Ten commercial antibodies for alpha-1-adrenergic receptor subtypes are nonspecific. Naunyn-Schmied Arch Pharmacol *379*, 409–412.

Jeppesen, J., Maarbjerg, S.J., Jordy, A.B., Fritzen, A.M., Pehmøller, C., Sylow, L., Serup, A.K., Jessen, N., Thorsen, K., and Prats, C. (2013). LKB1 regulates lipid oxidation during exercise independently of AMPK. Diabetes *62*, 1490–1499.

Jiang, G., and Zhang, B.B. (2003). Glucagon and regulation of glucose metabolism. Am. J. Physiol. Endocrinol. Metab. *284*, E671–E678.

Jitrapakdee, S. (2012). Transcription factors and coactivators controlling nutrient and hormonal regulation of hepatic gluconeogenesis. International Journal of Biochemistry and Cell Biology *44*, 33–45.

Jitrapakdee, S., Slawik, M., Medina-Gomez, G., Campbell, M., Wallace, J.C., Sethi, J.K., O'Rahilly, S., and Vidal-Puig, A.J. (2005). The Peroxisome Proliferator-activated Receptor- Regulates Murine Pyruvate Carboxylase Gene Expression in Vivo and in Vitro. J. Biol. Chem. *280*, 27466–27476.

Johannessen, M., Delghandi, M.P., and Moens, U. (2004). What turns CREB on? Cellular Signalling *16*, 1211–1227.

Jositsch, G., Papadakis, T., Haberberger, R.V., Wolff, M., Wess, J., and Kummer, W. (2008). Suitability of muscarinic acetylcholine receptor antibodies for immunohistochemistry evaluated on tissue sections of receptor gene-deficient mice. Naunyn-Schmied Arch Pharmacol *379*, 389–395.

Kaestner, K.H., Hiemisch, H., and Schütz, G. (1998). Targeted disruption of the gene encoding hepatocyte nuclear factor 3γ results in reduced transcription of hepatocyte-specific genes. Mol. Cell. Biol. *18*, 4245–4251.

Kanyo, R., Price, D.M., Chik, C.L., and Ho, A.K. (2009). Salt-inducible kinase 1 in the rat pinealocyte: adrenergic regulation and role in arylalkylamine N-acetyltransferase gene transcription. Endocrinology *150*, 4221–4230.

Karaman, M.W., Herrgard, S., Treiber, D.K., Gallant, P., Atteridge, C.E., Campbell, B.T., Chan, K.W., Ciceri, P., Davis, M.I., Edeen, P.T., et al. (2008). A quantitative analysis of kinase inhibitor selectivity. Nat Biotechnol *26*, 127–132.

Kasper, L.H., Boussouar, F., Ney, P.A., Jackson, C.W., Rehg, J., van Deursen, J.M., and Brindle, P.K. (2002). A transcription-factor-binding surface of coactivator p300 is required for haematopoiesis. Nature *419*, 738–743.

Katoh, Y., Takemori, H., Doi, J., and Okamoto, M. (2002). IDENTIFICATION OF THE NUCLEAR LOCALIZATION DOMAIN OF SALT-INDUCIBLE KINASE. Endocrine Research.

Katoh, Y., Takemori, H., Lin, X.-Z., Tamura, M., Muraoka, M., Satoh, T., Tsuchiya, Y., Min, L., Doi, J., Miyauchi, A., et al. (2006). Silencing the constitutive active transcription factor CREB by the LKB1-SIK signaling cascade. FEBS Journal *273*, 2730–2748.

Katoh, Y., Takemori, H., Min, L., Muraoka, M., Doi, J., Horike, N., and Okamoto, M. (2004). Salt-inducible kinase-1 represses cAMP response element-binding protein activity both in the nucleus and in the cytoplasm. European Journal of Biochemistry *271*, 4307–4319.

Kemper, J.K. (2011). Regulation of FXR transcriptional activity in health and disease: Emerging roles of FXR cofactors and post-translational modifications. BBA - Molecular Basis of Disease *1812*, 842–850.

Kemper, J.K., Xiao, Z., Ponugoti, B., Miao, J., Fang, S., Kanamaluru, D., Tsang, S., Wu, S.-Y., Chiang, C.-M., and Veenstra, T.D. (2009). FXR Acetylation Is Normally Dynamically Regulated by p300 and SIRT1 but Constitutively Elevated in Metabolic Disease States. Cell Metabolism *10*, 392–404.

Kim, Y.D., Park, K.G., Lee, Y.S., Park, Y.Y., Kim, D.K., Nedumaran, B., Jang, W.G., Cho, W.J., Ha, J., Lee, I.K., et al. (2007). Metformin Inhibits Hepatic Gluconeogenesis Through AMP-Activated Protein Kinase-Dependent Regulation of the Orphan Nuclear Receptor SHP. Diabetes *57*, 306–314.

Kioussis, D., Reshef, L., Cohen, H., Tilghman, S.M., Iynedjian, P.B., Ballard, F.J., and Hanson, R.W. (1978). Alterations in translatable messenger RNA coding for phosphoenolpyruvate carboxykinase (GTP) in rat liver cytosol during deinduction. J. Biol. Chem. *253*, 4327–4332.

Koh, H.-J., Toyoda, T., Fujii, N., Jung, M.M., Rathod, A., Middelbeek, R.J.-W., Lessard, S.J., Treebak, J.T., Tsuchihara, K., and Esumi, H. (2010). Sucrose nonfermenting AMPK-related kinase (SNARK) mediates contraction-stimulated glucose transport in mouse skeletal muscle. Proc. Natl. Acad. Sci. U.S.a. *107*, 15541–15546.

Koo, S.-H., Flechner, L., Qi, L., Zhang, X., Screaton, R.A., Jeffries, S., Hedrick, S., Xu, W., Boussouar, F., Brindle, P., et al. (2005). The CREB coactivator TORC2 is a key regulator of fasting glucose metabolism. Nature *437*, 1109–1111.

Koo, S.-H., Satoh, H., Herzig, S., Lee, C.-H., Hedrick, S., Kulkarni, R., Evans, R.M., Olefsky, J., and Montminy, M. (2004). PGC-1 promotes insulin resistance in liver through PPAR-α-dependent induction of TRB-3. Nat Med *10*, 530–534.

Korzus, E. (1998). Transcription Factor-Specific Requirements for Coactivators and Their Acetyltransferase Functions. Science *279*, 703–707.

Kowanetz, M., Lönn, P., Vanlandewijck, M., Kowanetz, K., Heldin, C.-H., and Moustakas, A. (2008). TGFbeta induces SIK to negatively regulate type I receptor kinase signaling. J. Cell Biol. *182*, 655–662.

Krebs, E.G. (1989). Role of the Cyclic AMP—Dependent Protein Kinase in Signal Transduction. Jama *262*, 1815–1818.

Kumagai, A., Horike, N., Satoh, Y., Uebi, T., Sasaki, T., Itoh, Y., Hirata, Y., Uchio-Yamada, K., Kitagawa, K., Uesato, S., et al. (2011). A potent inhibitor of SIK2, 3, 3', 7-trihydroxy-4'-methoxyflavon (4'-O-methylfisetin), promotes melanogenesis in B16F10 melanoma cells. PLoS ONE *6*, e26148.

Kumashiro, N., Beddow, S.A., Vatner, D.F., Majumdar, S.K., Cantley, J.L., Guebre-Egziabher, F., Fat, I., Guigni, B., Jurczak, M.J., and Birkenfeld, A.L. (2013). Targeting pyruvate carboxylase reduces gluconeogenesis and adiposity and improves insulin resistance. Diabetes.

Kurland, I.J., and Pilkis, S.J. (1995). Covalent control of 6-phosphofructo-2-kinase/fructose-2,6-bisphosphatase: insights into autoregulation of a bifunctional enzyme. Protein Sci. *4*, 1023–1037.

Kwok, R.P., Lundblad, J.R., Chrivia, J.C., Richards, J.P., Bächinger, H.P., Brennan, R.G., Roberts, S.G., Green, M.R., and Goodman, R.H. (1994). Nuclear protein CBP is a coactivator for the transcription factor CREB. Nature *370*, 223–226.

Lamers, W.H., Hanson, R.W., and Meisner, H.M. (1982). cAMP stimulates transcription of the gene for cytosolic phosphoenolpyruvate carboxykinase in rat liver nuclei. Proc. Natl. Acad. Sci. U.S.a. *79*, 5137–5141.

Lanjuin, A., and Sengupta, P. (2002). Regulation of chemosensory receptor expression and sensory signaling by the KIN-29 Ser/Thr kinase. Neuron *33*, 369–381.

Le Lay, J., Tuteja, G., White, P., Dhir, R., Ahima, R., and Kaestner, K.H. (2009). CRTC2 (TORC2) Contributes to the Transcriptional Response to Fasting in the Liver but Is Not Required for the Maintenance of Glucose Homeostasis. Cell Metabolism *10*, 55–62.

Lefebvre, D., BAI, Y., SHAHMOLKY, N., SHARMA, M., POON, R., DRUCKER, D., and ROSEN, C. (2001). Identification and characterization of a novel sucrose-non-fermenting protein kinase/AMP-activated protein kinase-related protein kinase, SNARK. Biochem J *355*, 297–305.

Leone, T.C., Lehman, J.J., Finck, B.N., Schaeffer, P.J., Wende, A.R., Boudina, S., Courtois, M., Wozniak, D.F., Sambandam, N., Bernal-Mizrachi, C., et al. (2005). PGC-1α Deficiency Causes Multi-System Energy Metabolic Derangements: Muscle Dysfunction, Abnormal Weight Control and Hepatic Steatosis. Plos Biol *3*, e101.

Li, X., Monks, B., Ge, Q., and Birnbaum, M.J. (2007). Akt/PKB regulates hepatic metabolism by directly inhibiting PGC-1α transcription coactivator. Nature *447*, 1012–1016.

Liang, H., and Ward, W.F. (2006). PGC-1 : a key regulator of energy metabolism. AJP: Advances in Physiology Education *30*, 145–151.

Lin, B., Morris, D.W., and Chou, J.Y. (1997). The role of HNF1alpha, HNF3gamma, and cyclic AMP in glucose-6-phosphatase gene activation. Biochemistry *36*, 14096–14106.

Lin, H.V., and Accili, D. (2011). Hormonal Regulation of Hepatic Glucose Production in Health and Disease. Cell Metabolism *14*, 9–19.

Lin, J., Wu, P.-H., Tarr, P.T., Lindenberg, K.S., St-Pierre, J., Zhang, C.-Y., Mootha, V.K., Jäger, S., Vianna, C.R., Reznick, R.M., et al. (2004). Defects in Adaptive Energy Metabolism with CNS-Linked Hyperactivity in PGC-1α Null Mice. Cell *119*, 121–135.

Lin, X., Takemori, H., Katoh, Y., Doi, J., Horike, N., Makino, A., Nonaka, Y., and Okamoto, M. (2001). Salt-inducible kinase is involved in the ACTH/cAMP-dependent protein kinase signaling in Y1 mouse adrenocortical tumor cells. Mol Endocrinol *15*, 1264–1276.

Linseman, D.A. (2003). Inactivation of the Myocyte Enhancer Factor-2 Repressor Histone Deacetylase-5 by Endogenous Ca2//Calmodulin-dependent Kinase II Promotes Depolarization-mediated Cerebellar Granule Neuron Survival. Journal of Biological Chemistry *278*, 41472–41481.

Liu, C., and Lin, J.D. (2011). PGC-1 coactivators in the control of energy metabolism. Acta Biochimica Et Biophysica Sinica *43*, 248–257.

Liu, Y., Dentin, R., Chen, D., Hedrick, S., Ravnskjaer, K., Schenk, S., Milne, J., Meyers, D.J., Cole, P., III, J.Y., et al. (2008). A fasting inducible switch modulates gluconeogenesis via activator/coactivator exchange. Nature *456*, 269–273.

Lizcano, J.M., Goransson, O., Toth, R., Deak, M., Morrice, N.A., Boudeau, J., Hawley, S.A., Udd, L., Mäkelä, T.P., Hardie, D.G., et al. (2004). LKB1 is a master kinase that activates 13 kinases of the AMPK subfamily, including MARK/PAR-1. Embo J. *23*, 833–843.

Lonze, B.E., and Ginty, D.D. (2002). Function and regulation of CREB family transcription factors in the nervous system. Neuron *35*, 605–623.

Louet, J.-F., Chopra, A.R., Sagen, J.V., An, J., York, B., Tannour-Louet, M., Saha, P.K., Stevens, R.D., Wenner, B.R., Ilkayeva, O.R., et al. (2010). The Coactivator SRC-1 Is an Essential Coordinator of Hepatic Glucose Production. Cell Metabolism *12*, 606–618.

Lönn, P., Vanlandewijck, M., Raja, E., Kowanetz, M., Watanabe, Y., Kowanetz, K., Vasilaki, E., Heldin, C.-H., and Moustakas, A. (2012). Transcriptional induction of salt-inducible kinase 1 by transforming growth factor β leads to negative regulation of type I receptor signaling in cooperation with the Smurf2 ubiquitin ligase. Journal of Biological Chemistry *287*, 12867–12878.

Luo, J., Deng, Z.-L., Luo, X., Tang, N., Song, W.-X., Chen, J., Sharff, K.A., Luu, H.H., Haydon, R.C., Kinzler, K.W., et al. (2007). A protocol for rapid generation of recombinant adenoviruses using the AdEasy system. Nat Protoc *2*, 1236–1247.

Ma, K. (2006a). Farnesoid X receptor is essential for normal glucose homeostasis. J. Clin. Invest. *116*, 1102–1109.

Ma, K. (2006b). Farnesoid X receptor is essential for normal glucose homeostasis. J. Clin. Invest. *116*, 1102–1109.

MacDonald, P.E., El-Kholy, W., Riedel, M.J., Salapatek, A.M.F., Light, P.E., and Wheeler, M.B. (2002). The multiple actions of GLP-1 on the process of glucose-stimulated insulin secretion. Diabetes *51 Suppl 3*, S434–S442.

MacKenzie, K.F., Clark, K., Naqvi, S., McGuire, V.A., Nöehren, G., Kristariyanto, Y., van den Bosch, M., Mudaliar, M., McCarthy, P.C., Pattison, M.J., et al. (2013). PGE(2) induces macrophage IL-10 production and a regulatory-like phenotype via a protein kinase A-SIK-CRTC3 pathway. J. Immunol. *190*, 565–577.

Magnusson, I., Rothman, D.L., Katz, L.D., Shulman, R.G., and Shulman, G.I. (1992). Increased rate of gluconeogenesis in type II diabetes mellitus. A 13C nuclear magnetic resonance study. J. Clin. Invest. *90*, 1323–1327.

Manning, G., Whyte, D.B., Martinez, R., Hunter, T., and Sudarsanam, S. (2002). The protein kinase complement of the human genome. Science *298*, 1912–1934.

Matsumoto, M., Ogawa, W., Akimoto, K., Inoue, H., Miyake, K., Furukawa, K., Hayashi, Y., Iguchi, H., Matsuki, Y., Hiramatsu, R., et al. (2003). PKCλ in liver mediates insulin-induced SREBP-1c expression and determines both hepatic lipid content and overall insulin sensitivity. J. Clin. Invest. *112*, 935–944.

Matsumoto, M., Pocai, A., Rossetti, L., DePinho, R.A., and Accili, D. (2007). Impaired Regulation of Hepatic Glucose Production in Mice Lacking the Forkhead Transcription Factor Foxo1 in Liver. Cell Metabolism *6*, 208–216.

Mayr, B., and Montminy, M. (2001). Transcriptional regulation by the phosphorylation-dependent factor CREB. Nature Reviews Molecular Cell Biology *2*, 599–609.

McGee, S.L., van Denderen, B.J.W., Howlett, K.F., Mollica, J., Schertzer, J.D., Kemp, B.E., and Hargreaves, M. (2008). AMP-Activated Protein Kinase Regulates GLUT4 Transcription by Phosphorylating Histone Deacetylase 5. Diabetes *57*, 860–867.

McKinsey, T.A., Zhang, C.L., Lu, J., and Olson, E.N. (2000). Signal-dependent nuclear export of a histone deacetylase regulates muscle differentiation. Nature *408*, 106–111.

MD, G.D., PhD, M.M.F., MSc, Y.L., PhD, G.M.S., MPH, M.J.C., PhD, C.J.P., John K Lin AB, MD, F.F., MD, P.Y.-H.K., DSc, G.A.S., et al. (2011). National, regional, and global trends in fasting plasma glucose and diabetes prevalence since 1980: systematic analysis of health examination surveys and epidemiological studies with 370 country-years and 2Â·7 million participants. The

Lancet *378*, 31–40.

Michel, M.C., Wieland, T., and Tsujimoto, G. (2009). How reliable are G-protein-coupled receptor antibodies? Naunyn-Schmied Arch Pharmacol *379*, 385–388.

Mihaylova, M.M., and Shaw, R.J. (2013). Metabolic reprogramming by class I and II histone deacetylases. Trends in Endocrinology & Metabolism *24*, 48–57.

Mihaylova, M.M., Vasquez, D.S., Ravnskjaer, K., Denechaud, P.-D., Yu, R.T., Alvarez, J.G., Downes, M., Evans, R.M., Montminy, M., and Shaw, R.J. (2011). Class IIa histone deacetylases are hormone-activated regulators of FOXO and mammalian glucose homeostasis. Cell *145*, 607–621.

Miller, R.A., Chu, Q., Xie, J., Foretz, M., Viollet, B., and Birnbaum, M.J. (2013). nature11808. Nature *494*, 256–260.

Montminy, M.R., Sevarino, K.A., Wagner, J.A., Mandel, G., and Goodman, R.H. (1986). Identification of a cyclic-AMP-responsive element within the rat somatostatin gene. Proc. Natl. Acad. Sci. U.S.a. *83*, 6682–6686.

Montminy, M.R., and Bilezikjian, L.M. (1987). Binding of a nuclear protein to the cyclic-AMP response element of the somatostatin gene. Nature *328*, 175–178.

Mora, A., Komander, D., Van Aalten, D.M.F., and Alessi, D.R. (2004). PDK1, the master regulator of AGC kinase signal transduction. Seminars in Cell & Developmental Biology *15*, 161–170.

Motta, M.C., Divecha, N., Lemieux, M., Kamel, C., Chen, D., Gu, W., Bultsma, Y., McBurney, M., and Guarente, L. (2004). Mammalian SIRT1 represses forkhead transcription factors. Cell *116*, 551–563.

Mueller, C.L. (1996). CREB-binding Protein Activates Transcription through Multiple Domains. Journal of Biological Chemistry *271*, 28138–28145.

Muraoka, M., Fukushima, A., Viengchareun, S., Lombès, M., Kishi, F., Miyauchi, A., Kanematsu, M., Doi, J., Kajimura, J., Nakai, R., et al. (2009). Involvement of SIK2/TORC2 signaling cascade in the regulation of insulin-induced PGC-1 and UCP-1 gene expression in brown adipocytes. AJP: Endocrinology and Metabolism *296*, E1430–E1439.

Nakae, J. (1999). Insulin Stimulates Phosphorylation of the Forkhead Transcription Factor FKHR on Serine 253 through a Wortmannin-sensitive Pathway. Journal of Biological Chemistry *274*, 15982–15985.

Nakae, J., Kitamura, T., Silver, D.L., and Accili, D. (2001). The forkhead transcription factor Foxo1 (Fkhr) confers insulin sensitivity onto glucose-6-phosphatase expression. J. Clin. Invest. *108*, 1359–1367.

Nakajima, T., Uchida, C., Anderson, S.F., Parvin, J.D., and Montminy, M. (1997). Analysis of a cAMP-responsive activator reveals a two-component mechanism for transcriptional induction via signal-dependent factors. Genes & Development *11*, 738–747.

Nedumaran, B., Hong, S., Xie, Y.-B., Kim, Y.-H., Seo, W.-Y., Lee, M.-W., Lee, C.H., Koo, S.-H., and Choi, H.-S. (2009). DAX-1 acts as a novel corepressor of orphan nuclear receptor HNF4alpha and negatively regulates gluconeogenic enzyme gene expression. Journal of Biological Chemistry *284*, 27511–27523.

Nie, Y., Erion, D.M., Yuan, Z., Dietrich, M., Shulman, G.I., Horvath, T.L., and Gao, Q. (2009). STAT3 inhibition of gluconeogenesis is downregulated by SirT1. Nat. Cell Biol. *11*, 492–500.

Nordlie, R.C., Foster, J.D., and Lange, A.J. (1999). Regulation of glucose production by the liver. Annu. Rev. Nutr. *19*, 379–406.

Nuttall, F.Q., Ngo, A., and Gannon, M.C. (2008). Regulation of hepatic glucose production and the role of gluconeogenesis in humans: is the rate of gluconeogenesis constant? Diabetes Metab. Res. Rev. *24*, 438–458.

Oakhill, J.S., Steel, R., Chen, Z.P., Scott, J.W., Ling, N., Tam, S., and Kemp, B.E. (2011). AMPK Is a Direct Adenylate Charge-Regulated Protein Kinase. Science *332*, 1433–1435.

Obenauer, J.C. (2003). Scansite 2.0: proteome-wide prediction of cell signaling interactions using short sequence motifs. Nucleic Acids Research *31*, 3635–3641.

Obici, S., Zhang, B.B., Karkanias, G., and Rossetti, L. (2002). Hypothalamic insulin signaling is required for inhibition of glucose production. Nat Med *8*, 1376–1382.

Okamoto, M., Takemori, H., and Katoh, Y. (2004). Salt-inducible kinase in steroidogenesis and adipogenesis. Trends in Endocrinology & Metabolism *15*, 21–26.

Ozcan, L., Wong, C.C.L., Li, G., Xu, T., Pajvani, U., Park, S.K.R., Wronska, A., Chen, B.-X., Marks, A.R., Fukamizu, A., et al. (2012). Calcium Signaling through CaMKII Regulates Hepatic Glucose Production in Fasting and Obesity. Cell Metabolism 1–13.

Papworth, C., Bauer, J.C., Braman, J., and Wright, D.A. (1996). Site-directed mutagenesis in one day with>80% efficiency. Strategies *9*.

Park, E.A., Roesler, W.J., Liu, J., Klemm, D.J., Gurney, A.L., Thatcher, J.D., Shuman, J., Friedman, A., and Hanson, R.W. (1990). The role of the CCAAT/enhancer-binding protein in the transcriptional regulation of the gene for phosphoenolpyruvate carboxykinase (GTP). Mol. Cell. Biol. *10*, 6264–6272.

Parker, D., Ferreri, K., Nakajima, T., LaMorte, V.J., Evans, R., Koerber, S.C., Hoeger, C., and Montminy, M.R. (1996). Phosphorylation of CREB at Ser-133 induces complex formation with CREB-binding protein via a direct mechanism. Mol. Cell. Biol. *16*, 694–703.

Perrot, V., and Rechler, M.M. (2005). The coactivator p300 directly acetylates the forkhead transcription factor Foxo1 and stimulates Foxo1-induced transcription. Mol Endocrinol *19*, 2283–2298.

Petersen, K.F., Price, T., Cline, G.W., Rothman, D.L., and Shulman, G.I. (1996). Contribution of net hepatic glycogenolysis to glucose production during the early postprandial period. Am. J. Physiol. *270*, E186–E191.

Pilkis, S.J., and Claus, T.H. (1991). Hepatic gluconeogenesis/glycolysis: regulation and structure/function relationships of substrate cycle enzymes. Annu. Rev. Nutr. *11*, 465–515.

Pilkis, S.J., and Granner, D.K. (1992). Molecular physiology of the regulation of hepatic gluconeogenesis and glycolysis. Annu. Rev. Physiol. *54*, 885–909.

Pilkis, S.J., el-Maghrabi, M.R., and Claus, T.H. (1988). Hormonal regulation of hepatic gluconeogenesis and glycolysis. Annu. Rev. Biochem. *57*, 755–783.

Pilkis, S.J., el-Maghrabi, M.R., and Claus, T.H. (1990). Fructose-2,6-bisphosphate in control of hepatic gluconeogenesis. From metabolites to molecular genetics. Diabetes Care *13*, 582–599.

Pocai, A., Lam, T.K.T., Gutierrez-Juarez, R., Obici, S., Schwartz, G.J., Bryan, J., Aguilar-Bryan, L., and Rossetti, L. (2005). Hypothalamic K(ATP) channels control hepatic glucose production. Nature *434*, 1026–1031.

Popov, S., Silveira, A., Wågsäter, D., Takemori, H., Oguro, R., Matsumoto, S., Sugimoto, K., Kamide, K., Hirose, T., Satoh, M., et al. (2011). Salt-inducible kinase 1 influences Na(+),K(+)-ATPase activity in vascular smooth muscle cells and associates with variations in blood pressure. J. Hypertens. *29*, 2395–2403.

Prawitt, J., Abdelkarim, M., Stroeve, J.H.M., Popescu, I., Duez, H., Velagapudi, V.R., Dumont, J., Bouchaert, E., van Dijk, T.H., Lucas, A., et al. (2011). Farnesoid X Receptor Deficiency Improves Glucose Homeostasis in Mouse Models of Obesity. Diabetes *60*, 1861–1871.

Previs, S.F., Brunengraber, D.Z., and Brunengraber, H. (2009). Is There Glucose Production Outside of the Liver and Kidney? Annu. Rev. Nutr. *29*, 43–57.

Purushotham, A., Schug, T.T., Xu, Q., Surapureddi, S., Guo, X., and Li, X. (2009). Hepatocyte-Specific Deletion of SIRT1 Alters Fatty Acid Metabolism and Results in Hepatic Steatosis and Inflammation. Cell Metabolism *9*, 327–338.

Qiang, L., Banks, A.S., and Accili, D. (2010). Uncoupling of Acetylation from Phosphorylation Regulates FoxO1 Function Independent of Its Subcellular Localization. Journal of Biological Chemistry *285*, 27396–27401.

Quinn, P.G., Wong, T.W., Magnuson, M.A., Shabb, J.B., and Granner, D.K. (1988). Identification of basal and cyclic AMP regulatory elements in the promoter of the phosphoenolpyruvate carboxykinase gene. Mol. Cell. Biol. *8*, 3467–3475.

Quinn, P.G., and Granner, D.K. (1990). Cyclic AMP-dependent protein kinase regulates transcription of the phosphoenolpyruvate carboxykinase gene but not binding of nuclear factors to the cyclic AMP regulatory element. Mol. Cell. Biol. *10*, 3357–3364.

Radziuk, J., and Pye, S. (2001). Hepatic glucose uptake, gluconeogenesis and the regulation of glycogen synthesis. Diabetes Metab. Res. Rev. *17*, 250–272.

Ramnanan, C.J., Edgerton, D.S., and Cherrington, A.D. (2012). Evidence against a Physiologic Role for Acute Changes in CNS Insulin Action in the Rapid Regulation of Hepatic Glucose Production. Cell Metabolism *15*, 656–664.

Rask-Madsen, C., and Kahn, C.R. (2012). Tissue-Specific Insulin Signaling, Metabolic Syndrome, and Cardiovascular Disease. Arteriosclerosis, Thrombosis, and Vascular Biology *32*, 2052–2059.

Ravnskjaer, K., Kester, H., Liu, Y., Zhang, X., Lee, D., Yates, J.R., and Montminy, M. (2007). Cooperative interactions between CBP and TORC2 confer selectivity to CREB target gene expression. Embo J. *26*, 2880–2889.

Rena, G., Pearson, E.R., and Sakamoto, K. (2013). Molecular mechanism of action of metformin: old or new insights? Diabetologia *56*, 1898–1906.

Rhee, J., Inoue, Y., Yoon, J.C., Puigserver, P., Fan, M., Gonzalez, F.J., and Spiegelman, B.M. (2003). Regulation of hepatic fasting response by PPARγ coactivator-1α (PGC-1): requirement for hepatocyte nuclear factor 4α in gluconeogenesis. Proc. Natl. Acad. Sci. U.S.a. *100*, 4012–

4017.

Ritter, S.L., and Hall, R.A. (2009). ritter_nrm2803_opt. Nature Reviews Molecular Cell Biology *10*, 819–830.

Roden, M., Petersen, K.F., and Shulman, G.I. (2001). Nuclear magnetic resonance studies of hepatic glucose metabolism in humans. Recent Prog. Horm. Res. *56*, 219–237.

Roden, M., and Bernroider, E. (2003). Hepatic glucose metabolism in humans—its role in health and disease. Best Practice & Research Clinical Endocrinology & Metabolism *17*, 365–383.

Rodgers, J.T., and Puigserver, P. (2007). Fasting-dependent glucose and lipid metabolic response through hepatic sirtuin 1. Proc. Natl. Acad. Sci. U.S.a. *104*, 12861–12866.

Rodgers, J.T., Haas, W., Gygi, S.P., and Puigserver, P. (2010). Cdc2-like Kinase 2 Is an Insulin-Regulated Suppressor of Hepatic Gluconeogenesis. Cell Metabolism *11*, 23–34.

Rodgers, J.T., Lerin, C., Gerhart-Hines, Z., and Puigserver, P. (2008). Metabolic adaptations through the PGC-1α and SIRT1 pathways. Febs Lett *582*, 46–53.

Rodgers, J.T., Lerin, C., Haas, W., Gygi, S.P., Spiegelman, B.M., and Puigserver, P. (2005). Nutrient control of glucose homeostasis through a complex of PGC-1α and SIRT1. Nature *434*, 113–118.

Romito, A., Lonardo, E., Roma, G., Minchiotti, G., Ballabio, A., and Cobellis, G. (2010). Lack of sik1 in mouse embryonic stem cells impairs cardiomyogenesis by down-regulating the cyclin-dependent kinase inhibitor p57kip2. PLoS ONE *5*, e9029.

Rothman, D.L., Magnusson, I., Katz, L.D., Shulman, R.G., and Shulman, G.I. (1991). Quantitation of hepatic glycogenolysis and gluconeogenesis in fasting humans with 13C NMR. Science *254*, 573–576.

Rudolph, D., Tafuri, A., Gass, P., Hämmerling, G.J., Arnold, B., and Schutz, G. (1998). Impaired fetal T cell development and perinatal lethality in mice lacking the cAMP response element binding protein. Proc. Natl. Acad. Sci. U.S.a. *95*, 4481–4486.

Ruiz, J.C., Conlon, F.L., and Robertson, E.J. (1994). Identification of novel protein kinases expressed in the myocardium of the developing mouse heart. Mech Dev *48*, 153–164.

Sakamoto, K. (2004). Activity of LKB1 and AMPK-related kinases in skeletal muscle: effects of contraction, phenformin, and AICAR. AJP: Endocrinology and Metabolism *287*, E310–E317.

Salt, I., Celler, J.W., Hawley, S.A., Prescott, A., Woods, A., Carling, D., and Hardie, D.G. (1998). AMP-activated protein kinase: greater AMP dependence, and preferential nuclear localization, of complexes containing the alpha2 isoform. Biochem J *334 (Pt 1)*, 177–187.

Saltiel, A.R., and Kahn, C.R. (2001). Insulin signalling and the regulation of glucose and lipid metabolism. Nature *414*, 799–806.

Saper, C.B. (2005). An open letter to our readers on the use of antibodies. J. Comp. Neurol. *493*, 477–478.

Sapkota, G.P., Deak, M., Kieloch, A., Morrice, N., Goodarzi, A.A., Smythe, C., Shiloh, Y., Lees-Miller, S.P., and Alessi, D.R. (2002). Ionizing radiation induces ataxia telangiectasia mutated

kinase (ATM)-mediated phosphorylation of LKB1/STK11 at Thr-366. Biochem J *368*, 507–516.

Sasagawa, S., Takemori, H., Uebi, T., Ikegami, D., Hiramatsu, K., Ikegawa, S., Yoshikawa, H., and Tsumaki, N. (2012). SIK3 is essential for chondrocyte hypertrophy during skeletal development in mice. Development *139*, 1153–1163.

Sasaki, T., Takemori, H., Yagita, Y., Terasaki, Y., Uebi, T., Horike, N., Takagi, H., Susumu, T., Teraoka, H., Kusano, K.-I., et al. (2011). SIK2 Is a Key Regulator for Neuronal Survival after Ischemia via TORC1-CREB. Neuron *69*, 106–119.

Schilling, M.M., Oeser, J.K., Boustead, J.N., Flemming, B.P., and O'Brien, R.M. (2006). Gluconeogenesis: Re-evaluating the FOXO1–PGC-1α connection. Nature *443*, E10–E11.

Screaton, R.A., Conkright, M.D., Katoh, Y., Best, J.L., Canettieri, G., Jeffries, S., Guzman, E., Niessen, S., Yates, J.R., Takemori, H., et al. (2004). The CREB Coactivator TORC2 Functions as a Calcium- and cAMP-Sensitive Coincidence Detector. Cell *119*, 61–74.

Shaw, R.J. (2005). The Kinase LKB1 Mediates Glucose Homeostasis in Liver and Therapeutic Effects of Metformin. Science *310*, 1642–1646.

Shaw, R.J., Kosmatka, M., Bardeesy, N., Hurley, R.L., Witters, L.A., DePinho, R.A., and Cantley, L.C. (2004). The tumor suppressor LKB1 kinase directly activates AMP-activated kinase and regulates apoptosis in response to energy stress. Proc. Natl. Acad. Sci. U.S.a. *101*, 3329–3335.

Shin, D.J., and Osborne, T.F. (2008). FGF15/FGFR4 Integrates Growth Factor Signaling with Hepatic Bile Acid Metabolism and Insulin Action. Journal of Biological Chemistry *284*, 11110–11120.

Short, J.M., Wynshaw-Boris, A., Short, H.P., and Hanson, R.W. (1986). Characterization of the phosphoenolpyruvate carboxykinase (GTP) promoter-regulatory region. II. Identification of cAMP and glucocorticoid regulatory domains. J. Biol. Chem. *261*, 9721–9726.

Siu, Y.-T., and Jin, D.-Y. (2007). CREB – a real culprit in oncogenesis. FEBS Journal *274*, 3224–3232.

Sjöström, M., Stenström, K., Eneling, K., Zwiller, J., Katz, A.I., Takemori, H., and Bertorello, A.M. (2007). SIK1 is part of a cell sodium-sensing network that regulates active sodium transport through a calcium-dependent process. Proc. Natl. Acad. Sci. U.S.a. *104*, 16922–16927.

Sonoda, J., Mehl, I.R., Chong, L.-W., Nofsinger, R.R., and Evans, R.M. (2007). PGC-1β controls mitochondrial metabolism to modulate circadian activity, adaptive thermogenesis, and hepatic steatosis. Proc. Natl. Acad. Sci. U.S.a. *104*, 5223–5228.

Staehr, P., Hother-Nielsen, O., and Beck-Nielsen, H. (2004). The role of the liver in type 2 diabetes. Rev Endocr Metab Disord *5*, 105–110.

Stapleton, D., Mitchelhill, K.I., Gao, G., Widmer, J., Michell, B.J., Teh, T., House, C.M., Fernandez, C.S., Cox, T., Witters, L.A., et al. (1996). Mammalian AMP-activated Protein Kinase Subfamily. Journal of Biological Chemistry *271*, 611–614.

Stapleton, D., Woollatt, E., Mitchelhill, K.I., Nicholl, J.K., Fernandez, C.S., Michell, B.J., Witters, L.A., Power, D.A., Sutherland, G.R., and Kemp, B.E. (1997). AMP-activated protein kinase isoenzyme family: subunit structure and chromosomal location. Febs Lett *409*, 452–456.

Stenström, K., Takemori, H., Bianchi, G., Katz, A.I., and Bertorello, A.M. (2009). Blocking the

salt-inducible kinase 1 network prevents the increases in cell sodium transport caused by a hypertension-linked mutation in human α-adducin. J. Hypertens. *27*, 2452–2457.

Stewart, R., Akhmedov, D., Robb, C., Leiter, C., and Berdeaux, R. (2013). Regulation of SIK1 abundance and stability is critical for myogenesis. Proc. Natl. Acad. Sci. U.S.a. *110*, 117–122.

Stumvoll, M., Goldstein, B.J., and van Haeften, T.W. (2005). Type 2 diabetes: principles of pathogenesis and therapy. The Lancet *365*, 1333–1346.

Suzuki, A., Kusakai, G.-I., Kishimoto, A., Minegichi, Y., Ogura, T., and Esumi, H. (2003). Induction of cell–cell detachment during glucose starvation through F-actin conversion by SNARK, the fourth member of the AMP-activated protein kinase catalytic subunit family. Biochemical and Biophysical Research Communications *311*, 156–161.

Takemori, H. (2002). ACTH-induced Nucleocytoplasmic Translocation of Salt-inducible Kinase. IMPLICATION IN THE PROTEIN KINASE A-ACTIVATED GENE TRANSCRIPTION IN MOUSE ADRENOCORTICAL TUMOR CELLS. Journal of Biological Chemistry *277*, 42334–42343.

Takemori, H., Doi, J., Horike, N., Katoh, Y., Min, L., Lin, X.-Z., Wang, Z.-N., Muraoka, M., and Okamoto, M. (2003). Salt-inducible kinase-mediated regulation of steroidogenesis at the early stage of ACTH-stimulation. J. Steroid Biochem. Mol. Biol. *85*, 397–400.

Takemori, H., Kanematsu, M., Kajimura, J., Hatano, O., Katoh, Y., Lin, X.-Z., Min, L., Yamazaki, T., Doi, J., and Okamoto, M. (2007). Dephosphorylation of TORC initiates expression of the StAR gene. Molecular and Cellular Endocrinology *265-266*, 196–204.

Takemori, H., Katoh Hashimoto, Y., Nakae, J., Olson, E.N., and Okamoto, M. (2009). Inactivation of HDAC5 by SIK1 in AICAR-treated C2C12 myoblasts. Endocr. J. *56*, 121–130.

Taniguchi, C.M., Emanuelli, B., and Kahn, C.R. (2006). Critical nodes in signalling pathways: insights into insulin action. Nature Publishing Group *7*, 85–96.

Taylor, S.S., Buechler, J.A., Slice, L.W., Knighton, D.K., Durgerian, S., Ringheim, G.E., Neitzel, J.J., Yonemoto, W.M., Sowadski, J.M., and Dospmann, W. (1988). cAMP-dependent protein kinase: a framework for a diverse family of enzymes. *53*, 121–130.

Thonpho, A., Sereeruk, C., Rojvirat, P., and Jitrapakdee, S. (2010). Identification of the cyclic AMP responsive element (CRE) that mediates transcriptional regulation of the pyruvate carboxylase gene in HepG2 cells. Biochemical and Biophysical Research Communications *393*, 714–719.

Tilghman, S.M., Hanson, R.W., Reshef, L., Hopgood, M.F., and Ballard, F.J. (1974). Rapid loss of translatable messenger RNA of phosphoenolpyruvate carboxykinase during glucose repression in liver. Proc. Natl. Acad. Sci. U.S.a. *71*, 1304–1308.

Tinti, M., Johnson, C., Toth, R., Ferrier, D.E.K., and MacKintosh, C. (2012). Evolution of signal multiplexing by 14-3-3-binding 2R-ohnologue protein families in the vertebrates. Open Biology *2*, 120103–120103.

Tombes, R.M., Faison, M.O., and Turbeville, J.M. (2003). Organization and evolution of multifunctional Ca2+/CaM-dependent protein kinase genes. Gene *322*, 17–31.

Uebi, T., Tamura, M., Horike, N., Hashimoto, Y.K., and Takemori, H. (2010). Phosphorylation of the CREB-specific coactivator TORC2 at Ser307 regulates its intracellular localization in COS-7 cells and in the mouse liver. AJP: Endocrinology and Metabolism *299*, E413–E425.

Uebi, T., Itoh, Y., Hatano, O., Kumagai, A., Sanosaka, M., Sasaki, T., Sasagawa, S., Doi, J., Tatsumi, K., Mitamura, K., et al. (2012). Involvement of SIK3 in Glucose and Lipid Homeostasis in Mice. PLoS ONE *7*, e37803.

van de Werve, G., Lange, A., Newgard, C., Méchin, M.C., Li, Y., and Berteloot, A. (2000). New lessons in the regulation of glucose metabolism taught by the glucose 6-phosphatase system. Eur. J. Biochem. *267*, 1533–1549.

van der Linden, A.M., Nolan, K.M., and Sengupta, P. (2007). KIN-29 SIK regulates chemoreceptor gene expression via an MEF2 transcription factor and a class II HDAC. Embo J. *26*, 358–370.

Vander Kooi, B.T. (2005). The Glucose-6-Phosphatase Catalytic Subunit Gene Promoter Contains Both Positive and Negative Glucocorticoid Response Elements. Mol Endocrinol *19*, 3001–3022.

Vega, R.B., Matsuda, K., Oh, J., Barbosa, A.C., Yang, X., Meadows, E., McAnally, J., Pomajzl, C., Shelton, J.M., Richardson, J.A., et al. (2004). Histone Deacetylase 4 Controls Chondrocyte Hypertrophy during Skeletogenesis. Cell *119*, 555–566.

Verdin, E., Dequiedt, F., and Kasler, H.G. (2003). Class II histone deacetylases: versatile regulators. Trends in Genetics *19*, 286–293.

Vogt, J., Traynor, R., and Sapkota, G.P. (2011). The specificities of small molecule inhibitors of the TGFß and BMP pathways. Cellular Signalling *23*, 1831–1842.

Walkinshaw, D.R., Weist, R., Kim, G.-W., You, L., Xiao, L., Nie, J., Li, C.S., Zhao, S., and Yang, X.-J. (2013). The tumor suppressor kinase LKB1 activates SIK2 and SIK3 to stimulate nuclear export of class IIa histone deacetylases. Journal of Biological Chemistry.

Wang, B., Goode, J., Best, J., Meltzer, J., Schilman, P.E., Chen, J., Garza, D., Thomas, J.B., and Montminy, M. (2008). The Insulin-Regulated CREB Coactivator TORC Promotes Stress Resistance in Drosophila. Cell Metabolism *7*, 434–444.

Wang, C., Tian, L., Popov, V.M., and Pestell, R.G. (2011). Acetylation and nuclear receptor action. Journal of Steroid Biochemistry and Molecular Biology *123*, 91–100.

Wang, N.-D., Finegold, M.J., Bradley, A., Ou, C.N., Abdelsayed, S.V., Wilde, M.D., Taylor, L.R., Wilson, D.R., and Darlington, G.J. (1995). Impaired energy homeostasis in C/EBP alpha knockout mice. Science *269*, 1108–1112.

Wang, Y., Inoue, H., Ravnskjaer, K., Viste, K., Miller, N., Liu, Y., Hedrick, S., Vera, L., and Montminy, M. (2010). Targeted disruption of the CREB coactivator Crtc2 increases insulin sensitivity. Proc. Natl. Acad. Sci. U.S.a. *107*, 3087–3092.

Wang, Y., Li, G., Goode, J., Paz, J.C., Ouyang, K., Screaton, R., Fischer, W.H., Chen, J., Tabas, I., and Montminy, M. (2012). Inositol-1,4,5-trisphosphate receptor regulates hepatic gluconeogenesis in fasting and diabetes. Nature *485*, 128–132.

Wang, Z., Takemori, H., Halder, S., Nonaka, Y., and Okamoto, M. (1999). Cloning of a novel kinase (SIK) of the SNF1/AMPK family from high salt diet-treated rat adrenal. Febs Lett *453*, 135–139.

Wasserman, D.H. (2009). Four grams of glucose. Am. J. Physiol. Endocrinol. Metab. *296*, E11–E21.

Winder, W.W., and Hardie, D.G. (1999). AMP-activated protein kinase, a metabolic master switch: possible roles in type 2 diabetes. Am. J. Physiol. Endocrinol. Metab. *277*, E1–E10.

Woods, A., Johnstone, S.R., Dickerson, K., Leiper, F.C., Fryer, L.G.D., Neumann, D., Schlattner, U., Wallimann, T., Carlson, M., and Carling, D. (2003). LKB1 is the upstream kinase in the AMP-activated protein kinase cascade. Curr. Biol. *13*, 2004–2008.

Wu, C., Okar, D.A., Kang, J., and Lange, A.J. (2005). Reduction of hepatic glucose production as a therapeutic target in the treatment of diabetes. Curr. Drug Targets Immune Endocr. Metabol. Disord. *5*, 51–59.

Wynshaw-Boris, A., Lugo, T.G., Short, J.M., Fournier, R.E., and Hanson, R.W. (1984). Identification of a cAMP regulatory region in the gene for rat cytosolic phosphoenolpyruvate carboxykinase (GTP). Use of chimeric genes transfected into hepatoma cells. J. Biol. Chem. *259*, 12161–12169.

Xia, Y., Zhang, Z., Kruse, U., Vogt, P.K., and Li, J. (2000). The New Serine-Threonine Kinase, Qik, Is a Target of the qin Oncogene. Biochemical and Biophysical Research Communications *276*, 564–570.

Xiao, B., Sanders, M.J., Underwood, E., Heath, R., Mayer, F.V., Carmena, D., Jing, C., Walker, P.A., Eccleston, J.F., Haire, L.F., et al. (2011). Structure of mammalian AMPK and its regulation by ADP. Nature *472*, 230–233.

Xie, M., Zhang, D., Dyck, J.R., Li, Y., Zhang, H., Morishima, M., Mann, D.L., Taffet, G.E., Baldini, A., and Khoury, D.S. (2006). A pivotal role for endogenous TGF-β-activated kinase-1 in the LKB1/AMP-activated protein kinase energy-sensor pathway. Proc. Natl. Acad. Sci. U.S.a. *103*, 17378–17383.

Xu, W., Kasper, L.H., Lerach, S., Jeevan, T., and Brindle, P.K. (2007). Individual CREB-target genes dictate usage of distinct cAMP-responsive coactivation mechanisms. Embo J. *26*, 2890–2903.

Yang, F.-C., Tan, B.C.-M., Chen, W.-H., Lin, Y.-H., Huang, J.-Y., Chang, H.-Y., Sun, H.-Y., Hsu, P.-H., Liou, G.-G., Shen, J., et al. (2013). Reversible Acetylation Regulates Salt-inducible Kinase (SIK2) and Its Function in Autophagy. Journal of Biological Chemistry *288*, 6227–6237.

Yang, X.-J., and Seto, E. (2007). HATs and HDACs: from structure, function and regulation to novel strategies for therapy and prevention. Oncogene *26*, 5310–5318.

Yao, T.P., Oh, S.P., Fuchs, M., Zhou, N.D., Ch'ng, L.E., Newsome, D., Bronson, R.T., Li, E., Livingston, D.M., and Eckner, R. (1998). Gene dosage-dependent embryonic development and proliferation defects in mice lacking the transcriptional integrator p300. Cell *93*, 361–372.

Yeo, R., and Sawdon, M. (2013). Hormonal control of metabolism: regulation of plasma glucose. Anaesthesia and Intensive Care Medicine *14*, 296–300.

Yoon, J.C., Puigserver, P., Chen, G., Donovan, J., Wu, Z., Rhee, J., Adelmant, G., Stafford, J., Kahn, C.R., and Granner, D.K. (2001). Control of hepatic gluconeogenesis through the transcriptional coactivator PGC-1. Nature *413*, 131–138.

Yoon, Y.S., Seo, W.Y., Lee, M.W., Kim, S.T., and Koo, S.H. (2009). Salt-inducible Kinase Regulates Hepatic Lipogenesis by Controlling SREBP-1c Phosphorylation. Journal of Biological Chemistry *284*, 10446–10452.

Yoshida, H., and Goedert, M. (2012). Phosphorylation of microtubule-associated protein tau by AMPK-related kinases. J. Neurochem. *120*, 165–176.

Yuan, J.S., Reed, A., Chen, F., and Stewart, C.N. (2006). Statistical analysis of real-time PCR data. BMC Bioinformatics *7*, 85.

Zagórska, A., Deak, M., Campbell, D.G., Banerjee, S., Hirano, M., Aizawa, S., Prescott, A.R., and Alessi, D.R. (2010). New roles for the LKB1-NUAK pathway in controlling myosin phosphatase complexes and cell adhesion. Science Signaling *3*, ra25.

Zhang, J., Yang, P.L., and Gray, N.S. (2009). Targeting cancer with small molecule kinase inhibitors. Nat. Rev. Cancer *9*, 28–39.

Zhou, G., Myers, R., Li, Y., Chen, Y., Shen, X., Fenyk-Melody, J., Wu, M., Ventre, J., Doebber, T., Fujii, N., et al. (2001). Role of AMP-activated protein kinase in mechanism of metformin action. J. Clin. Invest. *108*, 1167–1174.

Zhou, X.Y., Shibusawa, N., Naik, K., Porras, D., Temple, K., Ou, H., Kaihara, K., Roe, M.W., Brady, M.J., and Wondisford, F.E. (2004). Insulin regulation of hepatic gluconeogenesis through phosphorylation of CREB-binding protein. Nat Med *10*, 633–637.

(2008). The p300 Acetylase Is Critical for Ligand-activated Farnesoid X Receptor (FXR) Induction of SHP. Journal of Biological Chemistry *283*, 35086–35095.

8 Appendix

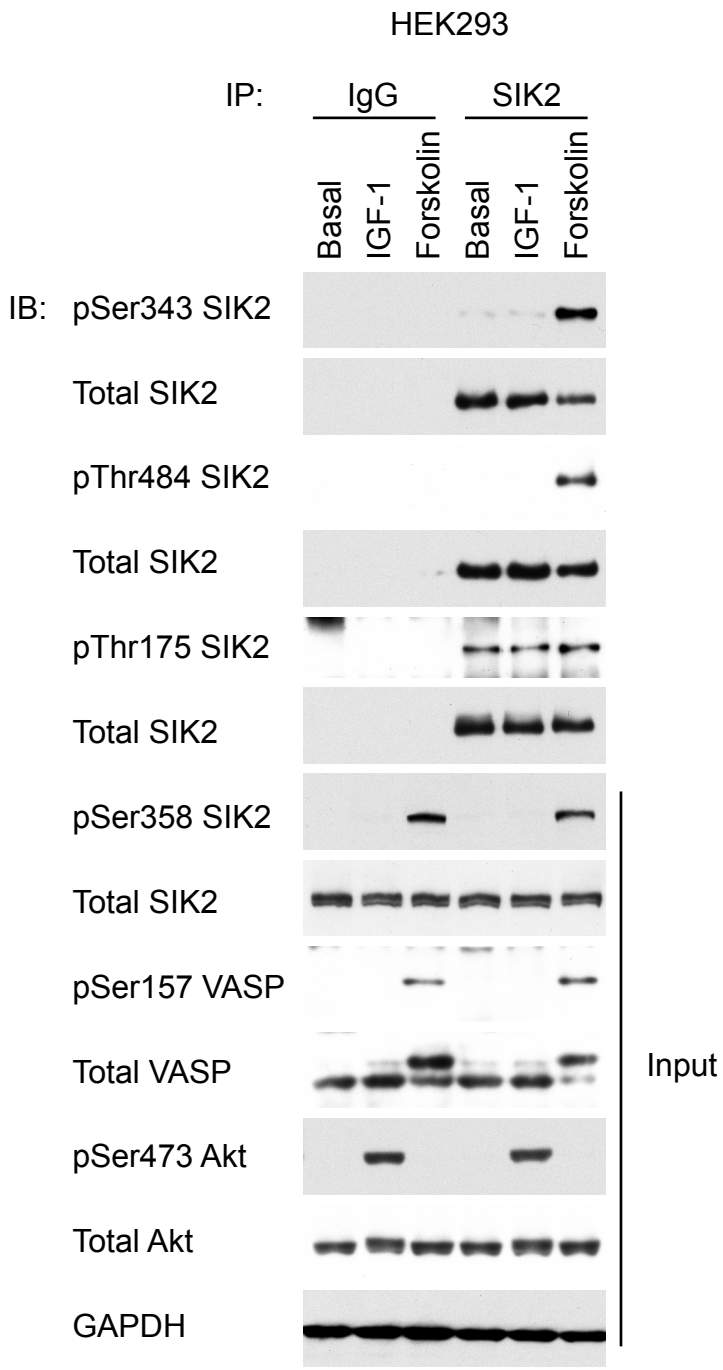

Appendix 1 SIK2 phosphorylation in HEK293 cells.

HEK293 cells were lysed following 10 min treatment of 10 µM forskolin or 50 ng/ml IGF-1. Endogenous SIK2 was immunoprecipitated from 0.5 mg lysates or pre-immune IgG as a negative control. The precipitates were immunoblotted (along with 40 µg of lysates as an input) with indicated SIK2 antibodies. The Akt and VASP antibodies were used to confirm the stimulation by insulin or PKA activation by glucagon respectively. The GAPDH antibody was used as a loading control.

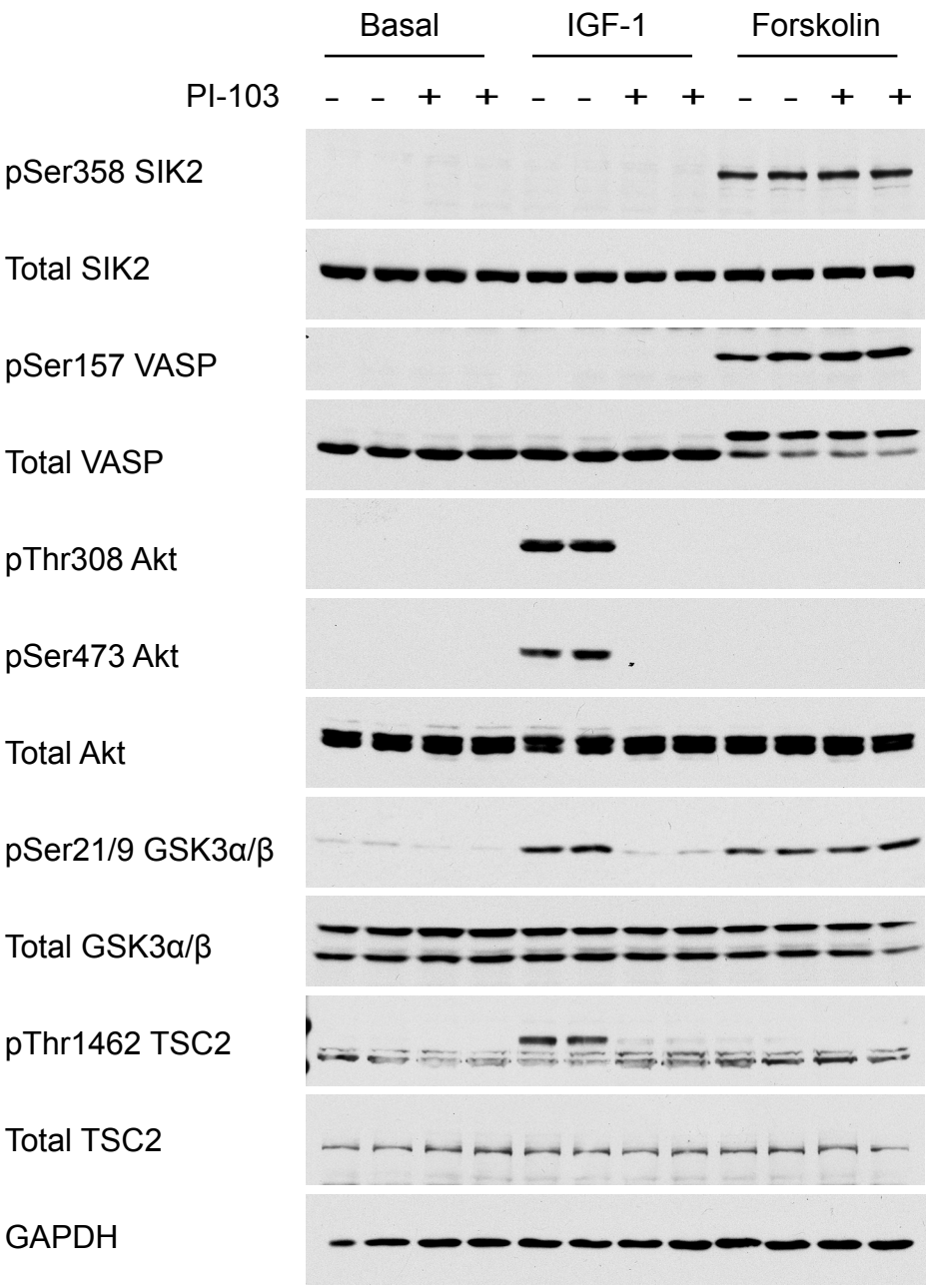

Appendix 2 SIK2 phosphorylation in HEK293 cells following PI3K inhibition.

HEK293 cells were pre-treated with 1 µM PI-103 (a PI3K inhibitor) for 30 min followed by stimulation with 10 µM forskolin or 50 ng/ml IGF-1 prior to cell lysis. Lysates were immunoblotted with indicated antibodies. The pAKt, pGSK3α/β and pTSC2 antibodies were used to confirm the effects of inhibitor and VASP antibodies were used to confirm PKA activation by forskolin. The GAPDH antibody was used as a loading control.

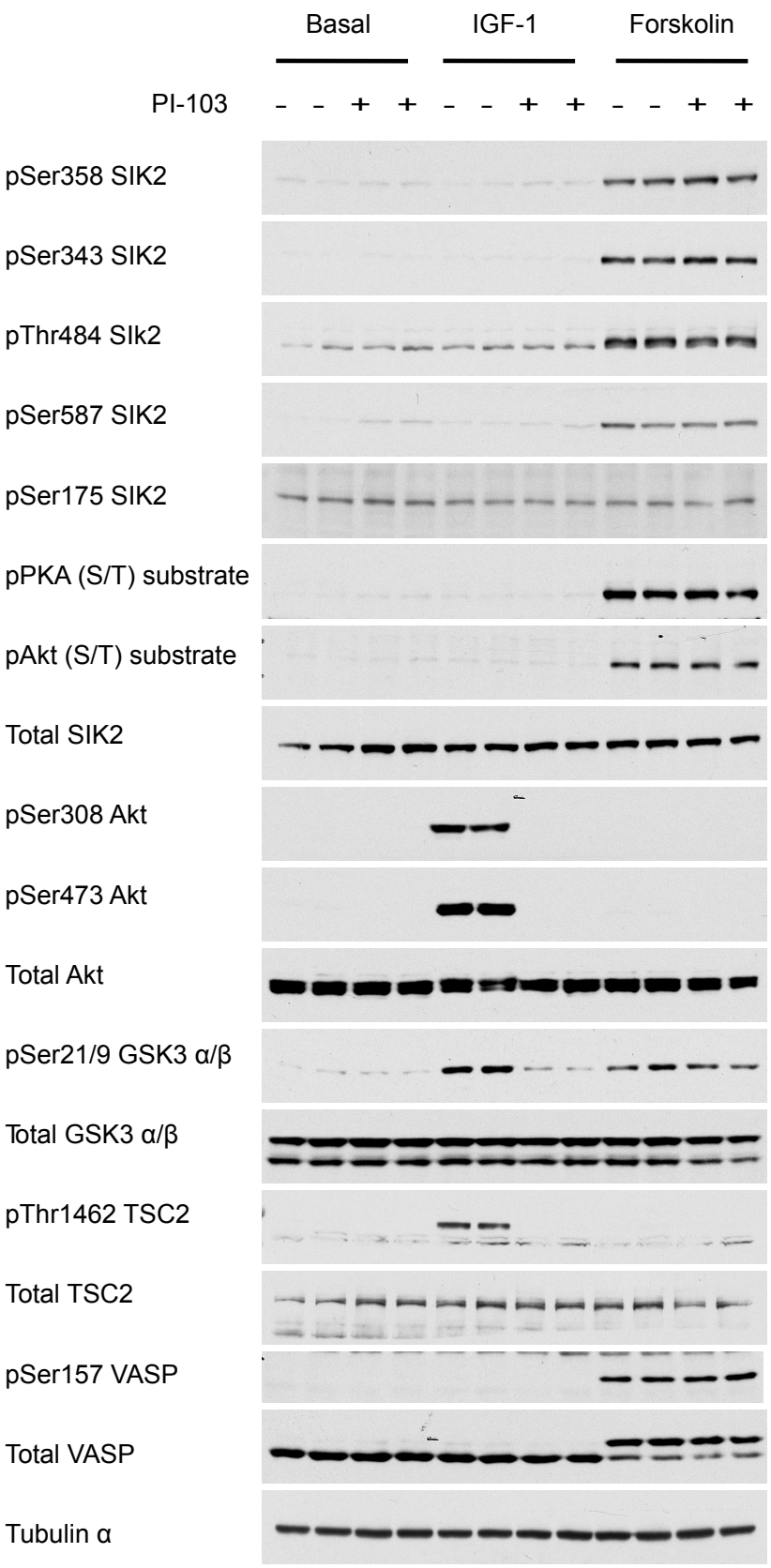

Appendix 3 SIK2 phosphorylation in HEK293 cells following PI3K inhibition.

HA-SIK2 was expressed in HEK293 cells for 36 h followed by pre-treatment with PI3K inhibitor PI-103 (1 µM for 30 min) and subsequently stimulation with 10 µM forskolin or 50 ng/ml IGF-1 prior to cell lysis. Lysates were immunoblotted with indicated antibodies. The AKt, GSK3α/β and TSC2 antibodies were used to confirm the effects of inhibitor and VASP antibodies were used to confirm PKA activation by forskolin. The GAPDH antibody was used as a loading control.

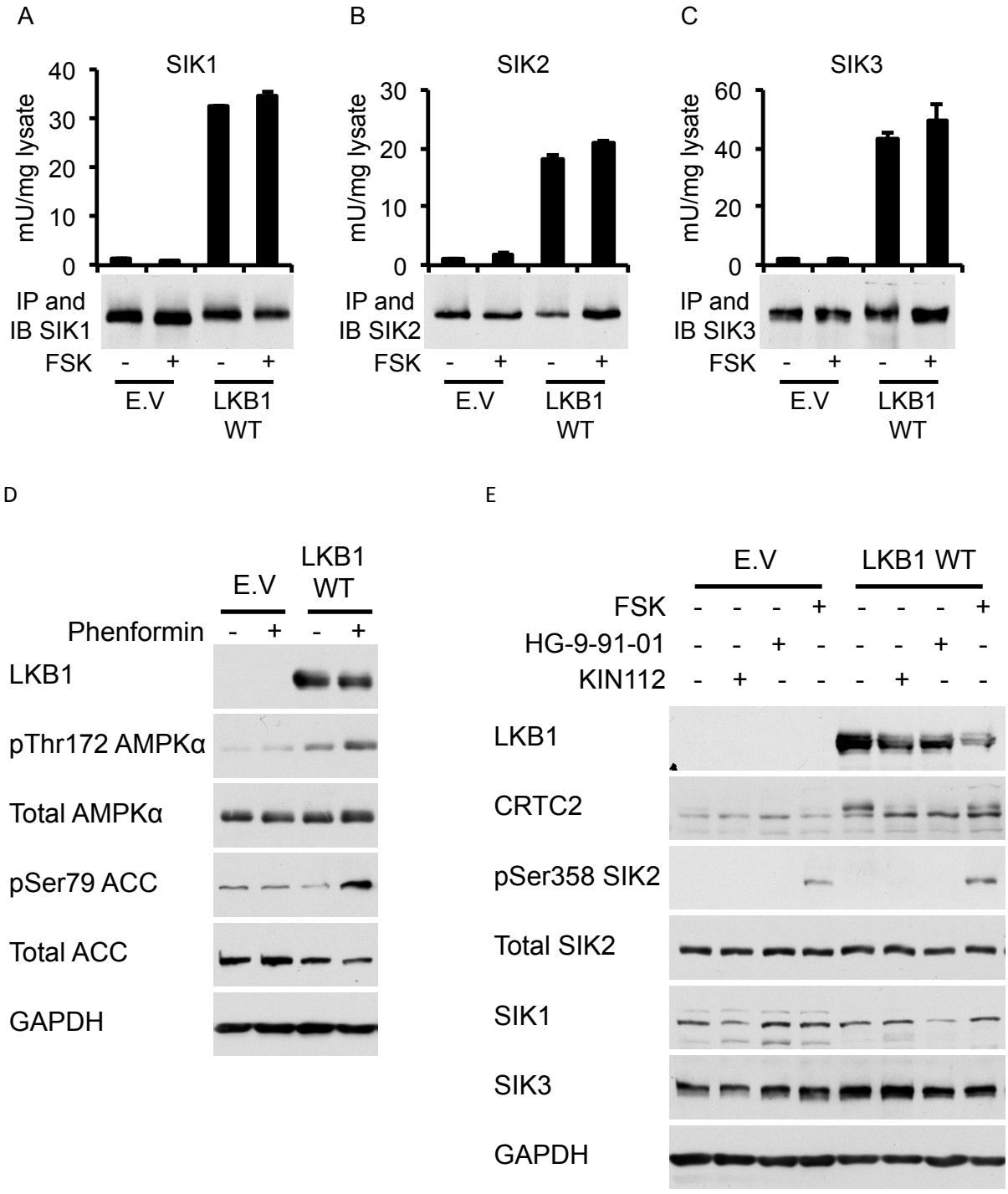

Appendix 4. HG-9-91-01 in HeLa cells.

Empty vector (E.V) or LKB1 wild-type (LKB1 WT) were stably transfected into HeLa cells. The resultant stable cell lines were incubated with or without 10 µM forskolin (FSK) for 10 min prior to cell lysis (A, B, C). SIK1 (A), SIK2 (B) or SIK3 (C) were immunoprecipitated from 0.5 mg of each lysate and subjected to *in vitro* kinase assay or immunoblotted with the respective SIK antibodies. Data is presented as mean ± SD, n=3. D) HeLa cells were treated with 10 mM phenformin for 60 min prior to cell lysis. Lysates were immunoblotted with the indicated antibodies. E) HeLa cells were treated with 10 µM FSK for 10 min, 4 µM HG-9-91-01 or 10 µM KIN112 for 1 h prior to cell lysis. Lysates were immunoblotted with the indicated antibodies. Empty vector and LKB1 WT stable HeLa cell lines were a generous gift from Dr Gopal Sapkota, MRC protein phosphorylation unit, Dundee, UK (Sapkota et al., 2002).

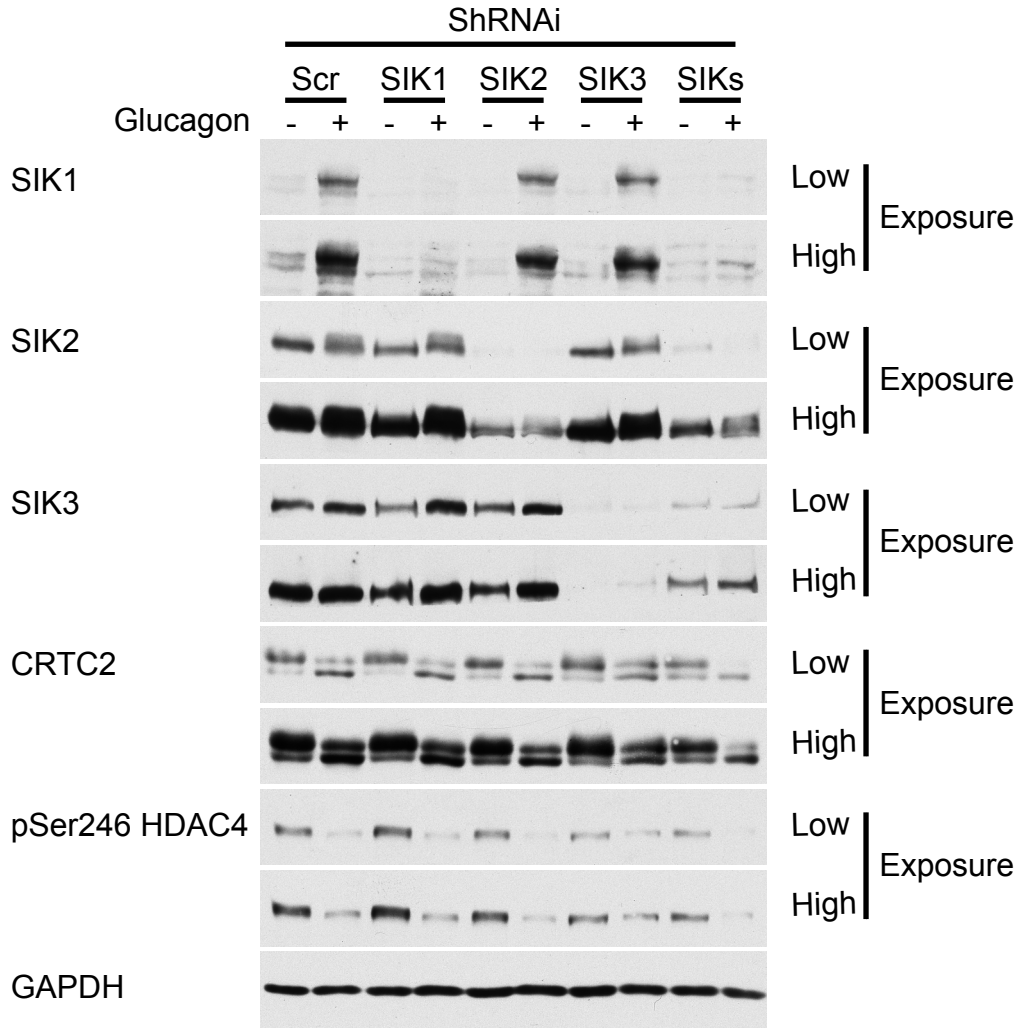

Appendix 5 ShRNAi mediated knock-down of SIKs in primary hepatocyte.

Primary hepatocytes were infected with adenoviral vectors of indicated SIK ShRNAi (1:30 MOI) for total 48 h and stimulated with 0.1 μM glucagon for the last 5 h prior to cell lysis. Lysates were immunoblotted with the indicated antibodies.